Multiplexed microfabricated cell culture device for stem cell process development

Marcel Reichen
Department of Biochemical Engineering
University College London

A thesis submitted for the degree of
Doctor of Philosophy (PhD)

2011

Declaration

I, Marcel Reichen confirm that the work presented in this thesis is my own. The work presented in this thesis was carried out under the supervision of Dr. Nicolas Szita at the Department of Biochemical Engineering, University College London between May 2007 and September 2011. This thesis has not been submitted, either in whole or in part, for another degree or another qualification at any other university.

Marcel Reichen
London, September 2011

Abstract

In this thesis, a multiplexed microfabricated cell culture device is presented to probe the soluble microenvironment of stem cells. A large number of biological, physical and chemical variables determine the microenvironment of stem cells and affect therefore their fate. The soluble microenvironment is believed to play a pivotal role in controlling stem cell fate and its optimisation may therefore allow exploitation of applications such as regenerative medicine or drug discovery.

However, novel tools are required to probe and optimise the soluble microenvironment. The ability to move small volumes of liquid and the minimal use of resources are important characteristics of microfluidic systems and thus, they are perfectly suited to study the microenvironment of stem cells. A microfluidic cell culture device must fulfil three important requirements to be of utility in stem cell bioprocess development.

The first aspect addresses the need for adaptability and flexibility to implement changes in microfluidic designs to take account of the rapid progress in stem cell research. To this end, a packaging solution specifically designed for a microfluidic cell culture device has been developed. The packaging system has thus been complemented with a rapid fabrication method using a micro-milling machine to quickly fabricate disposable and easily reconfigurable microfluidic chips. The packaging solution has a maximum burst pressure of approximately 7.5 bar and the fabrication method has a dimensional fidelity with less than 10% deviation from the nominal value.

The second aspect focuses on the scalability and comparability of results and the feasibility of continuous culture of stem cells - both critical elements for the success of a microfluidic cell culture system for stem cell bioprocess development. A novel cell seeding method has been developed using a pipette to directly and carefully seed cells into a culture chamber within a

microfluidic cell culture device. To prevent a wash-out of viable cells during continuous culture, a low hydrodynamic shear stress microfluidic chip has been developed. The cell culture device has been successfully tested using human embryonic stem cells (hESC) on feeder cells.

The third aspect concerns the automated monitoring of stem cell bioprocesses in the cell culture device. A multiplexed microfluidic bioreactor platform with time-lapse imaging has been developed to obtain data-rich experimental sets. The platform consisting of a cooled media reservoir and a pumping mechanism has been characterised and tested using mouse embryonic stem cells (mESC) as a proof of concept.

The combination of these three aspects provides a basis towards a multiplexed microfabricated cell culture device, which allows data-rich experimentation and comparability with current benchscale culture vessels for stem cell expansion and differentiation.

To my parents Robert and Marisa and my brother Rolf

Acknowledgements

First, I would like to express my gratitude to Dr. Nicolas Szita for his invaluable support, guidance and encouragement since my Master thesis in his lab back in 2006 in Denmark until now. I would also like to thank my advisor Dr. Farlan Singh Veraitch for his support, advice and suggestions for my research. I would also like to thank the Department of Biochemical Engineering for giving me the opportunity to pursue research at the cutting edge.

A number of colleagues around the world and fellow graduate students have influenced my research and my time at UCL. A big thanks goes to the members of the microfluidics lab. I would like to mention in particular my colleague Timothy 'Kirky' Kirk who entertained me in numerous situations with chats, music and humour, but also challenged me scientifically and engineering-wise with research problems.

I also thank Dr. Brian O'Sullivan for his compassion, support in the lab and comments on my work.

I am deeply grateful to the members of the regenerative medicine lab for their patience with the microfluidic 'intruder', in particular, Alex, Diana, Emily, Ludmila, Meg, Minal and Tristan.

I would also like to thank the MEng and M.Sc. students who suffered under my supervision: Sally James, Yong Hu, Matthew Li and Jamie Thompson. Without their work, it would not have been possible to progress.

In raising my interest in research, I am thankful to Dr. Peter Truog and his wife Tina who kindly supported me during my academic years.

I would not have made it without the support, compassion, friendship and kindness of all my friends in Switzerland and here in London. I would like to thank in particular David, Scutch, Blöms, Niccolo, Nina, Simon, John, Andy, Gareth, Rich, Lucy, Tarit, Rachel, Nick and Frank.

My thanks and gratitude goes to my parents and family. They have provided the necessary support, patience and encouragement.

Marcel
London, 2011

Contents

List of Figures

List of Tables

Glossary

ASC	Adult stem cell; a tissue specific stem cell which gives rise to a few progenitor and functional cells
CAD	Computer-aided design; virtual environment for the design process
CAM	Computer-aided manufacturing; use of computer software to control machine tools
CNC	Computer numerical control; automation of machine tools by abstractly programmed commands
DAPI	4',6-diamidino-2-phenylindole; a fluorescent stain that binds strongly to DNA and serves to marks the nucleus in fluorescence microscopy
DMEM	Dulbecco's minimal essential medium; cell culture medium used to maintain cells in tissue culture
ECM	Extracellular matrix; provides structural support to cells
EDTA	Ethylene-diamine-tetraacetic acid; a chelating molecule used to sequester most divalent metal ions, such as calcium (Ca^{2+}) or magnesium (Mg^{2+})
ESC	Embryonic stem cell; a stem cell which gives rise to nearly every type of cell
FBS	Fetal bovine serum; portion of the plasma remaining after coagulation of blood
FEM	Finite element method; numerical technique to find approximate solutions of partial differential equations or integral equations
FGF	Fibroblast growth factor; family of factors involved in angiogenesis, wound healing and embryonic development
GMEM	Glasgow's minimal essential medium; modification of Eagle's medium
hESC	Human embryonic stem cell; embryonic stem cells derived from a human blastocyst
iPSC	Induced pluripotent stem cell; a reprogrammed adult somatic cell exhibiting embryonic stem cell-like characteristics
ITO	Indium tin oxide; a transparent and electrically conductive coating
LIF	Leukemia inhibitor factor; interleukin 6 cytokine that affects cell growth and development
MEF	Murine embryonic fibroblasts; a cell that synthesizes the extracellular matrix and collagen
mESC	Mouse embryonic stem cell; embryonic stem cells derived from a mouse blastocyst
MSC	Mesenchymal stem cell; multipotent stem cells that can differentiate into various cells such as osteoblasts or chondrocytes
Oct-4	Octamer transcription factor 4; a protein which is critically involved in the self renewal of undifferentiated embryonic stem cells
PBS	Phosphate buffered saline; a usually isotonic buffer solution
PC	Poly(carbonate); a highly transparent thermoplastic polymer with high impact-resistance and strength
PDMS	Poly-(dimethylsiloxane); a silicone originally developed as an encapsulant, but widely used in microfluidics
PMMA	Poly(methyl methacrylate); a transparent thermoplastic polymer
PS	Poly(styrene); a widely used transparent thermoplastic polymer
SOX1	Sex determining region Y-box 1; a transcription factor of which the expression is restricted to the neuroectoderm
SSEA-3	Stage-specific embryonic antigen 3; one surface marker for pluripotency of embryonic stem cells or embryonic stem cell-like characteristics
TC-PS	Tissue culture poly(styrene); commonly used material for culture ware for adherent cells
Tra-1-81	Tumor rejection antigen; a surface marker for pluripotency of embryonic stem cells or embryonic stem cell-like characteristics

1

Introduction

Historically, medical advances have largely been limited to the management of the acute effects of diseases and symptoms, and the treatment of infections caused by pathogens, for example the discovery of penicillin. However, as we move into the twenty-first century, the attention of clinicians and researchers has begun to focus more on the treatment of a number of chronic diseases. The prevalence of such chronic diseases is increasing due to the demographic shift across the western world. For example, Parkinson's disease occurs in 1% of the population over the age of 60 (Morizane *et al.*, 2007). The majority of chronic diseases such as Parkinson's or Alzheimer's disease are largely managed by palliative care in the absence of disease reversing agents or therapies.

With the advances in medicine and life sciences, new possibilities arise to move on from merely fighting symptoms using compounds derived in chemical or biochemical processes to tackling the underlying causes of diseases or even repairing or replacing organs with more complex medicines.

A number of therapies are in development which use molecules such as cytokines to cure diseases like cancer, or *in vitro* grown cells to repair or even replace damaged tissues (Margolin, 2008).

Such future medicines will require cells with specific properties, either as a model tissue in drug discovery and development to test these molecules, or for direct use in cell based therapies (Nirmalanandhan & Sittampalam, 2009).

The discovery of stem cells, in particular embryonic stem cells (ESCs), has had an enormous impact on our society and has created a remarkable interest in this research

field - in the scientific community as well as in the broader public audience. The common belief that stem cells are the holy grail for numerous challenges and problems in healthcare, both as a cure for a variety of chronic diseases and for use in tissue engineering, is legitimate only so long as the solutions to these challenges and problems can be translated into products. In this context, an often neglected key aspect is the rapid translation of scientific discoveries or innovations into reproducible and scalable bioprocesses to obtain the cell numbers required for clinical testing or drug discovery applications. An understanding of the different types of stem cells and the variables involved which determine the fate of stem cells is necessary to develop a microfabricated cell culture device.

1.1 Stem cell sources

The potential of stem cells for regenerative medicine and tissue engineering applications is best described by starting with the definition of the properties of a stem cell. The classical definition of stem cells comprises two aspects: the capability of self-renewal and the potency of stem cells or differentiation into functional phenotypes (Darr & Benvenisty, 2006).

The self-renewal capability consists of two mechanisms to ensure that a stem cell population is maintained (Shenghui *et al.*, 2009). The asymmetric replication of a stem cell is one mechanism (Morrison & Kimble, 2006). This is the division of a stem cell into a daughter cell, which is identical to the original cell, and another daughter cell, which is a progeny. The second mechanism is the stochastic division of a stem cell, where one stem cell divides into two identical stem cells and another stem cell divides into two differentiated cells (Ho, 2005).

Potency is a measure of the differentiation capability of a stem cell or, in other words, at what level in the cell specialisation hierarchy a stem cell sits (Smith *et al.*, 2009). For example, embryonic stem cells are pluripotent, thus able to differentiate into one of the three germ layers - *ectoderm*, *mesoderm* and *endoderm*. Each of these layers gives rise to a specific subset of phenotypes after differentiation. It has been found that the *ectoderm* includes skin and neural cells, the *mesoderm* includes cardiovascular and blood cells and the *endoderm* includes cells from the gastrointestinal tissue. In contrast to ESCs, adult stem cells (ASCs), a type of stem cell found in mature animals,

are multipotent. Their differentiation capability is limited to a few progenitor cells and tissue-specific cells.
The two aspects - self-renewal and differentiation - are shown in figure 1.1 and formu-

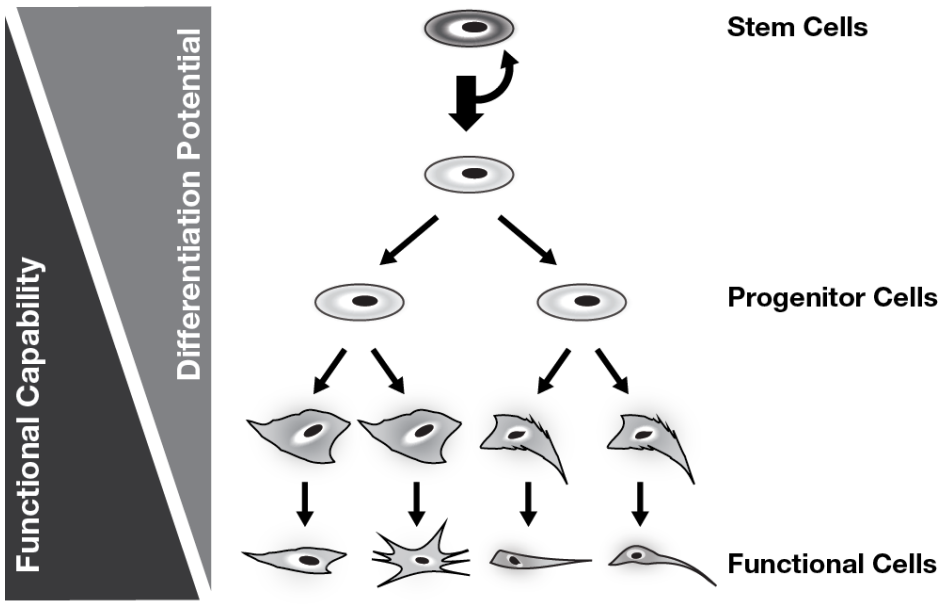

Figure 1.1: Hierarchy of self-renewal and differentiation - Stem cells either renew themselves or differentiate into progenitor cells that lead to terminally differentiated, functional cells. Further down the differentiation hierarchy, the differentiation capability decreases, but the cell functionality increases. Not every type of stem cell has the same differentiation potential and are thus classified for example into *pluripotent* and *multipotent* to name the most important.

lated in a definition by Melton & Cowen (2009):

> *A stem cell is a clonal, self-renewing entity that is multipotent and thus can generate several differentiated cell types.*

Unlike microbial bioprocesses, where a product such as a monoclonal antibody is recovered from cells, stem cell bioprocesses aim to produce cells with specific properties/deliver products, where cells themselves are the product. Regardless of the cell

donor origin, *autologous*[1], *allogeneic*[2] or *xenogeneic*[3], the selection of the appropriate cell source will influence the quality of the product in terms of functionality, safety and purity, and will affect the cost effectiveness of the bioprocess.
Stem cells can originate from multiple sources, either from adult or embryonic tissue or, more recently, by reprogramming functional, mature cells into induced pluripotent stem (iPS) cells - all with advantages and disadvantages (see table 1.1). A more detailed overview of the properties of the different types of established stem cell types is given in the following sections. Note that many of these definitions are based on current findings and are likely to change in the future as the field progresses and the characteristics of stem cells are determined more precisely, for example the definition of pluripotency for human ESCs and so-called induced pluripotent stem cells (Smith *et al.*, 2009).

Table 1.1: Overview of stem cell sources by origin - Advantages and disadvantages of ASCs, ESCs and induced pluripotent stem (iPS) cells under the aspect of usability for applications

	Adult Stem Cells	**Embryonic Stem Cells**	**Induced Pluripotent Stem Cells**
Advantages	Easily obtainable	Golden standard for characterisation	No ethical issues
	No ethical issues Autologous transplantation		Customised
Disadvantages	Short life *in vitro* compared to ESCs	Expensive culture *in vitro*	Little knowledge
		Ethical issues	No standard procedure for derivation
		Tumorgeneity	Tumorgeneity

1.1.1 Adult stem cells

Adult stem cells (ASCs), also known as somatic stem cells, are found in tissues throughout the body of juvenile and adult animals or humans. Their main function is to replace apoptotic cells or to rejuvenate tissue in a specific location. Due to their tissue-specific origin, ASCs are multipotent rather than pluripotent and thus restricted to a given tissue family, having a degree of lineage commitment (see also table 1.2). However, recent

[1]Donor and recipient are the same individual (reg, 2009)
[2]Donor and recipient are different individuals (reg, 2009)
[3]Donor and recipient belong to different species (reg, 2009)

studies suggest that tissue-specific stem cells still possess developmental capabilities. This characteristic is known as transdifferentiation or plasticity (Wagers & Weissman, 2004).

ASCs offer the advantage that an immune response is less likely if an autologous cell therapy can be used. Furthermore, ASCs can be relatively easily obtained from a donor and undergo directed differentiation.

Therapeutic interest in ASCs has particularly focused on the adult stem cells from the blood, the bone marrow, the brain, fat tissue and the umbilical cord blood (see table 1.2). Certain stem cells are limited to certain tissues, for example hematopoietic stem cells (HSCs) can only be found in blood, the bone marrow and the umbilical cord blood. Mesenchymal stem cells (MSCs) in particular gained fame for tissue engineering applications such as bone or cartilage formation (Caplan, 2010). MSCs have also been used to treat brain injuries, as an example for ASC plasticity (Ross & Verfaillie, 2008).

More recently, it has been shown as proof of concept that chondrocytes differentiated from donor-originated MSCs can be successfully transplanted into the donor by replacing the trachea without administering medication to suppress immune responses (Macchiarini *et al.*, 2008).

Table 1.2: An overview of tissue sources for different adult stem cells and their derived cells - Adult stem cells can be derived from various tissue sources and differentiated into many types of clinically relevant cell.

Tissue Source	Cell Type	Derived Cells	References
Blood	Hemapoietic stem cells (HSCs)	Blood cells	Czechowicz & Weissman (2011)
	Endothelial progenitor cells (EPCs)	Endothelial cells	Torsney & Xu (2011); Zampetaki *et al.* (2008)
Bone Marrow	Hemapoietic stem cells (HSCs)	Hepatocytes Blood	Thorgeirsson & Grisham (2006)
	Endothelial progenitor cells (EPCs)	Endothelial cells	
	Mesenchymal stem cells (MSCs)	Adipocytes	Muruganandan *et al.* (2009)
		Cardiomyocytes	Trivedi *et al.* (2010)
		Chondrocytes	Khan *et al.* (2010)
		Endothelial cells	Oswald *et al.* (2004)
		Neurons	Joyce *et al.* (2010)
Brain	Neural stem cells (NSC)	Adipocyte, chondrocyte, myocite, neural progenitor, osteocyte	Reynolds & Weiss (1992)
Fat	Processed lipoaaspirate (PLA)	Adipocyte, chondrocyte, myocite, neural progenitor, osteocyte	Gimble & Guilak (2003)
Umbilical Cord Blood	Hemapoietic stem cells (HSCs)	Blood cells	McKenna & Brunstein (2011)
	Mesenchymal progenitor cells (MPCs)	Adipocyte, endothelial cell, blood cells, osteoblast	Fan *et al.* (2011)

1.1.2 Embryonic stem cells

Embryonic stem cells (ESCs) are derived from the inner cell mass of a blastocyst, an early-stage embryo (Kim *et al.*, 2005). Unlike ASCs, ESCs are pluripotent and thus able to differentiate into any of the three germ layers - *ectoderm*, *mesoderm* and *endoderm*. Murine ESCs (mESCs) were first derived in 1981 by Evans & Kaufman (1981) and Martin (1981). It took nearly 20 years before Thomson *et al.* (1998) derived the first human ESCs.

A human ESC has been defined as a cell that 1) is isolated from the inner cell mass of the blastocyst, 2) proliferates extensively *in vitro*, and 3) retains the ability to differentiate into cell types of all three germ layers (Hoffman & Carpenter, 2005).
The number of hESC lines is rapidly increasing and variation of genomic expression of individual lines have been recognised (Rao *et al.*, 2004). Efforts have been thus undertaken to establish characterisation standards for human ESC research (Pal *et al.*, 2007).
Culture conditions for hESCs have been largely based on xenogeneic culture materials and are still under investigation for long-term expansion and differentiation. hESC lines have been cultured in media supplemented with animal sera and/or on immortalized mouse fibroblast feeder layers (Draper *et al.*, 2004; Reubinoff *et al.*, 2000; Skottman & Hovatta, 2006). However, the use of xenogeneic components raises a concern about introducing animal pathogens in clinical therapies (Lei *et al.*, 2007; Mallon *et al.*, 2006). To address this issue, efforts have been made to maintain hESCs on human feeder layers (Amit *et al.*, 2003; Choo *et al.*, 2004; Hovatta *et al.*, 2003; Richards *et al.*, 2002) or in feeder-free culture systems (Amit & Itskovitz-Eldor, 2006; Hernandez *et al.*, 2011; Rosler *et al.*, 2004). A complete synthetic culture system without animal sera-based medium supplements has been investigated, but has not been established as a standard culture protocol due to the high cost of its components (Ludwig *et al.*, 2006).
Although mouse ESCs share properties with hESCs and are frequently used as model for hESC research, it has to be noticed that self-renewal is regulated differently (Grigoryan & Kruglyakov, 2009). mESCs are grown in media with leukemia inhibitor factor (LIF) or on feeder cells such as immortalized fibroblasts (Tremml *et al.*, 2008). However, hESC may require feeder cells, serum, and bovine fibroblast growth factor (bFGF) instead of LIF (Xu *et al.*, 2005).
Differentiation can occur spontaneously or can be directed. *In vitro*, differentiation can be initiated by culturing cells in suspension to form embryoid bodies (EBs) or in monolayers. Differentiation protocols have been established to derive clinically relevant cells such as neuronal cells (Reubinoff *et al.*, 2001), myocardiocytes (Vidarsson *et al.*, 2010) and insulin producing hepatocytes (Kroon *et al.*, 2008).
Expression of intracellular markers such as Oct-4 and Nanog combined with surface markers such as Tra-1-60/Tra-1-81 and SSEA-3/-4 are an indication of pluripotency presence in an ESC culture.

1.1.3 Induced pluripotent stem (iPS) cells

An alternative source of stem cells, possessing the same properties as ESCs, would help to dispel the ethical concerns surrounding embryonic stem cells and their therapeutic risks (Condic & Rao, 2010; Wert & Mummery, 2003). A breakthrough has been achieved in 2006, when mouse fibroblasts were reprogrammed with four pluripotency genes (*Oct-3/4*, *SOX2*, *c-Myc*, and *Klf4*) also found in naturally-isolated pluripotent stem cells, exhibiting a similar phenotype and properties as their embryonic counterpart (Takahashi & Yamanaka, 2006). This type of cell is known today as induced pluripotent stem (iPS) cells (Stadtfeld & Hochedlinger, 2010). In 2007, human iPS cells were generated by reprogramming somatic stem cells (Yu *et al.*, 2007) or adult human dermal fibroblasts (Takahashi *et al.*, 2007).

Current research aims to improve the reprogramming method and efficiency by using other means than viral transfection of cells with genes. The use of an adenovirus (Stadtfeld *et al.*, 2008), plasmids (Okita *et al.*, 2008), recombinant proteins (Zhou *et al.*, 2009) or mRNA (Plews *et al.*, 2010) have all been investigated to address this issue.

Reprogramming fibroblasts into stem cells has also encouraged the efforts to reprogram mature cells directly into specialised, functional cells. For example, fibroblasts were directly converted into functional neurons by only three factors, *AScl1*, *Brn2* and *Myt1l*. These induced neurons expressed multiple neuron-specific proteins, generated action potentials and formed functional synapses (Braun & Jessberger, 2010; Vierbuchen *et al.*, 2010).

The derivation of iPS cells from cells of a patient itself makes them particularly attractive for regenerative medicine with a reduced risk of an immune response, or for drug discovery as a patient-specific disease model. As a safety measure, the absence of oncogenic genes such as *myc* and tumor formation is also required by regulatory bodies if iPS cells are to be used in regenerative medicine for patient safety (Carpenter & Couture, 2010; Smith, 2010).

1.2 The need for the production of human cells

1.2.1 Drug discovery

Drug discovery is the selection process of a target compound for a certain disease under the criteria of toxicity, efficacy and bioavalability of the active moiety in humans (Gad, 2005). Historically, drug discovery has been a heuristic approach, but has now shifted to a systematic search using technologies such as proteomics, genomics and high throughput screening of compound libraries (Drews, 2000). Nevertheless, drug discovery and development is an expensive and risky undertaking with increasing attrition rates (Kola & Landis, 2004; Paul *et al.*, 2010). For example, a recent study documents that only a fraction (less than a third) of all target compounds are approved (DiMasi *et al.*, 2010). To improve R&D productivity and thus reduce costs, an early elimination of non-active targets is desired (Paul *et al.*, 2010).

At present, reporter systems in genetically modified rodent or immortalised human cells are being used to indicate if a signalling pathway is activated by a target. However, these cell models may not represent the response in humans accurately enough. For example, an overexpression of a reporter gene at high levels may not reflect a physiological normal condition or their phenotype may be unrelated to the phenotype of the tissue of interest (Ebert & Svendsen, 2010; Pouton & Haynes, 2005). *In vitro*, primary cells of an appropriate tissue often dedifferentiate rapidly in culture and can only be propagated for a short time (Pouton & Haynes, 2005).

Progress in stem cell technology provides the opportunity to set up human models of diseases to elucidate the underlying disease mechanisms (Chien, 2008). By genotyping human pluripotent stem cells, it will be possible to measure the influence of genetic variations in drug response for example (Pouton & Haynes, 2005).

Certain small molecules have been recognised to have a negative impact on stem cell differentiation. Drug-like molecules have been identified, both *in vitro* and *in vivo*, which drive specific stem cell differentiation (McNeish, 2007). Specific human cells derived from pluripotent stem cells (PSCs) may therefore play a key role in target validation and/or toxicity, for example for hepatotoxicity and cardiotoxicity, and differentiation screens (Améen *et al.*, 2008; Rubin, 2008).

More accurate disease models could be derived directly from a patient's cells which

have been reprogrammed to resemble embryonic stem cells. For example, disease-specific ESC lines were derived from patients suffering genetic diseases like adenosine deaminase deficiency-related severe combined immunodeficiency, Shwachman-Bodian-Diamond syndrome, Gaucher disease type III, Duchene and Becker muscular dystrophy, Parkinson disease, Huntington disease, juvenile-onset, type 1 diabetes mellitus and the carrier state of Lesch-Nyhan syndrome (Park *et al.*, 2008).
In theory, reprogrammed ESCs could then be differentiated into patient-specific, functional cells for drug discovery, for example for personalised medicine. However, it remains unclear to which degree of cell specialisation these ESCs have to be differentiated to represent a sufficient accurate model (Rubin, 2008).
To take advantage of the properties of these ESC-derived, specialised cells, it is paramount to understand the mechanisms which control the expansion and differentiation of ESCs. This would then allow the efficient and economical mass production of specialised, functional cells.

1.2.2 Regenerative medicine

The lack of organ donors, for example for heart or liver transplants (Aubrey *et al.*, 2008), the life-long medication and its effects on diabetes patients (Rubin & Peyrot, 2001) or the non-existence of effective treatments for spinal cord injuries are some examples of issues in modern healthcare that need to be addressed.
Inspired by the Greek myth of Prometheus' liver regeneration which fed Zeus' eagle daily, the ideal treatment strategy would aim to repair the damaged tissue or organ to restore its functionality, thereby removing the need for long-term care (Power & Rasko, 2008).
However, the concept of using cells to treat diseases or trauma and restore tissue function is not outlandish. For example, the transplantation of hematopoietic stem cells derived from the donor bone marrow has been a successful treatment of myeloma and leukemia patients for over 50 years (Appelbaum, 2007).
Under the umbrella terms *regenerative medicine* or *tissue engineering*, new opportunities for stem cell based therapies and cures have subsequently arisen since then, with progress in stem cell research combined with other disciplines such as biomaterial science or bioengineering. The definition by Daar & Greenwood (2007) clarifies the difference between regenerative medicine and tissue engineering:

> *Regenerative medicine is an interdisciplinary field of research and clinical applications focused on the repair, replacement or regeneration of cells, tissues or organs to restore impaired function resulting from any cause, including congenital defects, disease, trauma and ageing. It uses a combination of several converging technological approaches, both existing and newly emerging, that moves it beyond traditional transplantation and replacement therapies. The approaches often stimulate and support the body's own self-healing capacity. These approaches may include, but are not limited to, the use of soluble molecules, gene therapy, stem and progenitor cell therapy, tissue engineering and the reprogramming of cell and tissue types.*

The range of potential applications for regenerative medicine is immense (see table 1.3) and it has also sparked now a growing interest of the pharmaceutical industry (McKernan *et al.*, 2010). To reflect this trend, the FDA[1] approved in 2009 the first Phase 1 trial with hESC-derived oligodendrocytes for spinal cord injuries (Alper, 2009). Very recently, two new neural stem cell trials have been approved in the UK and Switzerland (Mack, 2011). Despite the promises and hopes of regenerative medicine, some challenges and issues exist in translating laboratory findings into clinical procedures (Bongso *et al.*, 2008). First, the efficacy and safety of these therapies in patients needs to be thoroughly tested to avoid secondary malignancies (Carpenter *et al.*, 2009). For this reason, robust and functional assays need to be developed which are able to predict the clinical safety and efficacy (Rayment & Williams, 2010). After injection of cells or transplantation of cell-laden grafts into a patient, severe immune responses or malignancies are undesired secondary effects. This is particularly relevant for ESC based therapies where undifferentiated cells have been shown to trigger tumor formation (Anisimov *et al.*, 2010).

The long-term safety of stem cell based therapies has to be thoroughly proofed that side effect disorders are absent. In a recent study, it has been shown for example that up to 30% of the patients receiving hematopoietic stem cell transplants may suffer from diabetes mellitus after 2 years post-implantation (Griffith *et al.*, 2010).

Besides the aforementioned biological issues, practical issues such as the cell numbers required for a therapy are stalling the advancement of regenerative medicine. Mason &

[1] Food and Drug Administration

Dunnill (2009) estimate required cell numbers in the range of $10^5 - 10^9$ cells depending on the tissue to treat. It becomes a huge challenge to manufacture these cells as currently no culture system and strategy is in place to cope with cell numbers of these magnitudes (Oh & Choo, 2006).

This challenge could be addressed by more efficient expansion and differentiation protocols using novel bioreactor types which allow to control the microenviroment of stem cells. However, at this stage, there is no bioprocess development tool available which could assess the influence of different culture variables on cell numbers obtained in expansion or differentiation steps.

Table 1.3: Exemplary summary of potential future regenerative therapies - A few examples of potential stem cell therapies for different, clinically relevant tissues. Naturally, there are more applications for stem cell based therapies.

Clinical Application	Injury/Disease	Description	Current Treatment	Future Treatment	References
Neural	**Spinal cord injury (SCI)**	Defect of the spinal cord by interrupting axonal pathways. Loss of nervous tissue and consequently of motor and sensory ability.	Treatment include neuronal protection and preservation of residual axons and white matter.	Injection of stem cells can lead to functional benefits.	Lindvall & Kokaia (2010); Rossi & Keirstead (2009); Sahni & Kessler (2010); Schwarz & Schwarz (2010)
	Alzheimers's disease	Disorder is characterised by neuronal and synaptic loss throughout the brain. Memory and cognitive performance is progressively impaired	Acetylcholinesterase inhibitors are administered to enhance cholinergic function.	Genetically modified stem cells could be used for delivery of factors that can modify the course of the disease.	Gögel *et al.* (2011); Kim & de Vellis (2009)
	Parkinson's disease	Gradual loss of nigrostrial dopamine-containing neurons. Symptoms include rigidity, poverty of movements, tremor and postural instability.	Oral administration of L-dopa and dopamine receptor agonists, deep brain stimulation in the subthalamic nucleus.	Replacement with dopaminergic neurons generated *in vitro*.	Lindvall & Kokaia, 2010; Morizane *et al.*, 2007; Schwarz & Schwarz, 2010

continued on the next page

continued from the previous page

Clinical Application	Injury/Disease	Description	Current Treatment	Future Treatment	References
	Huntington's disease	Fatal, intractable disorder that is characterized by excessive spontaneous movements and progressive dementia.	-	Treatment is in infancy, but implanted NS cells in rat brains were found to reduce motor impairments in experimental HD through trophic mechanisms.	Gögel *et al.* (2011); Kim & de Vellis (2009)
Cardiovascular	**Myocardial repair**	Mycardial infarcts lead eventually to congestive heart failure	Heart transplantation	Cardomyocytes differentiated from stem cells could replace damaged heart tissue. Ideal response includes revascularisation and electrical synchronization with host myocardiocytes.	Braam *et al.* (2009); Sui *et al.* (2011); Wong & Bernstein (2010)
	Blood Vessel Substitute	Vascular lesions result in tissue loss.	Xenogenic or synthetic materials lack growth potential and pose a risk for complications	Vascular grafts using biodegradable scaffolds and autologous cells allow better tissue integration.	Atala (2009)
Orthopedic	**Articular Cartilage Damage**	Loss of lubrication functionality leads to severe pain. Causes are trauma, but as well arthritis.	Physiotherapy, weight loss, pain relief medication, intraarticular injections and orthotic interventions.	Cartilage derived from stem cells can be transplanted.	Ahmed & Hincke (2010)
Metabolic & Secretory	**Diabetes Type I & II**	Chronic disease by a deficit of β-cell mass and failure of glucose homeostasis	Rigorous and invasive regiment of repeated testing of blood sugar levels and injections of recombinant insulin	Implantation of ESC-derived β cells	Gonez & Knight (2010); Wen *et al.* (2011)

1.3 Stem cell bioprocessing

Stem cell bioprocessing is concerned with the manufacture of stem-cell derived products using robust and reproducible culture conditions and processes (see figure 1.2). Unlike traditional microbial up- and downstream bioprocessing, it has to be pointed out that stem cell bioprocessing may also include further bioprocessing steps such as the delivery of the final product to a patient for example (Mason & Hoare, 2007).

Three design principles are applied to stem cell bioprocessing: the *process components*, the *process requirements* and the *process functions* (Placzek *et al.*, 2009). *Process*

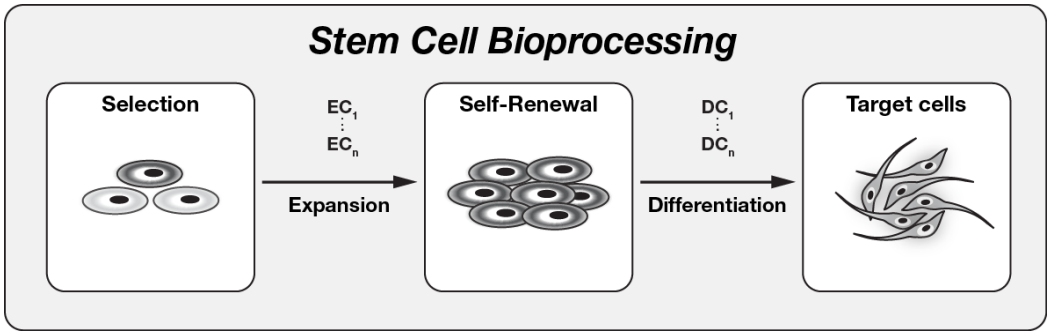

Figure 1.2: Basic concept of stem cell bioprocessing - A simple and basic description of stem cell bioprocessing. Stem cells are screened for and selected to meet specific process criteria. Stem cells are expanded under process conditions $EC_1...EC_n$ to the required cell density and kept pluripotent. These cells undergo directed differentiation under process conditions $DC_1...DC_n$ into target cells.

components are the cell source and type, the signalling required for cell development and the bioreactor design and implementation. Practical considerations of bioprocessing are addressed by *process requirements* and includes aspects of good manufacturing practice (GMP), bioprocess monitoring, control and automation and finally the delivery of the product. Both aspects - process components and process requirements - lead to product functionality and integration to name a few examples of *process functions*.

The systematic and cost-effective production of specific, stem cell-derived cells is required by both, drug discovery and regenerative medicine applications. The future success of regenerative medicine will rely on the bioprocessing capabilities to clear many of the current hurdles related to stem cells (see section 1.2.2). To address these issues and concerns, Kirouac & Zandstra (2008) proposed four criteria for stem cell bioprocess development and optimisation: 1) assessment of relevant cell properties, 2) measurement and control of key parameters, 3) robust predictive strategies for key parameters and 4) approaches to test the many different parameters that may affect cell output in a high throughput and scale-relevant manner.

Proliferation and differentiation protocols for stem cells are developed in simple, laboratory-scale open bioreactors such as Petri dishes or T-flasks. However, the transition of a biological, laboratory-scale problem (can cell A be turned into a cell B under culture condition C ?) into a system (can A cells be turned into B cells per volume and time unit under process conditions $C_1...C_n$?) requires engineering principles and

practices to achieve control, reproducibility, automation, validation and safety (Polak & Mantalaris, 2008).

To implement these criteria into an engineered system, the understanding of the so-called stem cell niche is necessary, a model to explain the survival, self-renewal and differentiation of stem cells. The niche is *in vivo* the microenvironment which consists of key components such as growth factors, cell-cell and cell-matrix interactions (Becerra *et al.*, 2010; Discher *et al.*, 2009). To resemble *in vitro* the complex and multi-factorial *in vivo* niches and taking the sensitivity of stem cells to their culture environment into account, the understanding of the microenvironment of stem cells and the interactions with other cells and the extracellular matrix (ECM) are paramount (see also figure 1.3 **A**) (Peerani & Zandstra, 2010). The following subsections elucidate the importance of the regulatory aspect of the stem cell niche - the cell interactions and the ECM - that are necessary for successful outcomes of stem cell bioprocessing. Due to the complexity of these interactions, this overview covers only two-dimensional culture systems, but it is inevitable that culture systems using engineered three-dimensional scaffolds will appear in the near future which mimic the *in vivo* niche more accurately. To resemble stem cell niches, cell culture systems have been developed which, in case of a two-dimensional culture, consists of a medium for expansion/differentiation with a cocktail of soluble cues, an ECM and a bioreactor.

1.3.1 Stem cell regulation & cellular interactions

A number of different molecular signalling pathways control and regulate whether a stem cell population proliferates or differentiates. For example, the *TGF-β/activin*, *Wnt* and *Nanog* pathways control and regulate pluripotency (Angers & Moon, 2009; Pera & Tam, 2010; Watabe & Miyazono, 2009), the *TGF-β*, *Hedgehog* and *c-Myc* pathways have been identified to regulate proliferation (Jenkins, 2009; Murphy *et al.*, 2005; Singh & Dalton, 2009; Taipale & Beachy, 2001). Although important pathways have been discovered and elucidated, a complete identification of all pathways and their interactions is lacking (Darr & Benvenisty, 2006; Stewart *et al.*, 2008).

To trigger these pathways in a controlled manner, it is necessary to understand the signalling factors, which trigger a signalling cascade and eventually lead to the start of a certain gene expression.

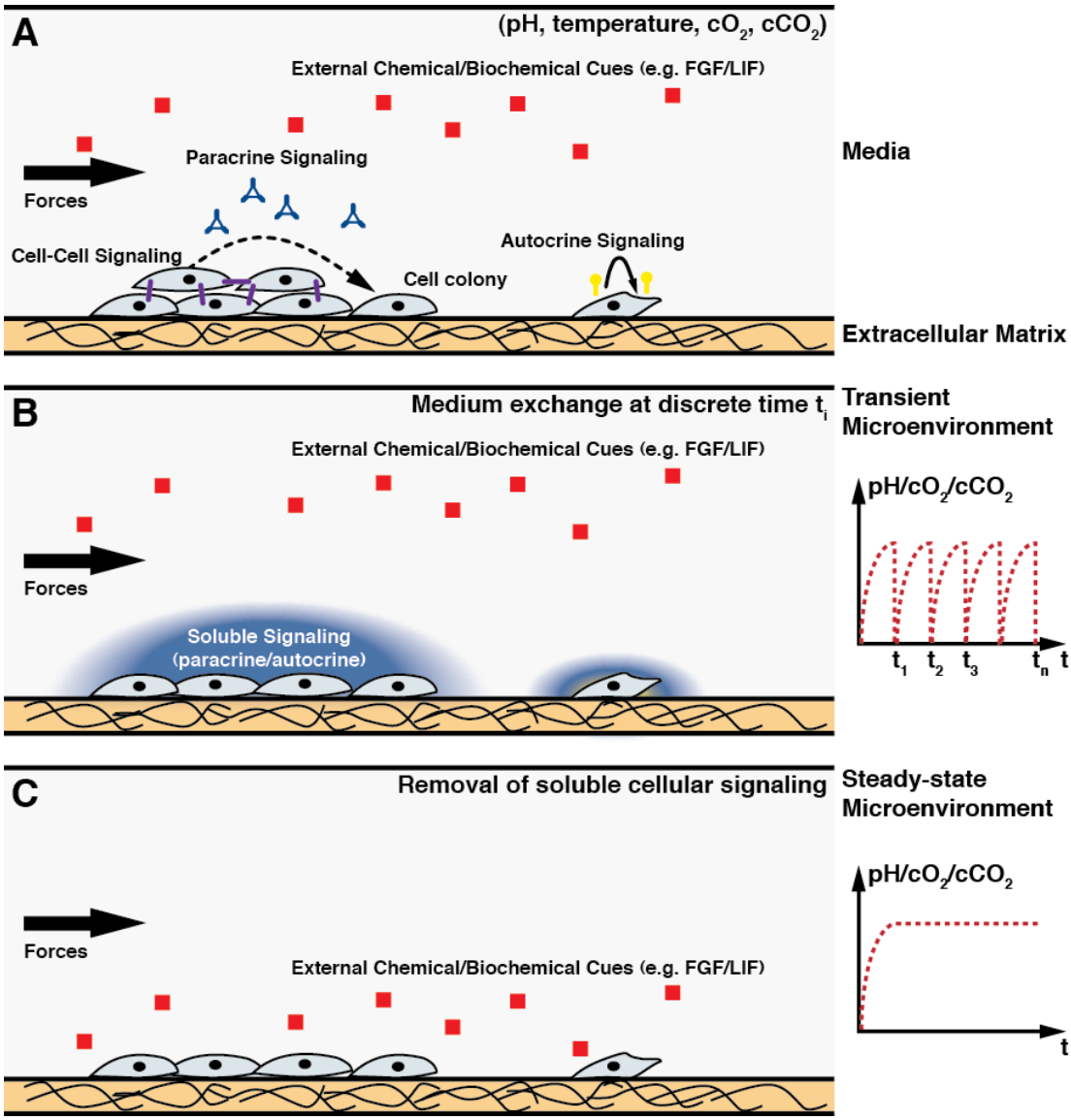

Figure 1.3: The in vitro microenvironment of ESCs - ESCs are grown on an extracellular matrix (ECM) and fed with media to either maintain their self-renewal capability or differentiate into a target cell. Cells communicate with itself (*autocrine*) or with other cells (*paracrine*) and interact with the ECM (**A**). In current culture protocols using T-flasks for example, media is exchanged daily (**B**). Medium exchanges impose time- and cell number dependent concentrations, which might not occur in a pseudo steady-state microenvironment with continuous medium exchange (**C**).

The *mTor* pathway has been identified as playing a major role in the cell cycle and proliferation (Fingar & Blenis, 2004). The cell cycle of stem cells in turn plays an important role in cellular fate decisions (White & Dalton, 2005). Whether a cell continues to proliferate or starts to differentiate is mainly decided in the G_1 phase of the cell cycle by a number of checkpoints (Burdon *et al.*, 2002; Neganova & Lako, 2008; Zhao & Xu, 2010). The cell cycle itself is regulated by pathways such as cyclin-dependent kinases (CDK) and *c-Myc* (Singh & Dalton, 2009). The majority of a mESC population for example is in the S phase of the cell cycle, where the DNA is replicated (White & Dalton, 2005). Not all cells in a stem cell cluster/colony are therefore at the same stage of the cell cycle either, so that different signalling cues are only released by a fraction of the cells. The elimination or minimisation of the effects of these concentration differences are likely to have a vast influence on the outcome of the entire bioprocess.

In vivo, there is a complex interplay of different soluble extrinsic and intrinsic signalling cues (Firestone & Chen, 2010; Kristensen *et al.*, 2005; Li & Ding, 2010), gap junctions[1] (Wong *et al.*, 2008) and the extracellular matrix (Tsang *et al.*, 2010) which control the fate of stem cells. Of particular interest for ESC bioprocesses are the extrinsic factors such as soluble signalling and the ECM due to their ease of control.

For example, leukemia inhibitor factor (LIF), a cytokine secreted by fibroblasts, regulates *STAT3*, *Oct-3/4* and *Sox-2*, which are transcription regulators for pluripotency (see section 1.1.2) (Okita & Yamanaka, 2006). The absence of LIF thus promotes ESC differentiation. Immortalised fibroblasts are traditionally used as feeders to keep ESCs pluripotent. However, murine ESCs remain pluripotent in the absence of feeder cells, if medium is supplemented with bone marrow protein 4 (BMP-4) and LIF (Okita & Yamanaka, 2006).

As discussed in the previous example, cells are capable of secreting signalling factors which bind to specific cell receptors on the surface of another cell; this mechanism is known as *paracrine* signalling (Baraniak & McDevitt, 2010). However, the receptor can also be located on the same cell, which released the signalling factor and is known then as *autocrine* cell signalling. For example, the transforming growth factor beta

[1] specialised intercellular connection which allows various molecules or ions to pass freely between cells

family *TGF-β* is a protein, which regulates pluripotency, and is secreted by ES cells themselves.

The last category of signalling mechanisms includes intrinsic mechanisms such as notch signalling, gap-junctions, and intercellular signalling such as endocrine signalling. Although intrinsic cues may not play an immediate part in stem cell bioprocess control, inhibition or promotion of intrinsic signalling might help to integrate such cells into an existing tissue. For example, gap junctions are important in myocardiac tissue to synchronise the heart beat frequency. Transplanted myocardiac cells or tissue have therefore to establish a connection with the existing tissue to synchronise the contraction for a heart beat.

So far, only extrinsic and intrinsic biochemical cues have been discussed. Physicochemical and topographical cues due to their direct interaction with cells play an important part to promote directed differentiation of stem cells into specialised, functional cells. For example, mesenchymal stem cells differentiate into osteochondrocytes under cyclic mechanical stimulation (Maul *et al.*, 2011). Hydrodynamic shear stress promotes the differentiation of human embryonic stem cells into endothelial-like cells (Ahsan & Nerem, 2010). Nano- and microstructured two-dimensional cell culture surfaces such as linearly aligned gratings for instance have a positive effect on the directed differentiation of a number of different types of stem cell (Martínez *et al.*, 2009). Valamehr *et al.* (2008) have demonstrated that the hydrophobicity of the cell culture surface plays a role in the embryoid body (EB) formation size and efficiency. The rigidity of cell culture substrate itself has also an influence on stem cell morphology as demonstrated by Yang *et al.* (2011). Chemical cues such as low oxygen tension levels may increase the differentiation efficiency, for example of ESC-derived neuronal progenitor cells (Mohyeldin *et al.*, 2010; Simon & Keith, 2008).

It is evident that the cellular environment of a stem cell is a complex and dynamic interplay of different cues - soluble factors, cell-cell signalling, mechanical load and the extracellular matrix. To precisely define a reproducible stem cell niche, engineered cellular environments are needed (Burdick & Vunjak-Novakovic, 2008; Peerani & Zandstra, 2010).

Static cultures, where medium is exchanged regularly, have a transient behaviour of the soluble microenvironment (see figure 1.3 **B**). Considering two arbitrary sized cell clusters/colonies in a static culture vessel for example, the larger sized cluster will

produce more signalling factors and toxic metabolites over time and consume more nutrients than the smaller cluster resulting in concentration gradients in the vessel.

However, a steady-state cellular environment is more likely to expose cell clusters to constant, spatially invariant concentration levels of nutrients and signalling factors (see figure 1.3 **C**). The choice of an appropriate bioreactor design and culture mode will therefore be critical to achieve steady-state conditions and yield large quantities of cells with specific properties.

1.3.2 The importance of the extracellular matrix

In vitro, some adherent cells require a biological glue, the extracellular matrix (ECM), to attach to a cell culture surface (Frantz *et al.*, 2010; Raymond *et al.*, 2009). The ECM is composed of different molecules such as collagens and other glycoproteins, hyaluronic acid, proteoglycans, glycosaminoglycans and elastins. ECM molecules have different functions: adhesive surfaces for cells, structure for cells, storage and mediation of growth factors and the sensing and transduction of mechanical signals (Rozario & DeSimone, 2010). The distribution of these molecules is not static, but rather changes dynamically with the development of a tissue.

The ECM has not only a structural support role, but also an interaction with receptors on the cell surface which transmit signals through the cell plasma into the cytoplasm (Daley *et al.*, 2008; Hynes, 2009). Stem cells communicate therefore not only via soluble signalling factors, interaction with the ECM regulates and controls also pluripotency/differentiation of stem cells via cell adhesion molecules signalling (Reilly & Engler, 2010; Yamashita, 2010). Cell adhesion molecules such as integrins and cadherins are proteins in the cytoskeletone which control cell-cell and cell-ECM communication. For example, integrin adhesion affects stem cell function and maintenance (Ellis & Tanentzapf, 2010; Lee *et al.*, 2010; Prowse *et al.*, 2011).

For embryonic stem cell expansion, different ECMs have been tested for culture of hESCs while maintaining their pluripotency (see table 1.4). Synthetic materials due to their cost and availability will become more important to deliver stem cell regulatory signals to direct stem cell fates (Lutolf *et al.*, 2009). Cell-generated physical forces and the stiffness of the extracellular matrix are increasingly linked to differentiation (Engler *et al.*, 2006; Guilak *et al.*, 2009; Reilly & Engler, 2010).

For scalable hESC culture systems, fully defined culture surfaces are required to ensure bioprocess reproducibility. Well defined synthetic surface components have proved that they are capable of maintaining long-term hESC pluripotency (Melkoumian *et al.*, 2010; Villa-Diaz *et al.*, 2010). Rodin *et al.* (2010) have shown that long-term culture of hESC on recombinant human laminin-511 while maintaining pluripotency is also possible. A controlled and quantifiable deposition of extracellular matrix proteins on a hyaluronic acid and chitosan surface has been demonstrated to promote culture of hESCs and MSCs (Doran *et al.*, 2010). These efforts are important steps towards scalable culture systems and the elucidation of the fundamental biological processes of expansion and differentiation.

Table 1.4: Summary of some different ECMs used for embryonic stem cells - ECMs used for expansion and differentiation of hESCs and mESCs.

ECM	Description	Role/Effect	References
Collagen	Group of proteins found especially in connective tissues. Of particular interest is collagen IV, which forms bases of the cell basement membrane and is found in gelatine.	Maintains pluripotency of stem cells.	Greenlee *et al.* (2005); Jones *et al.* (2010); Li *et al.* (2009)
Fibronectin	Group of proteins which are secreted by a number of cells. They play a critical role in wound healing and are necessary for embryogenesis	Fibronectin consistently supports hESC growth with feeder cells, conditioned medium and defined medium.	Lu *et al.* (2006); Pankov & Yamada (2002)
Laminin	Group of proteins of the ECM, structural components of basement membranes. Laminins play important roles in tissue morphoegensis and homeostasis by regulating tissue architecture, cell adhesion, migration and matrix-mediated signalling.	Maintains pluripotency of embryonic stem cells combined with conditioned medium. Only laminin 511 maintains pluripotency in human and murine ESCs.	Domogatskaya *et al.* (2008); Hamill *et al.* (2009); Rodin *et al.* (2010)
Matrigel™	Protein mixture secreted by Engelbreth-Holm-Swarm mouse sarcoma cells containing structural proteins like laminin and collagen. Exact composition unknown.	Maintenance of pluripotency over several days and passage numbers.	Hughes *et al.* (2010); Kleinman & Martin (2005); Rowland *et al.* (2010); Xu *et al.* (2001)

1.3.3 Bioreactors for stem cell bioprocessing

Media composition and ECM are not the only variables that affect the outcome of a stem cell bioprocess. The choice and operation mode of an appropriate bioreactor type will play an equally important role in the efficient large-scale and long-term manufacture of cells (King & Miller, 2007).

In general, a bioreactor is a device in which biological and/or biochemical processes occur under a controlled environment and operating conditions (Martin *et al.*, 2004). For stem cell bioprocesses, the condition of the media such as pH, temperature, dissolved gas tensions, nutrients, metabolites and regulatory molecules can be controlled by the bioreactor. Cues such as mechanical forces or signalling molecule concentrations are generated, applied to cells by the bioreactor. Furthermore, bioreactor designs for stem cell applications need to incorporate rigorous quality control (QC) and process control (PC) measures to guarantee product safety (Kino-oka & Taya, 2009). For regenerative medicine stem cell bioprocesses, a bioreactor will have more functions than cell expansion or differentiation, for example the delivery of cells to the patient in a clinical fashion.

Monitoring or even control over important culture parameters in bioreactors are thus important to ensure GMP production of cells. In microbial bioprocesses, optical density and dissolved oxygen are commonly monitored parameters to ensure product consistency (Harms *et al.*, 2002).

Although a real-time multi-channel systems to monitor pH, oxygen and carbon dioxide tension and temperature has been developed for stem cell culture processes (Yue *et al.*, 2008), real-time monitoring of cell morphology or even cell functionality has been rarely implemented as standard in bioreactor designs for stem cell bioprocesses. Due to the complex biological mechanisms involved in stem cell expansion and differentiation, sophisticated, non-invasive monitoring approaches are required (see figure 1.4).

However, non-invasive monitoring and controlling efforts are still at an early development stage. Hagenmüller *et al.* (2007) developed a bioreactor for the formation of bone-like tissue using time-lapsed micro-computed tomography (μCT) to monitor bone mineralisation in a scaffold over 44 days. The characterisation of the beating frequency of ESC derived cardiomyocytes is another example for innovative bioprocess monitoring and control. Digital video recording and analysis of pixel intensity were converted into

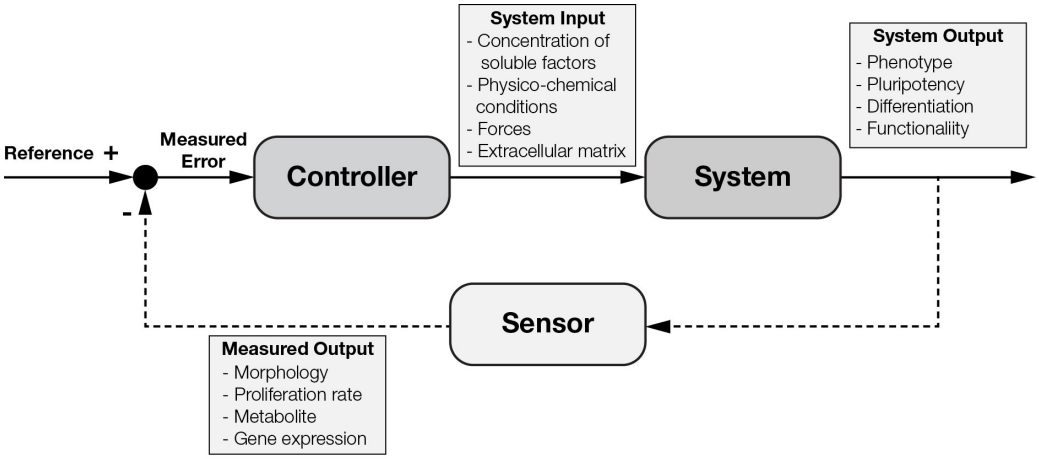

Figure 1.4: Theoretical innovative feedback loop for controlling stem cell bioprocesses - A reference value is given, for example ideal cell morphology, and processed by a controller by adjusting a number of parameters. System output such as phenotype or functionality are monitored by a sensor such as an advanced image processing algorithm which feeds back into the control chain.

time and frequency domains to characterise and categorise cardiomyocytes (Hossain *et al.*, 2010).

Microscope-based analysis is a simple and automated approach to monitor stem cell expansion or differentiation (Rubin, 2008). Stem cell populations tend to be non-homogenous and cells expressing relevant markers by means of a fluorescent protein or antibody can even be detected at single-cell level. Advanced fluorescent cell labelling methods are in development for labelling different locations in or on a cell, which allow data-rich monitoring for stem cell bioprocesses. Although these techniques are in their infancy, they will become necessary tools for stem cell bioprocess characterisation and optimisation.

An overview of commonly used bioreactors for stem cell culture is given in the following sections to highlight their advantages and disadvantages. Three-dimensional bioreactors involving scaffolds are not covered in this overview.

1.3.3.1 Static bioreactors

Current methods available for the expansion or differentiation of stem cells are two-dimensional bioreactors such as Petri dishes, T-flasks and roller bottles. These biore-

actors are generally used for monolayer culture of adherent cells, and are marked by ease of use, low cost and disposability. However, frequent subculturing is necessary to maintain an undifferentiated state in stem cells. Subculturing requires manual interaction such as dissecting ESC colonies or the use of collagenase or trypsin to remove cells from the flask. To reduce cellular stress during subculturing, synthetic coatings have been developed, which change their polymer chain length by a temperature decrease thereby releasing cells gently.

Petri Dishes and T-flasks are most commonly employed in early stages of stem cell bioprocess development and are available with surface areas between 20 and 175 cm^2. To achieve cell numbers required by regenerative medicine applications (see Section 1.2.2), in combination with a scale out approach, the growth areas of individual flasks have been increased up to 1720 cm^2 (Corning HYPER*Flask*) by parallel stacking of growth surfaces.

Spatial and temporal variances in nutrient and cytokine concentrations are likely to occur as described in Section 1.3.1. For example, Veraitch *et al.* (2008) have shown that manual processing changes the culture conditions in flasks and wells dramatically. This becomes even more critical when differentiation protocols require hypoxic conditions, for example to efficiently derive neurons from ES cells (Mondragon-Teran *et al.*, 2009). It is thus difficult to maintain long-term culture conditions using manual interaction.

Efforts have been also made to automate hESC culture in T-flasks using pipette robots (Terstegge *et al.*, 2007) and laser-assisted dissection tools for passaging hESC colonies to improve reproducibility (Terstegge *et al.*, 2009).

1.3.3.2 Stirred bioreactors and microcarriers

Stirred bioreactors, with control over parameters such as oxygen mass transfer and pH are well-established in the industry, and are suitable for large-scale culture processes delivering high cell densities (Nienow, 2006). Initial work using stirred bioreactors has been demonstrated for the expansion of different types of stem cell, for example hematopoietic and murine ES cells (Andrade-Zaldívar *et al.*, 2008; Fok & Zandstra, 2005). Krawetz *et al.* (2010) have demonstrated that a 25-fold expansion of hESC over a period of 6 days in a stirred bioreactor can be achieved while retaining high levels of pluripotency and maintaining a normal karyotype. Similar results have been presented

for the culture of hESCs and iPS cells supplemented with full-length IL6RIL6 chimera and bFGF over 20 passages (Amit *et al.*, 2010).

Suspension culture bioreactors have been also used for differentiation of mESC and hESC. Steiner *et al.* (2010) have demonstrated the expansion and differentiation of free-floating hESC clusters by optimising the expansion medium. After 10 weeks of expansion, hESC clusters were cultivated for 4 weeks in chemically defined medium to initiate neural differentiation.

Microcarriers which offer cells the ability to attach to a surface have also been used in stirred suspension bioreactors. Cylindrical, Matrigel coated cellulose microcarriers for the long-term culture (6 months) of hESC have been used to demonstrate a 2- to 4-fold increase over two-dimensional plastic surfaces (Oh *et al.*, 2009).

1.3.3.3 Continuous culture bioreactors

In continuous culture bioreactors, also known as perfusion bioreactors, cells are trapped in a contained system to which fresh medium is added while spent medium is removed at the same rate (Arathoon & Birch, 1986). Medium can be recirculated where fresh medium is added for replenishment of growth factors and nutrients or non-recirculating. Continuous culture bioreactors offer an immediate control over culture conditions such as pH, minimise problems associated with medium depletion and rapidly dilute and remove negative metabolic products. However, hydrodynamic shear stress on cells can cause metabolic changes and needs to be taken into account (Kretzmer, 2000).

Different designs for continuous culture bioreactors have been proposed such as hollow fiber bioreactors, perfused cartridges, tubular bioreactors and rotating wall vessel bioreactors. Continuous culture bioreactors are of particular interest for tissue engineering applications where mass transfer of oxygen and nutrients to cells in a 3-D scaffold would otherwise be limited.

An advantage of continuous culture for bioprocessing is the establishment of steady-state conditions and therefore yielding probably higher cell numbers. For example, continuous culture bioreactors employed for hematopoietic progenitor cell cultures have shown that an 11-fold increase for granulocyte-macrophage colony forming units compared to static cultures over 15 days can be achieved (Koller *et al.*, 1992, 1993a,b). Initial experiments with murine and human ESCs using a two stage perfusion bioreac-

tor system indicate that within 2 weeks of culture time in a 1 L scale 100 billions ESCs can be propagated (Ouyang & Yang, 2008).

Smaller bioreactor systems have been reported for hESC perfusion cultures where the medium in a modified organ culture dish was exchanged every 12 h for various pumping times increasing cell numbers by 70% in the best case compared to the static controls over a period of 7 days (Fong *et al.*, 2005). More recently, it has been shown that a perfusion reactor in combination with oxygen control produces a 12-fold increase in cell numbers of hESCs compared to static 2-D cultures (Serra *et al.*, 2010).

1.4 Micro-scale culture for stem cell bioprocess development

To speed up the delivery of products to market, the prediction of culture performance and efficiency is an important bioprocess challenge. Micro-scale technologies can address this challenge, which combine high-throughput screening with instrumentation (Rees & Wise, 2008). For microbial and mammalian bioprocesses, micro-scale culture vessels, predominantly microwell plates, have become a common and fast approach to screen in parallel for two or more culture conditions (Micheletti & Lye, 2006). Parallelised, automated and multiplexed culture systems fitted with instrumentation for data-rich bioprocess monitoring and control are important tools for bioprocess development and optimisation (Schäpper *et al.*, 2009).

For stem cell bioprocesses, dedicated and validated micro-scale culture systems for bioprocess development and optimisation have not yet been established. Two different systems are discussed in the following subsections - microwell plates and microfluidic systems. A comparative summary of advantages and disadvantages of the two systems is given in table 1.5.

Table 1.5: Comparative summary of microfluidic cell culture systems and microwell plates

	Microfluidic Systems	Microwell plates
Advantages	(+++) flexible in modes of operation (static, intermittent, continuous)	(+++) highly parallel
	(++) dynamic changes of the environment spatially and temporally	(++) culture of cells adherent to the well surface or on beads in a well
	(++) parts or entire process steps on chip in series	(++) different sizes of wells available
	(+) parallelisation allows screening of different conditions	(+) well established technology
	(+) implementation of optical and chemical monitoring (e.g. microscope or CCD-chip)	(+) automated (with pipette robot)
Disadvantages	(-) lack of large scale integration and parallelisation	(-) limited mode of operation
	(-) materials used not necessarily comparable with scale	(-) optical monitoring difficult to implement
	(-) Usability	

(+++) extremely favourable, (++) very favourable, (+) favourable, (-) disadvantageous

1.4.1 Microwell plates

A solution to minimise development and screening costs is to use well plates, because they are widely accepted. Traditionally, well plates have been used for micro-scale microbial and mammalian bioprocess studies offering parallel experimentation on a small foot print (Barrett *et al.*, 2010). They are available in various formats for cell culture, for example 6-well to 96-well plates. Reproducible results are crucial for a process and hence, manual interaction is undesired. Automated culture systems using well plates have been used for maintenance of pluripotent hESCs (Terstegge *et al.*, 2007; Thomas *et al.*, 2008).

A recent trend towards microfabricated microwells is observed to control EB size, formation and differentiation. It has been demonstrated that a differently sized moulded polyurethane microwell array coated with ECM influence the differentiation capability of EBs from hESCs into cardiomyocytes (Mohr *et al.*, 2010). A similar approach using a concave microwell array to control the size of EBs from murine ESCs has shown that cardiogenesis and neurogenesis is strongly regulated by the microwell size (Choi *et al.*, 2010). A comparative study of a microwell and a micropatterned chip for the proliferation and differentiation of EBs from murine ESCs indicates though that proliferation

was lower and EB differentiation proceeded slowly forming only a small amount of the endoderm (Sakai *et al.*, 2011).

1.4.2 Microfluidic systems

Microfluidic systems or devices are defined by their small volumes, usually in the microlitre to nanolitre range. Other sources define microfluidics by the size of the channel which are in the range of a few micrometer to a few hundred micrometers. These two physical aspects have been combined in the following definition (Li, 2008a):

> *Microfluidic system manipulate or process tiny ($10^{-9} - 10^{-18}$ L) volumes of fluids in channels with dimensions of tens to hundreds of micrometers.*

The origins of microfluidics are found in analytical chemistry applications where it was desirable to use small sample volumes, to separate and detect reagents with high resolution and sensitivity, and to have a small footprint and a low cost (Whitesides, 2006). Microfluidic systems are also often referred to as *lab on a chip* or *micro total analysis system* (Manz *et al.*, 1990).

For life sciences such as bioprocessing or systems biology, cell culture, high-throughput cell assays, gradient devices or single cell analysis are microfluidic applications which will benefit from the physical properties microfluidic systems offer (Andersson & van den Berg, 2003; El-Ali *et al.*, 2006; Feng *et al.*, 2009).

Faster response times, smaller reagent volumes and the potential integration of instrumentation are also important features. The unique characteristic of microfluidic systems is the ability to manipulate small volumes of fluids and this offers therefore an unmatched control over the cellular microenvironment (Young & Beebe, 2010). At present, three flow manipulation modes for cell culture are used, static, intermittent and continuous flow (see table 1.6).

Table 1.6: Comparison of the different flow manipulation modes in microfluidic systems - Flow modes of interest for micro-scale stem cell bioprocessing.

Static	Intermittent	Continuous
(+) studies of microenvironment by diffusion	(+) hydrodynamic shear stress lowered compared to continuous culture	(++) continuously controlling the soluble microenvironment (+) comparable with large scale perfusion bioreactors (+) ability to run in all modes
(-) no relevant information for bioprocesses	(-) no advantage over microwells	(-) hydrodynamic shear stress

(++) very favourable, (+) favourable, (-) disadvantageous

Microfluidic cell culture systems offer spatial and temporal control of soluble cues on a micro-scale, which can not be captured in conventional static culture equipment. For example, research for stem cell culture would greatly benefit from the study of cell-cell and cell-ECM interactions using gradients of cues generated in microfluidic systems (Gupta *et al.*, 2010; van Noort *et al.*, 2009).

Unlike a 96-well plate, microfluidic systems for cell culture offer the option of an undisturbed optical observation. The meniscus of fluid formed in well plates and the thickness of the well bottom distort the visualisation of cells by phase or fluorescence imaging, but this problem can be solved in microfluidic systems. For example, Yin *et al.* (2008) has demonstrated that the performance of a quantitive, on-chip calcium flux assay is comparable and allows the possibility for faster screening protocols with the potential ability for resolving sub-cellular information than in microtiter plate formats. However, the influence of hydrodynamic shear stress above a threshold in the microfluidic system has triggered responses in cells similar to chemical stimuli (Yin *et al.*, 2007).

In spite of the experimental advantages these microfluidic systems offer, they have yet to find acceptance and general use among biologists (Andersson & van den Berg, 2006; Paguirigan & Beebe, 2008).

Firstly, the challenges associated with fabrication, use and reliability of microfluidic devices are currently outweighing the potential experimental gain.

Secondly, existing cell analysis equipment such as plate readers, flow cytometry, microscopes or laboratory tools such as pipettors will need to be integrated to facilitate

the operation and the accessibility of microfluidic systems for cell culture. For example, plate reader compatible microfluidic systems for cell culture culture have been presented to analyse fluorescent labelled cells (Lee *et al.*, 2007; Sung *et al.*, 2009; Wen *et al.*, 2010).

Andersson & van den Berg (2007) raised the question of whether to analyse single cells or cell clusters in microfluidics. From a biological point of view both aspects are required to understand the mechanisms which regulate self-renewal or differentiation of stem cells. Microfluidic platforms have been developed to analyse the genetic profile of single iPS cells in a high-throughput screen for example. This has an implication on the dividing potential of individual cells and represents an opportunity to gain insight for basic stem cell research (Spiller *et al.*, 2010).

For translational research such as stem cell bioprocessing, microfluidic tools with the required functionalities are rarely available. An overview of specifically designed microfluidic culture systems for human and murine ESCs is given in table 1.7. All devices, except Kim *et al.* (2006); Villa-Diaz *et al.* (2009), are used in static cultures (medium is not replaced) or in periodic refeed cultures (medium is exchanged at discrete points in time). These devices thus lack the ability to create a steady-state soluble microenvironment over long periods of time.

Table 1.7: Chronological summary of microfluidic culture systems for embryonic stem cells

Reference	Cell type (line)	Culture time	Features
Khademhosseini *et al.* (2005)	mESC (R1)	N/A[1]	5 x 5,Orthogonal patterning and multiphenotype culturing
Kim *et al.* (2006)	mESC (ABJ1)	4d	4/12 chambers. Perfusion with concentration and shear gradient
Abhyankar & Beebe (2007)	hESC (N/A[1])	48h	Spatiotemporal patterning, static culture
Torisawa *et al.* (2007)	mESC (D3)	3d	Controlled EB formation on semi-porous membrane
Figallo *et al.* (2007)	hESC (H9/H13)	4d	12 chambers with optional inlet configuration, 3-D in gel
Lii *et al.* (2008)	mESC (R1)	N/A[1]	16 chambers, 3D culture in Matrigel, medium replacement every 12h
Korin *et al.* (2009b)	hESC (Rex1)	2d	Single channel, periodic refeed
Kamei *et al.* (2009)	hESC (HSF1/HSF6/H9)	max. 12d	6 parallel channels, semi-automated colony control, periodic refeed
Villa-Diaz *et al.* (2009)	hESC (hESCBGN-01/H9)	48h	Single channel/ delivery of different reagents
Ellison *et al.* (2009)	mESC (ESD3)	N/A[1]	Modelling approach for autocrine and paracrine signalling, verified with 6 microchannels and periodic refeed
Fung *et al.* (2009)	mESC (E14)	5d	Exposure of one EB to two different streams
Khoury *et al.* (2010)	hESC (H9 & H1 Oct4-EGFP) & mESC (Nestin-GFP mESC)	6d	Different sized microtraps for EB culture, monitoring of Oct4-GFP and Nestin-GFP.

[1] Information not available

Microfluidic devices designed for bioprocess development and screening must follow a scaling law for meaningful and translatable results. For suspension cultures for example, the design is based on either miniaturising existing bioreactors or the use of

an engineering constant like *kLa* as design principle for scale down bioreactors. The mass transfer coefficient *kLa* is a classical engineering constant used to describe mass transfer in large-scale suspension bioreactors. A microfluidic suspension bioreactor for *E. coli* with a similar *kLa* value to a shaker flask has been shown to match the growth characteristics of bioreactors (Szita *et al.*, 2005). Microfluidic bioreactors can thus be used as accurate predictors for scale up in process development and optimisation.

Unlike suspension cultures with a scaling technology already in place, a straightforward definition of design rules for stem cell microfluidic bioreactors is difficult at present (see section 1.3).

Firstly, basic research to understand the mechanisms of stem cell proliferation and differentiation is still ongoing and thus, methods are likely to change in future. Therefore, a predominant culture vessel technology has not been selected and adopted by researchers and industry. Secondly, embryonic stem cells and reagents used, for example media, are extremely costly, therefore process development and screening is limited.

However, the main advantage of microfluidic systems lies in manipulating very small volumes of fluid. This ability can thus be used to probe the microenvironment in transient and steady-steady state conditions with respect to cell numbers and process efficiency, and translated to implications and assess the impact for macro-scale bioprocesses (see figure 1.5).

Two important design principles for a microfluidic tool for stem cell bioprocessing can thus be formulated :

1. The design of the microfluidic system is adaptive to allow the incorporation of future changes in stem cell research and bioprocessing techniques

2. Culture outcomes are only affected by microfluidic operations and not by alterations or modifications to current culture protocols

These two design principles and how they are implemented are discussed in more detail in the following sections.

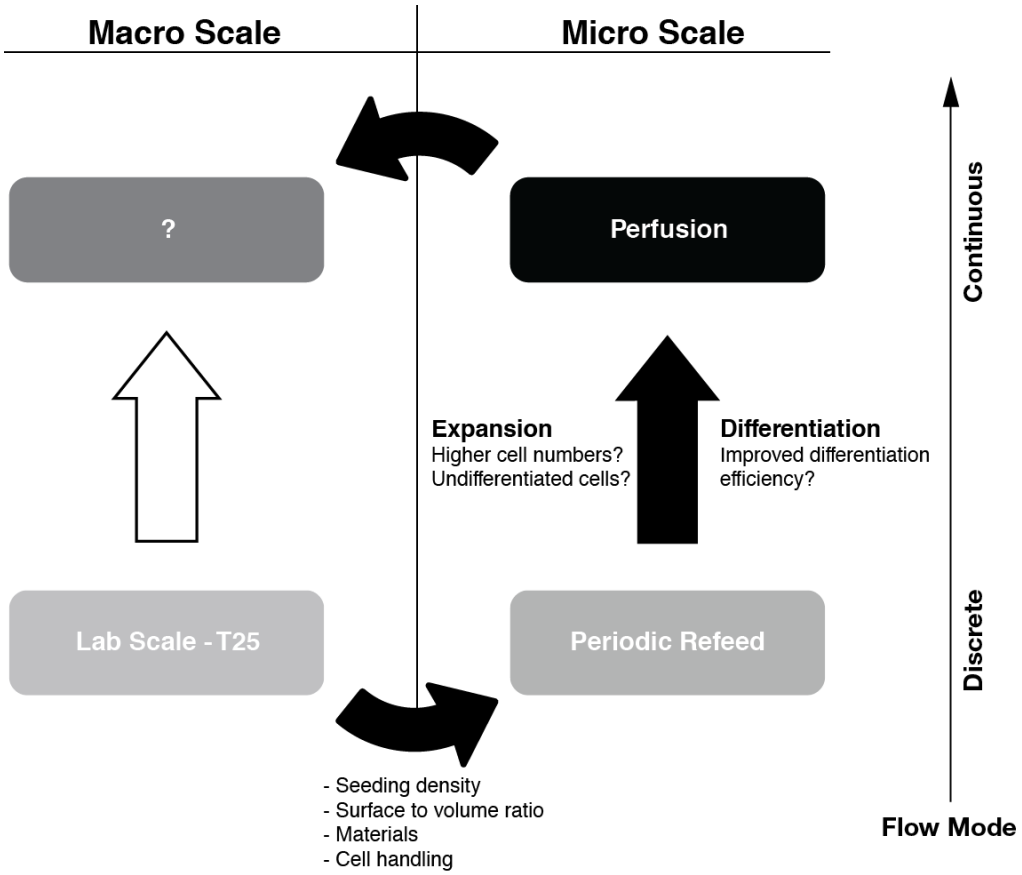

Figure 1.5: Micro-scale stem cell bioprocessing and its potential implication for macro-scale bioprocessing - The ability of microfluidic systems to manipulate volumes of fluid - *static*, *intermittent* and *continuous* - offers new possibilities to probe the microenvironment for stem cell expansion and differentiation. Scalability and comparability of micro-scale experimental outcomes are critical for the translation into meaningful implications for macro-scale bioprocesses.

1.4.3 Concept of a microfabricated stem cell bioprocess development platform

1.4.3.1 Requirements for a microfabricated stem cell bioprocess development platform

To elucidate the influence of discrete or continuous medium exchange in a microfluidic system on cell numbers, a complete microfluidic stem cell bioprocessing platform needs to be designed with well-defined functionalities and requirements. Bioprocessing of stem cells in static laboratory culture-ware involves generally a process of seeding, culture and analysis (see also figure 1.6).

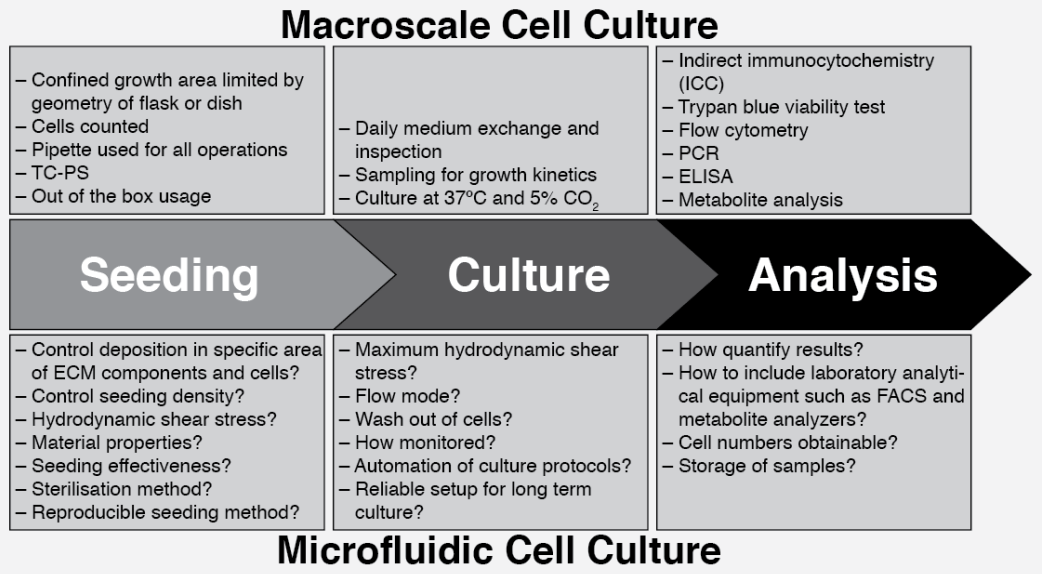

Figure 1.6: Comparison of macro-scale cell culture and microfluidic cell culture - Generally, a macro-scale cell culture experiment consists of three steps: *seeding*, *culture* and *analysis*. The translation of these steps for microfluidic cell culture represents a challenge in terms of dimensioning microfluidic devices properly and implementing the necessary functionalities for each step. For reproducible experimental outcomes, seeding is a critical step for a microfluidic stem cell bioprocessing platform. During culture, hydrodynamic shear stress needs to be under the critical threshold value. After culture, enough cells need to be available for quantitative analysis off-chip.

A laboratory-scale, stem cell experiment starts usually with coating a pre-sterilised tissue culture polystyrene (TC-PS) bioreactor with an ECM, usually 0.1% (w/v) gelatine, followed by incubation in a sterile environment. For pre-culturing cells, stem

cells grown in a monolayer are trypsinized and quenched with medium, spun down and re-suspended in fresh medium. To determine the correct seeding density, trypan blue exclusion and manual counting under a microscope is a commonly used viability assay in a separate experiment prior to any cell experiment. Cells are seeded by aspirating the necessary volume from the cell suspension with a pipettor and transferring the cell suspension to the new T-flask. Cell distribution is achieved by shaking the culture vessels gently before attachment of cells to the growth surface starts. Seeding for monolayer differentiation experiments for example requires an accurate seeding density. The density can be very low, in the range of thousands to ten-thousands cells per square centimetre, for example, for differentiation of murine ESCs into neuroectodermal precursor cells (Ying *et al.*, 2003). It has also been demonstrated that the plating density of human bone marrow stromal cells regulates the vascular lineage commitment (Whyte *et al.*, 2011).

A culture system often used for human ESCs expansion consists of a feeder layer and clusters of human ESCs (see section 1.1.2). The cluster size plays an important role for hESC expansions and it has been demonstrated that clusters with less than 10 cells often spontaneously differentiate (Reubinoff *et al.*, 2000). Hydrodynamic shear stress and the cross-sectional geometry in the loading channel will thus have a critical limit to deliver cell clusters intactly to the culture area. Cell seeding is therefore a critical step in any stem cell experiment/bioprocess, as it precisely defines the cell density or excludes undesired cell cluster sizes.

After seeding, static bioreactors are kept in temperature-controlled incubators and medium is usually exchanged daily by manual interactions using pipettors in a sterile environment. Furthermore, the cell culture medium needs to be protected from UV-exposure ($>$ 1d) and stored in a fridge to prevent degradation of glutamine for example during an experiment (Arii *et al.*, 1999).

Analysis of cells is also critical for optimisation of an experiment or protocol. Staining is a commonly used technique for qualitative or quantitative visualisation of cell properties via markers using flow cytometry. However, quantitative methods require a minimum cell number (approximately 5000 cells) to be accurate, for example for flow cytometry or trypan blue viability assays.

All aforementioned experimental steps in macro-scale cell culture need to be adequately addressed in a microfluidic system. Furthermore, to exploit and use the advan-

tages of a microfluidic system, three aspects in particular need to be considered when designing a microfluidic bioprocessing platform for stem cells:

1. The ability to adapt and change designs rapidly
2. Scalability and comparison criteria
3. Innovative monitoring solutions

Firstly, the platform needs an inherent flexibility to implement changes to optimise the microfluidic network, to design new microfluidic networks for future advanced assays or culture protocols and to implement advanced functionalities (see section 1.3.1). For example the implementation of a gradient generator for soluble cues or the integration of sensors in the platform, such as oxygen or pH sensors, need to be straightforward without redesigning the entire platform. Furthermore, the ability to implement future trends in stem cell bioprocessing needs also to be addressed by the microfluidic platform. Future stem cell bioprocessing trends may include for example cell reprogramming protocols or even three-dimensional culture of stem cells in scaffolds.

Secondly, for a microfluidic stem cell bioprocessing platform, comparability and scalability criteria are not currently developed, but these criteria can be adequately addressed in methods, in materials and in process conditions (see figure 1.7).

Comparability in methods means that the same stem culture protocols can be used in a microfluidic cell culture device as in a T-flask for example, but also the entire handling of cells is similar, exposing the cells for example to similar levels of shear stress during subculturing.

An important factor for expansion and differentiation of stem cells is the culture surface where cells grow. The culture surface in T-flasks consists of a mechanically stiff substrate, such as TC-PS, and an ECM coating such as gelatine, fibronectin or Matrigel. Cell adhesion is a function of the surface properties of the substrate, such as hydrophilicity (Carré & Lacarriè, 2010). A recent study to compare cell adhesion of mouse embryonic stem cells to various materials used for microfluidic culture systems has shown that TC-PS is superior than PDMS or glass (Liu *et al.*, 2010). Optimising the surface properties, for example Zeonor surfaces, by plasma treatment has not shown superior results in viability of HeLa cells compared to polystyrene surfaces (Beaulieu *et al.*, 2009). Optimised culture surfaces by mixing different ECMs for microfluidic

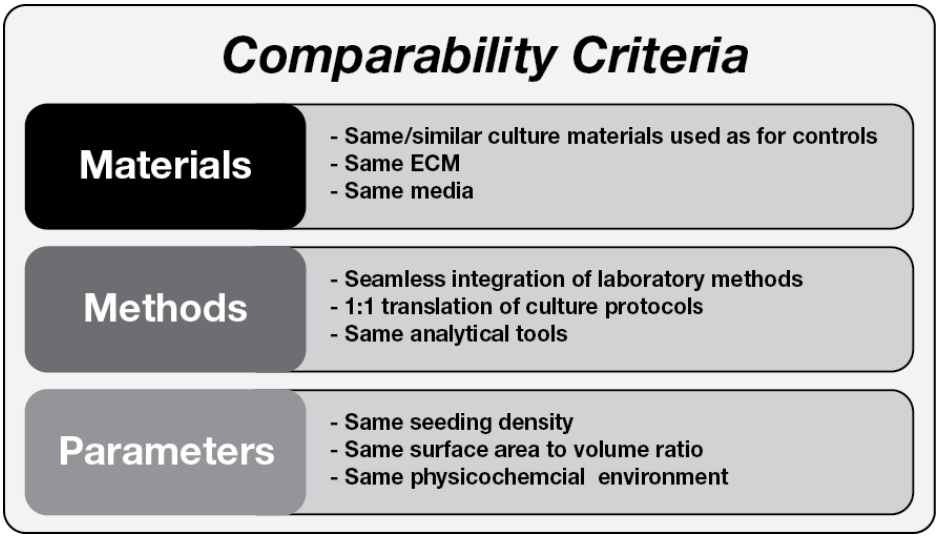

Figure 1.7: Comparability criteria for scale down of stem cell culture protocols and use in a microfluidic stem cell bioprocessing platform - Three areas to implement comparability have been identified which contribute to the scalability of microfluidic stem cell bioprocessing.

culture devices may be used (Kamei *et al.*, 2009). However comparison of a substrate material with an optimised surface or ECM composition is not possible with a control or a T-flask and thus, not applicable for stem cell bioprocessing. The impact of the properties of the culture surface on differentiation behaviour or pluripotency maintenance is tremendous and therefore comparability in materials is a necessary requirement.

Finally, the microfluidic experimental outcomes for stem cells need to be translatable and therefore criteria such as seeding density, surface area to volume ratio and the physicochemical environment need at least a similarity to the static controls prior to microfluidic experimentation by modulating flow. These three scalability and comparability criteria ensure that microfluidic operation will predominantly influence experimental outcomes and minimise effects resulting from miniaturisation. A summary of all requirements necessary for the microfluidic platform is given in table 1.8.

Table 1.8: Summary of requirements and functionalities for the microfluidic stem cell bioprocessing platform

	Requirement	Quantification	P[1]/S[2]	Description
1	Window for microscope	Diameter of the microscope stage: 10 cm (Nikon)	P	A time-lapse system is needed to get an optical feedback and automation of the culture
2	Pumping mechanism	N/A[3]	P	The pumping mechanism should be reliable over a long period of time, autoclavable and mobile.
3	Mixing gases	N/A[3]	S	For a dynamic cultivation it is required to modulate the gas composition
4	Store medium	4-8℃	P	Medium has to be kept cool and in the dark to prevent glutamin degradation at room temperature, this requires though a preheating of the medium prior to use in the microfluidic chip
5	Medium modulation	2 bottles	P	To proliferate/differentiate hESC, different media are required. Furthermore, staining and washing steps could be included and variations minimised
6	Thermal insulation	N/A[3]	S	To prevent thermal gradients, the incubator platform has to be insulated
7	Oxygen measurement	0-21% oxygen	S	Oxygen seems to have a critical impact on the culture of ESCs (Mohyeldin *et al.*, 2010)
8	pH measurement	N/A[3]	S	pH is another variable, which is interesting to monitor
9	Temperature control	30-40℃	P	Temperature seems to have an impact on proliferation/differentiation (unreported results)
10	Generation of gradients	N/A[3]	S	Chemical gradient on one chip and possibly within one channel for rapid screening
11	Cultivation area required	1 cm^2	P	A minimum cell culture surface is required for further cell analysis (e.g. Guava)
12	Different flow regimes	N/A[3]	P	Steady, semi-steady and continuous flow regimes under consideration of a reasonable amount of shear stress
13	Comparability criteria	N/A[3]	P	Comparability in materials, in methods and in parameters

[1] Primary requirement **P**: has to be incorporated in platform

[2] Secondary requirement **S**: desirable implementation, but not necessary

[3] Information not available

1.4.3.2 Design considerations for a microfabricated stem cell bioprocess development platform

To comply with the requirements defined in the previous section, a modular microfluidic platform design is proposed which addresses the flexibility to adapt changes and functionalities for future bioprocessing steps or developments. The advantages of such a modular design approach are compared to integrated microfluidic systems in table 1.9.

Table 1.9: Comparison of integrated versus modular microfluidic systems for stem cell bioprocessing

Integrated Systems	Modular Systems
(++) implementation of entire processes or sequences	(+++) highly flexible for changes in design
(++) application specific	(+++) parts/functionalities for different bioprocesses easily interchangeable
(+) small dead volume	(++) cheap or easily reproducible parts are disposed
(- - -) entire system will be disposed	(- -) reliable packaging and interconnection with off-chip components
(-) increased complexity of a system	(-) window of operation
(-) adaptions or changes can be difficult to implement	(-) dead volume

(+++) extremely favourable, (++) very favourable, (+) favourable, (-) disadvantageous, (- -) very disadvantageous, (- - -) undesired

Integrated systems are defined here as a microfluidic system which has a culture chamber, valves and pumps on-chip. Such microfluidic systems have been designed and developed most notably by the Quake group (Melin & Quake, 2007; Thorsen *et al.*, 2002). The proposed modular approach restricts the functionality of the microfluidic system to cell culture only and separates pumping and liquid storage from the microfluidic system.

By defining sub-assemblies, an independent development and later optimisation of each sub-assembly and its modules is possible without re-designing the entire microfluidic platform. Besides the engineering advantages, it facilitates the exchange or disposal of used or defect parts. Furthermore, such a modular platform allows to expand the system with more functionalities to address future bioprocessing requirements.

For the microfluidic platform, two sub-assemblies have been defined. The first subassembly is the modular microfabricated cell culture device and the second subassembly includes functionalities such as the pumping mechanism, storage of media and the mi-

croscope with a camera. The microfabricated cell culture device sub-assembly needs to incorporate two important design features: 1) disposability of the microfluidic chip and 2) an inherit flexibility to easily implement various microfluidic layouts for different assays, for example for shear stress studies (see figure 1.8). Seeding, culturing and

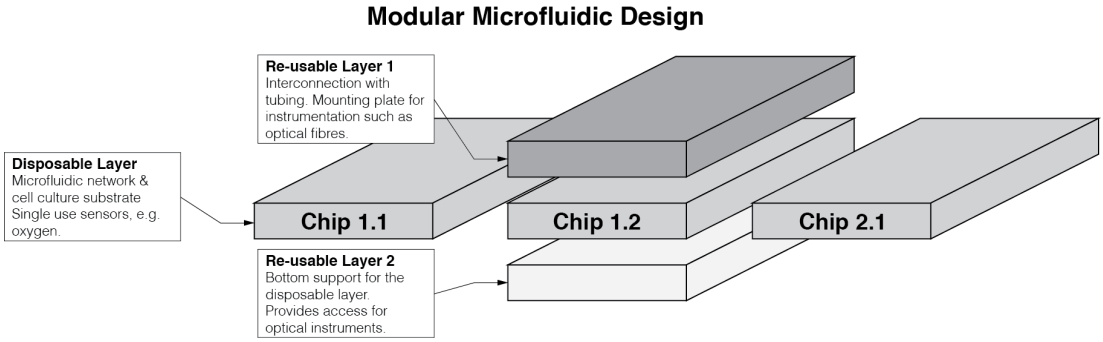

Figure 1.8: Packaging concept for a modular microfabricated cell culture device - The mo dular microfabricated cell culture device design consists of three layers: A disposable and customisable layer which includes the entire microfluidic network and sensors and two re-usable layers which serve as packaging for the disposable layer and can be used as mounting base for instrumentation such as optical fibres. The packaging concept allows to test or experiment with disposable layers of the same design (Chip 1.1, 1.2...1.n) or of a different microfluidic network layout (Chip 2.1) without affecting the re-usable layers.

harvesting the cell material for analysis are critical tasks in any stem cell experiment or bioprocess as outlined in section 1.4.3.1, a mechanism for seeding and harvesting has thus to be incorporated in the microfabricated cell culture device to facilitate these operations.

1.5 Organisation of the thesis

The previous sections have provided a description of stem cell sources, applications and stem cell bioprocessing to date. The need for the prediction of culture conditions has been elucidated by understanding the complex interplay of cellular functions with the microenvironment. The complexity of stem cell bioprocessing requires new bioprocess development and optimisation tools alongside existing development and optimisation tools for successful translation of laboratory findings into a large-scale production.

The aims of the thesis were to develop a microfabricated platform for stem cell bioprocess development by a) implementing a modular system to explore the capa-

bilities of culturing stem cells, b) developing a cell culture device which allows scaling and comparison with existing small scale bioreactors and c) obtaining data-rich process information.

The thesis covers in Chapter 2 the development of a modular packaging system for microfluidic devices for stem cell bioprocess development. Chapter 3 introduces issues associated with the seeding and continuous perfusion culture of embryonic stem cells in microfluidic devices. First, an overview of seeding methods and the theory of flow is given, followed by experiments with hESCs to prove the seeding method and the microfluidic concept.

Chapter 4 is based on the findings of Chapter 2 and 3 and uses the modularity and the seeding method for a microscope-based platform. Chapter 5 outlines the conclusion of the presented work and Chapter 6 suggests directions for future work on the modular microfabricated stem cell bioprocess development platform.

2

Development of a modular microfluidic cell culture device with rapid prototyping capability

Long-term microfluidic cell culture devices require reliable packaging and interconnection to off-chip components. The research progress to elucidate the complexity of the interactions between stem cells and the soluble microenvironment requires that unique design features can be rapidly implemented in a microfluidic cell culture device. Various features, for example the possible integration of a tissue-culture polystyrene slide, have to be integrated that the results obtained with such a microfluidic cell culture device are then more likely to be scalable.

The results in this chapter have also been presented as a conference proceeding at the Microtechnologies in Medicine and Biology conference 2011 in Lucerne, Switzerland (see Appendix G).

2.1 State of the art fabrication and packaging methods

Microfluidic cell culture devices have a hierarchy of requirements, beginning with the microfluidic chip function, then extending to fluidic connections, sensor and actuator integration, and subsequent levels of packaging. The development of microfluidic cell culture devices is usually an iterative process, outlined in figure 2.1, typically requiring a series of improvements in performance, function, or reproducibility, before arriving at a final design. Accordingly, an approach that allowed to concentrate the efforts on making these improvements for the microfluidic chip, with minimal modification of other system components, would streamline and accelerate the development process. It would also enable a better integration of the prototyping in the laboratory with the design and modelling stages, the so called 'virtual prototyping', such as finite element method (FEM) prototyping (Erickson, 2005). This would further allow the definition of design rules, turning the device development process into a truly *rapid* prototyping approach.

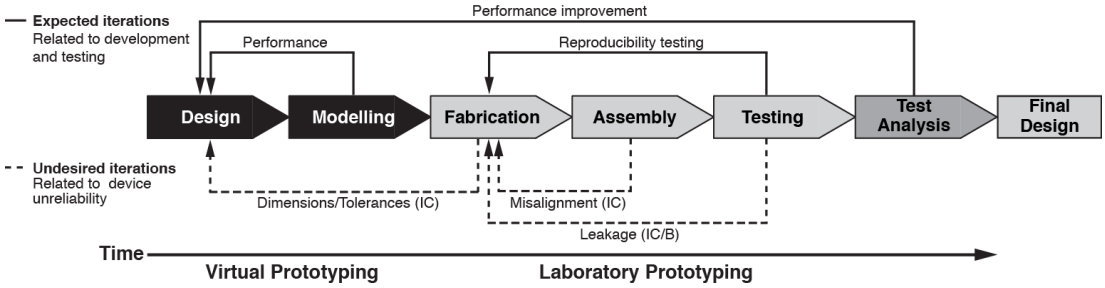

Figure 2.1: Microfluidic design & prototyping process - Design improvements can be divided into expected (*solid lines*) and undesired iterations (*dashed lines*). The expected iterations include a short phase of virtual prototyping, for example the use of design and modelling software to check the performance of a design idea. This is ideally followed by a rapid translation of the design to a reproducible number of working prototypes for verification of performance and reliability and as few as possible iterations for improvement. Undesired iterations, caused for example by deficiencies in the interconnect (**IC**) or by poor bonding (**B**) delay this translation to working microfluidic prototypes.

To achieve this, three key elements are required: 1) rapid fabrication of large numbers of prototype test chips for performance evaluations (Easley *et al.*, 2009; Nath *et al.*, 2010; Yuen & Goral, 2010); 2) reliable integration, via the packaging hierarchy, with off-chip components (Crane *et al.*, 2010; Whitesides, 2011); and 3) independent

development of chip and packaging design. In contrast, complex or expensive fabrication techniques, and unreliable interconnections, can introduce delays and sources of errors (Han & Frazier, 2005). To address this, the modular assembly of pre-fabricated chip components has been previously presented as a solution for rapid development of proof-of-concept devices (Rhee & Burns, 2008; Yuen, 2008). However, pre-fabricated components reduce the ability to customise the channel network and to integrate sensors and actuators which in turn limits the ability to tailor the microfluidic chip function.

2.1.1 Fabrication methods

The use of various inexpensive polymers to fabricate disposable test chips is widespread, and they can be machined using a variety of fabrication methods (Becker & Gärtner, 2008; Fiorini & Chiu, 2005) (see also table 2.1).

Table 2.1: Overview of transparent polymers and their fabrication technologies for microfluidic devices

Material	Fabrication technologies[1]	Autoclavable[2]	Remarks	References
COC/COP	Injection moulding, Hot embossing, Milling	Yes[3]	Limited availability of different sheet dimensions	Bundgaard *et al.* (2006); Mair *et al.* (2006)
PC	Milling, Hot embossing, Laser ablation	Yes	Tough material to mill (Young's modulus: approximately 2 GPa)	Ogonczyk *et al.* (2010); Qi *et al.* (2009)
PDMS	Soft lithography	Yes	Non-cured polymer chains may affect experimental outcomes	McDonald & Whitesides (2002)
PMMA	Laser ablation, Hot embossing, Milling	No	Variations in sheet thickness	Brown *et al.* (2006)
PS	Injection moulding	No	Not commercially available as sheet	Young *et al.* (2011)

[1] using commercially available materials
[2] 121°C for 20 min
[3] except Topas Series 8007

Direct writing methods, such as CO_2 laser writing (Klank *et al.*, 2002), are appeal-

ing for rapid fabrication of new chip designs with feature sizes in the range of 100 μm within minutes. However, writing a new microfluidic chip for each experiment can introduce unnecessary variations in dimensional fidelity and back end processing (bonding for example takes several hours in an oven). Injection moulding and hot embossing are fabrication techniques for large-scale production of chips, but are economically inefficient for the fabrication of prototypes (the mould alone costs several 1000), and there is a lack of flexibility for design changes. Direct writing, injection moulding and hot embossing require rigid, polymeric materials such as poly(methylmethacrylate) (PMMA), poly(carbonate) (PC), poly(styrene) (PS) or cyclo-oleofin copolymers (COC).

Soft polymers such as poly-dimethylsiloxane (PDMS) are frequently used materials for fabrication of multiple prototype chips by casting and moulding from a master (McDonald *et al.*, 2000; Sia & Whitesides, 2003) allowing feature sizes between 5 and 200 μm. This greatly reduces dimensional variations and the preparation time of an individual chip, yet the preparation of the master by photolithographic means can itself be time-consuming (including delivery of mask up to 5 days), precluding rapid implementation of changes to chip design. Silicones and in particular PDMS are well characterised materials for biomedical applications, however there are concerns about uncured polymer chains and their effects on cells.

Computer numerical controlled (CNC) micro-milling offers quick and simple direct writing of master moulds or chips with feature sizes down to 25 μm if necessary, allowing rapid fabrication of new chip designs and large numbers of high-fidelity replicas for reproducibility and performance testing within one day (Jung *et al.*, 2007; Mecomber *et al.*, 2006). Additionally, the versatility of micro-milling machines also allows fabrication of the microfluidic packaging.

2.1.2 Packaging and interconnect solutions

A wide range of interconnects, such as those reviewed by Fredrickson & Fan (2004), have been presented. These can be partitioned into two classes, *permanent* and *non-permanent*.

Permanent connections typically rely on adhesives, often epoxy resins, to attach tubing to the microfluidic chip either directly or via commercially available connection ports such as the NanoPort™ assembly. This approach requires an operator to repeat the interconnection attachment process for each test chip, and reproducibility may depend

on their manual skill (Gray *et al.*, 1999; Mair *et al.*, 2006; Nittis *et al.*, 2001). Adhesives may block the microfluidic channels and connections or may not be compatible with some applications or the solvents used (Sabourin *et al.*, 2009). Glueless solutions have also been presented using a press-fit to connect different microfluidic chips by a small metal tubing. Biocompatibility and sufficient thermal resistance to withstand autoclave sterilisation are particular concerns for a microfluidic cell culture device.

Non-permanent interconnect solutions have the advantage of being re-usable - an important consideration if multiple prototypes need to be tested rapidly, as repetition of interconnection attachment is avoided. Forming a reliable seal however requires a more complex design of the interconnect than with permanent systems, and a number of O-ring or custom gasket systems (Bhagat *et al.*, 2007; Miserendino & Tai, 2008; Perozziello *et al.*, 2008; Snakenborg *et al.*, 2007), press-fit designs (Dalton & Kaler, 2007; Li & Chen, 2003; Quaglio *et al.*, 2008; Saarela *et al.*, 2006), and even magnetic clamps (Atencia *et al.*, 2010) have been described. Non-permanent interconnects can be integrated into chip fabrication (Mair *et al.*, 2006) or can be decoupled entirely from the chip (Sabourin *et al.*, 2009). Decoupling may be preferred as it allows simplified chip fabrication and reuse of the same interconnects for multiple experiments, therefore reducing the variability of results.

2.2 Design of the modular packaging system

To address the need for an adaptive microfluidic bioreactor module that allows the implementation of changes in the microfluidic network layout, or the incorporation of new functionalities (see section 1.4.3.1), a simple fabrication and comprehensive packaging route for a modular microfabricated cell culture device for stem cell bioprocess development is required. Currently, the casting of PDMS in moulds created by photolithographic techniques is a commonly used fabrication method for disposable microfluidic chips, offering the ability to fabricate highly customised microfluidic network layouts. However, the need for special equipment such as a mask aligner for photolithography and the lack of standardised world-to-chip interfaces solutions are disadvantageous for rapid translations of design ideas. Functional microfluidic blocks and units made from thermoplastics allow a simple and rapid assembly for microfluidic systems, but the customisation and optimisation of individual blocks is difficult to

implement rapidly. A rapid prototyping approach which combined simple fabrication of customisable microfluidic channel networks with standardised world-to-chip interfaces and packaging, would allow to design, build and optimise microfluidic systems (see figure 2.2). A robust and versatile rapid prototyping process for fabricating all device components, combined with a reliable and reusable interconnect design, could fulfil all requirements for accelerating device development. Such an approach may further open the field of microfluidics to non-engineers (Andersson & van den Berg, 2006; Mukhopadhyay, 2009).

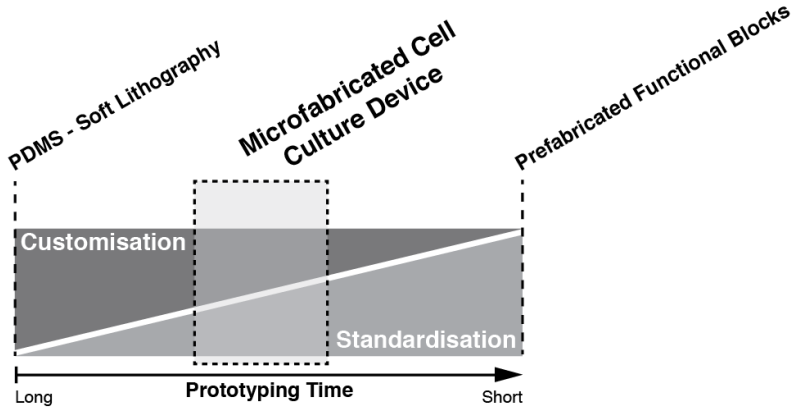

Figure 2.2: An ideal microfluidic rapid prototyping system for stem cell bioprocess development - Soft lithography and PDMS casting offer a high degree of microfluidic network customisation when compared with prefabricated functional blocks. However, the degree of standardisation of the prefabricated functional blocks allows short assembly times. A microfluidic stem cell bioprocess development tool requires both aspects to find an optimal balance - a high degree of microfluidic network customisation and short assembly times due to standardisation.

A key issue of microfluidic prototypes is the functional reliability across the prototypes, for example avoiding leakage. Due to the nature of planar, multi-layer microfluidic devices, leakages are most likely to occur at the interfaces of the layers. Therefore the number of layers is ideally reduced to a minimum, at the cost of a limited complexity of the channel network design. Modular microfluidic systems using hard polymers for the microfluidic layer require gaskets to seal the interface, thereby introducing a new set of undesired layers.

Using a sandwich of hard and soft polymer layers, functionalities such as interconnects for tubing or the microfluidic network can be separated. The hard polymer layers

serve as packaging plates to attach interconnects for tubing while the soft polymer layer contains the microfluidic network and uses its soft material properties to seal itself with the interconnect in the hard polymer layer. Using standard connectors for tubing such as Upchurch fittings facilitates development of microfluidic prototypes and increases the reliability of the interconnect. Furthermore, this modular packaging approach may also serve as an engineering basis for future add-on instrumentation modules such as the integration with microscope platforms or oxygen sensing systems.

2.2.1 First generation modular packaging system

The first generation of a modular packaging system was based on deforming a plate on the microfluidic chip to establish a fluidic connection. Two plates are clamped together around a microfluidic chip, which is made from a silicone rubber and acts as a gasket on the interconnect socket. While the the two plates are re-usable (interface plate and frame), the microfluidic layer and the glass slide can be disposed after use. All parts of the modular packaging assembly are depicted in figure 2.3.

The socket for the fitting itself was attached to a rigid interface plate with four countersink screws. The socket had a boss with a centred throughhole to fluidically link the microfluidic chip with tubing (see Appendix B.1 for dimensions). The boss protrudes by a height H (80 μm) of the interface plate and a diameter D of 6 mm has been chosen (see figure 2.4).

The microfluidic layer was made from PDMS and aligned with the interface plate via pins to prevent misalignment with the inlet and outlet ports. The microfluidic layer had a channel included which measured 1.5 mm in width, 36.5 mm in length and 125 μm in height (see Appendix B.4 for more dimensions). A microscope slide made from either glass or TC-PS was inserted in the frame to seal the microfluidic layer. 16 screws were used to secure all layers. After securing all screws, the microfluidic layer was compressed and formed a seal with the protruding boss of the interconnect socket at the inlet and outlet ports.

2.2.2 Second generation modular packaging system

The overall concept of the first generation was maintained, for example the re-usable packaging system with a disposable microfluidic chip. However, to implement microfluidic network layouts which would allow a larger cell culture area and multiple layers,

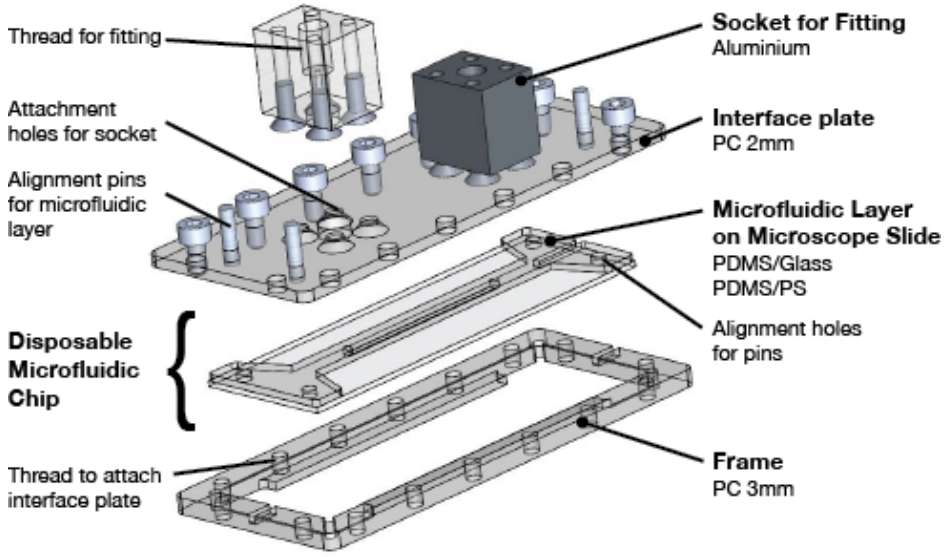

Figure 2.3: Exploded view of the first generation microfluidic packaging system - Basic microfluidic assembly with the reusable parts of the packaging system and the disposable microfluidic chip consisting of a microfluidic layer and a microscope slide.

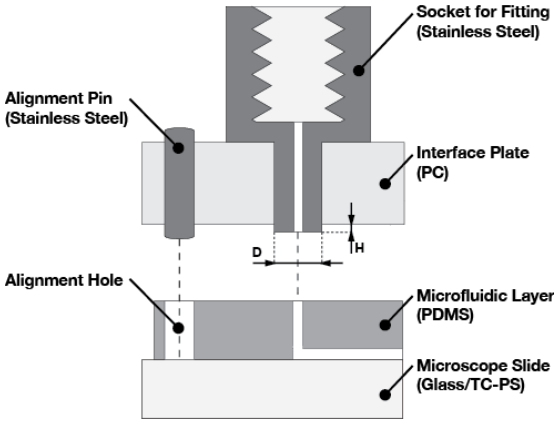

Figure 2.4: Working principle of the first generation interconnect and packaging system - Schematic of the interconnect, outlining critical dimensions of the boss (D, H). To keep the microfluidic layer in place, the microfluidic layer has holes included which align with the corresponding pin in the interface plate. The PDMS microfluidic layer forms a seal with the protruding boss of the interconnect socket when clamped together. Figure is not to scale and the interface plate and the microfluidic layer are shown in exploded view to facilitate labelling of the dimensions.

the microfluidic layer dimensions were altered to 18 mm width, 50 mm length and 1 mm thickness. Instead of using alignment pins and holes, the outer geometry of the microfluidic layer was used to align it with a corresponding recess in the interface and thus with the boss of the socket (see figure 2.5 **A** and Appendix B.7 for dimensions). The microfluidic channel was 1.4 mm wide, 32 mm long and 200 μm high (see Appendix B.9). The same interconnect socket was used as for the first generation (see Appendix B.1 for dimensions), however smaller cylindrical versions or versions which use only three attachment screws have also been designed and developed (see Appendix B.5 & B.6). A basic assembly of the second generation is shown in figure 2.6 **A** to highlight all components. To increase the mechanical stiffness of the frame, a support underneath the fluidic interconnects was left in the frame (see also Appendix B.8 for dimensions). Furthermore, the amount of screws to tighten the packaging was reduced from 14 screws to 10 screws to simplify assembly.

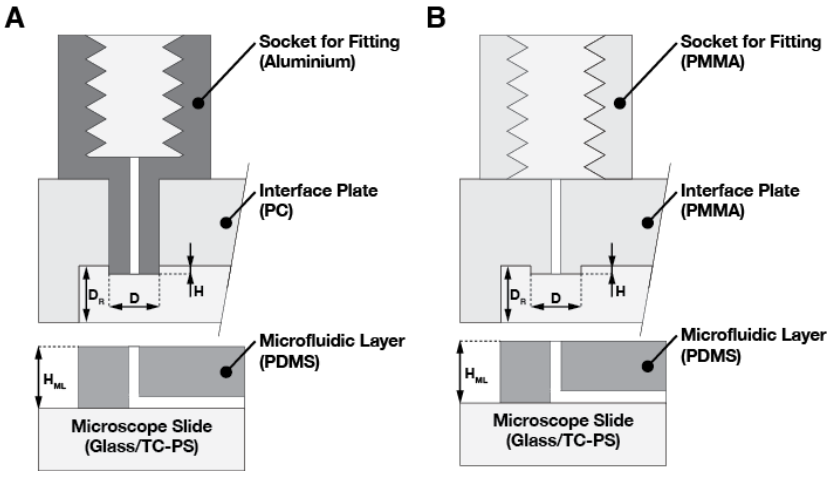

Figure 2.5: Working principle of the second and third generation interconnect and packaging system - Schematic representations of the working principle of the interconnect for the second (**A**) and third generation (**B**) are shown. Critical dimensions of the boss (D, H) and recess (D_R, H_{ML}) are outlined. The difference between the depth of the recess D_R and the height of the microfluidic layer H_{ML} limits the mechanical deformation of the microfluidic chip using the microscope slide as a bed stop. For these prototypes, a maximum mechanical deformation of approximately 50 μm for the second generation and 100 μm for the third generation has been allowed for the microfluidic chip. Therefore D_R has been set at 0.9 mm, H_{ML} at 1 mm. Figures are not to scale and the interface plate and the microfluidic layer are shown in exploded view to facilitate labelling of the dimensions.

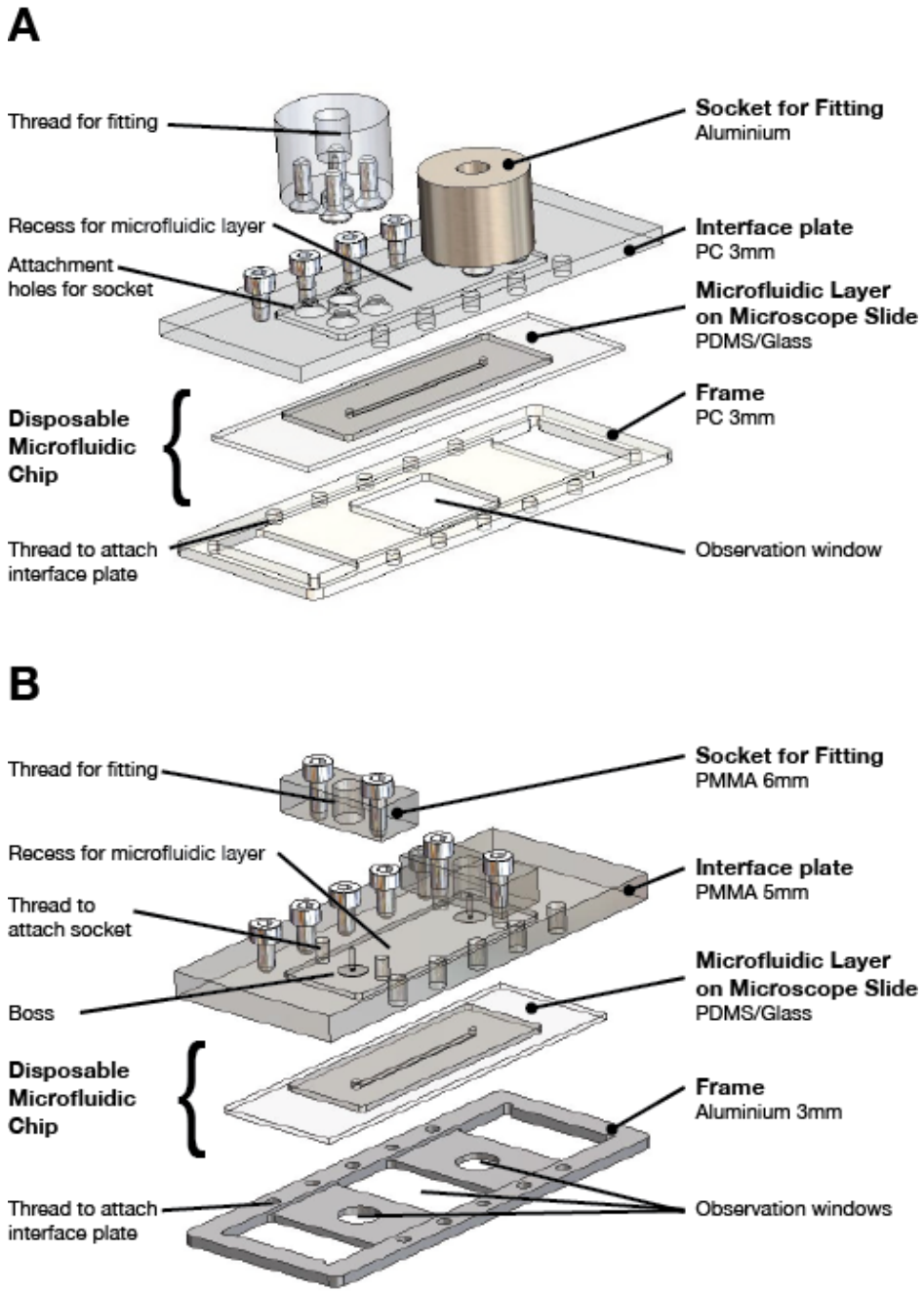

Figure 2.6: Exploded view of the microfluidic assembly of the second and third generation - Basic microfluidic assemblies of the second (**A**) and third generation (**B**) are shown. The disposable microfluidic chip is the same for both generations. The second and third generation differ in two areas: the socket design and structural improvements to the packaging. The third generation for example has an integrated interconnect while the second generation relies on a socket from the first generation. The third generation has also a stiffer interface plate and frame compared to the second generation.

2.2.3 Third generation modular packaging system

The third generation is based on the second generation, but includes an integrated interconnect boss in the interface plate and a screw-on socket for fittings on the interface plate (see figure 2.5 **B**). By separating the protruding boss from the socket, a thicker interface plate can be used, thus increasing the stiffness of the interface plate which is better for repeated use (see figure 2.6 **B** and Appendix B.11 for dimensions). For the second generation, the thickness of the interface plate was 3 mm which was determined by the height of the protruding boss of the aluminium sockets. For the third generation, a 5 mm thick interface plate was chosen which increased stiffness approximately 4.5 times compared to a 3 mm thick plate without sacrificing short machining times. The socket for the tubing fitting has been designed to be made from a 6 mm thick PMMA sheet (see Appendix B.10 for dimensions). The socket has 3 holes, a centred hole (5 mm in diameter) to cut a M6 thread and two holes with a diameter of 3.1 mm, each 7 mm from the centre hole apart to attach the socket to the interface plate with M3 screws.

The frame has been redesigned for simpler milling operation and the material has been changed to aluminium to increase stiffness of the frame (see Appendix B.12 for dimensions). To observe the inlet/outlet ports when assembled, the frame had observation holes (8 mm in diameter) cut out. In comparison with the second generation, these changes also allow the interconnect to be entirely manufactured using the micro-milling machine.

2.3 Materials & methods

2.3.1 Fabrication and characterisation of the packaging system

For all generations, all machined parts were designed with a 3-D CAD program (SolidWorks, Dassault Systems, France) and CNC-code was generated with a CAM program (Mastercam X2, Mastercam, USA). A micro-milling machine (M3400E, Folken Industries, USA) with a standard length, 2 flute, 2 mm diameter end mill (Kyocera Micro Tools, USA) was used to manufacture all parts of the packaging system and the mould. For the third generation packaging, the interface plate and the socket for the fittings were milled from 5 mm thick polymethylmetacrylate (PMMA) sheets, while for the first

a 2 mm thick polycarbonate sheet and for the seond generation a 3 mm thick polycarbonate sheet was used. M3 and M6 threads were manually cut in the appropriate bores for attachment of the sockets and the fittings. The frame and the mould were milled from 3 mm thick aluminium sheets. M3 threads for the screws to hold the interface plate in place were manually cut in the appropriate bores in the aluminium frame.

PDMS (Sylgard 184, Dow Corning, UK) was mixed according to the manufacturer's instructions, degassed in a vacuum desiccator and then poured into the mould (see figure 2.7). The mould with the PDMS was subjected to vacuum again to ensure all air bubbles were removed. The mould was closed with a 5 mm thick PMMA sheet or a 5 mm thick PC sheet and clamped between two rigid, 10 mm thick aluminium plates as reported in a similar procedure (Jo *et al.*, 2000). The thick aluminium plates were secured with four screws and tightened with a torque screw driver at 250 Ncm. The assembly was then placed in an oven at 85°C for at least one hour to cure the PDMS. After curing, the clamp was dismantled and the PDMS microfluidic layer released with tweezers. To seal the disposable microfluidic layer, a microscope glass slide was bonded to the PDMS microfluidic layer by an air plasma. Both parts were thoroughly cleaned with deionised water and ethanol and dried prior to bonding. To align the microfluidic layer with the microscope glass slide, the glass slide was placed in the frame and the microfluidic layer in the recess of the interface plate. The two surfaces to be bonded were placed in a plasma chamber (90 s, 30 W, 500 mTorr, PDC-002, Harrick Plasma, USA). The interface plate and frame were aligned and pressed together gently, ensuring that the PDMS and glass components of the chip were correctly placed. The microfluidic chip was then removed from the frame, and cured in an oven at 85°C for at least 2 hours.

The positive height of a microchannel feature in an aluminium mould, and the negative depth of the corresponding channel in a PDMS cast, were measured at the inlet, outlet and middle of the microchannel with a stylus profiler (Dektak 8, Veeco, USA). A stylus profiler is a measurement tool where a needle tip is dragged in direct contact over a surface. The deflection of the needle tip is measured and a 1-D plot generated displaying the heights and valleys. For these experiments, the stylus force was chosen to be 10 mg and the scan length was 2 mm. To measure the height of the protruding boss, a standard micrometer vernier calliper was used. Both bosses in an interface plate were measured six times and the mean and standard deviation

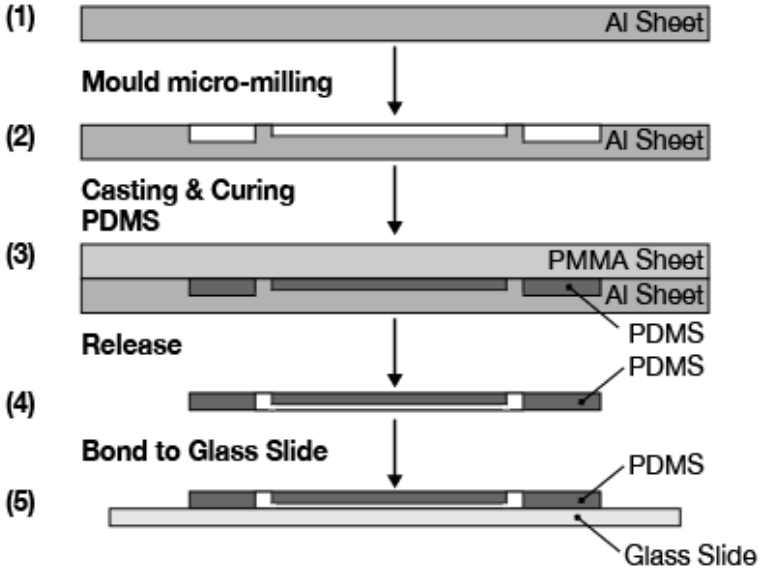

Figure 2.7: Fabrication process of a mould and a microfluidic chip created in the mould. - A 3 mm thick sheet of aluminium (**1**) was machined to a mould with standard CNC milling techniques (**2**). The mould was filled with PDMS monomer, degassed using vacuum and covered with a sheet of PMMA or PC and cured (85°C, 90min) (**3**). After curing, the PDMS microfluidic chip was released from the mould (**4**). The PDMS microfluidic chip and a microscope glass slide were exposed to an air plasma and immediately bonded together (**5**). Figure is not to scale.

calculated. A compact digital microscope (AM413T, Dino-Lite, USA) was used for imaging the different bosses, and the diameters measured using image analysis software (ImageJ, NIH, USA).

2.3.2 Setup for burst pressure measurement

To measure the effect of different boss geometries on the burst pressure of the interconnect, a syringe pump and tubing were connected to one of the fluidic ports of the microfluidic chip and a pressure sensor (40PC100G, Honeywell, USA) was glued into a fitting (P-207, Upchurch Scientific, USA) with an epoxy glue, and attached to the other end with a Luer lock (see figure 2.8 **A**). To generate pressure, a syringe pump was used to push air into the chip from a 5 ml syringe with a Luer lock connector. The force applied to the interface plate was controlled by tightening the screws to torques ranging from 2 Ncm to 5 Ncm using a torque screw driver. A LabView™ routine (LabView 8.2, National Instruments, USA) was used to log the pressure readings from a data acquisition card (USB-6229BNC, National Instruments, USA). The burst pressure was taken as the highest recorded applied pressure for a given experiment, and was measured six times for each torque setting.

2.3.3 Setup for flow rate measurement

To measure the deformation of the microchannel by the clamping procedure, a pressurised reservoir of water was used to deliver a constant flow rate, which was monitored by a flowmeter (see figure 2.8 **B**). The setup consists of a pressure regulator (ITV0011-2BL-Q, SMC, UK), a fluid reservoir, the microfluidic chip and a flowmeter (SLG1430-480, Sensirion, Switzerland). The fluid reservoir had two custom made ports built into the lid to connect to the pressure regulator and to the microfluidic chip, respectively. A Luer lock fitting was used to connect the reservoir with pneumatic tubing (SMC, UK) to the pressure regulator, which was connected to a compressed air supply. The other port had an M6 thread to accommodate a threaded flat bottom fitting. A fitting was attached to a 15 cm long PTFE tubing (ID: 0.8 mm, OD: 1.6 mm)(S1810-10, Bola, Germany) with the same fitting at the other end to connect to the microfluidic chip. The microfluidic chip was fitted on the other fluidic port with a male Luer lock adapter. A 5 cm long PTFE tubing was fitted on one end with an M6 fitting and a female Luer lock adapter to connect to the microfluidic chip and on the other end with

an adapter to connect to the flow meter. The adapter was fitted with a 300 μm inner diameter capillary, which was cut to a length of 5 cm. Flow rates for the minimum and maximum compression of the microchannel were recorded over 15 minutes, and the mean and standard deviation calculated.

2.3.4 Parametric simulation of microfluidic layer and microchannel dimensions

To study the influence of important dimensions, a simple two-dimensional model of a cross-section of the interface plate and the microfluidic layer (see figure 2.12 **A**) was analysed with a parametric model using a finite element software package (COMSOL 4.1, COMSOL AB, Sweden). The material properties of PMMA for the interface plate were taken from the material library of the software package. PDMS (microfluidic layer) was modelled as incompressible (Poisson number 0.499) with a Youngs modulus of 1 MPa (Gervais *et al.*, 2006).

Four critical parameters were defined: the width of the microfluidic layer *Pw*, the height of the microfluidic layer *Ph*, the width of the channel *Cw* and the height of the channel *Ch*. *Pw* was varied between 5 mm, 10 mm and 20 mm and *Ph*, between 1 mm, 1.5 mm and 2 mm. Values for *Ch* have been varied between 10 μm, 50 μm and 250 μm and for *Cw*, between 100 μm, 500 μm and 1.5 mm. The glass slide sealing the PDMS microchannel was assumed to be rigid, therefore imposing a zero-displacement boundary condition at the interface microfluidic layer/microscope glass slide. The torque applied to a screw results in an axial force on the interface plate, and point loads at the edges of the plate were used to represent this force generated by the screws. Friction losses between screw head and interface plate were neglected. The strain of the channel was calculated for the middle of the channel roof by dividing the displacement at this point by the nominal height.

2.4 Results & discussion

2.4.1 Design

A reusable, modular packaging system has been designed and developed, based on an adhesive-free connection of a reusable and mechanically stiff polymeric interface plate with a disposable, soft polymeric microfluidic chip under compression (see figure 2.9

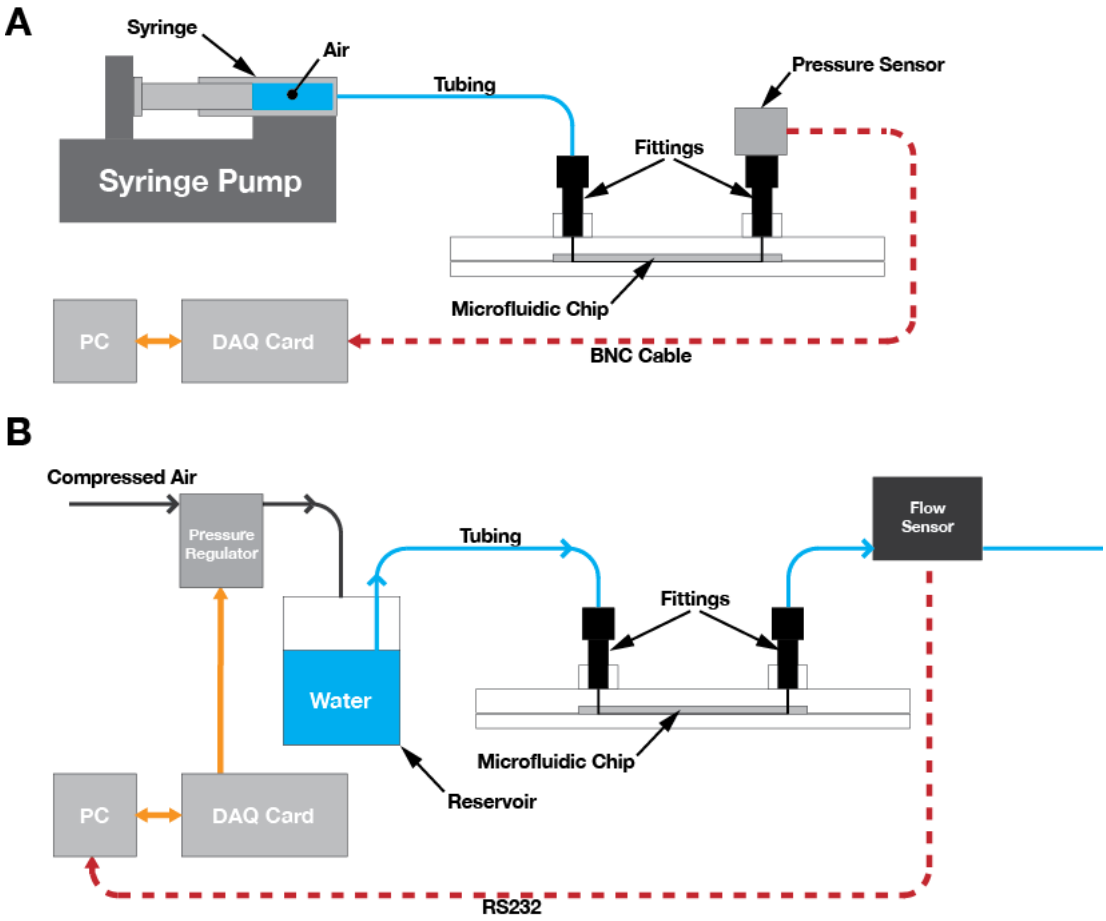

Figure 2.8: Schematic of the testing setup for burst pressure and flow rate - (**A**) Setup to measure the burst pressure of the interconnect. A syringe pump was used to generate pressure with air as medium. The exit of the microfluidic chip was blocked by a pressure sensor. The pressure sensor was read out and data logged on a PC. (**B**) Setup to measure the flow rate. The pressure in the reservoir was controlled and used to pump water at a constant flow rate through the microfluidic chip. A flow sensor was used to monitor the flow rate at the outlet of the microfluidic outlet for different compression forces of the interface plate. Figure is not to scale.

A, **B**). The packaging system enables the simple insertion and alignment of disposable poly(dimethylsiloxane) (PDMS)/glass chips or any other material. To attach and connect with standard and commercially available fittings, a socket is fixed with screws to the interface plate, and is easily aligned with the inlet and outlet bores in the interface plate. Self-alignment of the fluidic ports of the microfluidic chip with the corresponding bores in the interface plate is achieved by a recess in the interface plate. In the latest generation, the protruding boss to seal the microfluidic chip has been machined into the recess, and forms a tight seal with the microfluidic chip.

In the system presented here, the implementation of a standard microscope slide format (3 x 1 inches) for the rigid part of the microfluidic chip also allows the use of different commercially available materials, such as tissue culture polystyrene (TC-PS). This compatibility with this standard slide format also facilitates the integration of microfluidic chips with routine endpoint-analyses. For observation during the experiment, the centre opening in the bottom frame allows the objective of an inverted microscope to be placed in close proximity to the slide. It is thus possible to use the same microscope settings as employed with microscope slides to monitor the experiment in the microfluidic chip.

Further observation windows under the sockets enable visual verification that the fluidic connection is indeed leak-tight. Tubing is reliably connected to the interface plate with a commercially available flat-bottom fitting in the designated socket. The simple connection of tubing renders the preparation and set-up of a microfluidic experiment straightforward and without difficulties. Additionally, unlike other interconnect solutions, where only tubing can be connected, this socket can be used with different fitting types, for example Luer lock adapters (see figure 2.9 **B**), or can be modified for custom-made interconnects if required. In the past, such sockets for screw type fittings have been used in combination with injection moulded cyclooleofin copolymer (COC) microfluidic devices (Mair *et al.*, 2006), but this fabrication method is not suitable for rapid prototyping.

The force to compress the microfluidic chip is generated by screwing the interface plate with the microfluidic chip to a frame and can be varied by applying a different torque to the screws. It is thus important to properly characterise the effect of this force and the interconnect dimensions on the static burst pressure and on the flow rate.

To characterise the third generation interconnect, the dimensions of the boss have been varied for the diameter D between 3 mm and 5.5 mm and for the height H between 75 μm and 125 μm. These dimensions were tested in combination with a microfluidic chip consisting of a microfluidic layer and a standard microscope glass slide. The microfluidic layer had a single microchannel (nominal values: 200 μm in height, 1.25 mm in width and 36 mm in length) and two fluidic ports. Microfluidic layers with microchannel heights of 50, respectively 100 μm have been also designed and fabricated for the characterisation of the fabrication process.

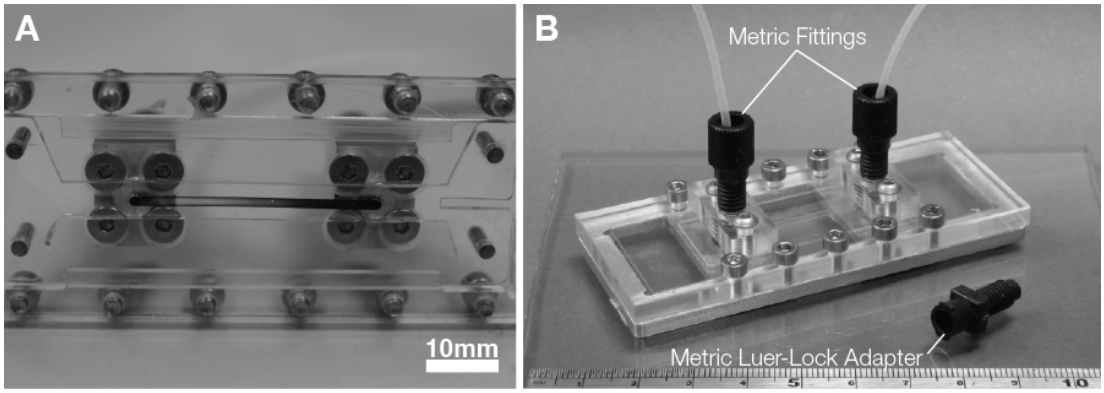

Figure 2.9: Modular microfluidic packaging - Filling test with the first generation of the modular microfluidic packaging system with water blue dye (5 g L^{-1}) (**A**) and an assembled microfluidic system of the third generation with different options for connectors such as a screw type fittings or Luer lock fittings (**B**).

2.4.2 Fabrication

The entire modular interconnect and packaging system and the mould for the microfluidic layer were fabricated with a CNC micro-milling machine. All materials are readily available at low cost. Feature sizes as small as 50 μm could be achieved by this technique. Allowing 3 - 4 hours for milling, and 2 hours for each curing step, the fabrication process takes less than two days. Surface modification for de-moulding is not required and moulds can be used repeatedly. The boss heights of the interconnect of the third generation have been measured with a micrometer calliper (see table 2.2) and the diameter has been measured using digital imaging (see table 2.3). The maximum difference between the nominal and measured heights was 10.7%. For all boss diameters, the maximum difference between nominal and measured diameter was 2.9%.

Nominal height (μm)	Measured height +/− std dev (μm)	Deviation from nominal height (%)
75	67 +/− 3	10.7
100	100 +/− 9	0
125	118 +/− 3	5.6

Table 2.2: Measurement of boss heights - Boss heights of the third generation. Boss heights were measured with a vernier calliper. Every boss in the interface plate was measured six times and the average, the standard deviation and the deviation of the average from the nominal boss height calculated (n=6).

Nominal diameter (mm)	Measured diameter +/− std dev (mm)	Deviation from nominal diameter (%)
3	3.02 +/− 0.04	0.6
4	3.94 +/− 0.02	1.5
5.5	5.66 +/− 0.03	2.9

Table 2.3: Measurement of boss diameters in the interface plate - Boss diameters of the third generation. Boss diameters were measure with a vernier calliper. Every boss in the interface plate was measured six times and the average, the standard deviation and the deviation of the average from the nominal boss diameter calculated (n=6).

To fabricate and rapidly test microfluidic chip designs, microfluidic layers were cast in an aluminium mould from PDMS. The mould contains the structures for the microchannel and the fluidic ports and defines the outer dimensions of the microfluidic layer. The negative microchannel height in the mould and the positive microchannel depth in the PDMS microfluidic layer were measured at three locations along the microchannel for nominal microchannel heights of 50 μm, 100 μm and 200 μm using contact profilometry (see figure 2.10 **A**–**H**). Table 2.4 shows the nominal and measured average values including standard deviation and deviation from the nominal height for different microchannel heights. To compare the dimensional fidelity of microchannel features in the PDMS microfluidic layers with the features in the moulds, microchannel depths of different PDMS microfluidic layers have also been measured (see table 2.5). Comparing the microchannel depths of PDMS microfluidic layers with the corresponding microchannel moulds shows either a difference which is within the measurement error margins (50 μm and 200 μm) or is less than 10 % of the average microchannel height of the mould (100 μm).

At the edges of the microchannels in the mould, bumps or spikes are observed (see figure 2.10 **C, E, G**). The height of these bumps is increasing with decreasing nominal

microchannel height in the mould. However, these bumps are less predominant in the PDMS microfluidic layer (see figure 2.10 **D, F, H**).

Milling generates generally burrs and burr generation is dependent on a few variables such as feed rate parameters, coolant and tool wear. The bumps observed for all microchannel heights are thus most likely burrs. To avoid burr generation, the number of moulds or parts milled with the same end mill has to be restricted.

Nominal height (μm)	Average height in mould +/− std dev (μm)	Deviation from nominal height (%)
50	32.9 +/− 2.2	34.2
100	88.9 +/− 2.1	11.1
200	185 +/− 2.3	7.5

Table 2.4: Profilometer measurements of microchannel heights in moulds - Every microchannel in the mould was measured three times at different locations along the microchannel and the average, the standard deviation and the deviation of the average from the nominal height calculated (n=3).

Nominal depth (μm)	Average depth in PDMS +/− std dev (μm)	Deviation from nominal value (%)
50	32.5 +/− 3.2	35.1
100	86.8 +/− 1.38	13.1
200	184.6 +/− 2.5	7.7

Table 2.5: Profilometer measurements of microchannel depths in PDMS microfluidic layer - Every microchannel in the PDMS microfluidic layer was measured three times at different locations along the microchannel and the average, the standard deviation and the deviation of the average from the nominal height calculated (n=3).

The variation in deviation of the nominal microchannel heights for decreasing microchannel heights may be a result of two causes - either due to the backlash in the Z-axis spindle drive of the micro-milling machine used for the fabrication of the moulds or due to an error by manually levelling the end mill on the work sheet.

Backlash is usually a clearance between two mating parts. In micro-milling machines, backlash occurs most likely in the bearing of the spindle drive. To level the end mill and define a machine origin on the work piece or the material to mill, a microscope is used to verify the contact of the end mill with the work piece surface. All moulds for the different microchannel heights were fabricated on the same aluminium sheet with a 2 mm end mill. The CNC program sequence is set to mill first the pocket

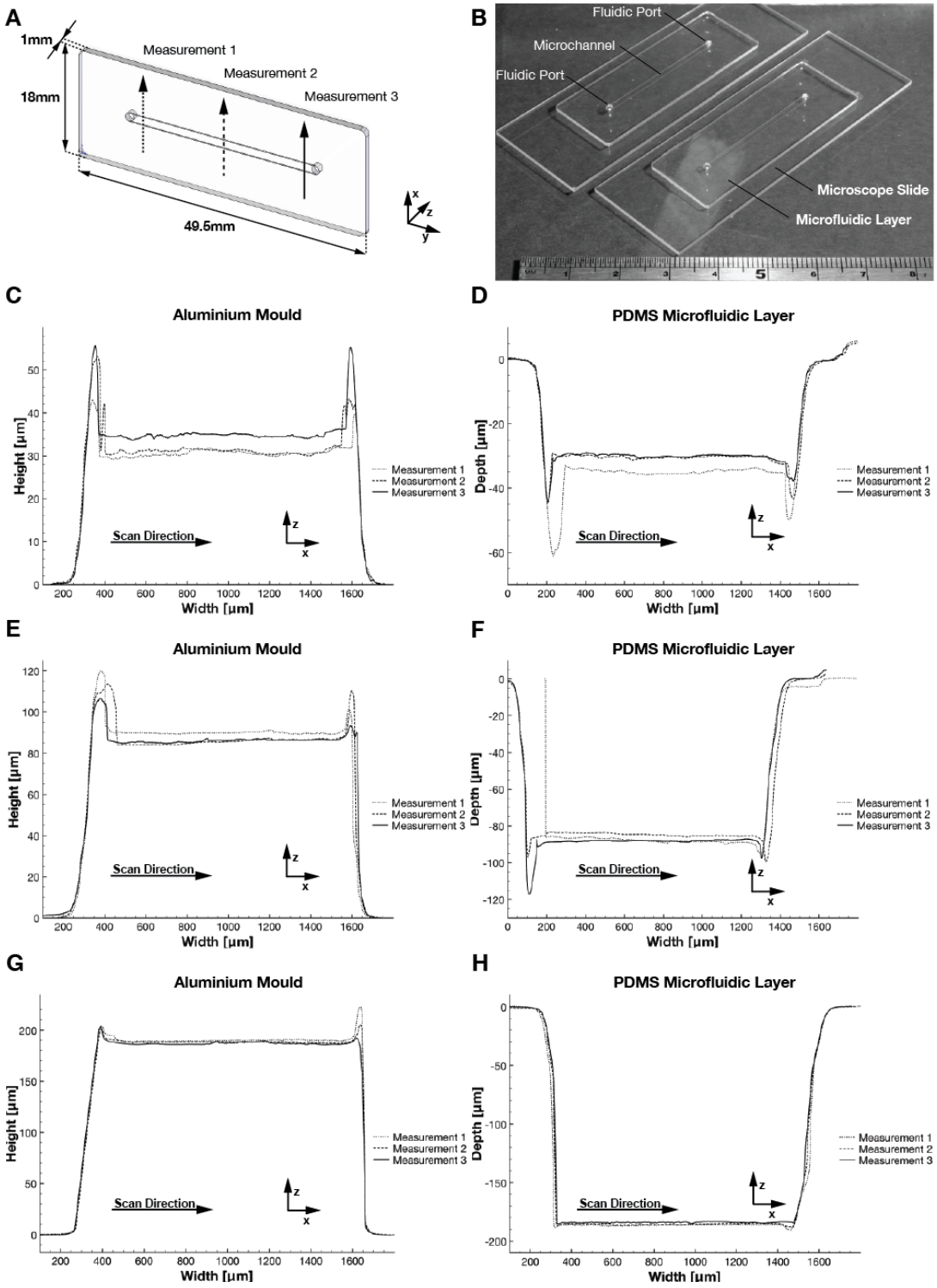

Figure 2.10: Characterisation of milling moulds with different channel heights and their cast PDMS parts - (**A**) Schematic of the microfluidic layer and the indicated scan locations. (**B**) Assembled microfluidic layer on a microscope slide. (**C** - **H**) Height and depth profiles of the microfluidic layer in the mould and the PDMS microfluidic layer for nominal values of 50 μm (**C**, **D**), 100 μm (**E**, **F**) and 200 μm (**G**, **H**).

defining the microfluidic layer dimensions and the inlet and outlet holes down to the features of the microchannel. The second milling step of the CNC program sequence defines the microchannel height and uses the same end mill level settings as for the first step. An end mill levelling error would therefore only lead to a decreased or increased overall microfluidic layer thickness, but not affect the height of the microchannel. It can therefore be assumed that the deviation from the nominal value occurs due to the backlash of the Z-axis spindle drive.

The accuracy of feature heights in the mould is thus limited by the micro-milling machine, in particular for features below 100 μm. However, a significant difference in height of the transferred features of the mould to a PDMS microfluidic layer has not been measured.

Before casting and curing, no surface treatment of the mould was required to prevent adhesion in the mould, and PDMS microfluidic layers from all mould geometries presented were de-moulded without difficulty. The subsequent plasma-assisted bonding of the PDMS microfluidic layer to a glass microscope slide was performed without any additional processing steps for the microfluidic layer (see figure 2.10 **B**), demonstrating that the mould fabrication method creates very smooth surfaces. Unlike silicon-photoresist masters, the monolithic aluminium mould is not prone to delamination of microfluidic structures. It is also more rapidly fabricated than other monolithic masters such as micro-machined silicon masters or plastic masters made from silicone (Desai *et al.*, 2009). Furthermore, micro-milling also allows to fabricate moulds with circular microchannel shapes as (Wilson *et al.*, 2011) has recently demonstrated. Milling moulds for the creation of microfluidic chips has a further advantage over directly milled parts. For directly milled parts, the end mill diameter defines the smallest feature possible. For moulds, the feature size is limited only by the accuracy of the micro-milling machine, and the robustness of the material being milled. However, these variations are considered to have a minimal effect on cells.

2.4.3 Burst pressure

The static burst pressure for all interface plate dimensions of the third generation was measured using the same microfluidic chip, indicating that the integrity of the PDMS bond to the glass slide was maintained, and that the eventual failure occurred between the microfluidic chip and the tubing interconnect. For the interface plates with varying

boss heights, the mean burst pressure ranges from 5.62×10^5 Pa to 6.89×10^5 Pa (see figure 2.11 **A**). For the applied screw torques (2 Ncm to 5 Ncm), no significant change in burst pressure values were observed. For the interface place where the boss diameters have been varied, the mean burst pressure ranges from 5.62×10^5 Pa to 7.26×10^5 Pa (see figure 2.11 **B**).

The measured values imply that the burst pressure can be considered virtually independent from the boss geometry for a 5 mm thick interface plate. The protruding boss is therefore a reliable approach to obtain leak-tight sealing, and it can compensate for manufacturing tolerances and small differences in the applied screw torque.

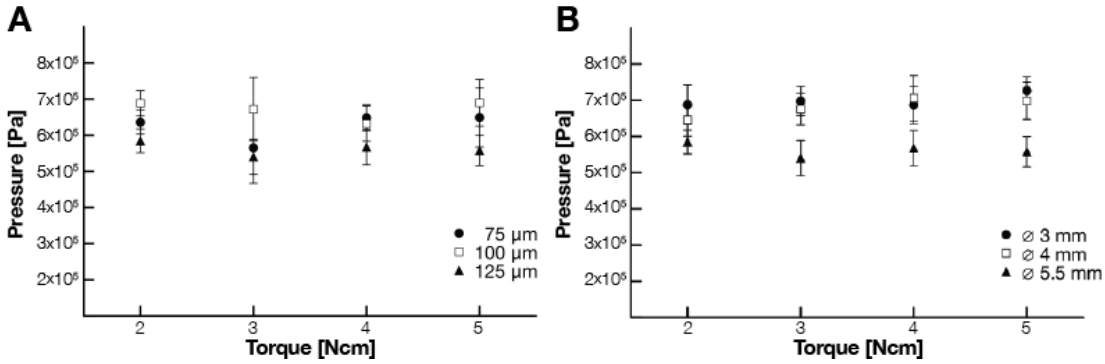

Figure 2.11: Burst pressure measurements using air - (**A**) Shows the mean burst pressures for varying boss heights (75 μm, 100 μm, 125 μm) with a constant diameter (5.5 mm) under different torques (2-5 Ncm). (**B**) shows the mean burst pressures for varying boss diameters (3 mm, 4 mm, 5.5 mm) with a constant height (H = 125 μm). $n = 6$.

2.4.4 Flow rate

To assess the effect of the compression on the flow rate, the flow rate of water through the microfluidic chip for a given pressure applied to the water reservoir has been measured at the lowest and highest torque (see figure 2.8). The decrease in flow rate for the highest applied torque is approximately 12% of the flow rate for the lowest torque (see Table 2.6). As expected a lower torque results in a less deformed microchannel and therefore, a higher flow rate is expected. However, the flow rates are highly reproducible at defined compressions of the microfluidic chip. For 2 Ncm for example, a coefficient of variation (i.e. the standard deviation over the mean) smaller than 1% from a total of 6 experiments was obtained. It has to be noted however, that the variation in flow rates

due to different torque settings is unlikely to affect cells within such a micro channel. These experiments were conducted independently, i.e. the system was re-assembled for each flow rate measurement. The measured variation is likely to be within the tolerance of the pressure-based pumping mechanism. Therefore, by precisely controlling the torque (which is straightforward when using a torque screw driver), it is possible to perform highly repeatable experiments. Finally, given that working pressures for most microfluidic applications are below 2.5 bar (Eddings *et al.*, 2008; Lee & Ram, 2009), it is recommend working at the lowest torque setting, minimising the mechanical stress on the entire microfluidic device.

Table 2.6: Difference in flow rate due to compression - (n=6)

Torque per screw (Ncm)	**Flow rate** ($\mu l\ min^{-1}$) +/− **std dev** ($\mu l\ min^{-1}$)
2	39.27 +/− 0.31
5	34.5 +/− 1.3

2.4.5 Design rules for a modular microfluidic packaging system

Due to the packaging, a compression of the microfluidic layer occurs which affects the dimensions of the microfluidic structures. To study this effect, a simple two-dimensional model of a cross-section of the interface plate with a microfluidic layer consisting of a single channel has been analysed (Calculations for translating screw torque into an axial force can be found in Appendix A). To formulate design rules, a number of finite element calculations were performed for different geometries. The width *Pw* and height *Ph* of the microfluidic layer, and the channel height, *Ch*, and width, *Cw*, were varied in a wide range (see figure 2.12 **A**). To plot the results, the different geometries were normalised against the channel height *Ch*. The figure 2.12 **B**, **C** show the impact on the strain at mid-width of the channel roof for $Ph = 1$ mm, for 2 Ncm and 5 Ncm torque, respectively. These are also the two torque settings which were subsequently used for the burst pressure (section 2.4.3) and flow rate analysis (section 2.4.4).

In general, for any given *Cw/Ch* ratio, the maximum strain occurs for low *Pw/Ch* ratios. A microfluidic layer which is significantly wider than the microfluidic structures thus reduces the strain. This effect was observed for all values of *Ph*. For *Cw/Ch* ratios below 10, strain in the channel is negligibly small for any torque setting. *Cw/Ch* ratios above 10 exhibit strains up to 1% for 2 Ncm torque, and up to 2.1% strain for 5 Ncm,

respectively (see figure 2.12 **B**, **C**). Increasing the height *Ph* decreases the strain on the microchannel. A *Ph* of 1 mm however is a good compromise which allows machining of the moulds in a reasonable time while keeping microchannel strain below 1 %.

2.4.6 Potential of the fabrication and packaging system

In order to demonstrate that the rapid prototyping method can easily be extended to more complex structures, a number of microfluidic demonstrators were prepared. A three-dimensional channel network (see figure 2.13 **A** - **D**), where coloured liquid streams (blue and yellow food dyes in water) pass over and under each other before being combined, was fabricated by using two layers of PDMS and a system of through holes. The moulds were machined with a single 2 mm end mill tool, using PMMA rather than aluminium, demonstrating also the versatility of the mould fabrication technique. The alignment of the PDMS layers before bonding was easily achieved, thanks to the standardisation of the outer dimensions. Feature sizes ranged from 125-1000 μm, much smaller than the 2 mm end mill tool used to mill the mould. A functioning leak-free prototype was successfully fabricated and tested within 24 hours of the final design being approved.

Similarly, a staggered herringbone mixer with grooves approx. 35 μm wide (50 μm spaced grooves under a 45°ängle) was prepared (using a 2 flute end mill with a 0.001 in. diameter), where negative mould was machined from brass stock (see figure 2.14). Various Y-channel mixing devices were also fabricated to demonstrate integration of multiple interconnect ports in the packaging system (see figure 2.15 **A**). Finally, a multiplexed microfluidic demonstrator has also been design and fabricated (see figure 2.15 **B**).

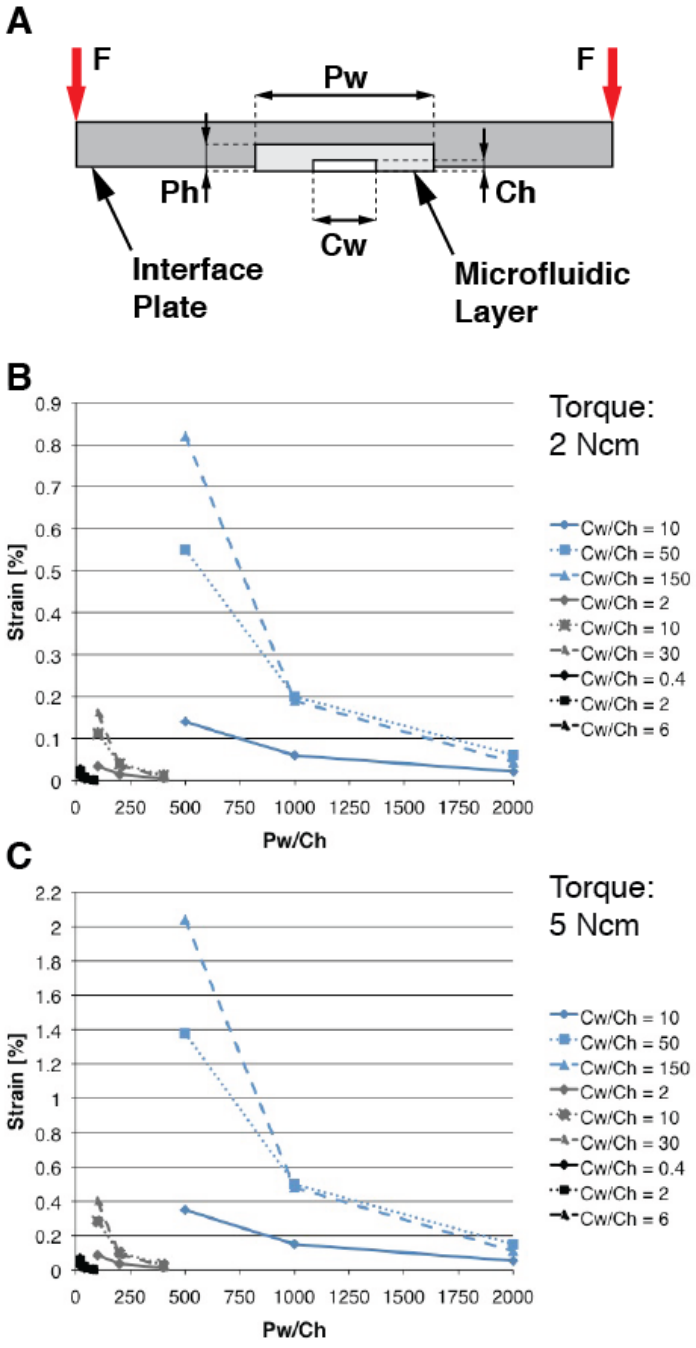

Figure 2.12: Model and compression under two different forces - (**A**) Schematic of the two-dimensional model to assess the influence of microfluidic layer (*Ph*, *Pw*) and microchannel dimensions (*Ch*, *Cw*) on strain experienced by the microfluidic layer. (**B**) *Ch* strain dependence on *Pw/Ch* ratios at different *Cw/Ch* ratios for *Ph* = 1 mm and a torque = 2 Ncm. (**C**) *Ch* strain dependence on *Pw/Ch* ratios at different *Cw/Ch* ratios for *Ph* = 1 mm and a torque = 5 Ncm. For (**B**) and (**C**) the blue, grey and black lines represent the values for *Ch* = 10 μm, *Ch* = 50 μm, *Ch* = 250 μm, respectively.

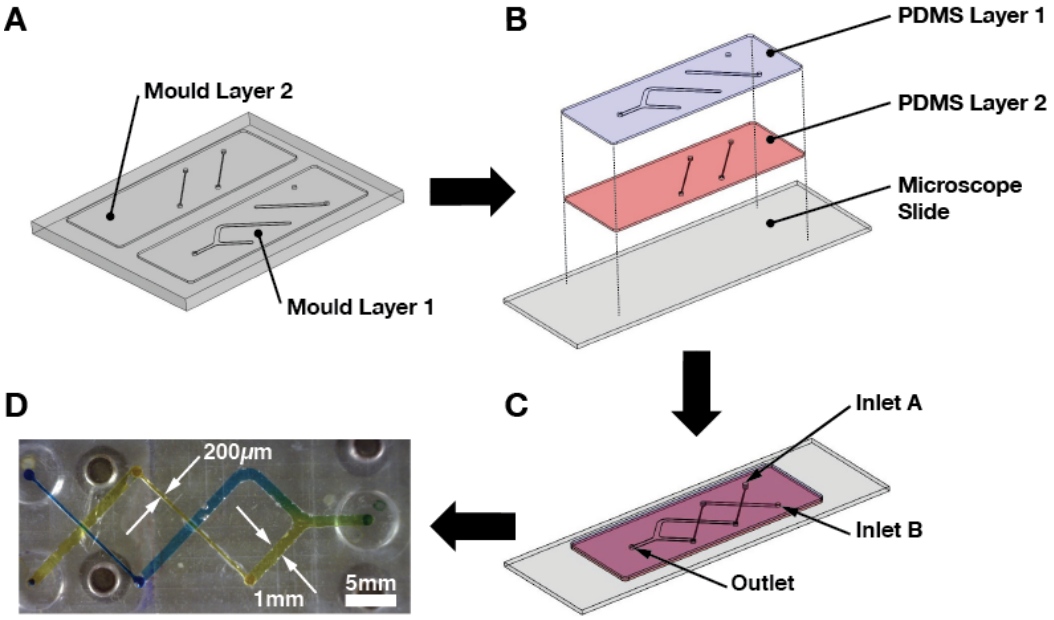

Figure 2.13: Fabrication and testing of a 3-D microfluidic demonstrator with two PDMS layers - Both microfluidic layers can be cast at the same time in the mould (**A**). The well-defined outer dimensions of the PDMS layers help to align the two layers for bonding (**B**). The assembled 3-D demonstrator has two inlets (A+B) for different fluids and a common outlet (**C**). The demonstrator was tested with yellow and blue food dyes (**D**). The entire microfluidic chip - from the design idea to a working prototype - has been realised in two days. For more details, see please Appendix B.13 & B.14.

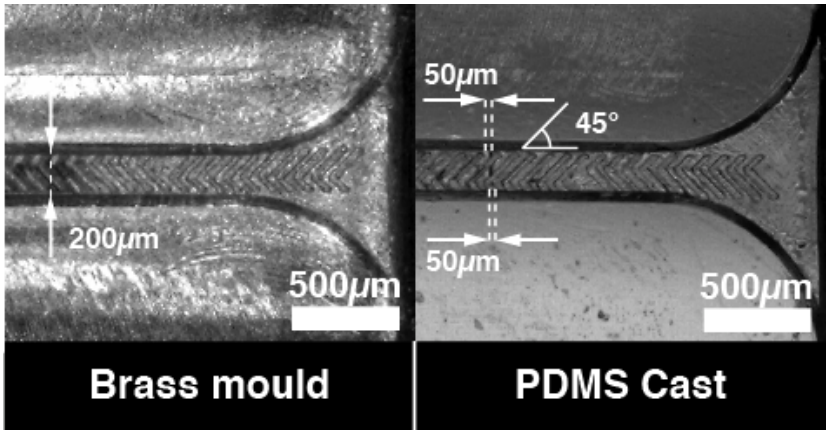

Figure 2.14: Brass mould and PDMS cast of a staggered herringbone mixer - Features as small as 35 μm can be fabricated, for example a mould with channel and a staggered herringbone mixer (Mixer structures are 20 μm deep, and 50 μm wide at a 45° angle to the channel wall. Dimensions of the microchannel: 200 μm (w)×100 μm (h)). See also Appendix B.15 for more details.

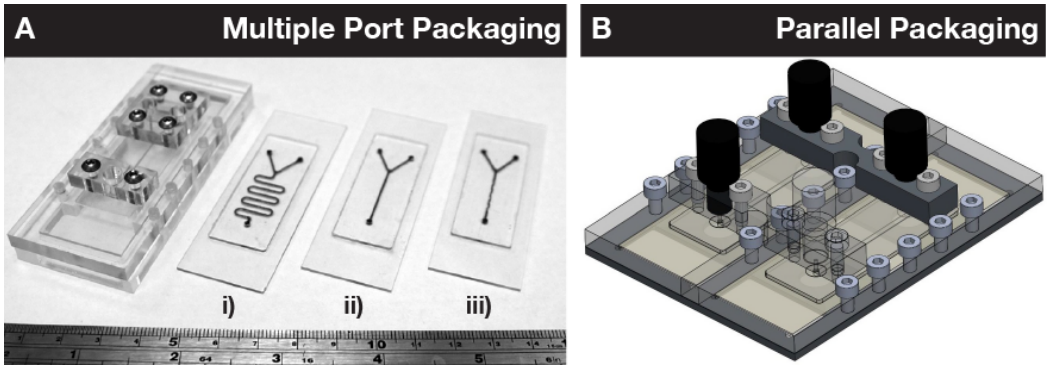

Figure 2.15: Multiple port and parallel chip packaging - Multiple ports can be realised, for example for mixer chips with different mixing lengths i)-iii) (**A**). These prototypes have been jointly developed with Dr. Brian O'Sullivan. To multiplex microfluidic chips, a packaging system for two microfluidic chips has been developed (**B**). Such a multiplexed system could be used for example to compare culture conditions, i.e. static versus perfusion culture.

2.5 Summary of findings

An integrated rapid prototyping approach has been developed and characterised, which offers a simple but comprehensive route to large numbers of ready-to-use microfluidic cell culture devices. The system consists of a casting method to deliver microfluidic prototype chips within two days, and a modular, robust, and adhesive-free interconnect and packaging system to rapidly test microfluidic chips for cell culture. This approach separates packaging and microfluidic chip, thus facilitating the rapid testing of microfluidic design concepts. The microfluidic devices are easy to fabricate and assemble, and do not require expert fabrication knowledge or specialised environments such as cleanrooms. Therefore it is also suitable for users with non-engineering backgrounds.

Micro-milling represents a cost-effective, rapid fabrication method for microfluidic prototypes. With the same machine, parts such as the interconnects and the packaging system can be fabricated directly, and moulds to cast soft microfluidic chips machined more quickly than with photolithography. All materials are widely available and at low cost. The packaging and fabrication method presented in this chapter will also serve as the basis for improved and optimised microfluidic cell culture chips.

3

Seeding and continuous culture of human embryonic stem cells in a microfabricated cell culture device

In the previous chapter, a packaging and fabrication approach to rapidly implement changes in the design of the microfluidic chip has been developed and tested using various configurations demonstrating the potential of the rapid prototyping approach. Critical aspects for a microfluidic tool for stem cell bioprocess development are cell seeding and the ability to culture cells in continuous perfusion, which are pivotal for successful experimentation. Besides these aspects, the culture chamber needs to be designed large enough to obtain a significant number of cells that off-chip analysis is feasible using flow cytometry for example.

The results in this chapter have also been presented as a conference proceeding at the Micro Total Analysis Systems conference 2009 in Jeju, Korea (see Appendix G).

3.1 Issues of adherent cell culture in microfluidic devices

Microfluidic devices for cell culture offer great advantages over current bioreactors (see also section 1.4.2) in terms of resources used and the data-rich experimental sets made possible by the parallel nature of the microfluidic devices. To take advantage of mi-

crofluidic cell culture devices, two particular requirements are of great importance - efficient and accurate cell seeding and low hydrodynamic shear stress microfluidic designs. A concise overview of the design of microfluidic cell culture devices for adherent cells is given by Kim *et al.* (2007). However, the requirements for a microfluidic stem cell bioprocess development and optimisation tool demand scalable and comparable methods as outlined in section 1.4.3.1.

3.1.1 First issue: Cell seeding

Every cell culture experiment is started with the seeding of cells into a bioreactor. Prior to seeding, an appropriate cell seeding density is calculated based on a cell viability count, which determines the amount of cell suspension to be added to a T-flask for example. It has to be pointed out that the seeding density plays an important role to control stem cell expansion or differentiation. For example, the differentiation of mESCs into neuronal precursor cells has been optimised for a low seeding density showing the importance (Ying *et al.*, 2003). The seeding process thus affects all subsequent process or experimental steps, and is therefore a critical element for successful and repeatable experimental outcomes.

Compared to off-the-shelf, ready-to-use T-flasks for example, traditional microfabricated cell culture devices for hESCs are cumbersome to operate (see figure 3.1).

Firstly, sterilisation procedures usually require a sequence of washing steps of the microfluidic channel network with ethanol and subsequent washings with phosphate buffer solution (PBS) or the exposure to a UV light source. However, both sterilisation methods are ineffective for long-term culture (>3 days), because these methods do not follow an approved standard sterilisation protocol.

Secondly, it would be desirable to follow the same seeding procedures of a macro-scale hESC experiment in a microfluidic device to facilitate scalable experimental results. However, traditional microfluidic cell seeding procedures differ from macro-scale cell culture by using volume units rather than area units.

These process steps prior to microfluidic cell culture may add a source of error which can affect device reliability during cell culture or the cell culture outcome itself. Common errors which may occur during microfluidic cell seeding are for example contamination by bacteria, incorrect seeding density or mechanical disruption of cells.

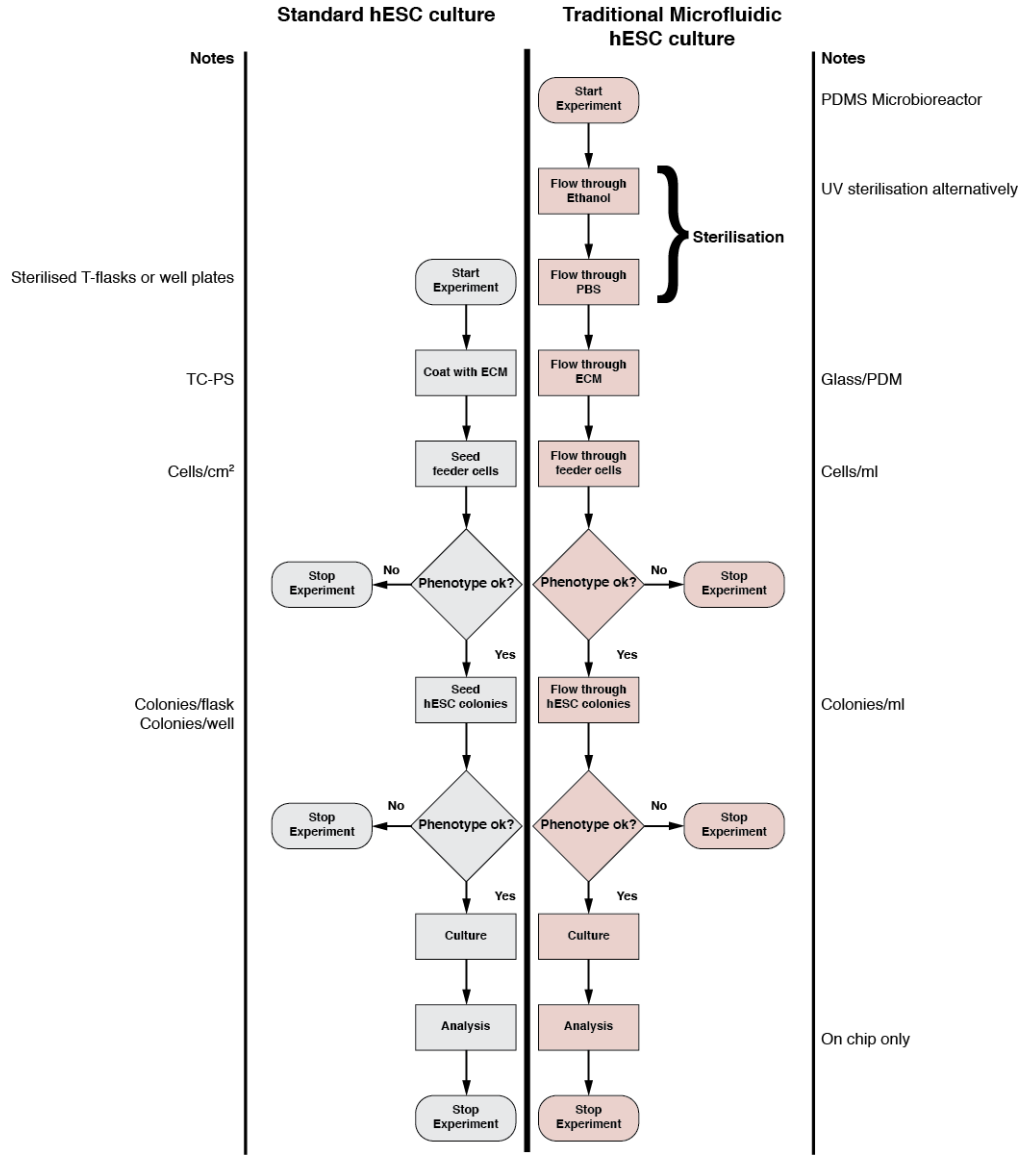

Figure 3.1: Comparison of seeding procedure - Comparison of seeding procedure in current small-scale cell culture methods (e.g. T-flasks) and a traditional microfluidic cell culture device for human ESCs on a feeder layer.

3.1.1.1 Flow-based seeding methods

The majority of microfluidic systems use flow-based seeding methods, where cells are seeded into a reservoir separate from the culture chamber and subsequently flowed to the culture chamber via fluidic connections (Kim *et al.*, 2007). This method has

also been applied to seed hESCs on human foreskin fibroblasts and on growth-arrested murine embryonic fibroblasts (mEFs) (Kamei *et al.*, 2009). Kamei *et al.* (2009) have reported a microfluidic selection port where only hESC clusters of a defined size were admitted into the downstream culture chambers.

While these methods offer a straightforward experimental procedure and allow the use of relatively simple microfluidic devices, they lack two important aspects for microfluidic cell culture. Firstly, flowing through ECM components results in coating the walls of the entire microfluidic channel network and therefore promoting cell adhesion throughout the entire microfluidic device. This can affect cells in the downstream culture area by exposing these cells with signalling cues secreted from cells in the upstream section. The definition of a dedicated cell growth area, and thus a precisely defined cell culture chamber within the microfluidic device, is difficult.

Secondly, loading a microfluidic chip with a cell suspension solution in long microchannels may result in cell settling due to gravity. A low flow rate during cell seeding has to be chosen to prevent hydrodynamic shear induced cell damage. However, low flow rates may also result in cell settling due to gravity before reaching a dedicated cell culture compartment. It is therefore difficult to find an appropriate flow rate, and such flow rate will also vary with different microfluidic chip designs and cell types.

Different solutions have been presented to address these flow-related effects during seeding. For example, Kim *et al.* (2006) have developed a microfluidic hydrodynamic shear stress gradient device with four chambers for mESC culture. Each chamber can be loaded over a seeding channel to ensure equal seeding densities across all chambers by manipulating valves. Gomez-Sjoberg *et al.* (2007) achieved an automatic seeding of MSCs by using a microscope and an image analysis algorithm to determine seeding density refilling the culture chamber accordingly with cell solution until the required seeding density was reached. To prevent cell adhesion outside the culture chamber, the microchannels were coated with Pluronic® F-68, a cell-repellent reagent.

Both examples demonstrate that the complexity of the microfluidic network design or experimental procedure in microfluidic devices increases with more advanced, flow-based solutions for cell seeding, which may reduce device reliability.

3.1.1.2 Alternative seeding methods

To simplify cell seeding and avoid the challenges described previously (see section 3.1.1.1), microfluidic networks which can be detached from a cell culture substrate allow a simple route to efficient cell seeding. Instead of waiting until cells are confluent in a microfluidic channel, cells are grown in a Petri Dish or on a microscope slide until cells are confluent or ready for experimentation and then closed with a microfluidic network. Various solutions to seal the microfluidic chip with the cell laden substrate have been presented using vacuum, magnets or clamps (Chung *et al.*, 2007; Tamanaha *et al.*, 2009; Tkachenko *et al.*, 2009). Tilles *et al.* (2001) have developed a method, in which a microscope glass slide was seeded, either with hepatocytes only or with fibroblasts and hepatocytes as a random co-culture, in a Petri dish. Once the glass slide was confluent, it could then be mounted in the bioreactor. However, these methods require special care when assembling the microfluidic device to avoid contamination.

3.2 Second issue: Hydrodynamic shear stress

Hydrodynamic shear stress caused by continuous culture can be a reason why cells detach from a substrate (Gutierrez *et al.*, 2008; Lu *et al.*, 2004), change their morphology (Metallo *et al.*, 2008) and, in the case of ESCs for example, may lose their pluripotency.

Microfluidic devices for the culture and manipulation of hESCs have been presented (Abhyankar & Beebe, 2007; Figallo *et al.*, 2007; Korin *et al.*, 2009b), but the continuous culture of hESCs remains a challenge. In case of a feeder culture system, hESC colonies must be attached to the feeder layer, before continuous culture can be started. However, hESCs in particular seem to be prone to wash out under continuous hydrodynamic shear stress (Korin *et al.*, 2009a).

Several examples of flow-stop modes or cell re-feeding schedules with long periods of static incubation have been reported, where cells remained pluripotent (Kamei *et al.*, 2009; Korin *et al.*, 2009a). However, for continuous culture culture the reports in literature are inconclusive. Wash-out of hESCs within a few hours was reported for a straight microchannel with a syringe-pump actuated flow rate of 0.05 ml h^{-1} (Korin *et al.*, 2006). To minimise hydrodynamic shear stress on cells, gentle pump methods such as gravitational flow have been proposed for handling of cells (Boettcher *et al.*, 2008).

In a Y-channel design and using gravitational flow up to 1.5 ml h^{-1}, for example an approximately ten-fold increase in hydrodynamic shear, viable cells did not wash out and in fact retained their undifferentiated state over 96 hours of culture (Villa-Diaz *et al.*, 2009). The latter study also used the gravitational flow to obtain a gentle seeding procedure. This indicates that the seeding method and the proper attachment to the cell growth surface are in fact critical for the success of continuous culture of hESC in microfluidic devices and may as well depend on the used cell line.

Other designs have been proposed, where cells are not directly exposed to hydrodynamic shear (Liu *et al.*, 2008; Toh *et al.*, 2007) or the shear stress distribution in the culture chamber has been adjusted with flow restrictors to a more uniform velocity profile (Petronis *et al.*, 2006).

3.2.1 Theoretical considerations for continuous culture in microfluidic devices

Shear stress at the wall in a rectangular channel can be expressed as a function of flow rate Q and channel dimensions h and w (the derivation of the equation can be found in the Appendix C):

$$\tau_{wall} = 6 \cdot \mu \cdot \frac{Q}{h^2 \cdot w} \tag{3.1}$$

Another important characteristic number represents the media residence time (MRT). This becomes an important characteristic when studying steady-state versus transient microenvironments of stem cells described in section 1.3.

A bioreactor might not be ideally designed and stagnant zones in the bioreactor might falsify concentration predictions. The residence time distribution unveils such non-ideal bioreactor performance. The mean media residence time can be predicted with a simple equation:

$$\bar{t}_{MRT} = \frac{V_{CC}}{Q} \tag{3.2}$$

where $\bar{t}_{MRT}$ is the mean media residence time, V_{CC} the volume of the culture chamber and Q the volumetric flow rate.

For a straight microchannel (W: 1.5 mm, L: 30 mm, H: 125 μm) shear stress levels can be as high as 0.2 dyne cm^{-2} at the cell culture plane and the MRT ranges from 40 s to 6 min (see figure 3.2).

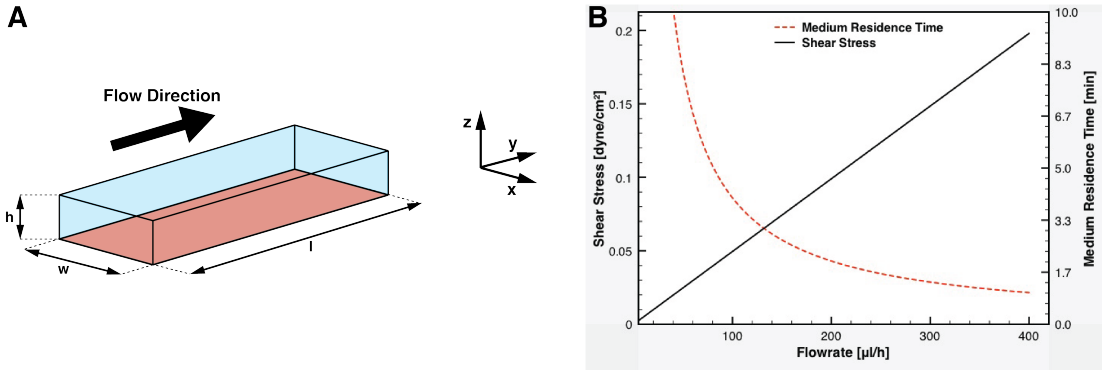

Figure 3.2: Shear Stress and MRT in a microchannel - Schematic of the microchannel and flow direction (**A**). Hydrodynamic shear stress and medium residence time in a microchannel can be calculated as a function of Q and the geometrical dimensions (W: 1.5 mm, L: 30 mm, H: 125 μm) of the microchannel section (**B**).

By analysing equation 3.1, hydrodynamic shear stress can be reduced by either lowering the flowrate Q and/or increasing the cross-sectional dimensions h and w. Medium residence time (MRT) is an important measure how long a molecule remains in a bioreactor chamber. As shear stress scales linearly with width and squared with height, a larger culture chamber design is advantageous. If compared with a straight microchannel, a large chamber design allows MRT to be changed/varied while the shear stress remains almost constant.

The calculations so far were based on average velocities across the entire microchannel section and do not represent the real physics. It has to be noted that flow in a tube or microchannel is generally known as Hagen-Poiseuille flow. The characteristics for Hagen-Poiseuille flow are that the maximum velocity is reached at the centre of the channel and equals zero at the walls.

3.3 Design of the microfabricated cell culture device

To address the issues associated with microfluidic continuous culture of adherent cells described in the section 3.1, a microfluidic continuous culture bioreactor is presented with a simple, yet reliable seeding method and a low hydrodynamic shear stress microfluidic network. The modular design of the microfluidic devices described in chapter 2 serve as basis for the microfluidic continuous culture bioreactor.

To streamline the seeding procedure in the microfabricated cell culture device with standard, laboratory scale cell culture techniques, a static seeding method with direct access to the microfluidic culture chamber using a standard laboratory pipette is proposed. In the open configuration, the microfluidic chip and the interface plate form a well with a depth D_W (see figure 3.3 **A**). The depth D_W can be adjusted by varying the thickness of the interface plate and the microfluidic chip to match the liquid film height in a standard T-flask for example (3 mm in a T25 flask with 5 ml working volume). By matching the surface-to-volume ratios in the microfabricated cell culture device during seeding, similar gaseous tension levels at the cell culture substrate can be expected.

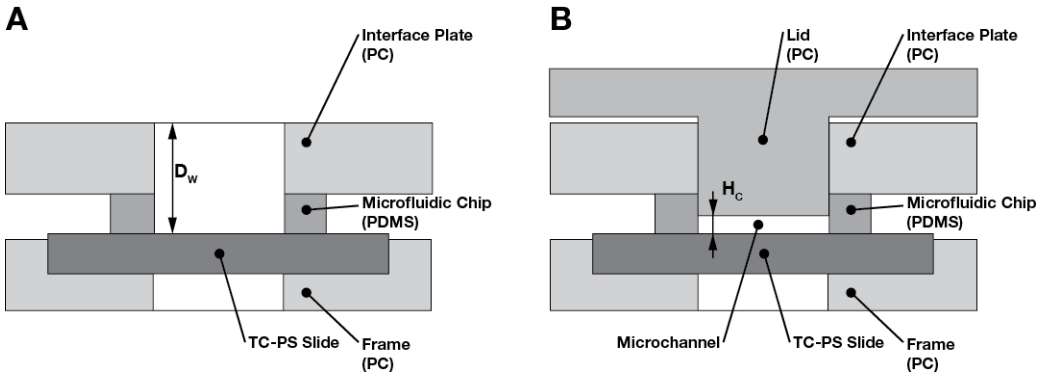

Figure 3.3: Cross-sectional schematic of the microfabricated cell culture device concept and its two modes - (**A**) shows a cross-sectional schematic of the modular bioreactor in the open configuration used for coating with ECM and seeding of cells. D_W defines the depth of the well during static incubation of ECM and cells. In continuous culture mode, a lid is used to form a microfluidic channel with a height H_C (**B**). Figure is not to scale.

Once cell seeding in the microfabricated cell culture device is completed and cells have attached to the culture substrate, a T-shaped lid made from PC seals the microchannel network in the microfabricated cell culture device (see figure 3.3 **B**). The horizontal bar of T-shape lid acts as bedstop and defines therefore the height H_C of the microchannel. The height H_C can be adjusted by altering the length of the vertical bar of the T-shape lid.

To prevent a wash out of viable cells during continuous culture, hydrodynamic shear stress due to flow has to be minimised. Three engineering parameters can be identified by analysing equation 3.1: flow rate Q, microchannel width w and microchannel height

h. To lower hydrodynamic shear stress level below the indicated maximum for hESCs (see figure 3.5), flow rate Q can be reduced, but this will also affect the medium residence time. Ideally, hydrodynamic shear stress should be engineered independently from MRT.

The modularity of the packaging system described in chapter 2 allows us to engineer hydrodynamic shear stress by adjusting the geometry parameters h and w. The design of the T-shape lid, for example, enables quick adjustments of hydrodynamic shear stress by altering the length of the vertical bar which defines the microchannel height H_C. By widening the microchannel width and increasing microchannel height in the cell culture chamber (in comparison with a straight microchannel, see figure 3.4), hydrodynamic shear stress can be lowered below the critical hydrodynamic shear stress causing a wash out of hESCs and remains almost constant for a wide range of different MRTs (see figure 3.5).

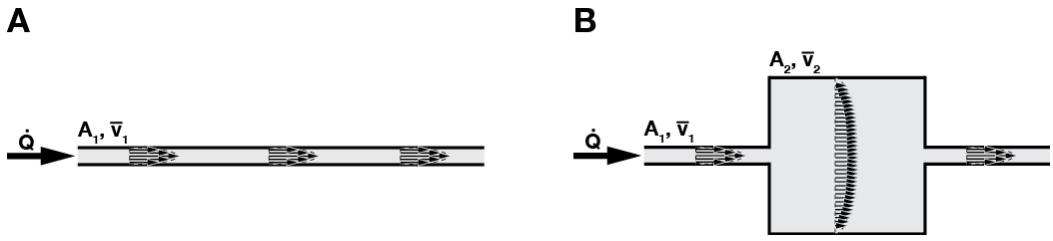

Figure 3.4: Schematic of an approach to lower hydrodynamic shear stress - (**A**) shows a schematic of a straight microfluidic channel and the velocity profile. To lower hydrodynamic shear stress, widening of the channel lowers the velocity field and therefore the shear tensor for the same volumetric flow rate Q (**B**). Conservation of mass imposes that $\overline{v}_2 = \overline{v}_1 \cdot A_1 \cdot A_2^{-1}$. Figure is not to scale.

3.4 Materials & methods

3.4.1 Modelling of critical parameters

The Navier-Stokes equations were solved using the finite element method (FEM) software package Comsol Multiphysics 3.5a/4.1 (Comsol, Cambridge, UK) for a set of parameters (see table 3.1). To solve the problem, it was assumed that a) the three-dimensional model is in steady-state, b) the flow is fully developed, c) no slip at the boundaries occurs, d) an incompressible fluid is used and e) the influence of cells at the

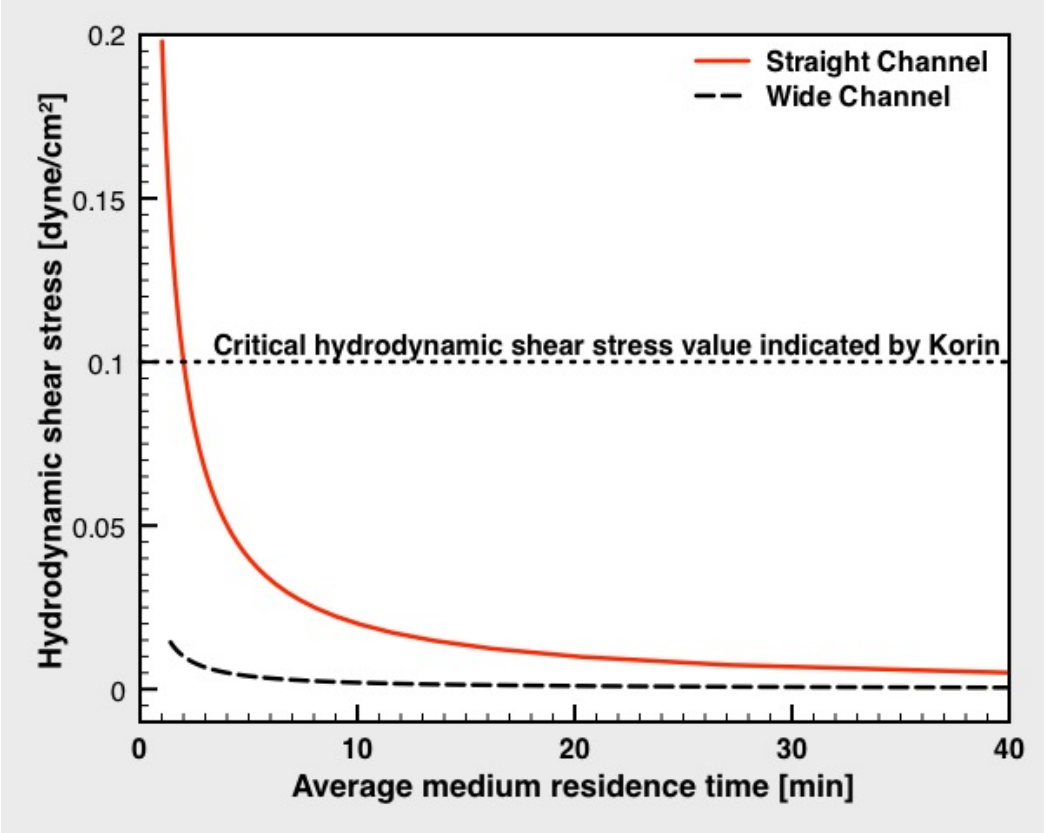

Figure 3.5: Hydrodynamic shear stress as a function of average medium residence time - Analytical equations were used to calculate hydrodynamic shear stress and average medium residence time for a straight channel (red solid line) (W: 1.5 mm, L: 30 mm, H: 125 μm) and a wide channel (black dashed line) (W: 12 mm, L: 4 mm, H: 450 μm). Korin *et al.* (2009a) indicated a maximum hydrodynamic shear stress of 0.1 dyne cm^{-2} at which a wash out of viable hESC colonies occured.

bottom of the channel can be neglected. Water at 37°C was used as working fluid and assumed to be sufficiently comparable with cell culture media. For all models simulated, the boundary conditions were set at the inlet to an average velocity (calculated from the flow rate), at the outlet to zero pressure and at the channel walls to non-slip.

Due to the longitudinal symmetry of the microfabricated cell culture device layout, only one half of the microfluidic chip was incorporated in the model to minimise computational time. For comparison, a straight channel (L: 30 mm, W: 1 mm, H: 125 μm) was incorporated as an entire model. The three dimensional domain of the microfabricated cell culture device and the straight channel were meshed using tetrahedral elements. For the microfluidic chip, the mesh size was varied between 2.5 to 7.5 μm, resulting in 527539 elements. The straight channel had a uniform mesh size of 5 μm, resulting in 54300 elements. Both models were solved with a built-in linear system solver UMFPACK. For both the microfluidic and the straight channel, hydrodynamic shear stress was calculated from simulated velocity profiles with the following equation:

$$\tau_h = \mu \cdot \dot{\gamma} \tag{3.3}$$

where τ_h is the shear stress at a height h from the surface, μ the dynamic viscosity and the $\dot{\gamma}$ shear rate. To verify and compare the calculated shear stress from the models, the analytical solution of the equation to determine the shear stress at the wall was used:

$$\tau_{wall} = 6 \cdot \mu \cdot \frac{Q}{h^2 \cdot w} \tag{3.4}$$

where τ_w is the shear stress at the wall, h the height of the microchannel, w the width of the microchannel, μ the dynamic viscosity and Q the volumetric flow rate.

Table 3.1: Parameters used for finite element models - Water has been considered a valid approximation for cell culture media as a fluid.

Parameters	Value	Unit	Reference
Density H_2O	993.249	kg m^{-3}	Interpolated from Lemon (2009)
Dynamic viscosity H_2O	6.96×10^{-4}	Pa s	Interpolated from Lemon (2009)
Volumetric flow rate	300	μl h^{-1}	Design specification

3.4.2 Fabrication of the cell culture device

The modular microfabricated cell culture device consisted of reusable and disposable parts based on the second generation packaging described in section 2.2.2. Reusable parts included a lid made from poly(carbonate) (PC) and a modified interface plate (PC). A gasket and a microfluidic chip made from poly(dimethylsiloxane) (PDMS), and a TC-PS slide (16004, Nunc, Denmark) were the disposable parts (see figure 3.6).

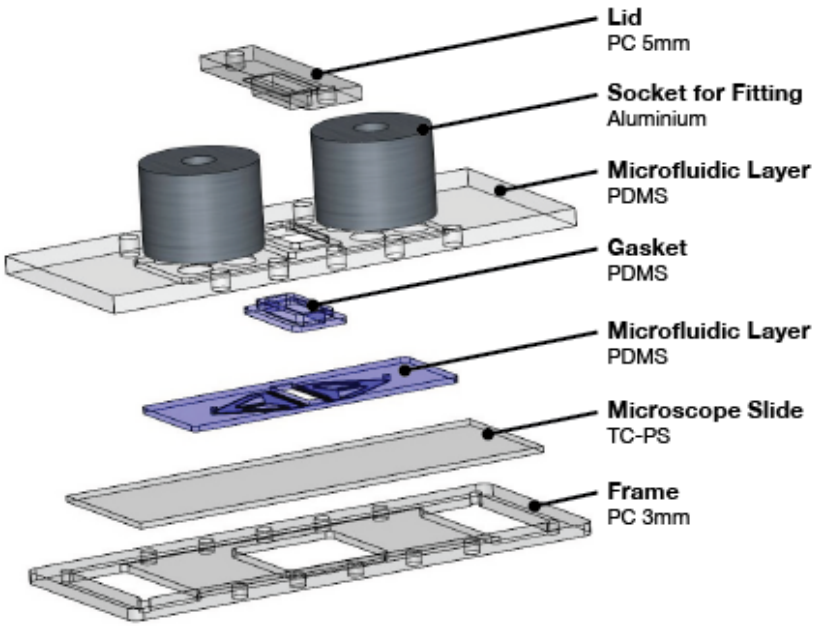

Figure 3.6: Exploded view showing all parts of the modular microfabricated cell culture device - The reusable world-to-chip interface was made from polycarbonate and aluminium and the disposable parts from poly(dimethylsiloxane) (PDMS). The tissue culture polystyrene (TC-PS) microscope slide and the microfluidic chip are compression-sealed between the top plate and the bottom frame. The opening in the microfluidic chip and the TC-PS slide then define the culture chamber body and the cell growth surface, respectively. To seal the chamber, the lid forms a press fit with the corresponding gasket. For cell culture imaging, an opening in the frame provides optical access to the TC-PS slide for the objective of an inverted fluorescence microscope.

The interface plate included an opening to hold the lid. The position of the opening matched the footprint of the culture chamber of the microfluidic PDMS chip. The interface plate also had two recesses included. The first positioned the microfluidic PDMS chip with respect to the interface plate, and the second deeper recess, accommodated the gasket. A set of bores in the interface plate enabled the two interconnects to be

mounted. A more detailed drawing of the interface plate can be found in Appendix B.16.

The frame had the same outer dimensions as the interface plate and its recess was of the dimensions of a microscope slide to hold the TC-PS slide (see Appendix B.8 for dimensions). The opening in the centre was designed to bring objectives from an inverted fluorescence microscope into close proximity with the TC-PS slide for cell culture imaging.

The lid was T-shaped with the upper horizontal bar acting as a bed stop when the lower vertical bar was pushed into the opening of the top plate. This defined the height of the culture chamber below (450 μm). The vertical bar formed a press-fit with the gasket to seal the chamber.

The microfluidic chip was made from two PDMS layers. The first layer included nineteen flow restrictors (200 μm $\times$ 1000 μm) on each side of the cell culture chamber (4 mm $\times$ 13 mm) (see figure 3.7, and for more dimensions, Appendix B.19).

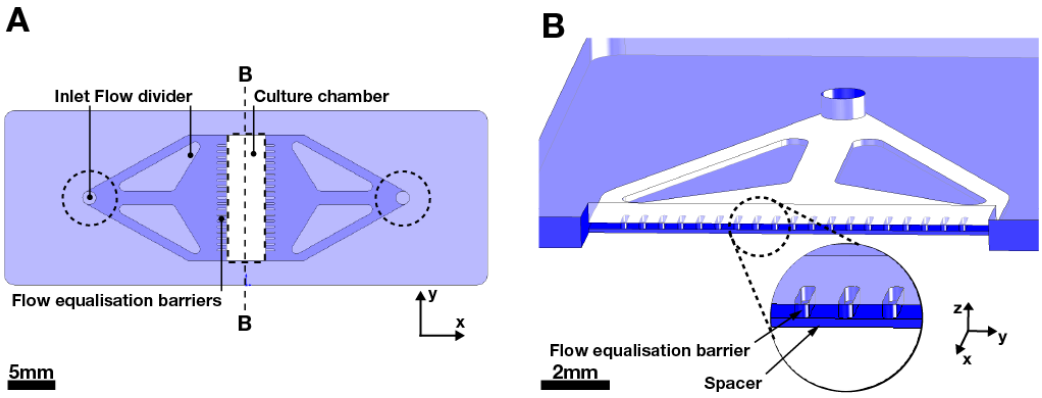

Figure 3.7: Schematic of the microfluidic continuous culture chip - (**A**) shows a schematic of the channel arrangement of the microfluidic chip with an inlet/outlet port, flow diffuser, flow equalisation barriers and a cell culture chamber body allowing access to the cell culture slide for cell seeding, which had an area of 4 mm $\times$ 13 mm (dashed rectangular). The dashed circles around the inlet and outlet ports depict the sealing areas of the cylinders of the protruding bosses of the fluidic connectors. (**B**) shows a section in the middle of the microfluidic chip. The height between the lower solid line and the dashed line depicts the membrane that elevates the flow restrictors, whereas the upper solid line approximately depicts the culture chamber height when the microfabricated cell culture device is in continuous culture configuration. Figure is to scale.

The apertures between the restrictors had rectangular cross-sections (400 μm $\times$ 200

μm). The inlet and outlet ports were connected with the chamber by three dividing channels on each side.

The second layer (spacer) elevated the first layer above the cell culture plane by 120 μm. For ease of seeding with a pipette, the dimensions of the cell culture area were chosen 4 mm wide and 13 mm long, resulting in a cell growth area of 52 mm^2.

A gasket made from PDMS was designed to fit into the recess in the top plate to ensure a leak-free operation both during seeding and continuous culture (see Appendix B.18 for dimensions).

The mould for the microfluidic manifold layer followed a similar procedure as described in section 2.3.1. The mould for the microfluidic manifold layer was milled (8,000-16,000 rpm, 104 mm min^{-1}) in Dural with 2 mm, 1 mm and 200 μm diameter end mills (2 flute standard length, Kyocera Micro Tools, USA). 2 mm and 1 mm diameter end mills were used to create the microfluidic manifolds or channels. A 200 μm diameter end mill was used to machine the flow restrictors. Poly(dimethylsiloxane) (PDMS) (Sylgard 184, Dow Corning, USA) was mixed in a ratio of 10:1, base to curing agent, and degassed under vacuum for approximately 15 minutes. The PDMS monomer was cast into the negative Dural mould and thoroughly degassed again until no air bubbles were visible. A 3 mm thick PC sheet was then placed on top of the mould and the stack clamped between two aluminium plates. Care was taken to prevent inclusion of air bubbles (see figure 3.8, **1-3**).

The clamped stack was placed in an oven at 85°C for 1 hour to cure the PDMS. After removing the aluminium plates, the enclosed mould was left to cool. The microfluidic manifold layer was then released from the mould with tweezers (see figure 3.8, **4**). Excess PDMS of the culture chamber body of the microfluidic manifold layer was cut out with a scalpel under a microscope.

A membrane at the bottom of the microfluidic chip determined the elevation of the flow restrictors with respect to the cell culture chamber bottom.

To fabricate the membrane, a 4 inch silicon wafer (Prolog Semicor, Ukraine) was silanised to prevent subsequent sticking of the PDMS. 200 μl of the trichloro(1H,1H,2H,-2H-perfluorooctyl)silane (448931, Sigma-Aldrich, UK) was dispensed into a vial and placed with the silicon wafer in a desiccator under vacuum for 1 hour. 5 ml of degassed PDMS was spun with a spin coater (P6708D, Specialty Coating Systems, USA) on the silanised wafer at 500 revolutions per minute for 50 seconds to obtain a thickness of

approximately 120 μm and placed in an oven at 85°C for 1 hour to cure (see figure 3.8, **3**).

To bond the thin PDMS membrane with the PDMS microfluidic manifold layer, an air plasma was used. Before bonding, the PDMS-coated wafer and the microfluidic manifold layer were rinsed with ethanol and subsequently dried. Both PDMS layers were then exposed to air plasma for 90 seconds at 30 W and 500 mTorr (PDC-002, Harrick Plasma, USA). The microfluidic manifold layer and the membrane on the wafer were then immediately brought into contact for bonding (see figure 3.8, **5**). To further strengthen the bond, the microfluidic chip was placed in an oven at 80°C for at least 2 hours.

The parts of the PDMS membrane which covered the cell culture chamber body of the microfluidic chip were cut away with a scalpel to provide free access to the cell culture slide underneath (see figure 3.8, **6**). The dimensions of the mould and the microfluidic chip were measured with a stylus profilometer (Dektak 8, Veeco Instruments Company, USA) and the quality of the mould was inspected with a SEM (XB1540 Cross-Beam, Carl Zeiss AG, Germany).

To cast the gasket, a negative mould was milled into a 5 mm thick poly(methylmethacrylate) (PMMA) (20070, Nordisk Plast, Denmark) using a 1 mm diameter end mill (2 flute standard length, Kyocera Micro Tools, USA). The gasket was cast in a similar manner as the microfluidic chip.

3.4.3 Cell culture

The Shef-3 hESC line (< passage 70) was obtained from the UK Stem Cell Bank and used for all experiments. Primary mouse embryonic fibroblasts (MEFs) (< passage 5), used as a feeder layer, were maintained in Dulbecco's Modified Eagle Medium (DMEM) (41965, Invitrogen, USA) supplemented with 10 % (v/v) heat inactivated foetal bovine serum (FBS) (10270, Invitrogen, USA) and 1 % (v/v) Modified Eagle Medium Non-Essential Amino Acids (MEM NEAA) (11140, Invitrogen, USA), passaged every 3 days into T25-flasks (159910, Nunc, Denmark) and cultivated in a humidified incubator at 37°C and 5% CO_2.

To inactivate the MEFs the growth medium was replaced with 5-7 ml of normal MEF growth medium supplemented with 1 mg ml^{-1} of mitomycin C (M4287, Sigma-Aldrich, UK), and incubated for 2 hours at 37°C. After inactivation cells were washed

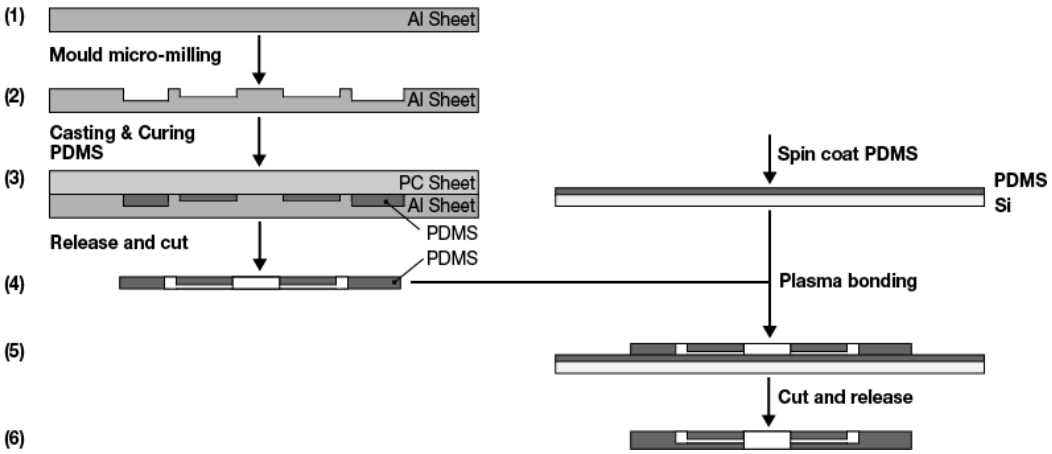

Figure 3.8: Fabrication process of a mould and a microfluidic chip created in the mould - (**1**) A sheet of dural was machined with a micro-milling machine to a mould (**2**). (**3**) PDMS was casted into the mould and then vacuum degassed. A PC sheet was placed on top of the mould and clamped together. Concurrently, a silanised silicon wafer was spin coated with PDMS to form a membrane. The PDMS-coated wafer and the clamped mould were then cured for 1 hour at 85°C in an oven. (**4**) The microfluidic manifold layer was released from the mould and the culture chamber body was cut out. (**5**) The microfluidic manifold layer and the PDMS membrane were exposed to an air plasma and immediately brought into contact for bonding. (**6**) The membrane at the bottom of the culture chamber body was cut out and the microfluidic chip was cut to shape and released from the wafer. Figure is not to scale.

three times with Dulbecco's phosphate buffer solution (DPBS) (D1408, Sigma-Aldrich, UK) detached with a trypsin:EDTA solution (T4049, Sigma-Aldrich, UK) for 3 minutes, quenched with normal MEF medium, centrifuged and re-suspended in MEF media before being seeded at a density of 15,000 cells cm^{-2} into T25-flasks which had been pre-coated with a 0.1 % (w/v) in DPBS gelatine solution (G1890, Sigma-Aldrich, UK) for 10 minutes at room temperature.

hESCs were cultivated in KnockOut DMEM (10829, Invitrogen, USA) supplemented with 20 % KnockOut Serum Replacement (10828, Invitrogen, USA), supplemented with 1 % MEM NEAA (11140, Invitrogen, USA), 2 mM L-Glutamine (21051, Invitrogen, USA), 0.1 mM β-mercaptoethanol (M3148, Sigma-Aldrich, UK) and 4 ng ml^{-1} FGF2 (4114-TC, RD Systems, USA). For passaging, flasks were incubated with 1.5 ml of 0.025 mg ml^{-1} collagenase solution (17104, Invitrogen, USA) for 5 minutes, before being replaced with fresh hESC medium. hESC colonies were then dissected into medium-sized colonies using pasteur pipettes and transferred into a new flask containing feeder cells prepared as outlined above.

3.4.4 Experimental procedure

Before every cell culture experiment, all parts of the microfabricated cell culture device and all tubing and tools required for assembly were autoclaved. The microfabricated cell culture device was then assembled with a sterile TC-PS slide in a laminar flow hood. For substrate coating and cell seeding, the lid was removed (open configuration, Figure 3.9 **A**). Laboratory pipettes with 200 μl pipette tips were employed for all steps. The TC-PS surface of the culture chamber and three single-well dishes (353653, BD Biosciences, USA) were coated with 0.1 % (w/v) gelatine in DPBS solution, and left to incubate at room temperature for 15 min. Then, each dish was seeded with 40,000 inactivated MEFs (seeding density of 13,800 cells cm^{-2}). The microfabricated cell culture device was seeded with 20,000 inactivated MEFs (40,000 cells cm^{-2}) in a suspension of 200 μl culture medium (Figure 3.9 **A**) (A higher cell density was chosen for the microfabricated cell culture device to ensure confluency.) The dish and microfabricated cell culture device were transferred to incubator (37°C, 5% CO_2). For transfer between laminar flow hood and incubator, the microfabricated cell culture device was placed in a large sterile glass Petri Dish (2175553, Schott, USA) (Figure 3.9 **C**). 1 day later, 6-8 dissected hESC colonies (250 μm to 1 mm in diameter) were

seeded in the microfabricated cell culture device, 10-12 dissected hESC colonies in the dishes, and incubated (37°C, 5% CO_2) for 1 day (Figure 3.9 **B** & **C**). Before perfusing the cell culture in the microfabricated cell culture device, the medium in the culture chamber was aspirated and the microfabricated cell culture device closed with the lid (closed configuration, Figure 3.9 **D**). The microfabricated cell culture device was manually primed with culture medium using a syringe. Two tubings, an autoclavable tubing (R1230, Upchurch Scientific, USA) with Upchurch fittings (P207, Upchurch Scientific, USA) and a gas-permeable silastic tubing (R3607, Tygon, USA), connected the syringe with the microfabricated cell culture device (see figure 3.10). The two tubings were attached to each other via Luer adapters (F331 and P659, Upchurch Scientific, USA). After priming of the microfabricated cell culture device, the syringe was placed on the syringe drive (Model100, KD Scientific, USA) and the cell culture in the microfabricated cell culture device perfused for 2 days with culture medium at a flow rate of 300 μl h^{-1}. Medium in the control dishes was exchanged every day.

3.4.5 Immunocytochemistry

For immunocytochemistry, the lid of the microfabricated cell culture device was removed and all operations carried out with a standard laboratory pipette (see figure 3.9 **E**). hESC colonies were fixed with 4 % (v/v) paraformaldehyde (PFA) in phosphate buffered saline (PBS) for 20 minutes and washed three times in PBS supplemented with 10% (v/v) FBS to block non specific binding. Primary monoclonal antibodies Oct-4 (SC-5279, Santa Cruz, USA), Tra-1-81 (MAB4381, Chemicon, UK) and SSEA-3 (MAB4303, Chemicon, UK) were used at a dilution of 1:200, incubating them with the cells for one hour at 37°C. The fixed cells were washed with PBS three times and incubated with secondary antibodies that had an excitation wavelength of 488 nm (A21212, Invitrogen, USA) and 555 nm (A21426, Invitrogen, USA) for an hour at room temperature. Finally, the cells were stained with 4',6-diamidino-2-phenylindole (DAPI) (D1306, Invitrogen, Carlsbad, CA, USA). DAPI at a dilution of 1:200 was incubated with cells at room temperature for 10 minutes. Daily cell culture inspections and end-point assay imaging were performed with an inverted microscope (Eclipse TE2000-U, microscope camera DS-Fi1, Nikon, Japan).

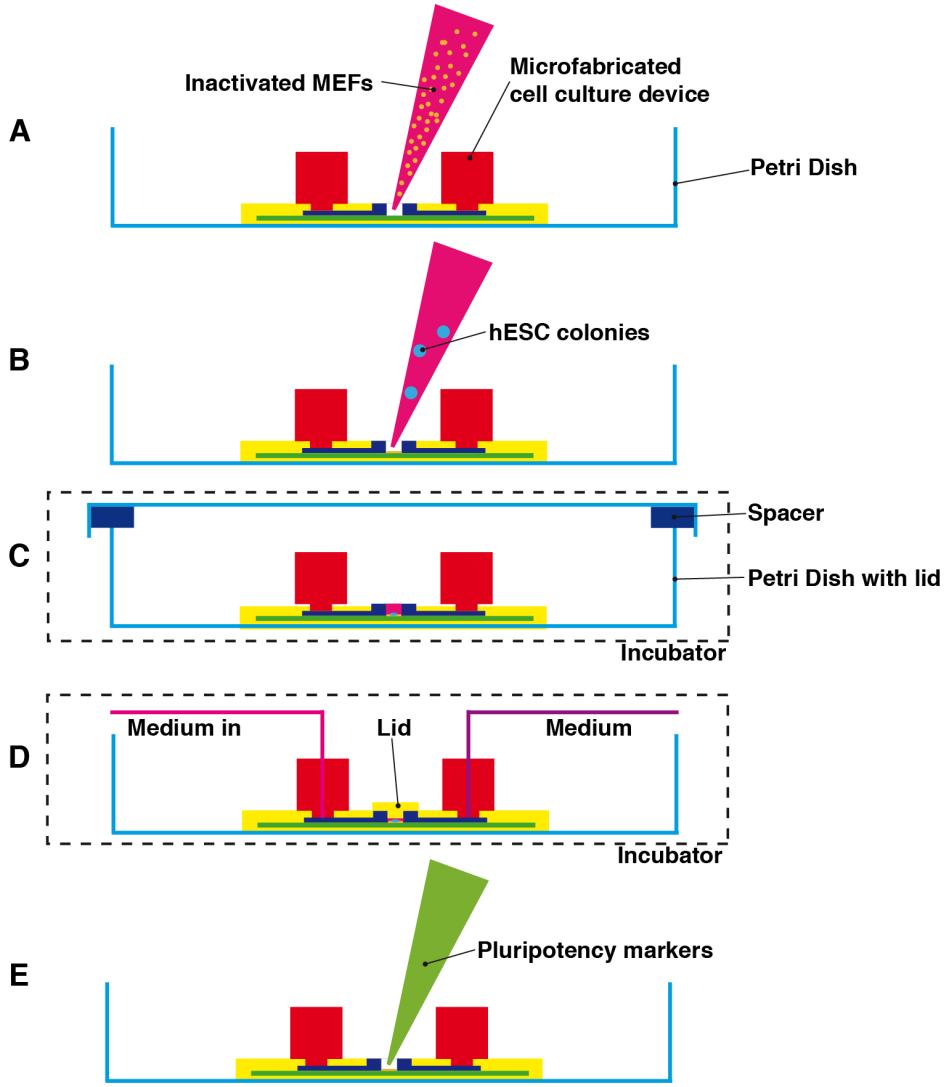

Figure 3.9: Seeding procedure - Schematic of the procedure for the microfabricated cell culture device in seeding and continuous culture configurations. (**A**) The TC-PS in the microfabricated cell culture device was coated with 0.1% gelatine with a pipette prior to seeding of the feeder cells. Inactivated MEFs were seeded subsequently with a pipette directly into the cell culture chamber of the microfabricated cell culture device and left overnight in an incubator to attach to the surface. A Petri dish fitted with spacers for gas exchange was used to accommodate a microfabricated cell culture device and kept in an incubator at 37°C and 5% CO_2 (**C**). hESC colonies were added into the culture area with a pipette (**B**), the Petri dish subsequently closed and the microfabricated cell culture device placed back into an incubator (**C**). Prior to changing to the perfusion configuration, medium was aspirated and the culture chamber closed with a lid. Tubing was connected to the microfabricated cell culture device and perfusion started using a syringe pump for 48 hours in an incubator (**D**). On the last day of experiment, medium was aspirated, cells fixed and stained with pluripotency markers to assess the effect of seeding and perfusion of hESC in a microfabricated cell culture device (**E**). Figure is not to scale.

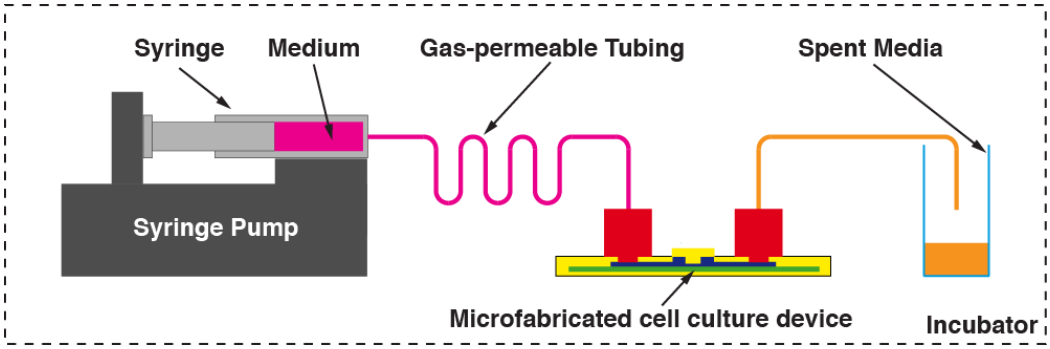

Figure 3.10: Schematic representation of the continuous culture setup - A syringe pump is used to pump media through gas-permeable tubing to adjust gaseous tension levels before entering the microfabricated cell culture device. A waste container is used to collect media from the outlet of the microfabricated cell culture device. The entire setup is placed in an incubator to maintain the culture temperature.

3.5 Results & discussion

The objectives of this chapter were to establish a microfabricated cell culture device which i) can be configured with cell growth surfaces typically employed in current routine hESC maintenance, ii) is compatible with standard laboratory procedures, and iii) maintains viable hESCs in continuous culture in order to fully harness the advantages of microfluidics for the probing of hESC behaviour and the implications for stem cell bioprocessing.

3.5.1 Design of the microfabricated cell culture device

To this end, a microfabricated cell culture device has been developed, where each part fulfils a specific function. The modularity of the packaging system allowed the optimisation of each part individually, i.e. without having to re-design the entire microfabricated cell culture device. To further facilitate the rapid re-design of the microfabricated cell culture device, the microfluidic chip was fabricated using the rapid prototyping technique described in chapter 2 (see also Appendix E.1 for additional characterisation using stylus profilometry and scanning electron microscopy). Additionally, the reusable parts of the microfabricated cell culture device (lid, interface plate, bottom frame, sockets) form a world-to-chip interface that can accommodate any microfluidic chip re-design as long as the inlet/outlet ports remain at the same position on the chip. Furthermore,

to ensure sterile long-term cultivations, all parts are fabricated from autoclavable materials such as poly(carbonate).

The interface plate and the frame provide the scaffold for the modular design. They align and reversibly seal all parts to each other and therefore offer an easy assembly of the microfabricated cell culture device. The frame of the microfabricated cell culture device holds a TC-PS slide or any slide of that size. Integration of TC-PS with microfluidic devices would normally be difficult, since TC-PS is not compatible with conventional bonding techniques. With this microfabricated cell culture device, slides of different material can easily be integrated.

The PDMS microfluidic chip controls the distribution of cell culture medium in the microfabricated cell culture device (see figure 3.7). The top layer contains a rectangular culture chamber body and flow restrictors on its sides. The flow restrictors promote a homogeneous velocity field during continuous culture. The efficacy of such restrictors to create uniform flow velocity fields was previously demonstrated with slightly larger apertures (Petronis *et al.*, 2006), and with smaller rectangular apertures (Hung *et al.*, 2005). The perfusion barriers were implemented to minimise non-uniform cell growth patterns which can arise from variations in velocity fields and thus, difficult to interpret (Aunins *et al.*, 2003).

The bottom PDMS spacer layer elevates the main plane of medium flow above the cell growth surface. This elevation reduces the hydrodynamic shear stress on the cells and therefore minimises the risk of cell dislodgement during medium perfusion.

Since the thickness of the layer is determined by spin-coating parameters, the elevation can easily be changed, for example to optimise shear stress levels versus mass transport conditions in the culture chamber or to conduct shear stress assays. Physical separation of medium flow plane and cell growth surface has been shown previously, but either required a large minimum separation distance to allow needle insertion for cell seeding (Stangegaard *et al.*, 2006) or was not combined with flow restrictors (Figallo *et al.*, 2007).

In this configuration, the separation distance can be freely chosen and is independent of the restrictor geometry that controls the flow. The re-sealable lid provides a simple means to open and close the culture chamber. To close the chamber the lid is inserted into the corresponding opening of the interface plate and forms a press fit with the compressible PDMS of the gasket. Due to the T-shape of the lid, i.e. due to the

horizontal bar acting as a bed stop, the same chamber height is attained in every experiment. Additionally, the hard material of the lid does not deform during medium perfusion ensuring reproducible fluid flow patterns from experiment to experiment.

PDMS has been reported to absorb small hydrophobic molecules such as proteins on the walls of microfluidic networks or to leach uncured oligomers (Regehr *et al.*, 2009; Toepke & Beebe, 2006).

However, alternatives have to be found to avoid negative effects caused by PDMS on experimental outcomes. Surface modifications of the PDMS microchannels may address these concerns (Wong & Ho, 2009). For example, it has been shown that the microchannels are rendered more hydrophilic by adding Pluronic®to the PDMS mixture before casting (Wu & Hjort, 2009). Such an approach could also be used to prevent for example protein adsorption on the walls of the microfluidic network. However the high diffusivity of oxygen in PDMS may represent an issue for oxygen sensitive applications such as differentiation of ESCs under hypoxic conditions in intermittent flow.

Materials such as medical grade silicones or polyurethanes have been investigated in preliminary experiments to offer an alternative to PDMS (James, 2007; Thompson, 2009). In contrast to PDMS, the fabrication methods for these materials are though immature at present for use in microfluidic devices.

For example the higher viscosity of medical grade silicones requires longer vacuum desiccation times to remove air bubbles than PDMS and casting of microfluidic layers becomes problematic to prevent air bubble inclusion in the mould.

The fabrication of polyurethane microfluidic devices is a lengthy process requiring a PDMS mould and a solvent to dissolve polyurethane granulates. It allowed thus only a layer by layer deposition to prevent bubble formation when evaporating the solvent.

Using the second generation packaging system has also facilitated rapid set-up of the cell culture experiment and achieved leak-free long-term operation, an easy and robust interconnection with the macro-world. In this reactor, the protruding structures of the interconnects press on the inlet/outlet ports of the PDMS microfluidic chip, which provides a leak-tight seal upon device assembly. Additionally, the interconnects accept standard Upchurch fittings and therefore permit simple connection with tubing for manipulation of medium.

Finally, to analyse and quantify the cell culture outcome, for example for real-time monitoring of molecular markers, the microfabricated cell culture device fits onto an inverted fluorescence microscope stage and the bottom frame has an opening to bring objectives into close proximity with the cell culture.

3.5.2 FEM analysis of the microfluidic chip

The Navier-Stokes equations for three dimensional models of the microfluidic chip of the microfabricated cell culture device and, for comparison, a straight channel have been solved by using a FEM software package. Previous reports indicated that shear stress is a critical parameter (Korin *et al.*, 2009b), which were confirmed in preliminary experiments (see Appendix D).

To evaluate the performance of our design, we compared it with a straight microchannel and analysed the velocity fields and shear stress for both configurations.

The uniformity of the flow velocity in the microfabricated cell culture device field has been confirmed at various heights above the culture plane. In comparison with the straight channel microfabricated cell culture device (for details, Appendix D.1) the velocity field at half the height of the inlet channel is one order of magnitude lower than in the straight channel with the same flow rate of 300 μl h^{-1} (see figure 3.11 **A**, **D**). 15 μm above the cell culture plane, the velocity field is approximately two orders of magnitude lower than in the straight channel (see figure 3.11 **B**, **E**). The flow restriction barriers produce an evenly distributed flow velocity field across the culture chamber (see figure 3.11 **C**), similar to the straight channel (see figure 3.11 **D**). An increased velocity at the boundaries of the microfabricated cell culture device can be observed due to the larger gap between flow restrictor and the boundary (see figure 3.11 **C**). Air bubbles included during closing or filling are likely to be removed through this gap when the bioreactor is positioned vertically.

Hydrodynamic shear stress was calculated 15 μm above the cell culture plane with a flow rate of 300 μl h^{-1} in both the microfabricated cell culture device and the straight channel. For the microfabricated cell culture device, an average of 1.1×10^{-3} dyne cm^{-2} and a standard deviation of 0.14×10^{-3} dyne cm^{-2} was obtained from the model. In contrast, the straight channel had an average hydrodynamic shear stress of approximately 0.16 dyne cm^{-2}. The calculated value of 1.3×10^{-3} dyne cm^{-2} using the analytical

solution for shear stress in the microfabricated cell culture device supports the result obtained through finite element modelling.

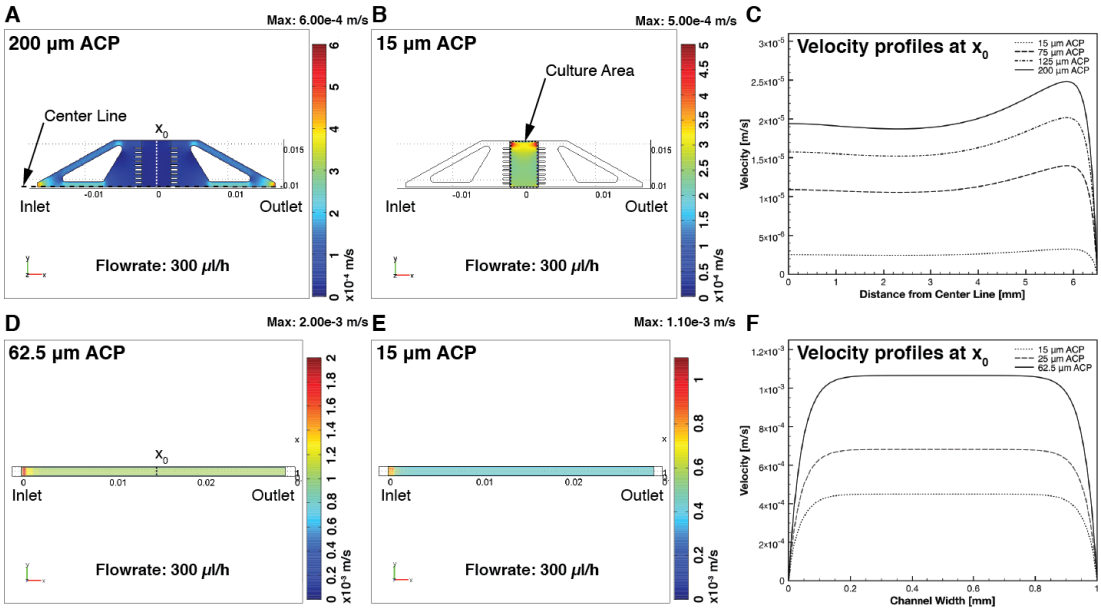

Figure 3.11: Modelling of flow conditions in the microfluidic chip and a straight channel - (**A**-**C**) relate to the microfluidic chip, and (**D**-**F**) to a straight channel. (**A**) and (**D**) represent the velocity field at half the height of the inlet channel. (**B**) and (**E**) represent the velocity field 15 μm above the culture plane (ACP). (**C**) and (**F**) show velocity profiles at x_0 along the Z-axis.

A conservative calculation of hydrodynamic shear stress has been applied for the design of a microfluidic culture device for murine embryonic stem cells (Kim *et al.*, 2006). The lowest values achieved in the reported microfluidic design are comparable with the range in which the microfabricated cell culture device is operated. It is therefore assumed that wash-out of viable cells is unlikely, as hydrodynamic shear stress is below the critical value of 1 mPa (1×10^{-2} dyne cm^{-2}) previously reported (Korin *et al.*, 2009a).

To verify the influence of the height in the culture chamber of the microfabricated cell culture device on hydrodynamic shear stress, three different configurations of the microfluidic chip have been analysed (see figure 3.12). The first model to analyse was a basic configuration of the microfluidic chip with a channel height of 200 μm (Figure 3.12 **A**). The second model contained the basic configuration of the first, but a a recessed

culture plane was added resulting in a channel height of 320 μm (Figure 3.12 **B**). The third model had the configuration which was used for all experiments and had a channel height of 450 μm (Figure 3.12 **C**).

By adding a recessed culture plane to the basic microfluidic model, a reduction of approximately 50% in hydrodynamic shear stress across the culture chamber was achieved (see figure 3.12 **B**, **D**). Hydrodynamic shear stress levels have been further reduced by adding a recessed culture plane and lid compared to the basic configuration shown in figure 3.12 **A**) resulted in a reduction of approximately 80% in hydrodynamic shear stress (see figure 3.12 **F**).

These quantitative measurements confirm that the height of the cell culture chamber in the microfabricated cell culture device plays an important role, showing also the flexibility of the design.

3.5.3 Integration with current laboratory procedures

To perform hESC cultures, the microfabricated cell culture device can be operated in an open configuration without the lid, and a closed configuration with the lid attached. In the open configuration, the culture chamber is directly accessible with laboratory pipettes. This makes it easy to apply the cell transfer methods typically employed in routine hESC maintenance at laboratory scale. Additionally, the exposure to hydrodynamic shear stress occurring with the flow-based dynamic seeding methods (Kim *et al.*, 2007) in closed microfluidic perfusion devices is avoided. Minimising exposure to hydrodynamic shear is particularly crucial for the handling of embryonic stem cells, since shear stress can affect the phenotype (Veraitch *et al.*, 2008).

Also, flow-based seeding could potentially even dissociate the multi-cellular hESC colonies before attachment to the feeder layers. Furthermore, in the open configuration, the depth of the culture fluid overlay in the microfluidic culture chamber is similar to the overlay in T25-flasks or in standard control dishes. During cell settling and attachment, the cells should thus experience a similar microenvironment as in traditional culture systems.

To test this concept, the microfabricated cell culture device was seeded with cells according to the protocol employed in our regenerative medicine laboratory (see Materials and Methods for more details). All parts of the microfabricated cell culture device were autoclaved, assembled to the open configuration with a TC-PS slide, and

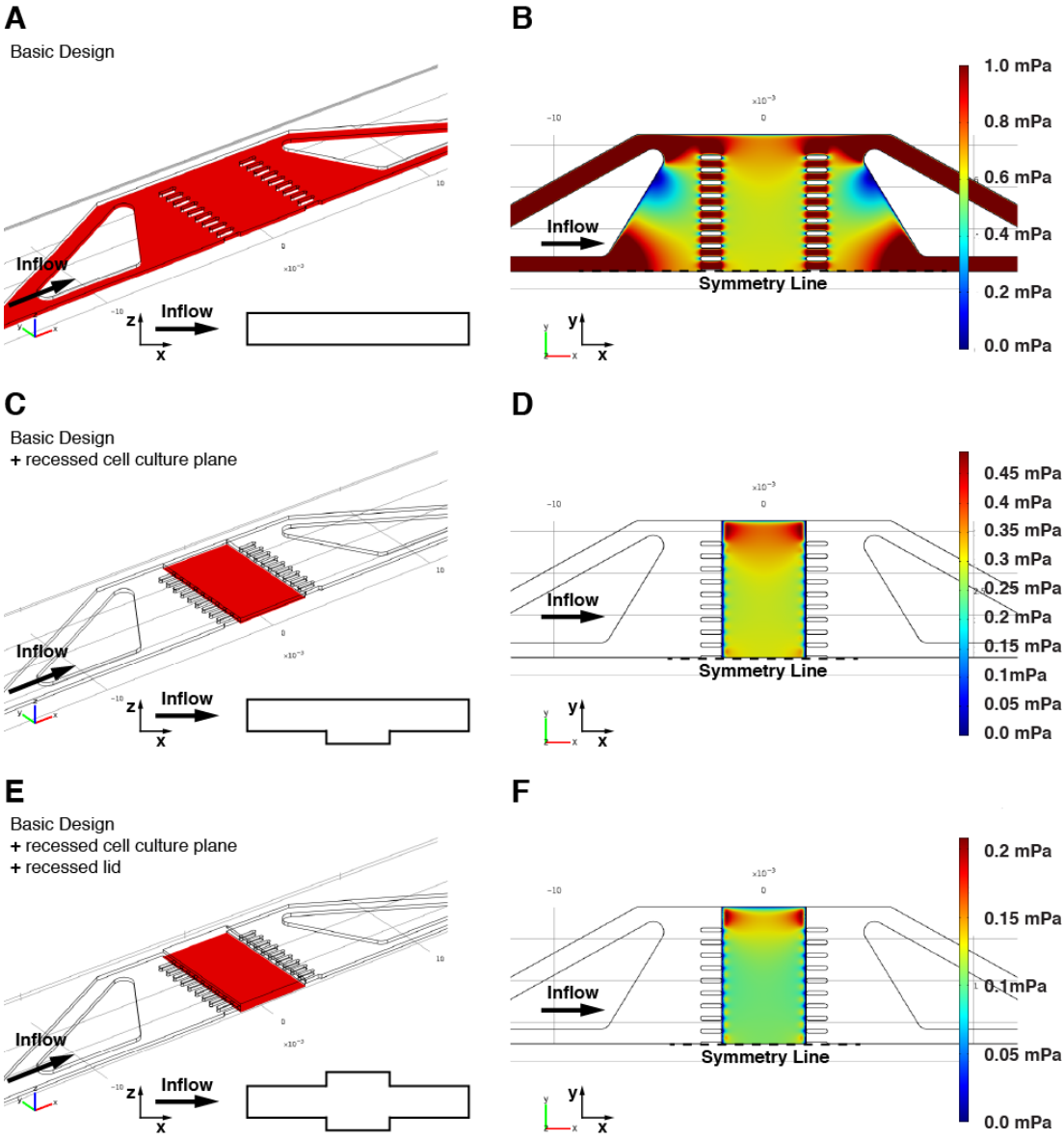

Figure 3.12: Influence of channel height on hydrodynamic shear stress in the microfabricated cell culture device - To gauge the influence of different channel heights, the microfluidic continuous chip was analysed in a basic configuration (**A**, **B**), the basic design and a recessed cell culture plane (**C**, **D**) and the basic design with a recessed cell culture plane and lid (**E**, **F**). A flow rate of 300 μl h^{-1} has been used for all models. Due to symmetry, only one half of the chip was simulated.

the culture chamber area coated with a 0.1 % (w/v) gelatine solution. To compare the outcome with traditional culture vessels, we seeded three single-well dishes in parallel to the microfabricated cell culture device.

In the microfabricated cell culture device and the control dishes, the inactivated mouse embryonic fibroblasts (iMEF) started to attach within 2 hours. After one day, the cells had attached and uniformly spread to attain their characteristic morphology in both systems (see figure 3.13 **A**, **E**). Furthermore, the cells did not grow into the apertures of the flow restrictors, demonstrating that the gelatine-coating step spatially defined the growth area for the cells in the microfabricated cell culture device. hESC colonies seeded to the uniform iMEF layer attached within 1 day. All colonies maintained an undifferentiated morphology and were comparable to the colonies in the control dishes (see figure 3.13 **B**, **F**).

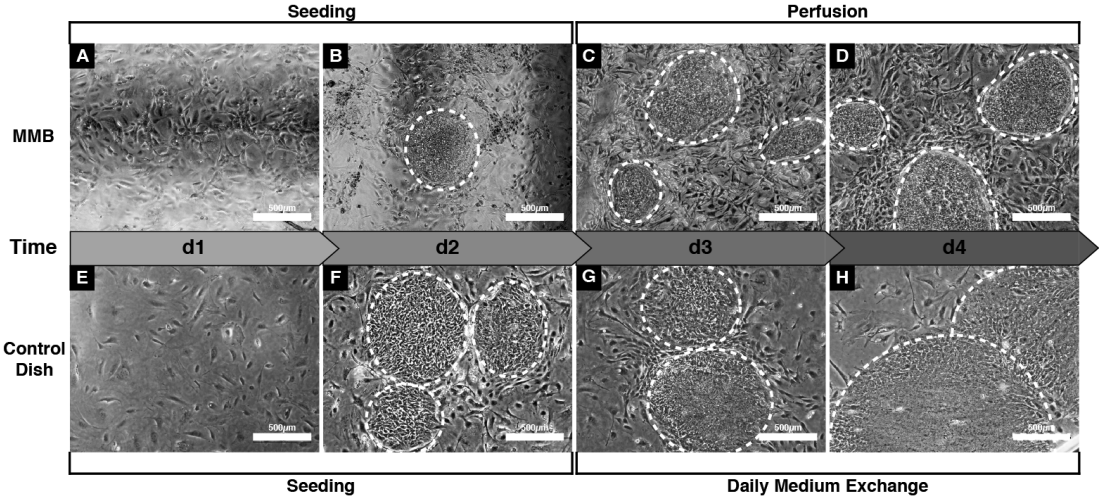

Figure 3.13: Comparison of morphology in control dishes and microfabricated cell culture device - Representative phase contrast images of iMEF feeder cells and hESC colonies cultured in the microfabricated cell culture device (**A** -**D**) and in the control dishes (**E** -**H**). All images were taken with 4× magnification, scale bar is 500 μm. Feeder cells attained their characteristic morphology in both systems 1 day after seeding (**A**, **E**). 1 day later, hESC colonies (highlighted with dashed lines) had attached to the feeder cells (**B**, **F**). After one day of culture, hESC colonies in the continuously perfused microfabricated cell culture device retained the characteristic morphology of undifferentiated hESCs and were of similar size to the colonies in the control dishes (**C**, **G**). After two days of culture, the hESC colonies continued to retain their undifferentiated morphology and were still of comparable size to the colonies in the control dishes (**D**, **H**)

3.5.4 hESC morphology & pluripotency after microfluidic continuous culture

After seeding, the microfabricated cell culture device was closed and the hESC culture was continuously perfused with a flow rate of 300 μl h^{-1} which resulted in a low medium residence time of approximately 5 min. In the control dishes, the medium was replaced once a day in line with standard manual cell culture practice. After 1 day, the colony sizes in the continuously perfused microfluidic chamber were comparable to the colonies in the control dishes (see figure 3.13 **C**, **G**). Additionally, the cells within the colonies were small and tightly packed together - a characteristic morphology of undifferentiated hESCs. A similar outcome was observed after a total of 2 days of continuous continuous culture: the hESCs were proliferating at a similar rate and maintained an undifferentiated morphology in both the microfabricated cell culture device (see figure 3.13 **D**) and in the control dishes (see figure 3.13 **H**). Furthermore, wash-out of viable colonies was not observed.

Immunocytochemistry for several pluripotency markers was carried out in the micro fabricated cell culture device after continuous culture. The cells from the first culture experiment were stained for Oct-4 (and co-stained with DAPI), and the cells from the second and third experiment were stained for Tra-1-81 and SSEA-3 (and co-stained with DAPI). The immunostaining sequences of antibody incubation and washing buffers were directly performed in the open configuration and according to typical immunostaining protocols. As can be seen in figure 3.14, the hESC colonies stained positively for Oct-4, Tra-1-81 and SSEA-3. The positive staining results confirmed the morphology observation that the hESC colonies maintained their undifferentiated state during seeding and continuous culture.

Continuous culture of feeder-attached hESC colonies in a microfabricated cell culture device without wash-out of viable colonies has thus successfully demonstrated. Additionally, the hESC colonies maintained the expression of the pluripotency markers after 2 days of constant medium perfusion. While these results must be further verified with feeder cell densities that match more closely the densities from the control dishes, the results indicate that in microfluidic devices the maintenance of pluripotent hESCs is not constrained to specific cell re-feeding schedules. It will therefore be possible to use the precise spatio-temporal control of the soluble microenvironment that microfluidics offer to probe the behaviour of hESCs. Additionally, by using the open access facility

of this MMB, the impact of a wide range of combinations of ECM components can be evaluated. Given the high costs of stem cell culture media, such a microfabricated cell culture device would be ideal to perform these investigations in a cost-effective manner.

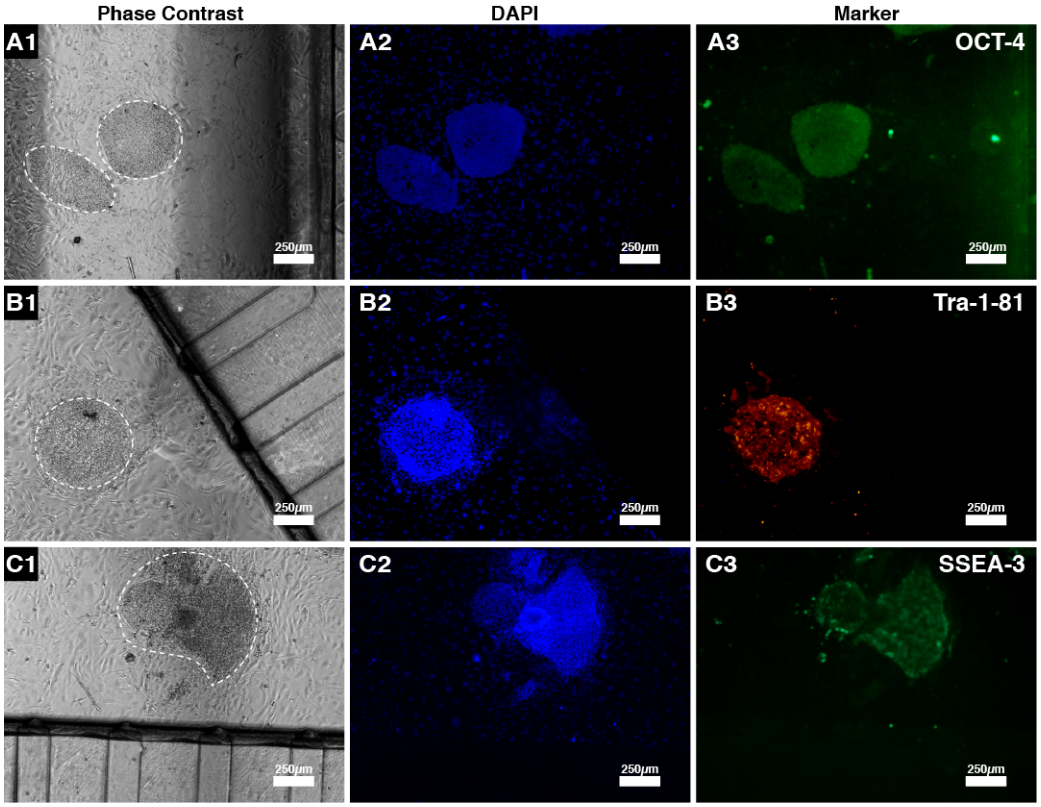

Figure 3.14: Representative images of the feeder-attached hESC colonies after 2 days of continuous culture perfusion in the microfabricated cell culture device - All images 4× magnification, scale bar is 250 μm. Each row shows the phase contrast images (**A1**, **B1**, **C1**) of the feeder-attached hESC colonies (highlighted with dashed lines) and the corresponding results from DAPI (**A2**, **B2**, **C2**) and pluripotency marker staining (**A3**, **B3**, **C3**). The phase contrast images (**B1**, **C1**) show the culture chamber area and the adjacent flow restrictors. Comparison with the corresponding DAPI images demonstrates that the feeder cells stayed in the culture chamber and did not outgrow into the flow restrictors. Viable colonies did not wash out and stained positively for Oct-4 (**A3**), Tra-1-81 (**B3**) and SSEA-3 (**C3**) confirming that the hESCs retained their undifferentiated state.

3.6 Summary of findings

A versatile and robust microfabricated cell culture device has been developed that can be autoclaved. The microfabricated cell culture device can easily be assembled and includes an interface which reversibly seals a disposable microfluidic chip with any culture substrate of microscope slide format. A lid offers direct access to the culture chamber which facilitates surface coating and cell seeding. The microfabricated cell culture device can therefore be configured with different cell growth surfaces. Additionally, a deep media overlay in the open configuration permits long incubation times during cell seeding, enabling the complete attachment of slowly and weakly adhering cells.

In FEM simulations, it was shown that the shear stress generated in the microfabricated cell culture device is two orders of magnitude lower than in a straight microchannel. Furthermore, changing the thickness of the spacer layer of the microfluidic chip enables to vary the hydrodynamic shear over the cells. It is therefore possible to rapidly test different microfluidic designs and fully exploit the versatility and the flow control offered by microfluidic perfusion devices.

In the open configuration, feeder-attached hESC colonies were seeded on a gelatine-coated TC-PS substrate in static conditions and according to current laboratory procedures. The feeder cells spread uniformly and attained their characteristic morphology in the same time as in the control dishes. The hESC colonies remained intact and retained their undifferentiated morphology. With the culture chamber closed, the feeder-attached hESC colonies were cultured in the continuous culture mode. Viable colonies did not wash out of the chamber. Furthermore, after 2 days of continuous perfusion, the hESC colonies stained positively for a set of typically used pluripotency markers.

These efforts address so far two important aspects of a microfluidic cell culture tool for stem cell bioprocess development. The flexibility to change and adapt the microfluidic chip has been shown by switching from the straight microchannel chip to a more complex low hydrodynamic shear stress microfluidic chip design. To address the scalability of results obtained with this cell culture device, three comparability criteria have been considered. Firstly, the use of TC-PS meets the requirement that the same materials are used as in small scale cell culture devices (e.g. T-flask). Secondly, the direct access to the cell culture chamber allows the use of seeding density units used in

small scale cell culture devices. Finally, the positive continuous perfusion experiments with delicate cells such as hESC on feeder cells encourage the efforts made to study the soluble microenvironment of stem cells.

However, to achieve throughput, a multiplexed system is required, which at least offers an experimental triplicate. Furthermore, to be of utility as a tool for stem cell bioprocess development or optimisation, an innovative monitoring solution to track the phenotypes needs to be incorporated into such a multiplexed system.

4

Development of a microfluidic platform with time-lapse imaging

The integrated rapid prototyping approach for microfabricated cell culture devices presented in chapter 2 has addressed the need for an adaptable and flexible packaging and fabrication methodology to take account of the rapid progress in stem cell research. In the previous chapter, a seeding method closely mimicking bench-scale seeding procedures has been developed using a lid to reseal a culture chamber within the microfabricated device. To prevent a wash out of viable cells, a low hydrodynamic shear stress microfluidic chip has been designed and both, seeding method and the low hydrodynamic shear stress microfluidic chip, successfully tested using hESC colonies. However, to serve as an automated and data-rich microscale stem cell bioprocess development and optimisation tool, a monitoring system is missing to link stem cell phenotypes to soluble cues in the microenvironment. This chapter addresses the last of the three aspect required for a microfluidic tool for stem cell bioprocess development and optimisation.

The results in this chapter have been presented in conference proceedings at the Micro Total Analysis Systems conference 2010 in Groningen, The Netherlands and at the Microtechnologies in Medicine and Biology conference 2011 in Lucerne, Switzerland (see Appendix G).

4.1 Integrating image-based monitoring techniques

Since the beginning of the nineteenth century, light microscopy has enabled biologists to describe the morphology of different cells, but the underlying functionalities and fundamentals of cellular processes remained largely undiscovered. Responses of living systems to cues were described, but the underlying molecular details required for a thorough understanding were not available.

Fluorescent antibody labelling techniques for proteins or DNA have enhanced the experimental capabilities to elucidate the underlying complex cellular pathways which control proliferation, differentiation or apoptosis, albeit only by sacrificing or fixing cells. However, the 'when and where' of cellular events in living cells can not be exactly pinpointed and fast cellular processes can not be tracked with these techniques.

The discovery of the green fluorescent protein (GFP) and other visible fluorescent probes has enabled to target specific gene expressions and therefore to monitor their expression over time without sacrificing cells (Chalfie, 2009; Tsien, 1998).

Light microscopy and visible fluorescence offer therefore a simple non-invasive route to monitor stem cell fates (Fu *et al.*, 2009). A few applications to characterise cells or entire organisms use already an imaging approach, for example to monitor the development of fish embryos (Clarke, 2009), cellular metabolites and ions using genetically encoded biosensors (Okumoto, 2010), or to characterise bona fide iPS cells (Chan *et al.*, 2009).

An automated microfluidic system with a time-lapse imaging system would therefore greatly benefit from the combination of phase contrast and fluorescence microscopy and thus enable automated analysis of experimental outcomes (see figure 4.1). In comparison to microfluidic tools for microbial bioprocesses where the cells are monitored for example using oxygen and pH sensors, this non-invasive imaging approach would also allow the direct monitoring of phenotypes *in situ* in real-time, if necessary, to obtain data-rich experimental sets. Furthermore, such an imaging approach would allow the study of phenotype variations under different culture parameters such as flow modes, hydrodynamic shear stress or oxygen tension levels and the measurement of proliferation kinetics or pluripotency *in situ* using advanced image processing algorithms for example.

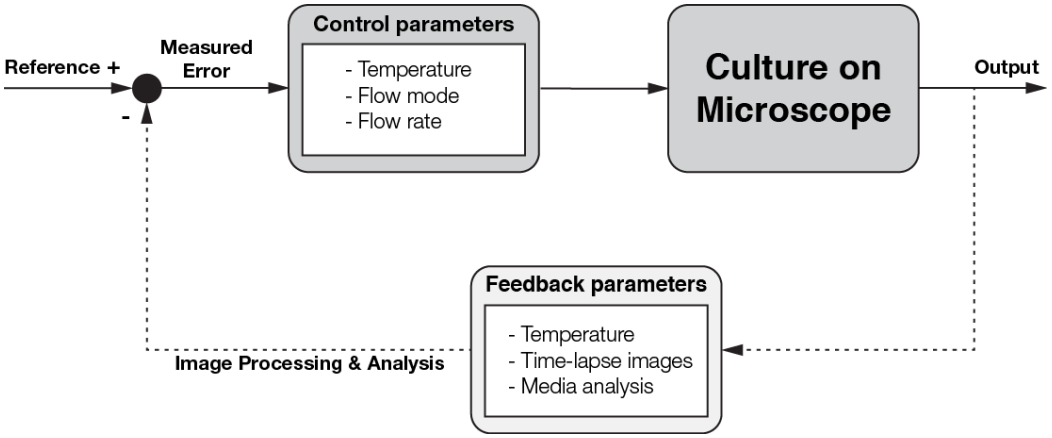

Figure 4.1: Feedback loop of the microfluidic platform for stem cell bioprocess development - A reference input to the system controls process parameters such as temperature, flow mode and flow rate during the culture on the microscope. A feedback loop automatically takes readings of all temperatures and images. Analysis of images and metabolites can be done in a semi-automated fashion. Traditional bioprocess parameters such as dissolved oxygen or pH can be added to the feedback loop for data-rich monitoring and control.

However, integration of real-time optical monitoring with microfluidic culture devices remains challenging, particularly for long-term culture (Charvin *et al.*, 2010), for example to maintain to sterility and gaseous tension levels in the media. Plate reader compatible, microfluidic culture systems have been recently reported to measure fluorescent tags as outlined in section 1.4.2. However, the analysis of cell morphology, a daily routine task in cell culture, still has to be carried out manually on an inverted microscope. Therefore, returning to a microscope and tracking of a specific area within such a microfluidic device may be difficult.

A charged-coupled device (CCD) has been directly mounted to a microfluidic cell culture device to count cells, but this solution may not be suitable for high resolution imaging of cell morphology or fluorescent labels (Ozcan & Demirci, 2008).

An inverted microscope is used when high quality images of cells are required for image analysis of phenotype or for determining cell numbers. A microfluidic culture chamber on an inverted microscope has been previously implemented with a transparent heater to monitor the proliferation of HeLa cells and to maintain culture temperature for the duration of inspection on the microscope (Petronis *et al.*, 2006). Albrecht *et al.* (2010) have presented a microfluidic platform with time-lapse imaging in a 96-well

format for mouse embryonic stem cells for the duration of 5 days.

All are examples for the experimental advantages microfluidic platforms with time-lapse imaging offer. However, the results obtained with these systems focus mainly on the handling of cells and the manipulation of medium in the microfluidic system. The time-dependent properties of medium are not taken into account, which arise from storage of medium at room temperature and its effects on various relevant culture conditions, for example pH. The interpretation and translation of the results obtained with these platforms, and therefore their relevance for scale, are thus difficult under such uncontrolled conditions.

4.2 Design of the microfluidic platform

The design of the platform follows the design requirements and considerations described in section 1.4.3.2. All functionalities of an incubator and a microfabricated cell culture device have to be integrated and combined to enable long term proliferation or differentiation of stem cells on an inverted microscope. This will serve as the basis towards the implementation of a feedback loop to link phenotype with culture conditions)(see also figure 4.1) By defining different sub-assemblies, an independent development and optimisation of modules and their functionalities can be achieved. Two sub-assemblies have been thus defined for the microfluidic platform - the microscope module and the media handling module (see figure 4.2). Both sub-assemblies are designed to be mobile that the platform can be used in different settings, for example during seeding or end-point analysis, or even in another cell-specific laboratory (for example our hESC laboratory).

4.2.1 Media handling module

The media handling module contains functionalities such as cooled storage and pumping of medium to the microscope module. Two autoclavable reservoirs provide medium for up to ten days of culture and can be selected by a set of valves. Each reservoir has a sparger for medium aeration, an exhaust port for pressure relief when not in use and a medium port for transporting medium to the microscope module. The set of valves controls which reservoir is pressurised with cell culture gas to move medium. Flow rates are controlled by the pressure in the reservoir using a computer controlled regulator.

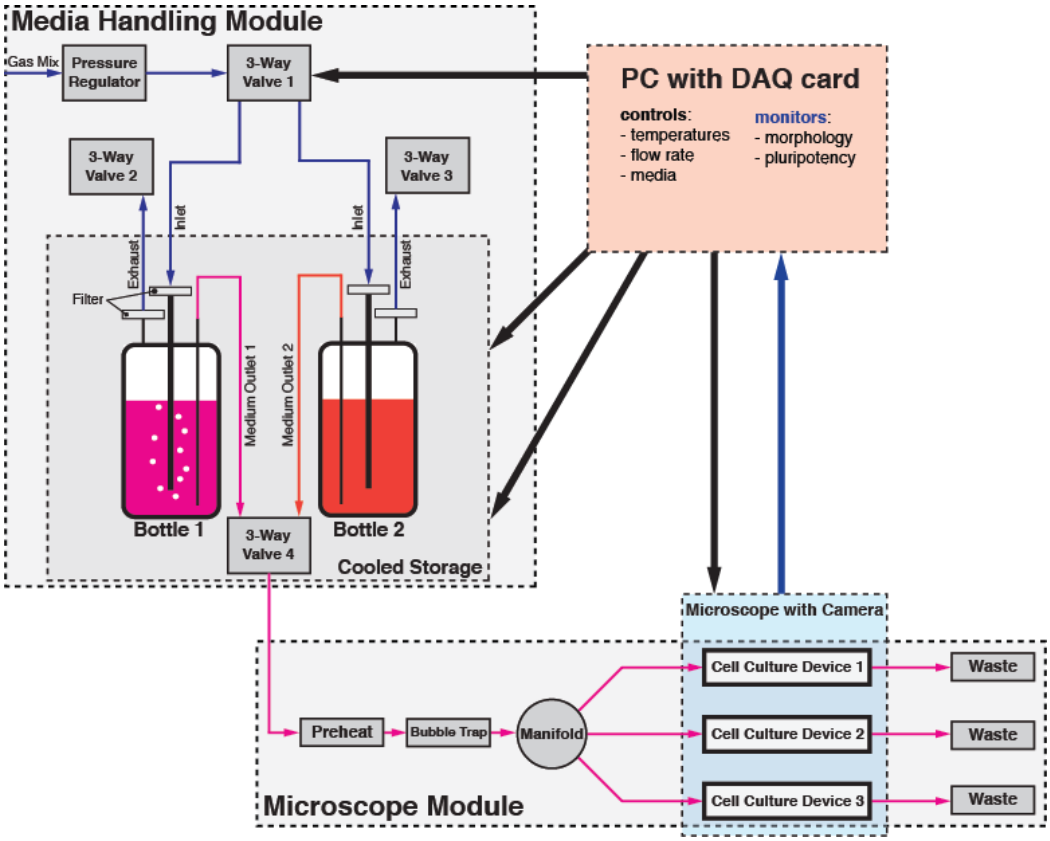

Figure 4.2: Schematic of the microfluidic platform - The microfluidic platform consists of two modules - the microscope module and the media handling module. The media handling module provides cooled storage of media and a set of valves and pressure regulators to pump media. In the microscope module, medium is heated up before it enters a bubble-trap and is split up to feed three parallel cell culture devices. A LabView™ routine is used to control all important culture parameters such as temperatures, media selection and flow rate.

Using pressure-based pumps allows a nearly instantaneous control of flow rates and thus preventing further dilution or transport of signalling factors into the cell culture chamber.

The media reservoirs are stored in a dark cabinet and cooled to prevent degradation of medium.

4.2.2 Microscope module

The microscope module consists of a preheat element, a bubble trap, a manifold, three microfabricated cell culture devices and waste containers.

The preheat element is designed to prevent a temperature shock to the cells in the microfabricated cell culture devices when medium is pumped from the cooled reservoir. Medium then passes through a bubble trap. A perpendicular bore is aligned and connected with the horizontal bore. When an air bubble enters the horizontal bore, it will rise in the perpendicular bore and therefore be removed from the medium entering the microfabricated cell culture devices (more details and dimensions can be found in Appendix B.27).

The modular microfabricated cell culture device is based on the third generation packaging described in chapter 2 and uses the seeding method described in chapter 3. For the platform, the microfabricated cell culture device has been modified to maintain the culture temperature for stem cells for the entire duration of an experiment. For that reason, a transparent resistive glass microscope slide is used instead of TC-PS as a heating element in the microfabricated cell culture device. Temperature on the cell growth surface is measured with a thermistor and controlled with a software-based PID[1] controller. The first generation microfluidic chip introduced in chapter 3 has been optimised to facilitate priming with medium.

A software-controlled microscope camera is used for phase contrast and fluorescent imaging. Spent medium is collected in waste bottles for each microfabricated cell culture device.

[1]PID stands for proportional-integral-derivative and is a widely used feedback controller

4.3 Materials & methods

4.3.1 Cell culture device

The third generation packaging system and the microfabricated cell culture device described in the sections 2.2.3 & 3.4.2 have been adapted and modified for use on an inverted microscope (see figure 4.3). A 5 mm thick poly(carbonate) plate was chosen to increase the stiffness of the interface plate. The interface plate has been fitted with four bores (3.15 mm in diameter) for M3 screws to keep the microfabricated cell culture device in place when mounted on the microscope. A pocket has been milled into the interface plate to fit a thermocouple for the temperature feedback loop. The pocket had a width and depth of 1.6 mm and a length of 22.8 mm. A M3 thread was made in the pocket to secure and hold the thermistor in position (see Appendix B.20 for dimensions). Two M3 threads for M3 × 30 mm standard brass screws (Clerkenwell Screws, UK) were manually cut on the other side of the interface plate to electrically connect an indium tin oxide (ITO) microscope glass slide (576352, Sigma-Aldrich, UK).

The frame was altered to minimise the contact area with the ITO microscope slide. The frame had one large opening (49.5 mm long, 26 mm wide), which made observation of the entire microfluidic chip possible (see Appendix B.21 for dimensions). The bearing area for the microscope slide had a raised middle part to separate the electrical contacts from the rest. The bearing area was covered with Kapton® tape (5413 (3/4"), 3M, USA) to electrically insulate it from the ITO microscope slide (see figure 4.3).

Both sockets at the inlet and outlet were fitted with Luer lock adapters (P-686, Upchurch, USA) to quickly connect tubing. At the inlet of the microfabricated cell culture device, an autoclavable 3-way valve (PMMM-700-156W, Fisher Scientific, UK) was attached to the Luer lock adapter.

The microfluidic layer manifold described in section 3.4.2 has been optimised to simplify priming by omitting the split channels into three microchannels (see Appendix B.25 for dimensions). A second microfluidic layer has been designed with a split cell culture chamber to culture two different cell lines in the same microfabricated cell culture device (see Appendix B.26 for dimensions). The lid to close the cell culture chamber of the microfabricated cell culture device has been simplified and adapted to the thickness of the interface plate (see Appendix B.22 for the single chamber version and Appendix B.23 for the split chamber version).

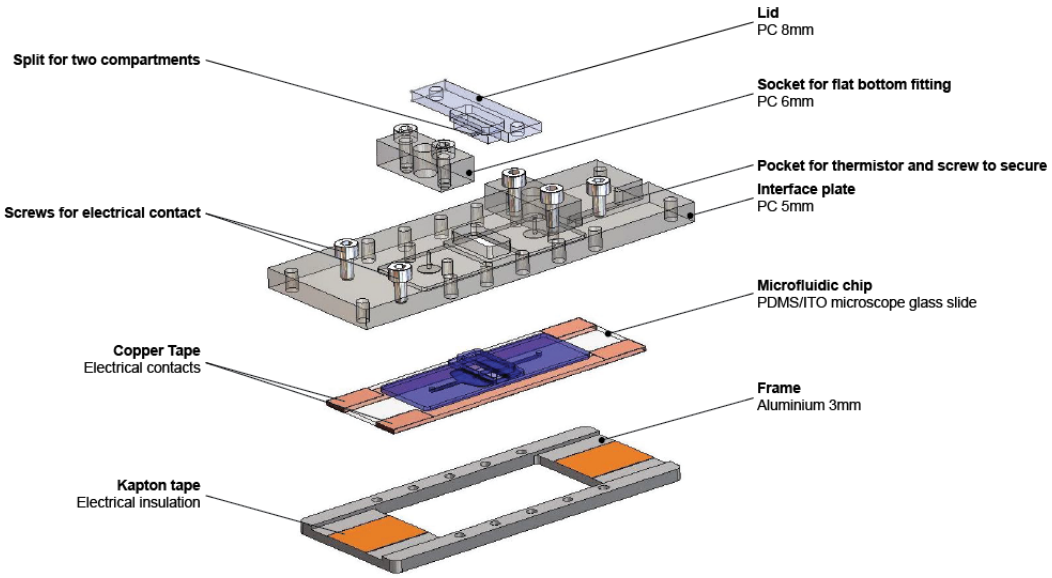

Figure 4.3: Exploded view of the cell culture device for the platform - Exploded view of the microfabricated cell culture device with the reusable parts of the packaging system and the disposable microfluidic chip consisting of a microfluidic layer, gasket and a resistive indium tin oxide (ITO) microscope slide. The frame has been improved for use on an inverted microscope and has been electrically insulated with Kapton® tape. The packaging system is based on the third generation described in section 2.2.3 and uses the the seeding method and a modified microfluidic layer described in section 3.4.4.

For the split cell culture chamber microfluidic layer, a seeding lid has been designed to avoid mixture of the different cell solutions (see Appendix B.24). All parts and moulds were fabricated using the rapid prototyping method described in section 3.4.2. However, all PDMS parts (gasket for lid, microfluidic layer and spacer) were first bonded and then the bonded PDMS microfluidic chip to the ITO microscope slide using the same plasma bonding technique described in section 3.4.2.

4.3.2 Pump

The pump consists of two 125 ml, autoclavable media reservoirs (2116-0125, Nalgene, USA). Each reservoir is fitted with three ports.

The inlet port is made from a stainless steel M6 hex screw. The hex cap has been machined into a round plate and a centred bore has been machined into the screw with a lathe. A stainless steel pipe was fitted into the centred bore by a press fit. An O-ring was placed at the former screw cap and the port was hold in the lid by a nut. The threaded end was fitted with a Luer lock adapter (P-660, Upchurch, USA) for a filter.

The second port was used as an exhaust port and was made in a similar fashion, except that the pipe has not been included. To fit two syringe filters as close as possible next to each other, a shorter thread was chosen for this port.

The third port was used as a fluid outlet. An M10 stainless steel screw was used as the basis for this port. The hex cap has been converted into a disc with a lathe. A centred bore was machined into the screw to provide a fluidical link. On the threaded end, a M6 thread has been machined in to accommodate a flat bottom fitting. A stainless steel pipe was also fitted into the centred bore by a press fit. An O-ring was placed at the former screw cap and the port was hold in the lid by a nut. The threaded end was fitted with a Luer lock adapter (P-660, Upchurch, USA).

A set of four 3-way valves was used to switch between the two media reservoirs. One valve (S070B-6CC, SMC, UK) was linked with the pressure regulator (ITV0011- 2BL-Q, SMC, UK) and controlled which medium reservoir was pressurised. Each valve was connected to the inlet port which has been fitted with a sterile filter (Minisart 16596, Sartorius Stedim, Germany). Medium was pumped by controlling the pressure in the reservoir. Each reservoir had an exhaust valve (S070B-6CC, SMC, UK) connected to the exhaust port (fitted with a sterile filter (Minisart 16596, Sartorius Stedim, Germany)) to release the pressure in the medium reservoir when not in use. The fluid

outlet of both reservoirs were linked to another switching valve (LHDA243115H, Lee Corporation, USA) (switching at the same time as the valve for the reservoir selection) which was connected to microscope module.

Medium was pumped from the reservoir through the preheat element (described in section 4.3.3) and a bubble trap in polytetrafluorethylene tubing (ID: 0.8 mm) (S1810-10, Bola, Germany) which was fitted with standard nut fittings (P-207, Upchurch, USA) and Luer lock adapters (P-657, Upchurch, USA).

The bubble trap had a T-shaped arrangement of bores. Fluid entered the trap in the horizontal bore (1 mm in diameter), while the bore perpendicular and vertical (5 mm in diameter) to the flow direction was fitted with a Luer lock adapter (P-686, Upchurch, USA) and a manual valve (W2-30600–2, Cole Parmer, UK) (see Appendix B.27 for dimensions).

Medium was distributed to three microfabricated cell culture devices using a manifold (P-150, Upchurch, USA) and 12 cm long capillary tubing (ID: 500 μm) (1532, Upchurch, USA) was attached to each port used of the manifold.

The three valves in the media handling module were driven with a custom-built electrical circuit (see Appendix B.31). The valve which fluidically linked the media reservoirs with the microfabricated cell culture devices was controlled by a fast switching relay (DMO063, Crydom, USA). The entire set of valves was controlled by a LabViewroutine.

The pump was characterised with a flow rate sensor (SLG1430-480, Sensirion, Switzerland) in a similar set up described in section 2.3.3 at the the flow splitter, when switching reservoirs and at the outlet of each microfabricated cell culture device. Flow rates were measured for three pressure regulator settings (300 mV, 400 mV, 500 mV).

4.3.3 Temperature feedback loop

The media reservoirs were stored in a cooled water bath to prevent media decomposition due to thermal exposure. The water bath consisted of an aluminium box with two holes (80 mm in diameter) in the lid (1590D, Hammond, Canada) and a converted Peltier cooling element (AA-60-12-00-00, Supercool, Sweden). A negative temperature coefficient (NTC) thermistor (B57703M103G, Epcos, Germany) was mounted on the inside wall of the aluminium box. The thermistor output was read with a custom made

circuit over the analog input port of a data acquisition (DAQ) card (USB-6221, National Instruments, USA) (see Appendix B.30). A LabView™ routine converted the read out voltage into a temperature reading. Temperature was controlled by a software-based PID feedback loop algorithm and pulse width modulation (PWM) (see figure 4.4). The PWM has been realised with a LabView routine (LabView 8.2, National Instruments, USA) using the digital outputs of the DAQ card.

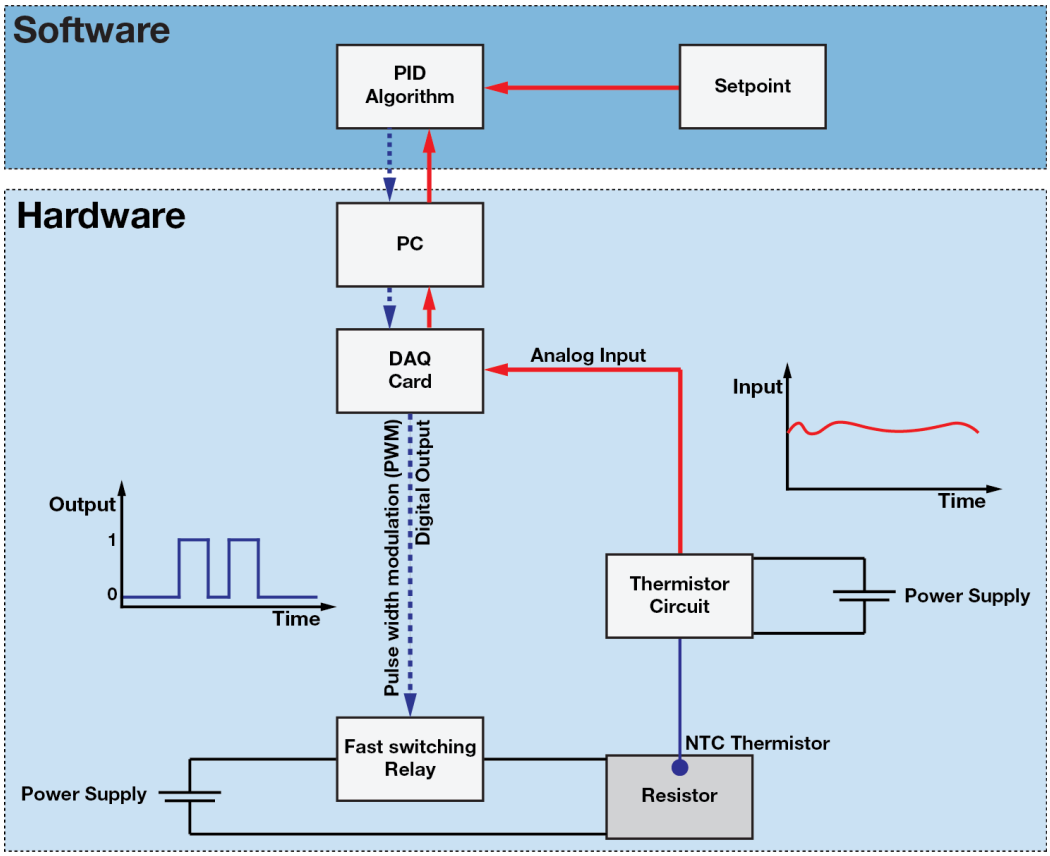

Figure 4.4: Schematic of the temperature control loop - Temperature control loop consists of a software PID algorithm and a sensor mounted on the microfluidic chip. The resistive heater is controlled by a relay which is actuated with the PWM using the digital output ports of the data acquisition (DAQ) card. Temperature is monitored with a negative temperature coefficient (NTC) thermistor and fed back to the DAQ card using the analog input ports. The PID algorithm processes the temperature reading and defines the pulse width.

The same PID control algorithm with pulse width modulation (PWM) was also used to control the temperature on the cell growth surface of each microfabricated cell

culture device (see figure 4.4). The routine controlled a solid state relay (CMX60D10, Crydom, USA) to switch the current of the power supply on or off. A NTC thermistor (B57861S103F40, Epcos, Germany) was used to measure the temperature on the cell growing surface of an ITO microscope slide. The custom-built circuit was also used to deliver a constant current for the thermistor and was read out using the analog input ports of the DAQ card (USB-6221, National Instruments, USA).

A 12 cm long conductive tape strip (1181 (1/4"), 3M, USA) was applied on the resistive side of the ITO microscope slide.. The tape was placed that on each side of the ITO microscope slide an excess of approximately 20 mm was made available. The excess was wrapped around to the non-conductive side of the microscope slide and cut off with a scalpel at the edge of the microfluidic chip.

The preheat element consisted of 4 parts and used the PID temperature controller described above. A resistive heating foil (HK5160R157L12B, Minco, USA) was controlled by the feedback loop algorithm using a fast switching relay (DMO063, Crydom, USA) and a NTC thermistor (B57045K103K, Epcos, Germany). The thermistor was screwed into part B of the housing (see Appendix B.29) and was facing towards the surface of the heating foil which was placed in part A of the housing (see Appendix B.28). Tubing was centred in a milled channel (1.6 mm $\times$ 1.6 mm) in part B of the housing. When the preheat element was assembled, the tubing in part B was facing the heating foil in part A.

4.3.4 Platform setup

For each module, a box was used to house all parts of the pump and temperature control. The microscope module consisted of a two modified boxes. The first box (PCM 175/150 G, Fibox, UK) housed on a mounting plate (MIV 175, Fibox, UK) all electrical circuits to control the temperature on the ITO microscope slides of the microfabricated cell culture devices, and the preheat element and the relay to control the switching valve between the two media reservoirs. The second box (6011324, Fibox, UK) was attached to first box and modified to accommodate three microfabricated cell culture devices and on a custom-made poly-carbonate mounting plate, the manifold, the bubble trap and the preheat element. The entire microscope module was attached using standard M3 screws to the manual stage of an inverted microscope (Eclipse TE2000-U, Nikon, Japan) with a camera (Scout scA1400, Basler Vision Technologies, Germany).

The media handling module was housed in a modified box with a hinged lid (CAB PC 303018 G, Fibox, UK) and was fitted with two 25 mm thick, 10 cm high and wide, custom made PMMA stands. The box contained the pressure regulator, the 3 valves, the cooling plate with the two media reservoirs and the circuits to control the valves and the temperature of the cooling plate.

Two power supplies (IPS 2303, Iso-Tech, UK) were used for the three microfabricated cell culture devices (12V, max. 1 A) and the cooling plate (24 V, 3 A). The fan of the cooling plate was powered by an unregulated power adapter at 5 V (UG01B, Maplin, UK).

An unregulated power adapter (L48BQ, Maplin, UK) at 12 V was used to power the circuits for the valves in the media handling module. The pressure regulator was powered using a 12 V power source (EP-920, Eagle Technologies, South Africa). The preheat element (24 V, 1 A) and the valve used for fluidic switching (24 V) were powered by a fourth power supply (LT30-2, Farnell Instruments, UK).

All relevant parameters of the platform were controlled and recorded by a LabView™ routine. LabView™ routines have also been programmed to tune the PID settings of all heaters (microfabricated cell culture device, preheat element and cooling plate) and to calibrate all thermistors.

4.3.5 Cell culture

Mouse embryonic stem cells (mESCs) with an Oct-4-GiP reporter (named Oct4-GFP hereafter) and 46Cs (mESC with a Sox-2 GFP reporter) were obtained from Stem Cell Sciences, Edinburgh, UK.

mESCs (all below p40) were routinely cultured on 0.1 % (w/v) filtered water porcine gelatin (G1890, Sigma, UK) coated T25 flasks (136196, Nunc, Denmark) in a humidified, 5% CO_2 controlled incubator. Medium in flasks was exchanged daily with 6 ml, fresh and warm medium. Medium consisted of Glasgow Minimal Essential Medium (GMEM) (G5154, Sigma, UK) and was supplemented with 10 % (v/v) fetal bovine serum (FBS) (EU-000-F, Sera Laboratories International, UK), 1 % (v/v) glutamax (35050-038, Invitrogen, USA), 1 % (v/v) sodium pyruvate (11360-039, Invitrogen, USA) , 0.2 % (v/v) of 2-β-mercaptoethanol (31350, Invitrogen, USA) and 1 % (v/v) ml of antibiotic-antimytotic solution (15240-062, Invitrogen, USA). After filter sterilisation,

500 μl leukemia inhibitor factor (LIF) (ESG1107, Millipore, UK) was added to the medium.

Cells were passaged every two days into new T25 flasks. New flasks were incubated each with 3 ml of 0.1 % (w/v) filtered water porcine gelatin solution at least 10 min prior to passaging in a laminar flow hood at room temperature. Cells were washed first with approximately 3 ml of Dulbecco's phosphate buffered saline (DPBS). DPBS was aspirated and 500 μl of trypsin added to the cells in the flask and incubated at 37°C for 3 min. To quench trypsin, approximately 4.5 ml of complete medium was added to a flask. The cell suspension was aspirated and added to a 50 ml centrifuge tube (210 261, CellStar Tubes, Greiner Bio-One). Cells were spun in a centrifuge (Centrifuge 5810R, Eppendorf, Germany) at 1200 revolutions per minute for 3 min at room temperature. The supernatant was aspirated and the pellet re-suspended in warm, fresh complete media. Cells were usually split in ratios of 1 to 8 or 10.

4.3.6 Experimental procedure

Prior to seeding, all microfabricated cell culture devices were placed in a glass Petri Dish and both sterilised using an autoclave. A standard laboratory pipette (Pipettor 20-200μl, Eppendorf, Germany) with an autoclaved tip (Ultratip 739295, Greiner Bio-One, Germany) a was used to coat the cell growth surface in the microfabricated cell culture device with 200 μl of 0.1 % (w/v) filtered water porcine gelatin solution. The microfabricated cell culture device was incubated for at least 1 h at room temperature in a laminar flow hood.

Cells were counted with a cell counter (CASY TTC, Roche Diagnostics, Switzerland) to determine the seeding density for both configurations, the improved microfluidic layer and the split microfluidic layer. 46C and Oct4-GFPs were processed as followed: Media in a T25 flask was aspirated. The cells were washed with 3 ml of DPBS (autoclaved) using a 5 ml pipette (86.1253.001, Sarstedt, Germany). 500 μl of trypsin were added with a 2 ml pipette (40502, Bibby Sterilin, UK). The T25 flasks were then incubated at 37°C and 5% CO_2 for 3 min (MCO-18M, Sanyo, UK). Trypsin was quenched with 4.5 ml of warm media using a 5 ml pipette (86.1253.001, Sarstedt, Germany) and pipette (Matrix, Thermo Scientific, UK). Cells were aspirated and transferred into a 50 ml tube. Tubes were spun at 1200 revolutions per minute for 3 min in a centrifuge (Centrifuge 5810R, Eppendorf, Germany). The supernatant was

aspirated with a 5 ml pipette and the remaining pellet broken off by taping the tube three times with a finger. The pellet for each cell line was re-suspended in 7 ml of fresh and warm media.

9.95 ml of filtered CasyTon were dispensed in the CasyTubes with an Anachem (25ml, Anachem, Germany). 50 μl of cell suspension were three times gently titurated and then added to the 9.95 ml of CasyTon (dilution factor 200). The tube was then turned three times to ensure mixing and immediately measured.

The Casy TTC was set to take a sample of 400 μl 5 times from the cell suspension to be counted. Between each sample, a count deviation tolerance of 20 % was allowed.

A target cell concentration of 260,000 cells ml^{-1} was achieved by taking 1 ml of the cell suspension, which has been used for the first measurement, and dilute to the correct concentration and measure again with the Casy TTC as described above. The gelatine solution was removed first from the cell culture chamber in the microfabricated cell culture device. The cell culture chamber has then been washed with 200 μl of media and 100 μl of cell suspension (corresponds to a seeding density of 10,000 cells cm^{-1}) have been added to each compartment (Oct-4: compartment 1, 46C compartment 2). 75 μl of medium has been used to top up each culture chamber. If the single culture chamber microfluidic chip was used, 200 μl of cell suspension using Oct-4 GFPs (corresponds to a seeding density of 10,000 cells cm^{-1}) has been added to the cell culture chamber, but no medium has been added as top up.

To prevent evaporation of medium in the microfabricated cell culture device, a cap of a 50 ml tube filled with 3 ml of sterile DPBS has been placed at the bottom of the Petri dish. Approximately 30 min later, media levels in the microfabricated cell culture devices were controlled.

Both complete media reservoirs, lids to close the microfabricated cell culture device and screws were autoclaved and subsequently dried before moving the platform onto the inverted microscope. The following day after cell seeding, all microfabricated cell culture devices were closed and primed as described in section 3.4.4.

Tubing which has been in contact with medium has been sterilised using the following procedure. One end of the tubing which connects to the fluid outlet of the media reservoirs and the other end which connects with the microfabricated cell culture devices have been fitted with pre-sterilised filters. All tubing was filled then with ethanol or isopropanol using a syringe and left in the tubing for at least 30 min. The tubing

was rinsed after at least two times with sterile DPBS, followed by applying a vacuum to remove residual fluid. During the entire sterilisation procedure, the filters were not removed from the tubing.

The microscope module was moved into a laminar flow hood, all three microfabricated cell culture devices inserted and secured in the box of the module. The filters on the tubing were removed and tubing attached to the manual valve at the inlet of the microfabricated cell culture devices and the fluid outlet ports of both media reservoirs (each filled with 50 ml of media). Each microfabricated cell culture device was electrically connected to the microscope module by fixing the spade crimps to the brass screws on the microfabricated cell culture device and the resistance of each heater in the microfabricated cell culture device quickly tested with a multimeter.

The entire microscope module was transferred then to the inverted microscope. The microscope module was connected to the PC and power supplies and the media reservoirs stored in the media handling platform and connected with the gas inlet port.

The manual valve attached to the bubble trap was fitted with a sterile a filter and opened while the pressure regulator was set at 1500 mV for each medium reservoir. Once the tubing for each reservoir was primed and medium reached the bubble trap, the manual valve was closed. Each microfabricated cell culture device was also fitted with a manual 3-way valve. Each valve was opened sequentially to prime the capillary tubing which connected the microfluidic cell culture device with the flow splitter. Once each microfabricated cell culture device was primed, the valve was closed to start continuous culture in the microfabricated cell culture devices and the pressure regulator set to 1200 mV.

Phase contrast images were taken automatically every 15 min, fluorescent images were daily taken manually using the LabView routine.

4.4 Results & discussion

4.4.1 Microfluidic platform

A microfluidic platform has been developed to monitor cells in microfabricated cell culture devices using time-lapse imaging. The platform presented consists of two modules - a microscope module and a media handling module (see figure 4.5).

The microscope module was designed to accommodate three cell culture devices in parallel to obtain experimental triplicates. Furthermore, a preheat element, a bubble trap and a manifold were also integrated into this module. Compared to integrated microfluidic systems, the modularity of the microscope assembly allowed independent development and optimisation of each component, most notably the microfabricated cell culture device.

The media handling module contained a set of valves, a pressure regulator, a cooled bath and two media reservoirs. Two functionalities, cooled storage of media and pumping, were integrated into this module.

Practical laboratory cell culture usually consists of more than just the periodic replacement of medium, or the manipulations required by an experiment. The proper storage of media in a cold and dark environment, the heating up of media in a water bath to 37°C before adding to cells and the frequent microscope inspection of cells for cell morphology or checking for contamination, play an equally important role in guaranteeing the success of an experiment. These functionalities need also be considered for microfluidic cell culture systems. Sophisticated, multiplexed microfluidic platforms for long-term culture, most with integrated pumps and valves, have been presented for various applications, for example for the three-dimensional perfusion culture of liver cells in scaffolds in a 12-well plate (Domansky *et al.*, 2010) or more recently, the culture of murine ESCs in a microfluidic cell culture array (Albrecht *et al.*, 2010). However, the influence of the proper storage and handling of medium in microfluidic cell culture systems on experimental outcomes has not been discussed yet in the literature.

The microfluidic platform presented combined with analytical methods such as metabolite analysers allows therefore the study of the relevance of temperature-dependent effects affecting the media quality on microfluidic experimental results.

The second functionality of the platform is a pumping mechanism that allows to switch between two different media reservoirs. Generally, two types of pumps for microfluidic devices can be distinguished, on-chip pumps and off-chip pumps. The advantages of on-chip pumps such as small dead volumes are offset by the limitations they impose on the microfluidic channel design, for example when a braille display or a series of pneumatically actuated valves is used to move liquid within a microfluidic network (Gu *et al.*, 2004; Melin & Quake, 2007). In this thesis, an off-chip pump solution has been chosen to maintain the flexibility of the microfluidic platform as there are no

geometrical constraints on the microfluidic network design of the microfabricated cell culture device.

A LabView™ routine has been developed to control and record all relevant parameters (Li, 2008b). The routine allows the user to either run an experiment manually or fully automatically using a file which contains all setpoints for the experiment. The routine worked stably over a week of experimentation.

4.4.2 Cell culture device for the platform

The microfabricated cell culture device developed in chapter 3 has been adapted for use in the microscope module using the third generation packaging system (see section 2.2.3). The modularity of the packaging system has allowed to integrate a heating element controlled by a feedback loop while other parts have either not been altered (gasket) or the alterations have not affected the packaging system (microfluidic layer).

The heating element consisted of a transparent resistive ITO microscope slide and a thermistor for the feedback loop control. The area bearing the resistive heater with the aluminium frame was electrically insulated with Kapton® tape to avoid an electrical short circuit. The electrical connection between the resistive microscope slide and the platform was made using brass screws which protruded by approximately 75 μm from the interface plate. The protruding screws were pressed against a copper strip wrapped around the ITO microscope glass slide. The brass screws acted as attachment points for the electrical wires. Spade crimps at the end of the electrical wires were secured to the brass screws with nuts.

The thermistor was placed in a pocket in the interface plate, which was secured with a screw, and was in direct contact with the cell growth surface plane of the ITO microscope slide. The temperature uniformity of the ITO microscope slides reported by Lin *et al.* (2010) (see also Appendix E.2) allowed the positioning of the thermistor next to the PDMS microfluidic chip.

The possibility of using ITO heaters to precisely control temperature dependent processes has already been demonstrated in various microfluidic devices used for DNA amplification (Zhang & Ozdemir, 2009). For microfluidic cell culture devices, solutions using ITO foil heaters or resistive wire heating have been presented (Alam *et al.*, 2010; Petronis *et al.*, 2006). Resistive wire heating is simple to integrate and embed into a microfluidic device when optical access for a microscope is not required, for example

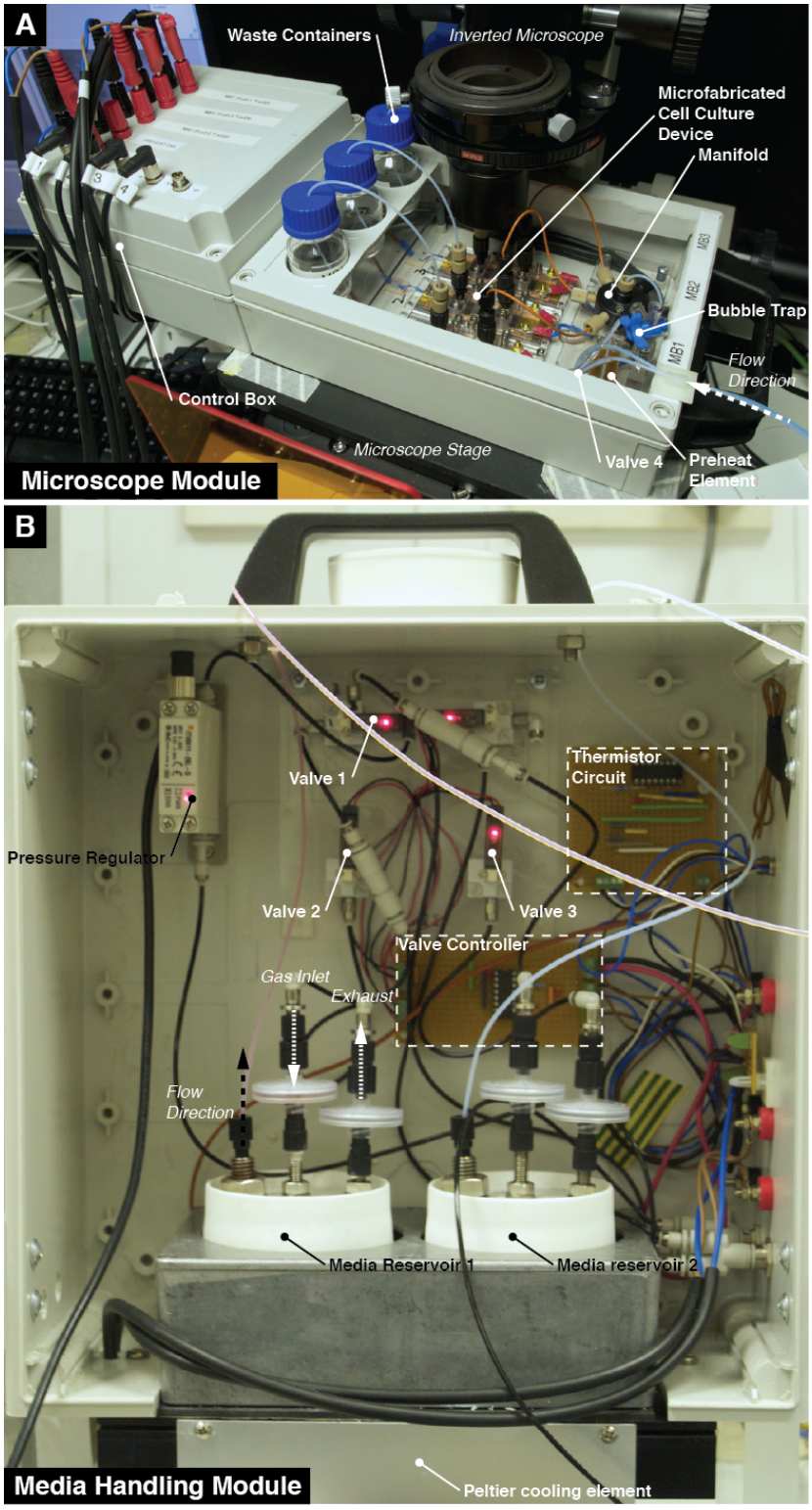

Figure 4.5: Microfluidic platform - The microfluidic platform consists of two modules - the microscope module (**A**) and the media handling module (**B**). A LabView™ routine is used to control parameters such as temperatures, media selection, flow rate and image capture frequency.

for suspension culture of cells in microbioreactors. However, this type of heater is not suitable for the optical monitoring and imaging of of adherent cells such as stem cells. For microscope based cell culture devices, an ITO foil heater has been compressed into the layers of a PMMA microfluidic device for the culture of HeLa cells (Petronis *et al.*, 2006). An automated microfluidic cell platform using a bespoke ITO heater and platinum thermistor has been demonstrated for the culture of bronchioloalveolar carcinoma cells (Huang & Lee, 2007). The ITO heater presented in this work uses off-the-shelf components, required minimal work to attach the microfluidic chip and therefore the microfabricated cell culture device assembly and the electrical connection to the temperature controller are straightforward, also in comparison with the ITO heaters described above.

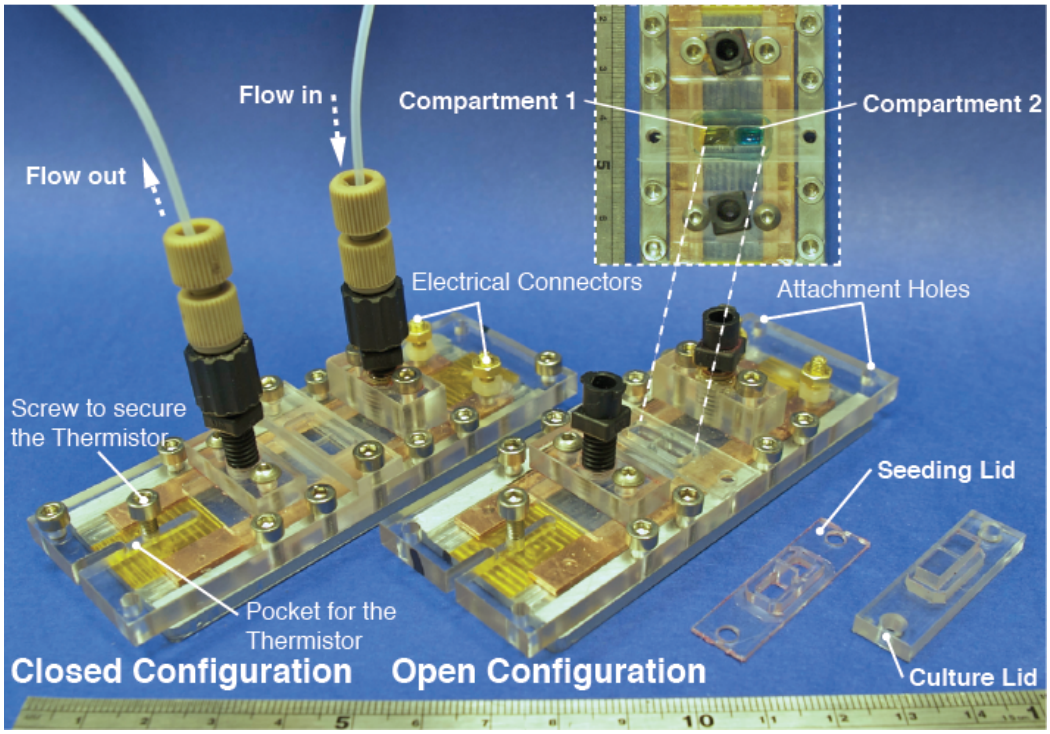

Figure 4.6: Cell culture device for use in the microscope module - The cell culture device used for the platform had two configurations - an open configuration used for seeding and a closed configuration used for culture. A split culture chamber in the microfluidic chip accommodated two compartments.

A simplified, second generation microfluidic layer has been developed and fabricated

by reducing the inlet and outlet manifold to one single channel. Two configurations of the second generation microfluidic layer have been tested: one configuration had one single culture chamber and the other configuration had a cell culture chamber equally split in two halves allowing the culture of two different cell lines, in this case, the Oct4-GFP and the 46Cs. Hydrodynamic shear stress levels were characterised using the same FEM parameters used in section 3.4.1 for both versions of the microfluidic layer. Changes in hydrodynamic shear stress compared to the first generation were not expected, this has been confirmed in the FEM analysis (see Appendix E.3). For the split microfluidic chip, a seeding lid has been designed to avoid mixing of the different cell types.

4.4.3 Temperature characterisation

A temperature control system with a feedback loop has been developed for the microfabricated cell culture device, the cooled storage and the preheat element. The feedback loop uses a thermistor, a software based PID algorithm and pulse width modulation to control the temperature. A tuning routine has been developed to easily adjust PID settings and calibrate thermistors (Li, 2008b). Changes in temperature ranging from 35 to 37°C in 1°C steps have been measured to characterise the heaters in the three bioreactors (see figure 4.7). Generally, the accuracy and reproducibility of the temperature on the cell growth surface is well controlled over long time periods (over 24 h) (see figure 4.7 **A**, **C**). Higher temperatures than the setpoint were recorded for only one heater due to poor PID settings (see figure 4.7 **B**).

The temperature setpoints for the preheat element and the cooling plate were not reached (see figure 4.8 **A**, **B**). For both the preheat element and the cooling plate, the determination of proper PID settings is difficult due to their thermal mass. The cooling element is also restricted by its power supply which is only capable of delivering 3 A. Using a higher rated power supply could rectify However, the temperature of the cooling element is below the storage temperature of 10°C recommended by the media manufacturer and therefore, thermal degradation of media can be excluded for long time experiments.

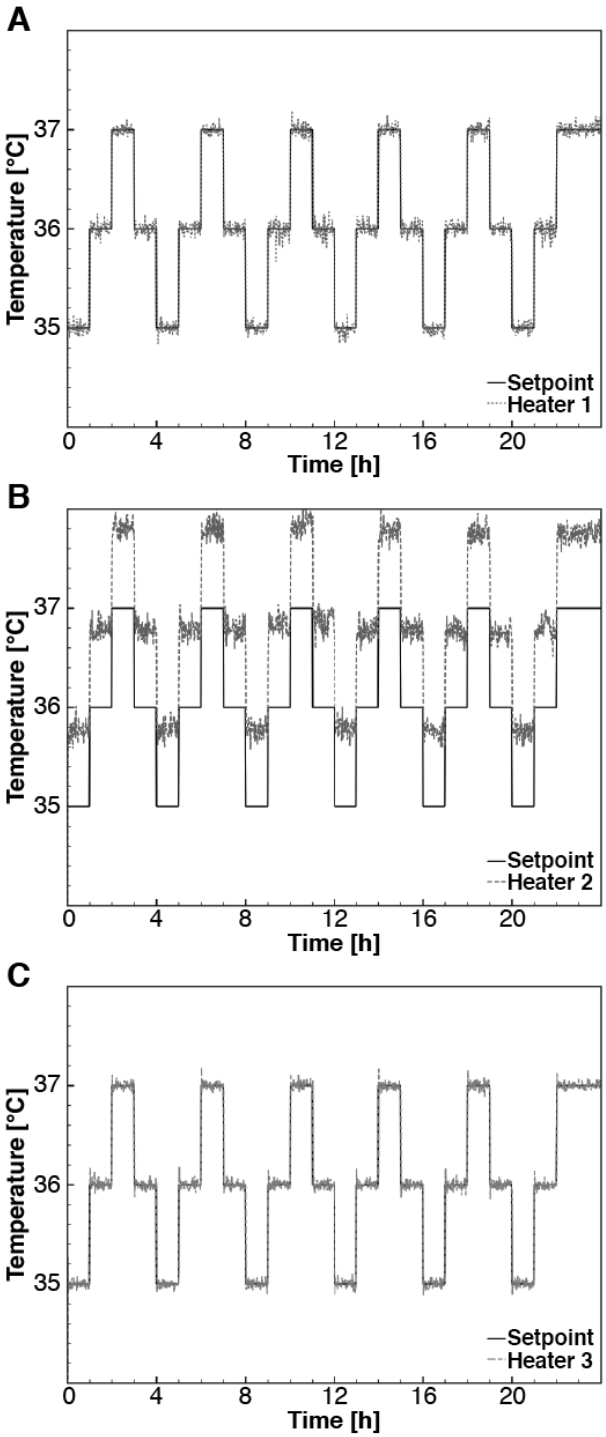

Figure 4.7: Temperature control in each of the three cell culture devices - The temperature of each cell culture device has been varied between 35°C to 37°C in 1°C steps and maintained for 1 h. Reproducible and accurate temperature readings which closely match the setpoint can be achieved when the PID settings are properly adjusted (**A**, **C**). In case of poor PID settings, temperature readings are at least reproducible (**B**).

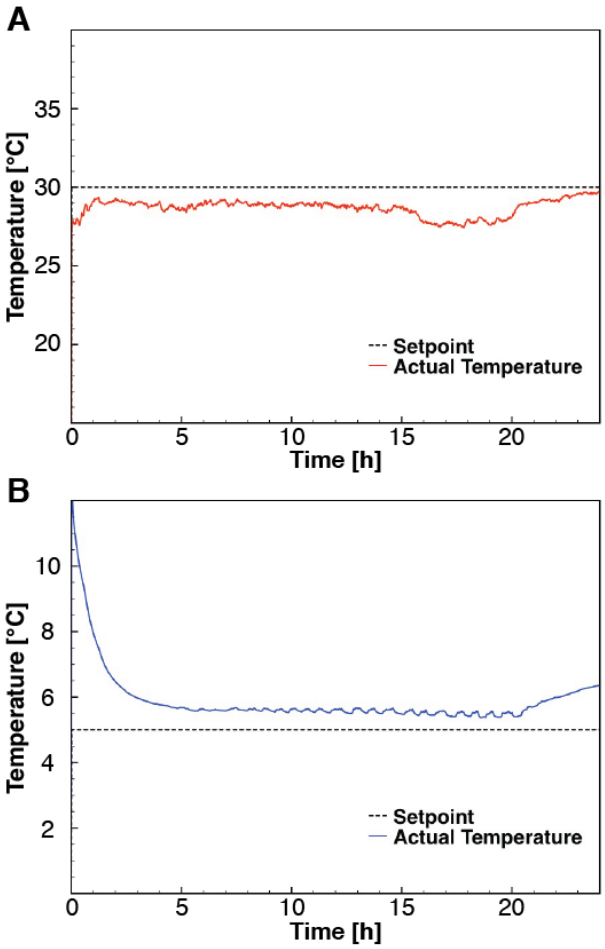

Figure 4.8: Temperature control in the preheat and cooling element - Temperature control in the preheat (**A**) and in the cooling element (**B**). In case of the cooling plate, the power supply is limiting its maximum output current to 3 A and thus, the performance of the cooling element.

4.4.4 Pumping characterisation

A pump with short response times has been developed to generate different flow modes (continuous, intermittent). Furthermore, a valve system has been developed as part of the pumping system to switch between the two media reservoirs. A LabView routine is used to control the flow rate and the medium reservoir to be pumped (Li, 2008b).

Flow rates have been characterised with a flow rate sensor, at three different locations in the fluid delivery chain. Typical for all flow rate measurements was the periodical 'sawtooth' flow rate curve (see figure 4.9). This effect is typical for this type of pressure regulator and was predominant at low flow rates and decreased with higher flow rates. Pressure is controlled with a series of solenoids and a pressure sensor in the regulator. The output pressure is fed back to a control circuit which actuates the solenoids until the pressure becomes proportional to the input signal. The actuation of these solenoids causes therefore the periodical flow rate curve. However, the pressure regulator is a low cost one and a more sophisticated replacement may be able to reduce this effect.

Apart from this effect, the response time of the pump is superior than for example that of a syringe pump (see Appendix E.4 for comparison).

Firstly, the flow rates at each port of the manifold have been measured for three different pressure regulator settings and over 30 min (see figure 4.9, **A**). The average and the standard deviation for each port and pressure setting have been calculated and are summarised in table 4.1. The standard deviations of the flow rate differ only by 2 % to 5.5 % from the average of the flow rate. It can therefore be assumed that each port delivers the same flow rate.

Secondly, the flow rate at the same fluidic port was measured when switching between media reservoir 1 to media reservoir 2 and then back to the first media reservoir (see figure 4.9, **B**). The average and the standard deviation for each port and pressure setting have been calculated and are summarised in table 4.2. For all three pressure settings, the first switch increased the flow rate, while in the second switch flow rates decreased as table 4.3. The difference in flow rates during switching may be a result of an increased fluidic resistance for the flow path of media reservoir 1. Currently, tubing can move freely from each media reservoir which may cause the increased fluidic resistance. By fixing the position of the tubing, the effects of the tubing position on

the flow rate could be eliminated. Compared to table 4.1, the flow rates are within an acceptable range even after switching between the two media reservoirs.

Pressure regulator setting (mV)	Port 1	Port 2	Port 3
300	9.17 +/− 0.27	8.68 +/− 0.36	8.15 +/− 0.45
400	15.09 +/− 0.51	16.13 +/− 0.34	15.89 +/− 0.58
500	20.64 +/− 1.11	23.24 +/− 0.46	21.49 +/− 0.53

Table 4.1: Flow rates for each port used at the manifold - Flow rate was measured at each port of the manifold used for a microfabricated cell culture device. During a measurement, the other ports of the manifold were closed. The average and the standard deviation for the flow rate at each port were then calculated (n=3). Units for the flow rate at each port are μl min^{-1}.

Pressure regulator setting (mV)	Media Reservoir 1	Media Reservoir 2	Media Reservoir 1
300	8.86 +/− 0.25	9.32 +/− 0.29	8.02 +/− 0.26
400	14.63 +/− 1.41	15.85 +/− 0.92	14.23 +/− 0.27
500	21.02 +/− 1.96	24.19 +/− 0.44	20.27 +/− 1.34

Table 4.2: Flow rates measured at the same port during media reservoir switching - Flow rate was measured at the same while switching between media reservoir 1 and 2. The average and the standard deviation for the flow rate at each port were then calculated (n=3). Units for the flow rate at each port are μl min^{-1}.

Pressure regulator setting (mV)	Switch 1	Switch 2
300	4.17 %	- 9.41 %
400	8.32 %	- 2.71 %
500	15.07 %	- 3.56 %

Table 4.3: Increase/decrease in flow rate after switching - The increase or decrease in flow rate was calculated by using the average flow rate achieved in media reservoir 1 as the basis. Switch 1 referrs to switching from media reservoir 1 to media reservoir 2, while switch 2 referrs to switching from media reservoir 2 back to media reservoir 1.

Finally, the flow rate after each microfabricated cell culture device has been measured using the same pressure settings and port as in the switching test. (see figure 4.10). The average and the standard deviation for each microfabricated cell culture device and pressure setting have been calculated and are summarised in table 4.4. For the lowest pressure setting, the flow rates achieved were not consistent for all microfabricated cell culture devices. Most likely the inclusion of an air bubble caused the

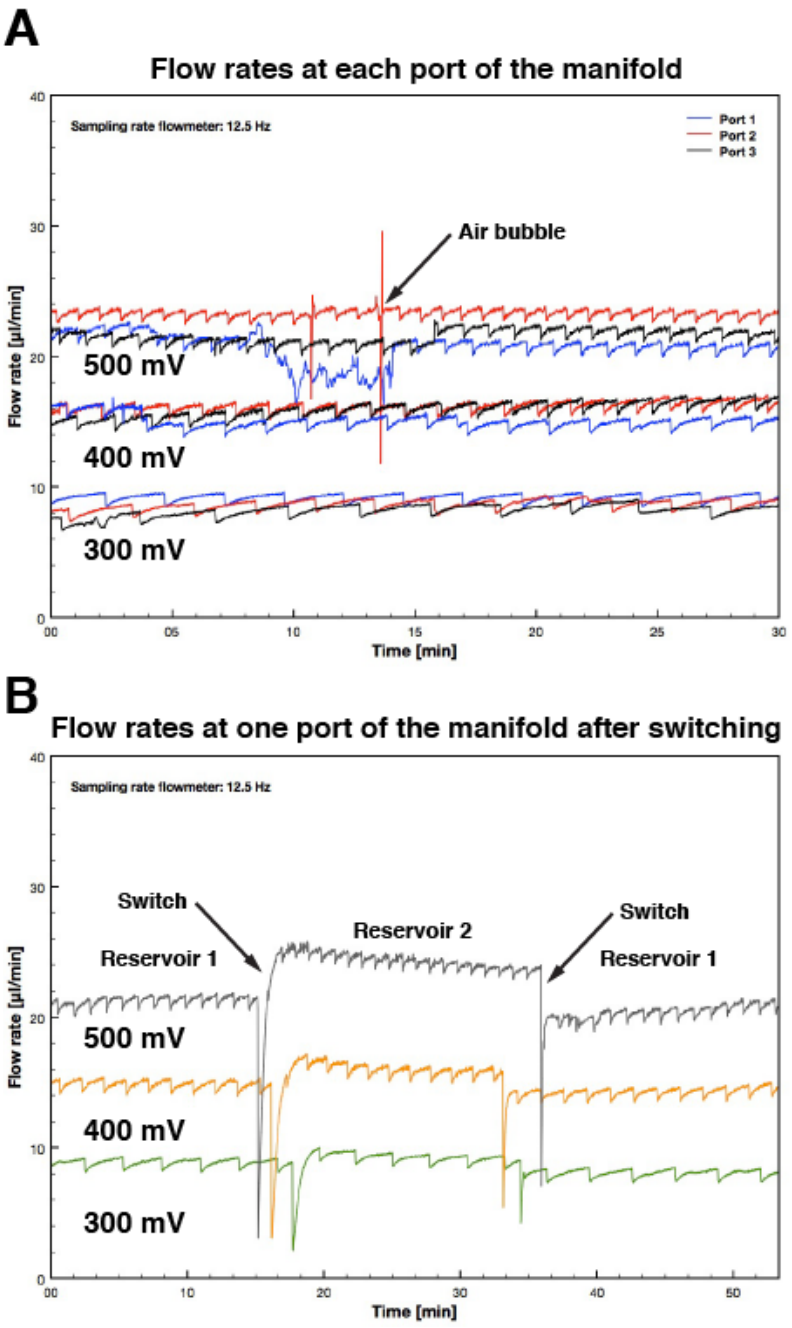

Figure 4.9: Flow rate measurements at the manifold using water - Flow rates have been measured using water for three pressure regulator settings (300 mV, 400 mV and 500 mV) at all three ports used for the microfabricated cell culture devices (**A**). Air bubble inclusion in the flow rate sensor is characterised by sharp spikes (port 2) or noise-like curves (port 1), here occuring at the highest flow rate. Using the same pressure settings, the flow rates have been measured when switching from media reservoir 1 to media reservoir 2 and then back to the first media reservoir (**B**).

variation across all three microfabricated cell culture devices. However, for the two other pressure settings the flow rates were comparable to the flow rates obtained at each port used at the splitter (compare with table 4.1). Furthermore, the flow rates measured after the microfabricated cell culture device remain almost the same compared to the flow rates measured at the splitter. It can be safely assumed that the fluidic resistance of the microfabricated cell culture device can be neglected and its influence thus minimal on the overall pumping system. The length of the capillary tubing at the inlet or at the outlet of the microfabricated cell culture device can therefore be used to fine tune the flow rates.

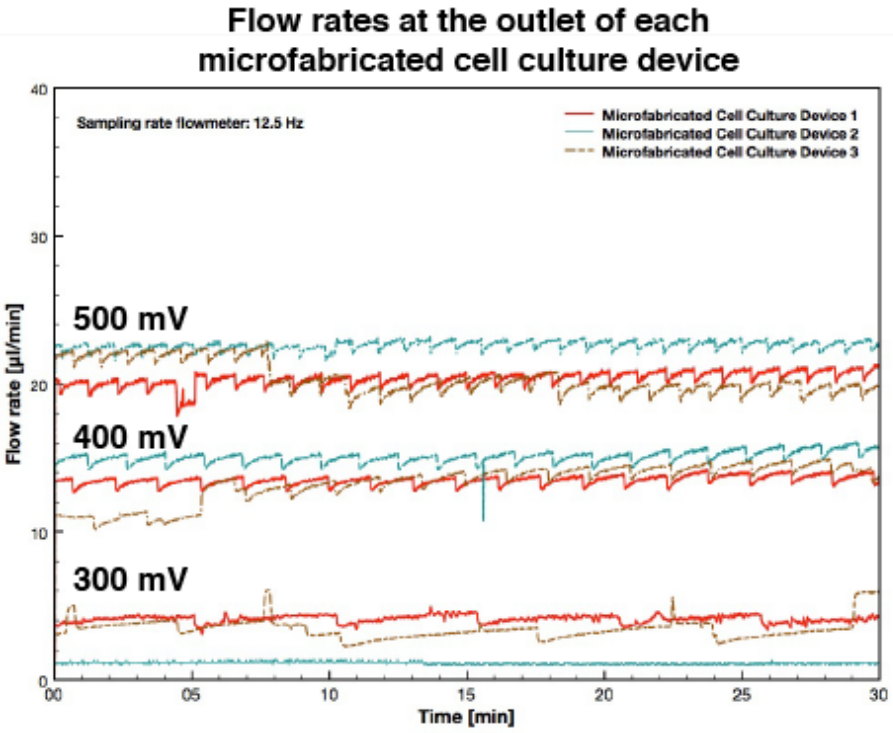

Figure 4.10: Flow rate measurements for each microfabricated cell culture device at three different pressure settings - Three pressure regulator settings (300 mV, 400 mV, 500 mV) were applied to each of the three microfabricated cell culture devices.

Pressure regulator setting (mV)	MB 1	MB 2	MB 3
300	9.94 +/− 0.29	1.17 +/− 0.09	3.46 +/− 0.676
400	16.35 +/− 0.41	15.10 +/− 0.43	13.28 +/− 1.24
500	23.58 +/− 0.40	22.57 +/− 0.29	20.33 +/− 1.06

Table 4.4: Flow rates after each cell culture device at the same port - Flow rate was measured at the same port of the manifold for all three microfabricated cell culture devices. The average and the standard deviation for the flow rate at each port were then calculated (n=3). Unit for the flow rate at each port is μl min^{-1}.

A flow rate chart has been compiled from the results of the flow rate measurements after the manifold, after the microfabricated cell culture device and switching of the media reservoirs by using the average of three measurements (see figure 4.11). A fitted curve for these average flow rates after the manifold shows the expected linear correlation between applied voltage to the pressure regulator and flow rate. The average flow rates obtained in each microfabricated cell culture device and for both media reservoirs for the three pressure regulator settings have also been plotted in the same figure. A deviation in flow rate from the fitted curve can be interpreted as a change in fluidic resistance along the flow path.

A media transport system has been developed to pump reproducibly medium through the cell culture devices. Compared to syringe pumps, it offers storage capabilities for enough medium for prolonged experiments (up to 7 days with a flow rate of 1.2 ml h^{-1}) and can easily be expanded if necessary. Currently, a 'sawtooth' effect in the flow rate curve is observed due to the pressure regulator used. However, such effects can also be observed in miniaturised peristaltic pumps with flow rate changes of up to 0.2 μl min^{-1} (Skafte-Pedersen *et al.*, 2009). In the system presented flow rate fluctuations of up to 1.1 μl min^{-1} were observed. These were minimised when multiple microfabricated cell culture device are operated, possibly because the bubble trap in the flow path may act as a capacitor, damping the flow rate fluctuations.

4.4.5 Experimental procedure & time lapse imaging

Finally, the microfluidic platform has been tested using mESC cell lines. Cells were seeded using the method described in chapter 3. After 1 day of incubation at 37°C, the culture chamber of each microfabricated cell culture device was closed and the microfluidic chip primed with medium. After priming, the microfabricated cell culture

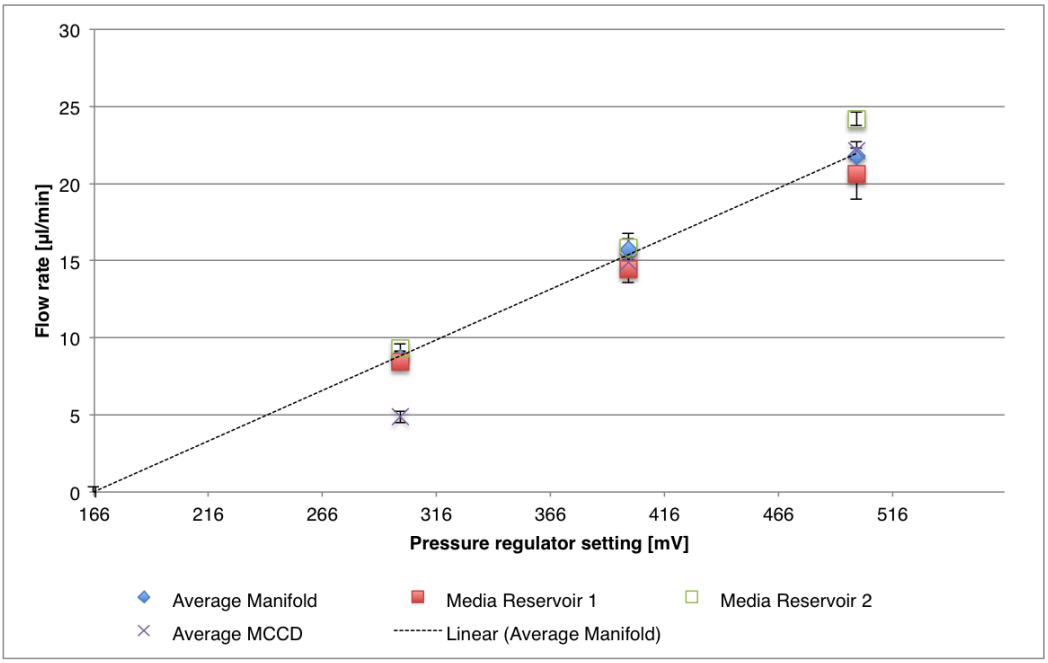

Figure 4.11: Flow rate chart for a given pressure setting - The average flow rates measured after the manifold for each port, after each cell culture device and for both media reservoirs for the three pressure regulator settings (300 mV, 400 mV and 500 mV) have been plotted. A linear curve fit of the flow rates measured after the manifold (R^2 = 0.99826) can be used to predict the flow rate due to the linear correlation of pressure and flow rate.

devices were inserted into the microscope module in a laminar flow hood and then continuously cultured on an inverted microscope for up to 4 days (see figure 4.12).

Cells were seeded according the seeding method described in chapter 3. mESC attached within 24 h to the cell growth surface within the microfabricated cell culture device and the culture chamber was subsequently sealed with the lid. Under continuous flow, cell proliferation and movement have been recorded by the time-lapse system (see figure 4.12 **A**, **B**). Changes in proliferation has been recorded in a time period of over 5 h (see figure 4.12 **C**). The GFP expression system allowed to monitor pluripotency over time. To avoid damage to cells by exposure to UV light, pluripotency was assessed every 24 h (see figure 4.12 **A**, **B**).

Whether cell proliferation or pluripotency were affected by flow, the light illumination or the properties of the cell growth surface (combination of 0.1% (v/v) gelatine/ITO microscope slide) is difficult to determine and thus, the biological interpretation not possible at present. However, as a proof of concept, it has been shown that the microfabricated cell culture devices remained sterile for up to 4 days and the requirements defined in section 1.4.3.1 were met. Seeding in the split microfluidic chip has been proven to be difficult, even when the seeding lid is used. Either cells accumulated in one part of their compartment or, when tried to seed cells without the seeding lid, mixed with the cells from the other compartment.

Air bubbles were a frequent occurrence in the microfabricated cell culture devices blocking the microchannel network, thus preventing medium reaching the cells. As a consequence of the increase in fluidic resistance in a blocked device by air bubbles the flow rates in the other cell culture devices has been raised. Besides this issue, the individual fluidic interconnection of each microfabricated cell culture device offered also an experimental advantage over integrated microfluidic systems. The affected microfabricated cell culture device could be disconnected and the flow rate in the unaffected devices accordingly adjusted. Failure of one or more microfabricated cell culture devices did therefore not affect or scrutinise the entire experiment, albeit the ability to obtain a triplicate was lost.

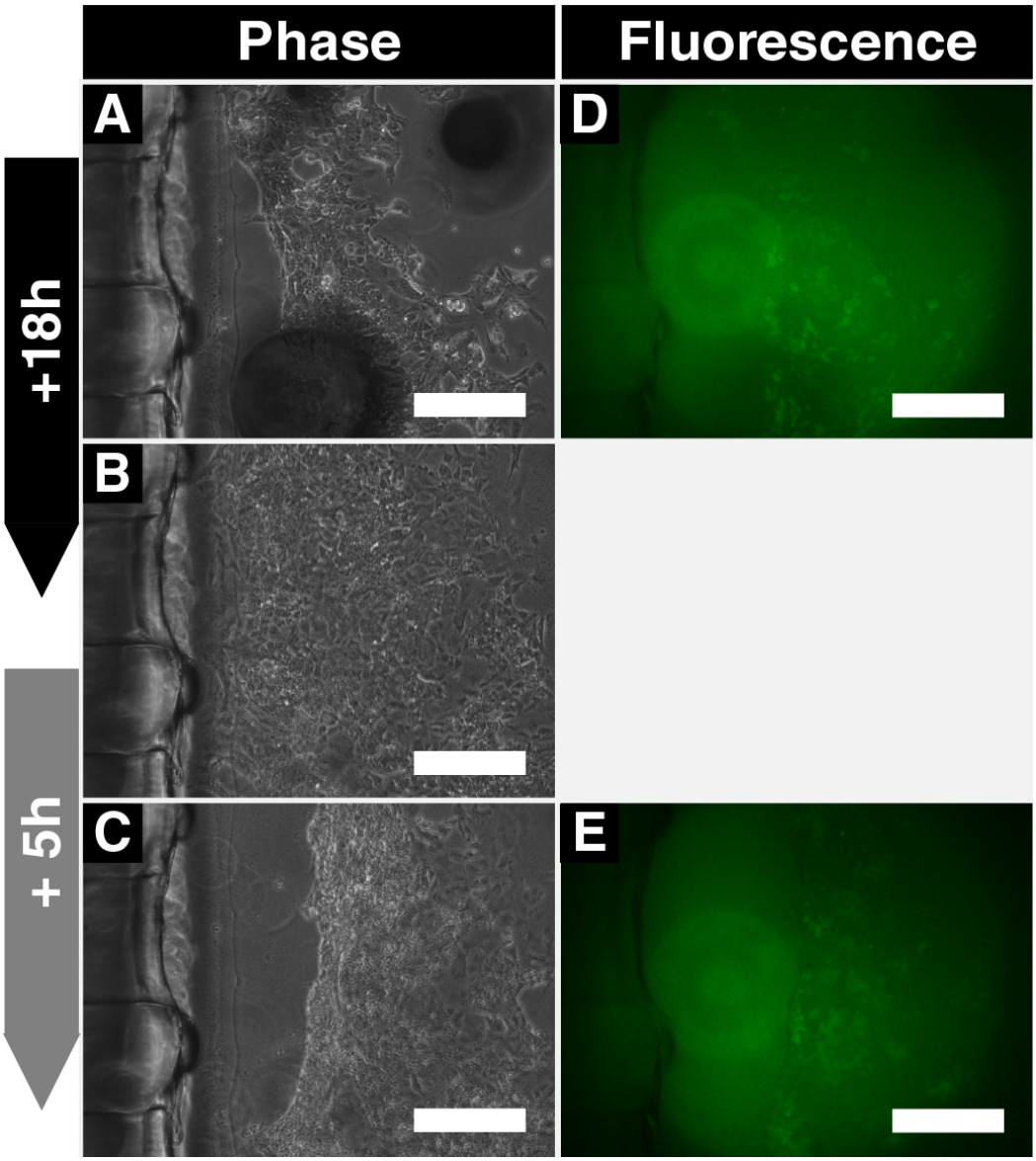

Figure 4.12: Time-lapsed image sequence of mESC Oct-4 GFPs - The time-lapse images of mESC Oct-4 GFPs in the single culture chamber of the cell culture device reveal the movement in phase images (A-C) and the pluripotency in fluorescent images (**D**, **E**). All images are taken at 10× magnification. The scale bar is 200 μm long.

4.5 Summary of findings

An automated microfluidic platform with time-lapse imaging has been developed that can be used for stem cell bioprocessing. The microfluidic platform consisted of two modular sub-assemblies, a microscope module and a media handling module. The microscope module contained all microfabricated cell culture devices while the media handling module kept the pumping solution and media reservoirs.

The pumping solution presented for the microfluidic platform is reproducible and also enables to aerate the medium at the same time. To maintain a constant culture temperature in the microfabricated cell culture device, a transparent heater has been incorporated into the existing microfabricated cell culture device presented in chapter 3.

A LabView routine controls and records all relevant parameters such as temperature, flow rate and image capture frequency. Furthermore, the routine allowed to read in a sequence of setpoint commands for all parameters or when necessary, manually changed. The pumping system and the heaters have been characterised for repeatability and accuracy. In experiments using mESCs, the microfluidic platform has been tested on an inverted microscope. Images were taken every 15 min and showed the movement of mESC under continuous flow with major changes within 5 h for example.

5

Conclusion

Stem cells are the subject of a remarkable scientific and commercial interest due to their ability to differentiate into tissue-specific functional cells. Paramount to the successful manufacture of any stem cell based product is the thorough understanding of the bioprocess conditions and parameters involved.

Microfluidic cell culture devices will ring in a new era of micro-scale bioprocessing of stem cells for applications such as regenerative medicine and drug discovery. These devices can be used as an advanced experimentation tool to dynamically probe multiple conditions due to their ability to be parallelised, all on a small footprint, for the development of stem cell bioprocesses.

However, a greater understanding of the cellular processes which drive stem cell proliferation or differentiation pathways is still required. Additionally, a number of stem cells are still not fully characterised.

The aim of this thesis was therefore to develop a multiplexed microfluidic cell culture device which can alter the soluble microenvironment of stem cells. The presented microfluidic device offers the flexibility to incorporate and adapt present culture protocols and future research findings, and to define the basis for scaling and comparison of experimental outcomes. Combining the experimental adaptability and comparability with an innovative image-based monitoring system enables the generation of data-rich experimental sets which can be correlated to different important culture parameters such as flow rate or temperature. All these requirements have been met with the microfluidic platform presented within this thesis.

Given the lack of standardised packaging and fabrication solutions for microfluidic devices, the need for the required design flexibility has been addressed with the development of a holistic rapid prototyping approach for microfluidic devices.

The system consists of a casting method to deliver PDMS microfluidic prototype chips within 2 days and a modular, robust, and adhesive-free interconnect and packaging for rapid testing of the PDMS microfluidic prototype chips. The geometry parameters of the interconnect and packaging system have been varied and their influence on performance such as burst pressure and flow rate elucidated.

The prototyping approach presented separates packaging from the microfluidic chip, thus facilitating the rapid testing of microfluidic design concepts. The microfluidic chip and the packaging system do not require any particular fabrication knowledge or specialised environments such as cleanrooms. Thus, it is also suitable for a range of different users with non-engineering backgrounds.

The seeding and culture in a microfluidic cell culture device are both critical steps in obtaining reliable and data-rich experimental sets. Scalability and comparability criteria have been defined to implement current cell culture protocols for embryonic stem cells in a microfluidic cell culture device. The holistic rapid prototyping approach has been used to fabricate microfluidic cell culture devices specifically for the culture of these cells. Direct access to the cell culture chamber of the microfluidic device enabled the translation of the seeding sequence of current cell culture protocols with the same liquid height. Furthermore, the modularity of the microfluidic cell culture device also enabled the use of an industry standard TC-PS microscope slide to provide the same surface properties found in T-25 flasks. These results represent the first results obtained for human embryonic stem cells grown in microfluidic cell culture devices which are specifically designed to be scaled.

Sealing of the cell culture chamber of the microfluidic device with a lid permits to switch from static seeding to continuous cell culture. Hydrodynamic shear stress levels in the cell culture chamber have been engineered to prevent a wash out of viable hESC colonies which were used as model. Under these conditions, continuous culture of hESC in a microfluidic system has been demonstrated for the first time without a washout of cells. Positive Oct-4, Tra-1-81 and SSEA-3 stains confirm that hESC colonies cultured within the microfluidic cell culture device retain their self-renewal capability. These

results are thus important indicators that continuous culture experiments with ESCs are worth pursuing.

The flexibility to easily change parts of the microfluidic cell culture device and the positive results obtained with continuous culture have set the stage to monitor cell culture in the microfluidic device using an image-based approach. A microfluidic platform has been developed and tested for three microfluidic cell culture devices. Functionalities of the platform included cooled media storage, media pumping and an inverted microscope fitted with a camera. This platform has been controlled with a LabView routine, which allows to carry out experiments either automatically with predefined experimental protocols or permits the manual intervention to adjust a specific parameter.

Using time-lapse imaging, cell morphology and pluripotency of mESC with a Oct-4 GFP expression system have been monitored. The results have shown that mESC move around within the microfluidic cell culture device under flow (approx. 300 μl h^{-1}). These results demonstrate that stem cell bioprocesses require an advanced monitoring approach to directly observe the fate of stem cells. This information would be lost using traditional bioreactors such as T-flasks where continuous monitoring is not possible. However, to fully exploit the experimental advantages of the microfluidic cell culture platform, all factors which can affect the outcome of a microfluidic cell culture experiment need to be tested so that the results obtained can be correlated with manipulated parameters such as flow or temperature.

This work represents the first step and serves as basis towards a microfluidic cell culture tool for stem cell bioprocess development and optimisation. The design and the development of such a microfluidic framework is an iterative process and many practical problems associated with microfluidic cell culture devices have been addressed. However, further technical efforts need still to be made to generate relevant and validated results for stem cell bioprocessing.

6

Future Work

The design and the development of a novel experimental tool is usually an iterative process and the microfluidic cell culture device presented in this thesis is no exception. Many problems such as efficient seeding or low hydrodynamic shear stress in the culture chamber of the device have been addressed. However, other engineering challenges emerged for which improvements and solutions need to be found. The cell culture device for stem cell bioprocess development in this work offers therefore a range of exciting research and engineering opportunities from microfluidic device development and optimisation, characterisation and validation of the multiplexed cell culture platform to micro-scale stem cell bioprocess development and optimisation.

The main aims of current research are to increase the usability of microfluidic chips for stem cell bioprocessing, and the impact of different culture modes on stem cell bioprocess outcomes. By characterising the physical performance of the microfluidic platform such as temperature, flow patterns and mass transfer of nutrients and oxygen, the interpretation of experimental outcomes of cells is facilitated and thus the obtained experimental data sets.

The current packaging and fabrication system is reliable, but some improvements can already be seen:

- The disposable microfluidic chip is currently made from PDMS in a casting process. However, it has been pointed out by (Regehr *et al.*, 2009) that PDMS may not be ideal for cell culture applications and thus, another material would have to be found. For example, biomedical materials such as polyurethane or medical

grade silicone could be used to replace PDMS, but fabrication processes would need either to be adapted or to be developed and characterised first.

- In the latest iteration of the packaging system, the frame is made from aluminium and the interface plate is made from poly(carbonate) or poly(methyl methacrylate). While these materials are fine and easy to machine for prototypes, mechanically stiffer materials with higher glass temperatures T_g such as poly(sulfone) would be better suited for repeated sterilisation with an autoclave to provide long-term mechanical stability.

- The packaging system uses currently screws to secure the stack of interface plate, microfluidic chip and frame. While the number of screws has been already reduced, a solution without screws would greatly benefit handling, for example in a laminar flow cabinet. The system could then be expanded into a disposable cartridge system.

- Although multiple inlet and outlet configurations have been explored, high density arrays of inlet and outlet ports have not been explored. Such high density interconnects would allow the integration of pneumatically actuated pumps and valves as shown by Quake and colleagues for on-chip control of flow for example, but represent a considerable challenge to the fabrication engineering.

Along with improvements to the fabrication and packaging system, another possible area of future work is more concerned with exploring cell culture within the microfluidic device:

- It has been demonstrated that seeding in a open culture chamber using a pipette is possible even with delicate and rare cells such as hESCs. This could be further expanded to seeding in a microfluidic cell culture device with multiple compartments and different types of cells to explore co-culturing for example, as has been shown in a similar approach by Chin *et al.* (2004). This would allow to obtain well defined and separated cell populations while cellular signalling is maintained for example for the guided differentiation of stem cells.

- The modularity of the microfluidic cell culture device allows the inclusion of any slides in microscope format. In preliminary experiments, a micro-milling

machine has been used to pattern a TC-PS slide to restrict cell growth within the microfluidic bioreactor by removing the specially treated cell growth surface (Hu, 2008). The open configuration of the microfluidic cell culture device would also enable the seeding of ESCs for example, to form well defined embryoid bodies in wells in a microscope slide.

- The open access to the cell culture compartment would also enable surface patterning using a stamp. Such a stamp could be used to precisely define cell growth surfaces within the microfluidic cell culture device, with well-established surface modifications as shown by Tang *et al.* (2010) or Séguin *et al.* (2010).

- Two types of low hydrodynamic shear stress microfluidic chips have been currently tested and used for ESC culture. These microfluidic chips could be further refined and optimised in a virtual prototyping setting using a similar design approach using tree-like inlet architectures to adjust the flow velocity in the cell culture chamber as proposed by Saias *et al.* (2011).

- At this stage, the low hydrodynamic shear stress microfluidic chips have been analysed using FEM. These simulations would need to be verified in experiments, for example using micro particle image velocimetry (μPIV) experiments.

- A recurring issue during priming and filling of a microfluidic system is the occasional inclusion of air bubbles in the system. The microfluidic cell culture device presented is no exception and therefore, an on-chip bubble trap would facilitate priming of the microfluidic cell culture device and maintain a bubble-free operation for the entire duration of an experiment. A system has been presented to remove air bubbles from a designated chamber with a vacuum which could be adapted for the microfluidic cell culture device (Skelley & Voldman, 2008). Such a solution for air bubble removal would be more gentle on the cells in the cell culture chamber than pushing out air bubbles by applying pressure at the inlet.

Only the microfluidic cell culture device has been considered in this chapter so far. The microfluidic platform is functional, but would also need some degree of refinement and improvements to achieve reproducible experiments:

- The microscope module has currently to be moved manually on the inverted microscope. Integration of a motorised microscope stage and z-axis to adjust focus would further automate the existing microfluidic platform. The system could be therefore expanded to multiple microfluidic cell culture devices (more than three) to probe different cell culture conditions at the same time.

- Time-lapsed images are taken in the current setup, but a real-time image analysis algorithm is missing in the current setup to determine key culture parameters such as cell density and pluripotency. The generation of these processed data would allow the linking of the input parameters such as temperature and flow rate with the experimental outcomes.

- A feedback loop to control the flow rate would allow the precise control of hydrodynamic shear stress and medium residence time in the cell culture chamber of the microfluidic cell culture device.

- Integration of different sensors, for example to measure the oxygen tension levels at various locations in the microfluidic cell culture device, would complement the data-rich experimentation with stem cells.

- In the current setup, an ITO microscope glass slide is used to maintain the temperature in the microfluidic cell culture device. A custom-made resistive polystyrene slide as heater would better suit the imposed scalability and comparability criteria. Integrating a temperature sensor with the slide would also facilitate the experimental procedure to connect the heater/temperature sensor unit.

- A multiplexed system would also require an improved experimental procedure to set up and prime the system with media. The system would preferably use an automated procedure to ensure experimentation reproducibility. Automation of the seeding procedure using pipette robots would also greatly support these efforts (Puccinelli *et al.*, 2010).

Finally, a fair amount of future work may be carried out to prove the usefulness of the microfluidic technology for stem cell bioprocess development:

- Experiments with intermittent and continuous flow in the microfluidic cell culture device using stem cells could demonstrate their implications for proliferation or

differentiation. For intermittent flow, the lid to close the cell culture chamber of the microfluidic device may need to be fitted with an gas permeable membrane to provide enough oxygen to the cells.

- Dynamic soluble signalling could be studied using the platform by switching between the individual media reservoirs in a similar manner as shown by Azizi & Mastrangelo (2008) or Paliwal *et al.* (2008).

- The microfluidic cell culture device has been successfully tested with human and murine ESCs. Adult stem cells such as MSCs or other adherent cells could be used to test the microfluidic cell culture device to demonstrate its capability as a stem cell bioprocess development and optimisation tool.

- The modularity of the microfluidic cell culture device and the open access would also be suitable for three dimensional cultures of cells in gels or entire tissue biopsies as shown by Huang *et al.* (2011) and Webster *et al.* (2010).

The work presented in this thesis serves as the basis to implement these further steps. The microfluidic cell culture platform is functional and many challenges of working with microfluidic systems (for example a standardised packaging and fabrication method) have been addressed.

It is necessary now to move from the proof-of-concept setting to a real tool for stem cell bioprocessing. The points outlined above present some ideas how the development of the microfluidic framework might lead to such a tool for stem cell bioprocess development.

The route to a functional microfluidic tool would encompass first the optimisation and experimental verification of the microfluidic chip layout and the integration of an efficient bubble trap, whether on- or off-chip needs to be determined. The next development step would address the multiplexing and increased automation of the microfluidic platform by integrating a motorised stage and z-axis. Alongside the refinement of the microfabricated cell culture device and the extension of a refined multiplexed platform, a consolidated software package which allows the integration of a real-time kinetic growth measurement routine with the existing automation routine would complement the technical efforts made towards a truly useful microfluidic stem cell bioprocess development platform. In such an advanced platform configuration, it should be technically

feasible to assess the influence of soluble signalling of stem cell on proliferation and monolayer differentiation.

A few design criteria and requirements have been derived from existing cell culture bioreactors, for example the ability to use TC-PS with the microfabricated cell culture device. Whether or not TC-PS is required for use in a microfluidic cell culture device, would need thorough testing of the materials and ECM coatings used using surface chemistry characterisation methods such as time of flight mass spectroscopy or X-ray photoelectron spectroscopy and then the surface characteristics compared with those of T-flasks. This study would then facilitate to decide whether TC-PS in a microfluidic stem cell bioprocess development platform could be made obsolete and therefore potentially further simplify the fabrication and packaging of the microfabricated cell culture device.

Appendix A

Calculations for forces acting on a PDMS microfluidic layer

A.1 Calculation of axial force in a screw

To determine the force acting on the PDMS microfluidic chip, it is necessary to calculate the axial force of a screw, which is used to clamp the microfluidic chip between the top plate and the frame.

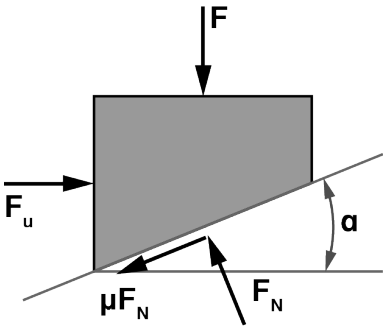

Figure A.1: Infinitesimal unit and the acting forces on the screw

$$M_T = F_u \cdot \frac{d_2}{2} \tag{A.1}$$

where M_T is the applied screw torque, F_u is the perimetric force and d_2 the pitch diameter.

$$F_u = F \cdot (tan(\alpha) - \mu) \tag{A.2}$$

where F is the axial force in the screw, α the pitch angle and μ the friction coefficient between screw and thread.

$$F_u = F \cdot \left(\frac{p}{d_2 \cdot \pi} - \mu \right) \tag{A.3}$$

where p is the pitch and d_2 is the pitch diameter.

$$M_T = F \cdot \left(\frac{p}{d_2 \cdot \pi} - \mu \right) \cdot \frac{d_2}{2} \tag{A.4}$$

after rearranging and solving for F:

$$F = M_T \cdot \frac{1}{\left(\frac{p}{d_2 \cdot \pi} - \mu \right)} \cdot \frac{2}{d_2} \tag{A.5}$$

$$F = M_T \cdot \frac{2}{\left(\frac{p}{\pi} - \mu \cdot d_2 \right)} \tag{A.6}$$

The relationship between torque and axial force for a M3 screw as used to hold the packaging system described in chapter 2.2 is given in figure A.2.

A.2 Calculation of compression of the PDMS microfluidic chip

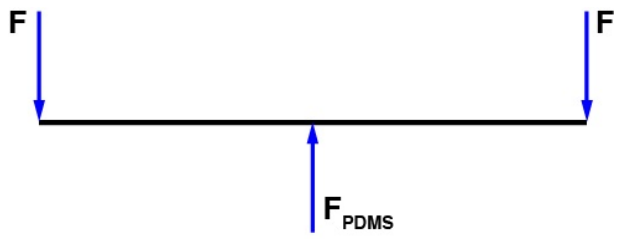

Figure A.3: Forces acting on the top plate and the resulting force on the PDMS microfluidic chip

The following assumptions were made: i) the top plate, the glass slide and the frame are rigid bodies, ii) the problem is two dimensional and iii) gravitational forces are

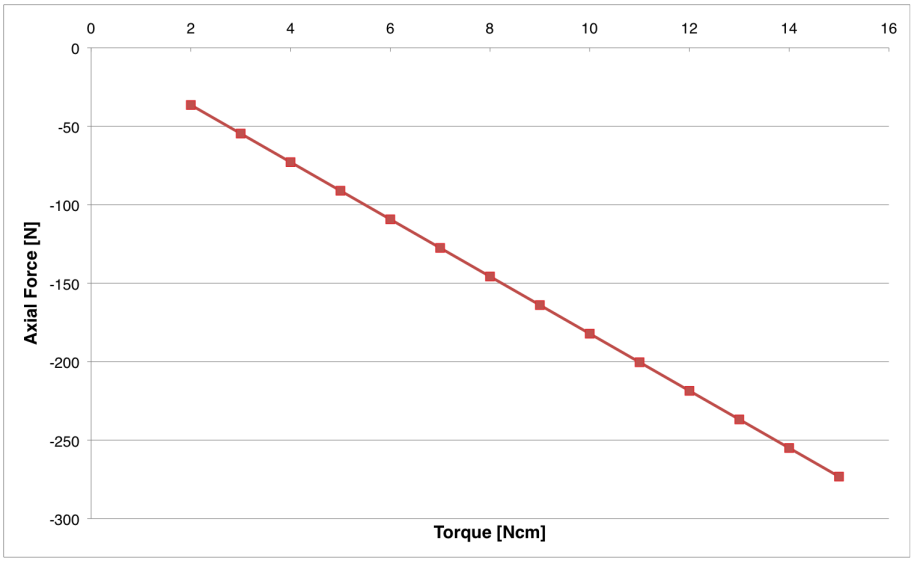

Figure A.2: Axial force F generated by sinking a M3 screw as a function of applied torque M_T. A friction factor of 0.47 is assumed between aluminium (frame) and steel (screw).

neglected. The force acting on the PDMS microfluidic chip F_{PDMS} was calculated by modelling the top plate as a beam (see Figure A.3). The sum of all forces in each direction and momentums has to be zero. In this case, no momentum is applied and no forces are acting in the X-direction , therefore:

$$\sum F_y = 0 \tag{A.7}$$

where F_y is the sum of all forces acting in the Y-direction.

$$F_{PDMS} - F - F = 0 \tag{A.8}$$

where F_PDMS is the force acting on the PDMS microfluidic chip and F is the axial force generated in the screw. After rearranging and solving for F_{PDMS}:

$$F_{PDMS} = 2 \cdot F \tag{A.9}$$

axial stress can be calculated by:

$$\sigma = \frac{F_{PDMS}}{A_{PDMS}} \tag{A.10}$$

where A_{PDMS} is the area of the PDMS chip the force is acting on.

To calculate the strain ϵ_{PDMS}, Hooke's law is used as an approximate model:

$$\sigma = E_{PDMS} \cdot \epsilon \tag{A.11}$$

where σ is mechanical stress and ϵ the strain. axial stress is replaced and from the following equation the axial strain is calculated:

$$\frac{F_{PDMS}}{A_{PDMS}} = E_{PDMS} \cdot \epsilon \tag{A.12}$$

where E_{PDMS} is the Young's modulus of PDMS.

$$\epsilon = \frac{F_{PDMS}}{A_{PDMS} \cdot E_{PDMS}} \tag{A.13}$$

To compute the deformation of a PDMS microfluidic layer in the Z-direction:

$$\epsilon = \frac{\triangle h}{h} \tag{A.14}$$

where h is the undeformed height of the PDMS microfluidic layer and $\triangle h$ the deformation of the PDMS microfluidic layer. After rearranging the equation, the deformation in height can be computed:

$$\triangle h = \epsilon \cdot h \tag{A.15}$$

The same calculations can be made for the lateral deformation of the PDMS microfluidic layer.

$$\epsilon_l = -\nu \cdot \epsilon = \frac{\triangle w}{w} \tag{A.16}$$

where w is the undeformed width of the PDMS microfluidic layer and $\triangle w$ the deformation of the PDMS microfluidic layer in lateral direction.

$$\triangle w = \epsilon_l \cdot w \tag{A.17}$$

References

M. Meier, Dimensionieren I, Lecture notes ETH Zurich, 2005.

Appendix B

Drawings & part list

B.1 Material and part list & drawings for the first generation packaging system

Material and part list required to fabricate and assemble the first generation packaging system described in chapter 2.2.1.

Table B.1: Part list for the first generation packaging system

Part	Cat. No.	Supplier
Poly(carbonate) sheet 2 mm thick	258-6613	RS Components
Poly(carbonate) sheet 3 mm thick	681-637	RS Components
Dow Corning Sylgard 184	634165S	VWR International
M3×6 Stainless Steel Socket Head Cap Screw	187-1207	RS Components
M3×6 Stainless Steel Countersink Screw	304-4788	RS Components
Steel parallel dowel pin 2.5 mm × 10 mm	270-524	RS Components

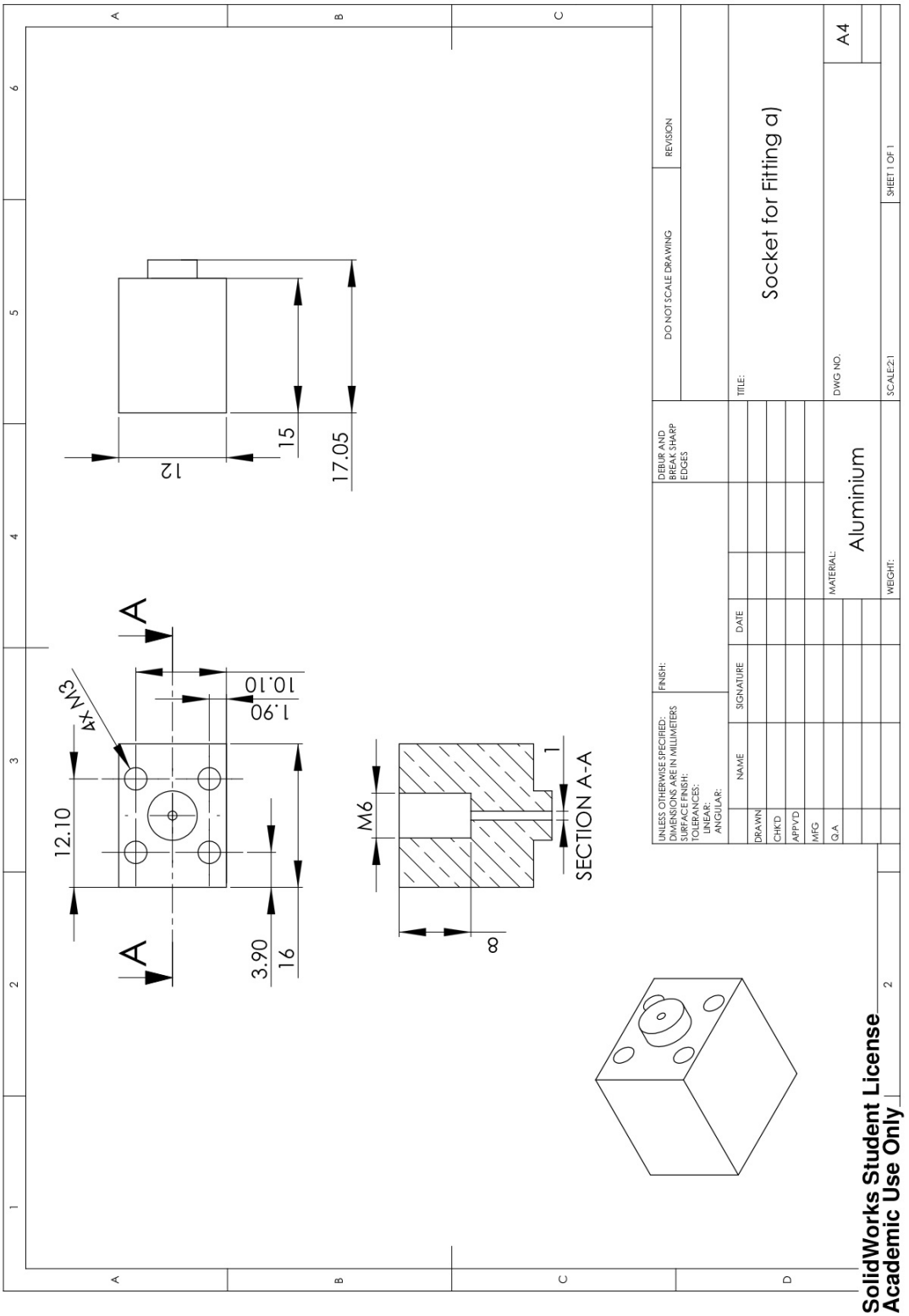

Figure B.1: Socket for fitting - Type A - Dimensions in mm.

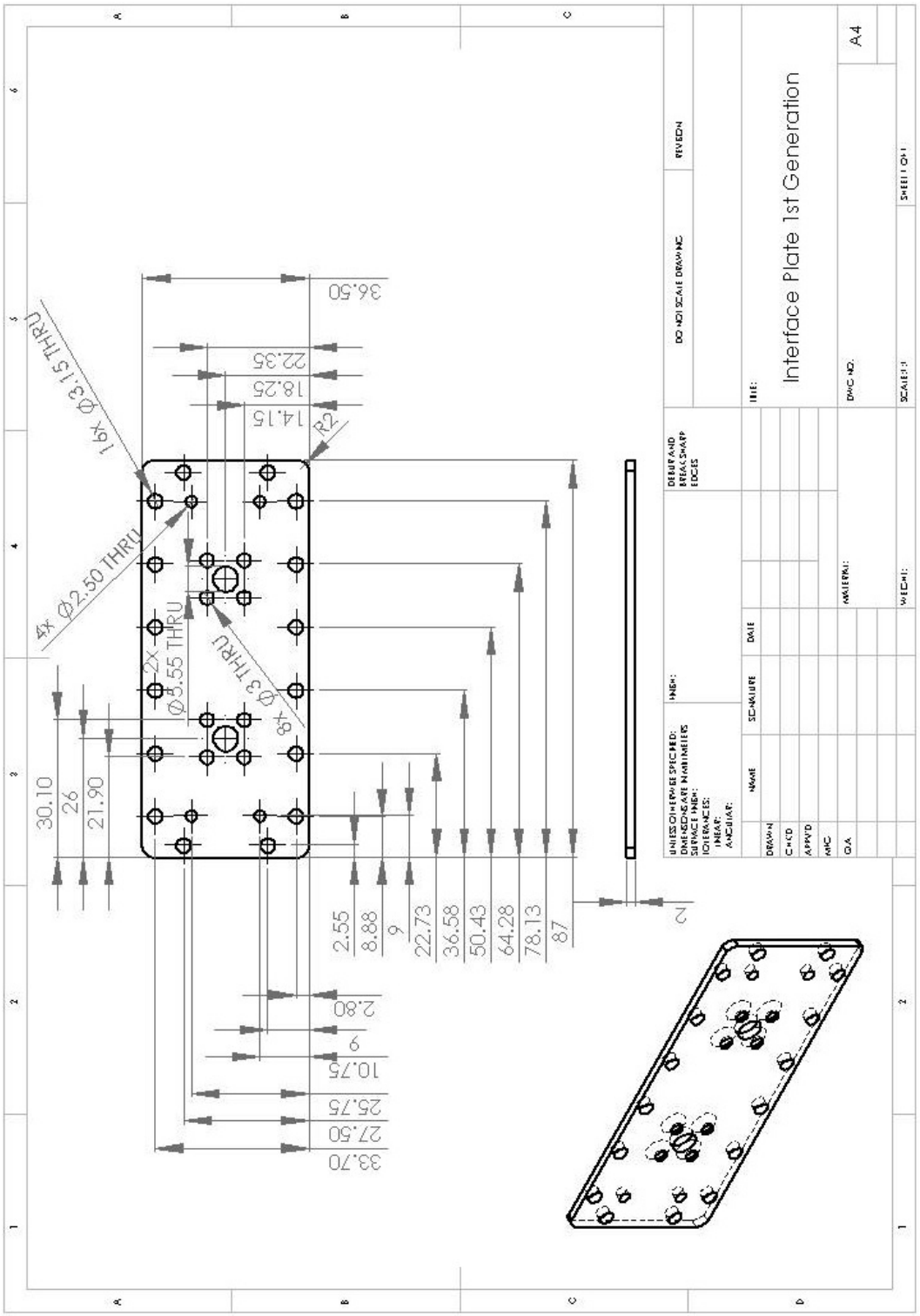

Figure B.2: Interface plate for the first generation packaging system - Dimensions in mm.

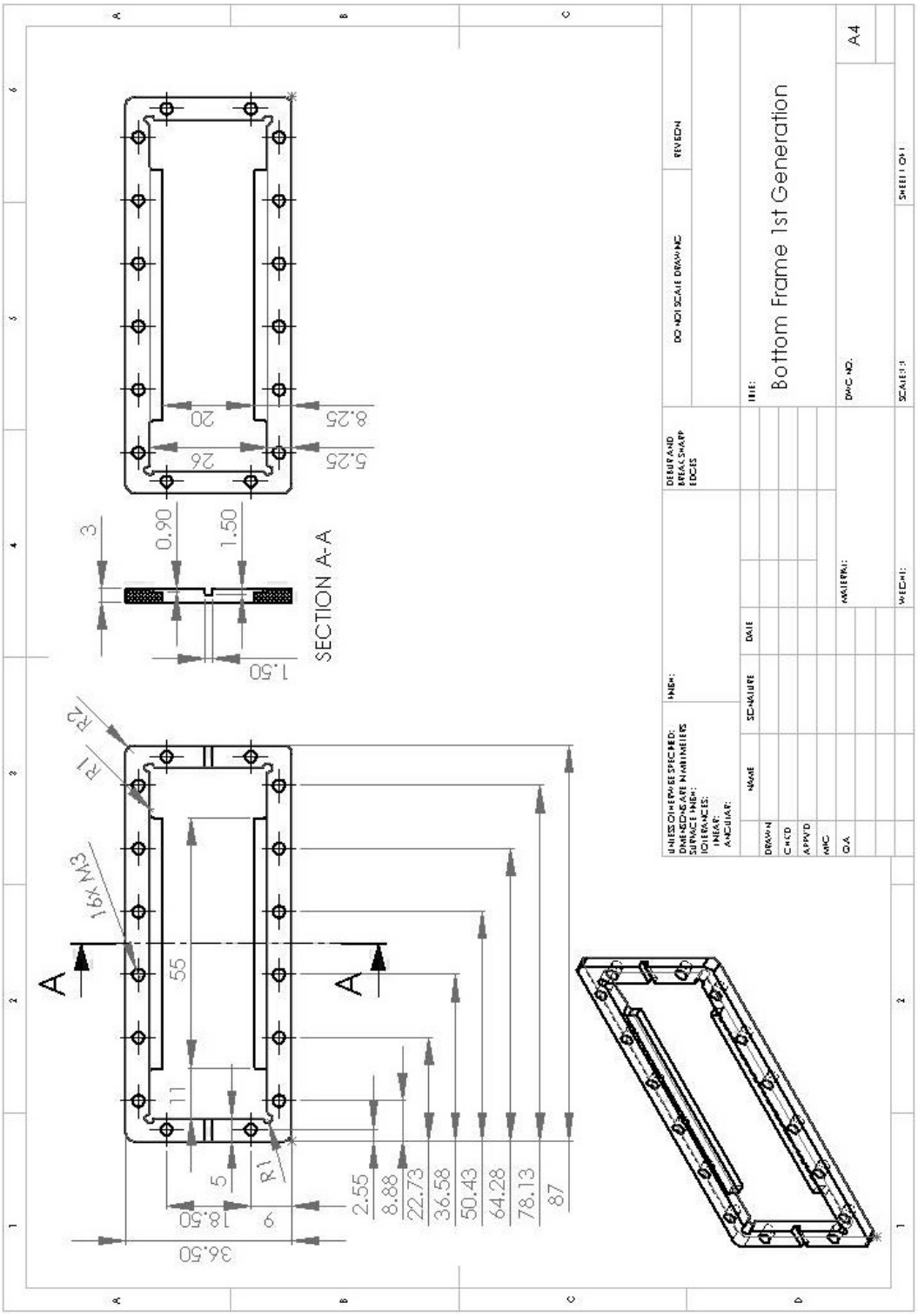

Figure B.3: Frame for the first generation packaging system - Dimensions in mm.

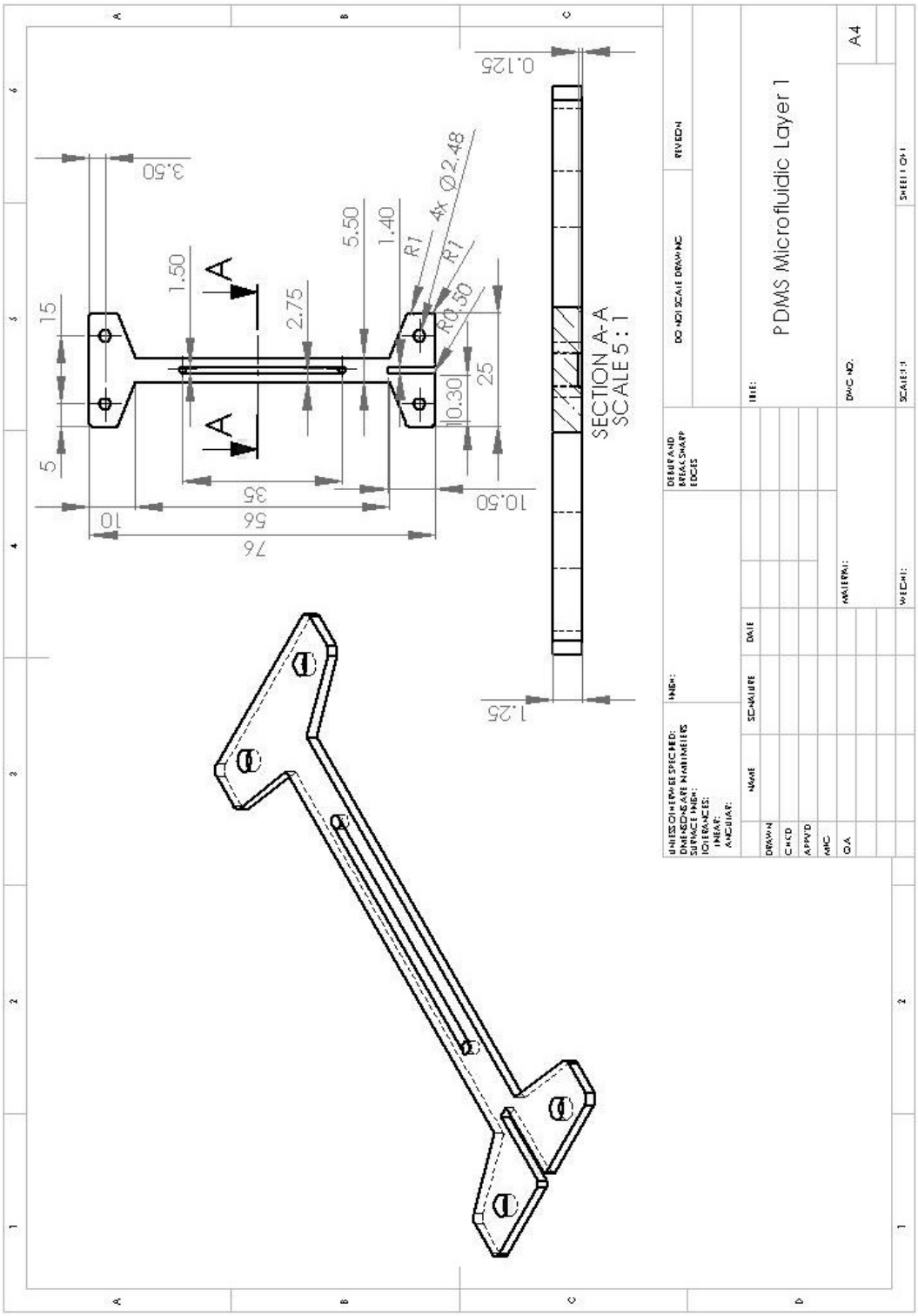

Figure B.4: Microfluidic layer for the first generation packaging system - Dimensions in mm.

B.2 Material and part list & drawings for the second generation packaging system

Material and part list required to fabricate and assemble the second generation packaging system described in chapter 2.2.2.

Table B.2: Part list for the second generation packaging system

Part	Cat. No.	Supplier
Poly(carbonate) sheet 3 mm thick	681-637	RS Components
Dow Corning Sylgard 184	634165S	VWR International
M3×6 Stainless Steel Socket Head Cap Screw	187-1207	RS Components
M3×6 Stainless Steel Countersink Screw	304-4788	RS Components

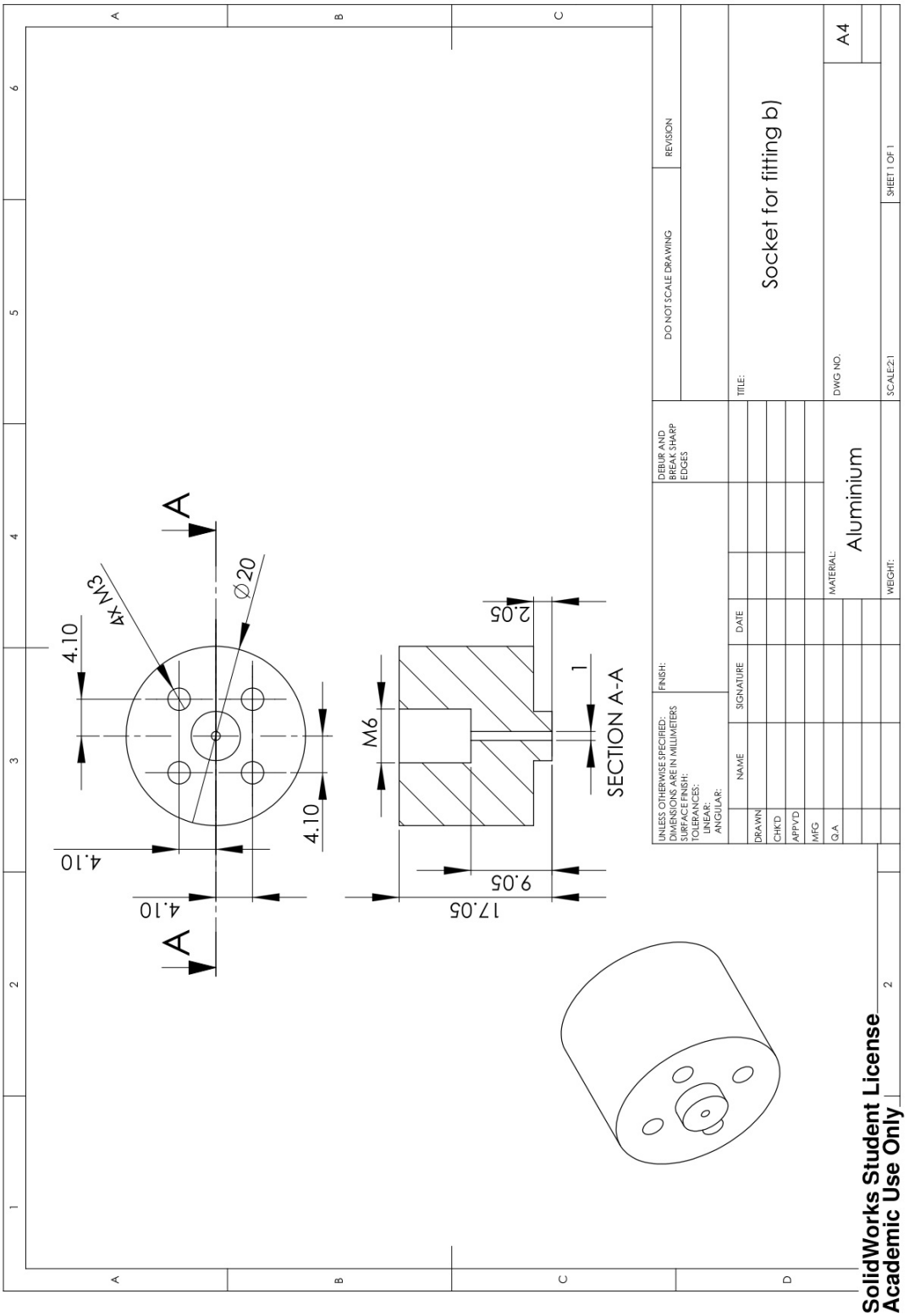

Figure B.5: Socket for fitting - Type B - Dimensions in mm.

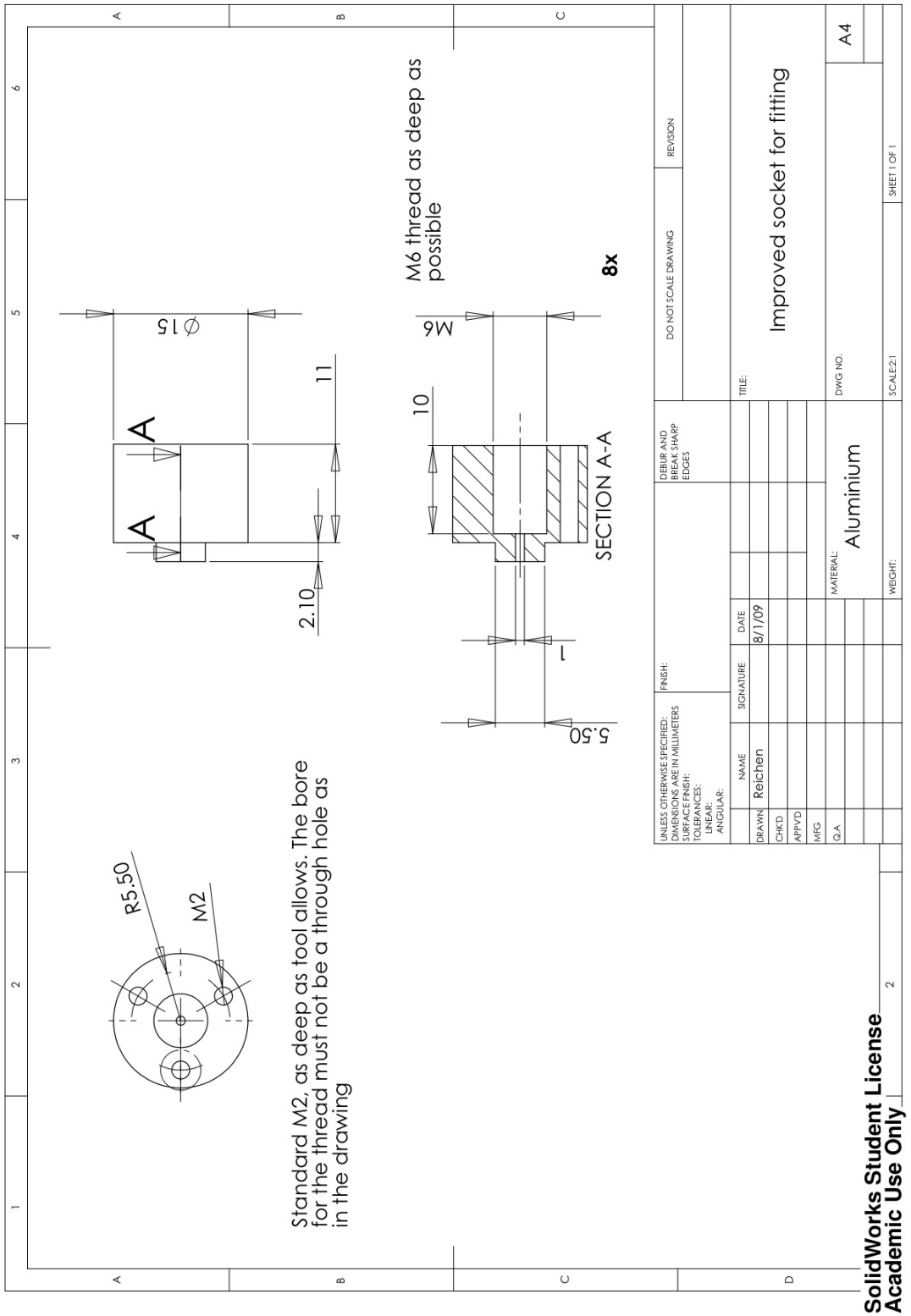

Figure B.6: Socket for fitting - Type C - Dimensions in mm.

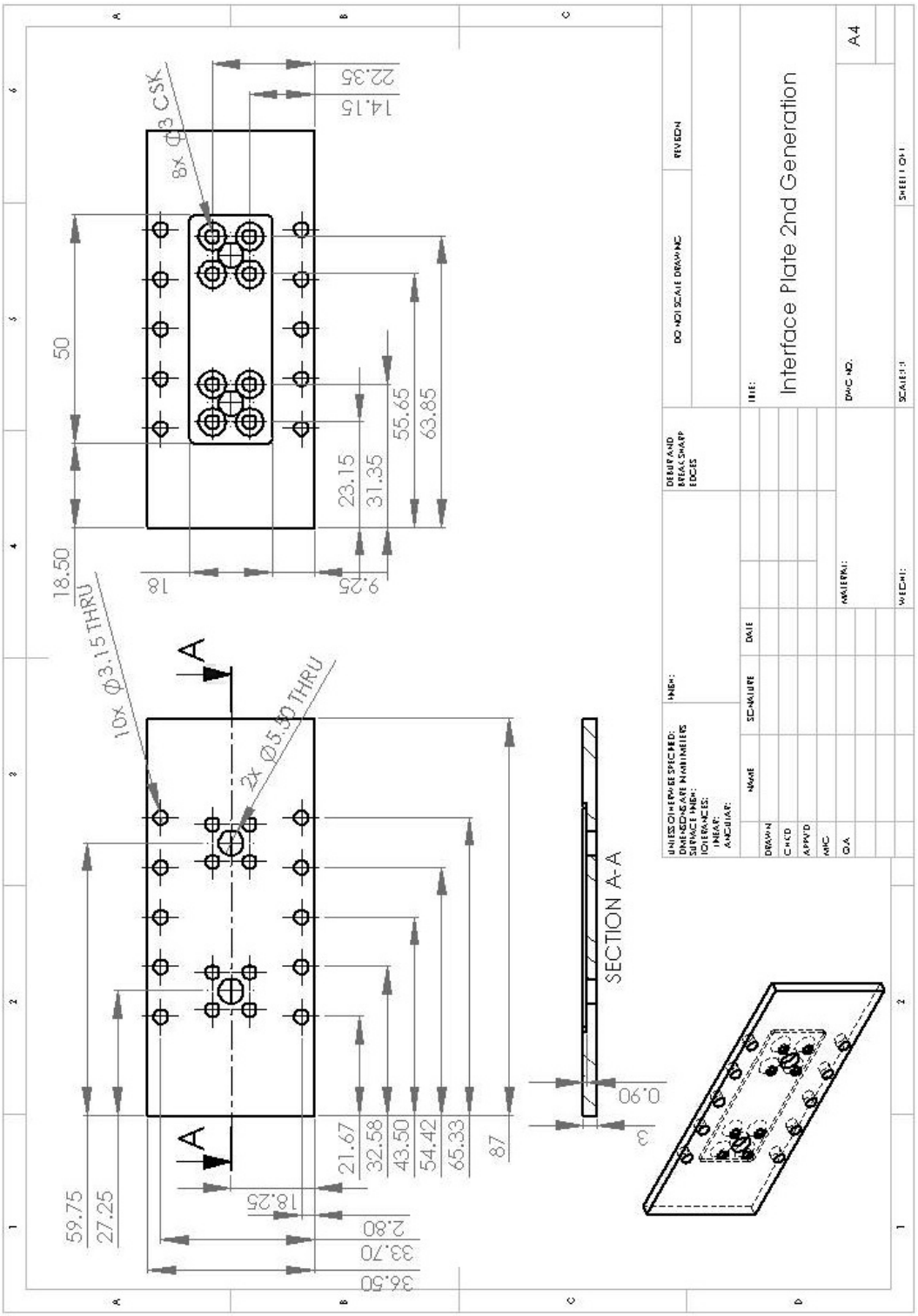

Figure B.7: Interface plate for the second generation packaging system - Dimensions in mm.

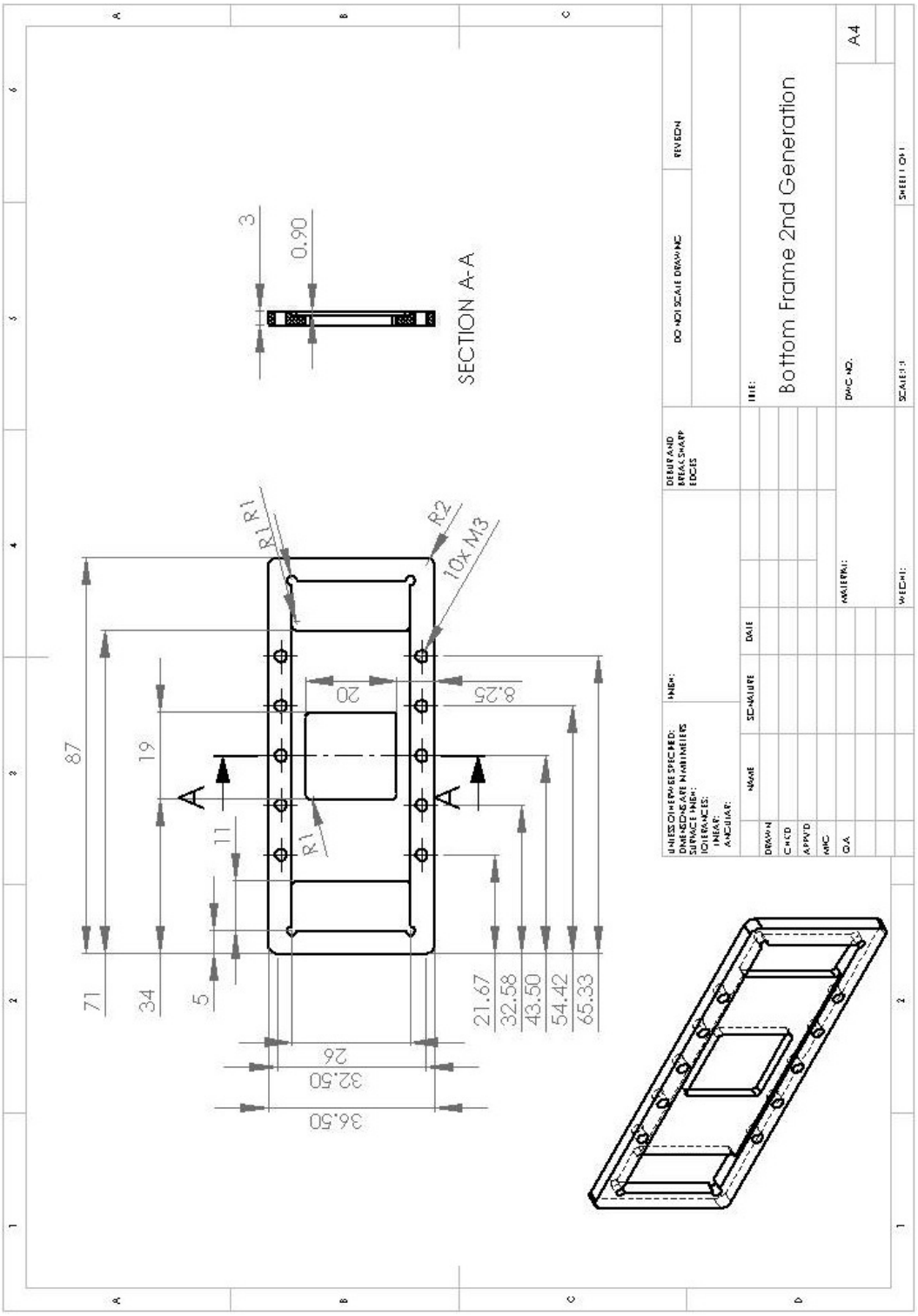

Figure B.8: Frame for the second generation packaging system - Dimensions in mm.

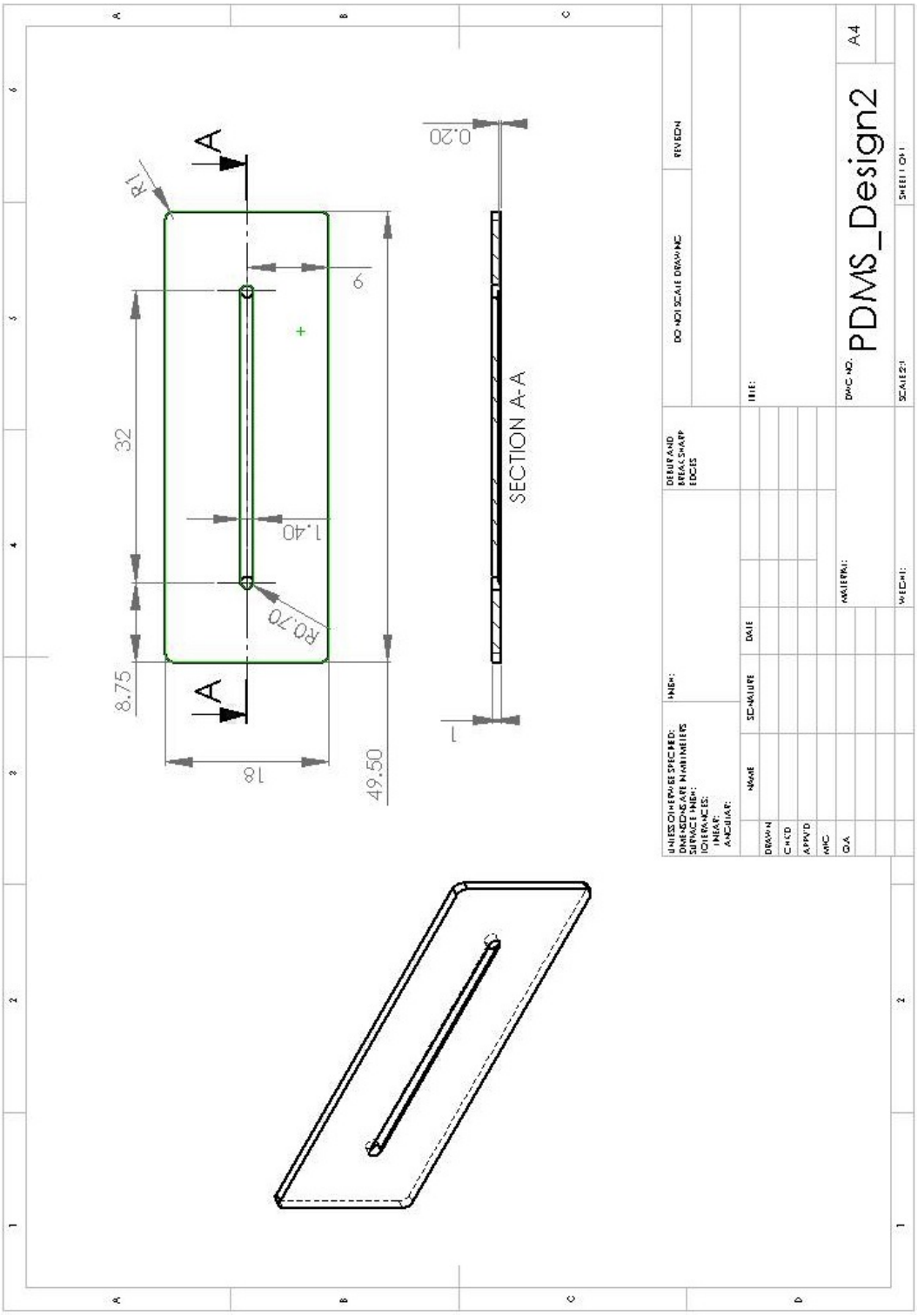

Figure B.9: Microfluidic layer for the second and third generation packaging system - Dimensions in mm.

B.3 Material and part list & drawings for the third generation packaging system

Material and part list required to fabricate and assemble the third generation packaging system described in chapter 2.2.3.

Table B.3: Part list for the third generation packaging system

Part	Cat. No.	Supplier
Poly(methylmethacrylate) sheet 5 mm thick	824-525	RS Components
Poly(methylmethacrylate) sheet 6 mm thick	680-886	RS Components
Aluminium sheet 3 mm thick	ALU-35	HABA
Dow Corning Sylgard 184	634165S	VWR International
M3×6 Stainless Steel Socket Head Cap Screw	187-1207	RS Components
M3×8 Stainless Steel Countersink Screw	187-1213	RS Components

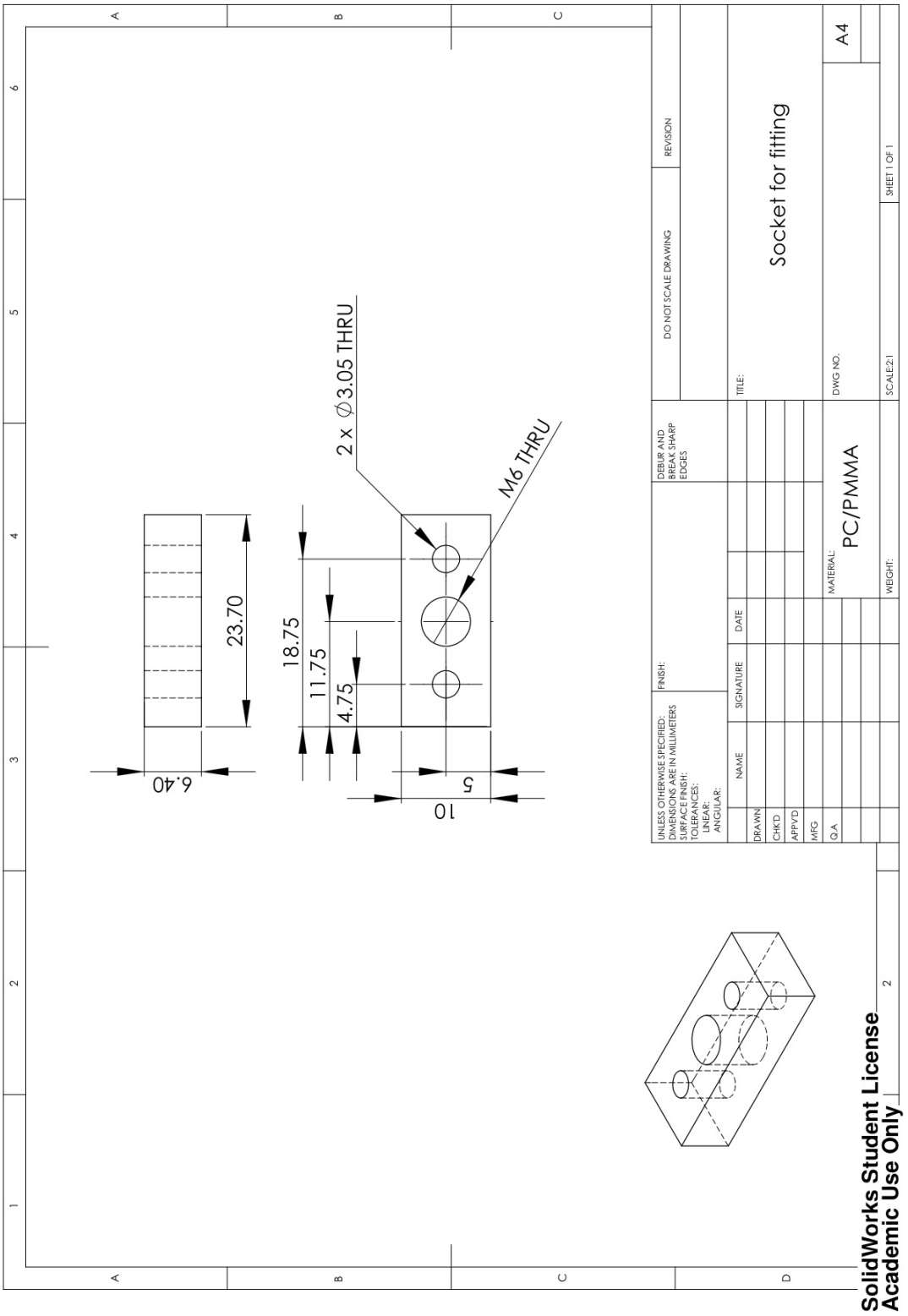

Figure B.10: Socket for fitting - Type D - Dimensions in mm.

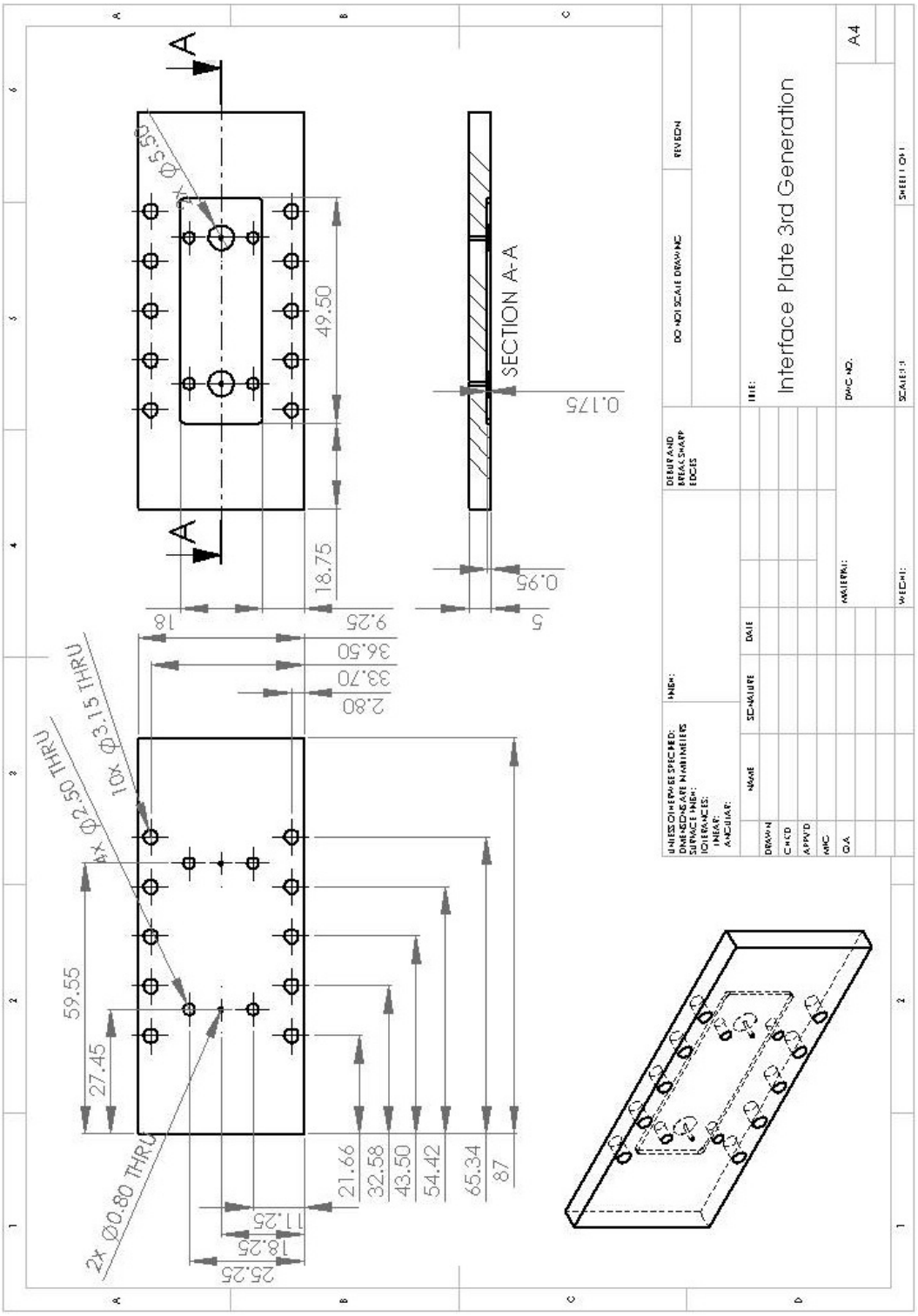

Figure B.11: Interface plate for the third generation packaging system - Dimensions in mm.

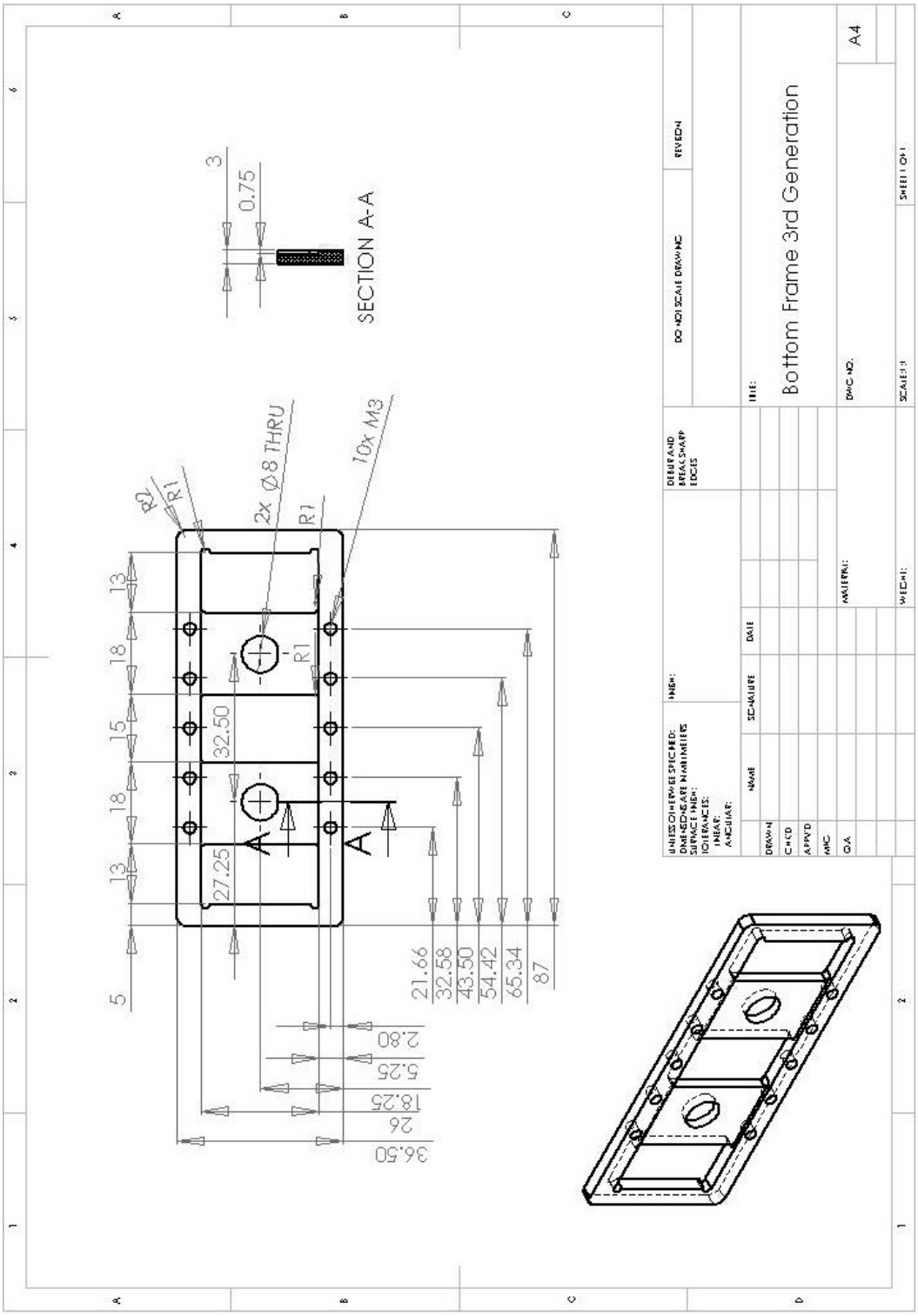

Figure B.12: Frame for the third generation packaging system - Dimensions in mm.

B.4 Drawings for the 3-D microfluidic demonstrator and the staggered herringbone mixer

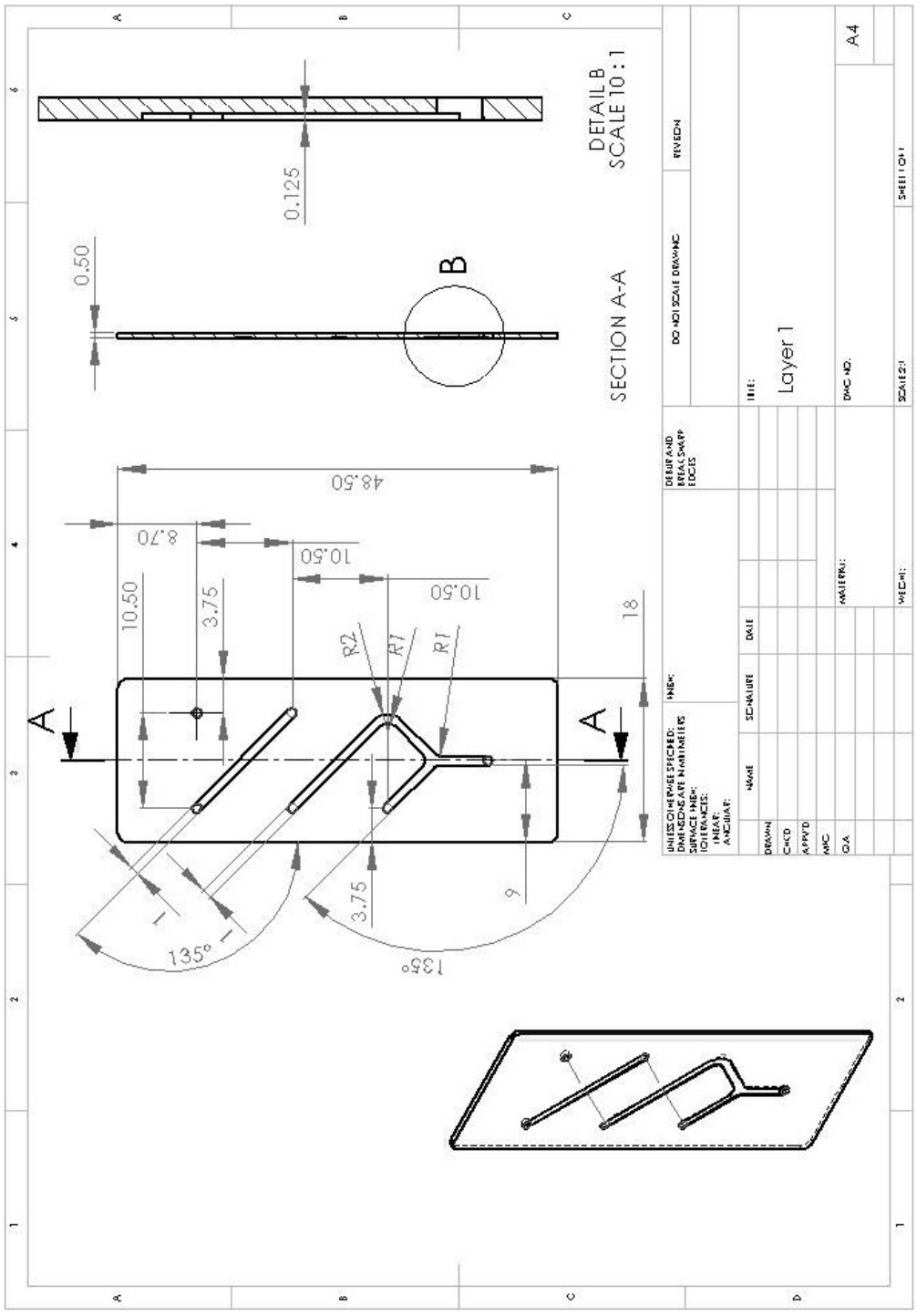

Figure B.13: Layer 1 of the 3-D microfluidic demonstrator - Dimensions in mm.

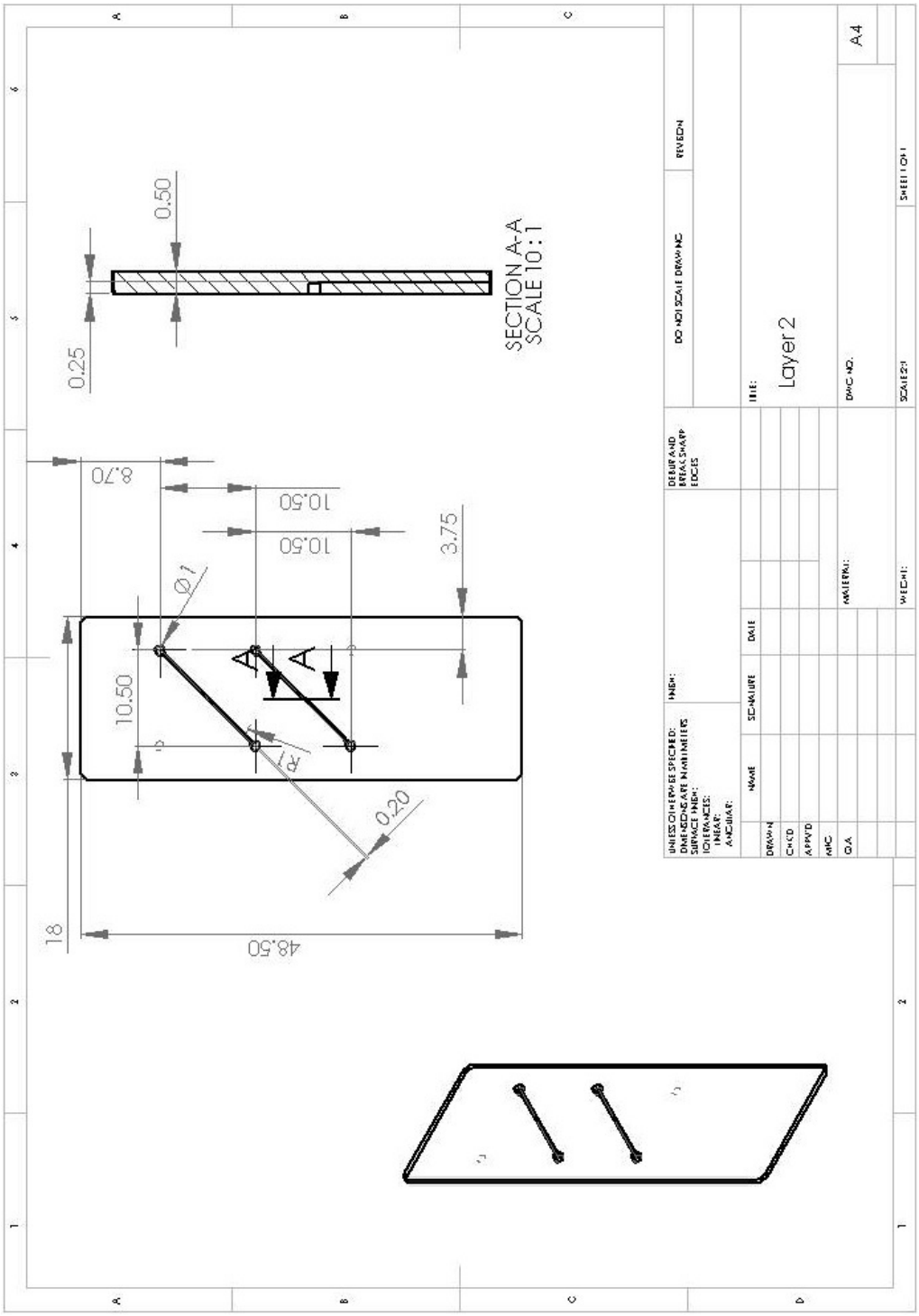

Figure B.14: Layer 2 of the 3-D microfluidic demonstrator - Dimensions in mm.

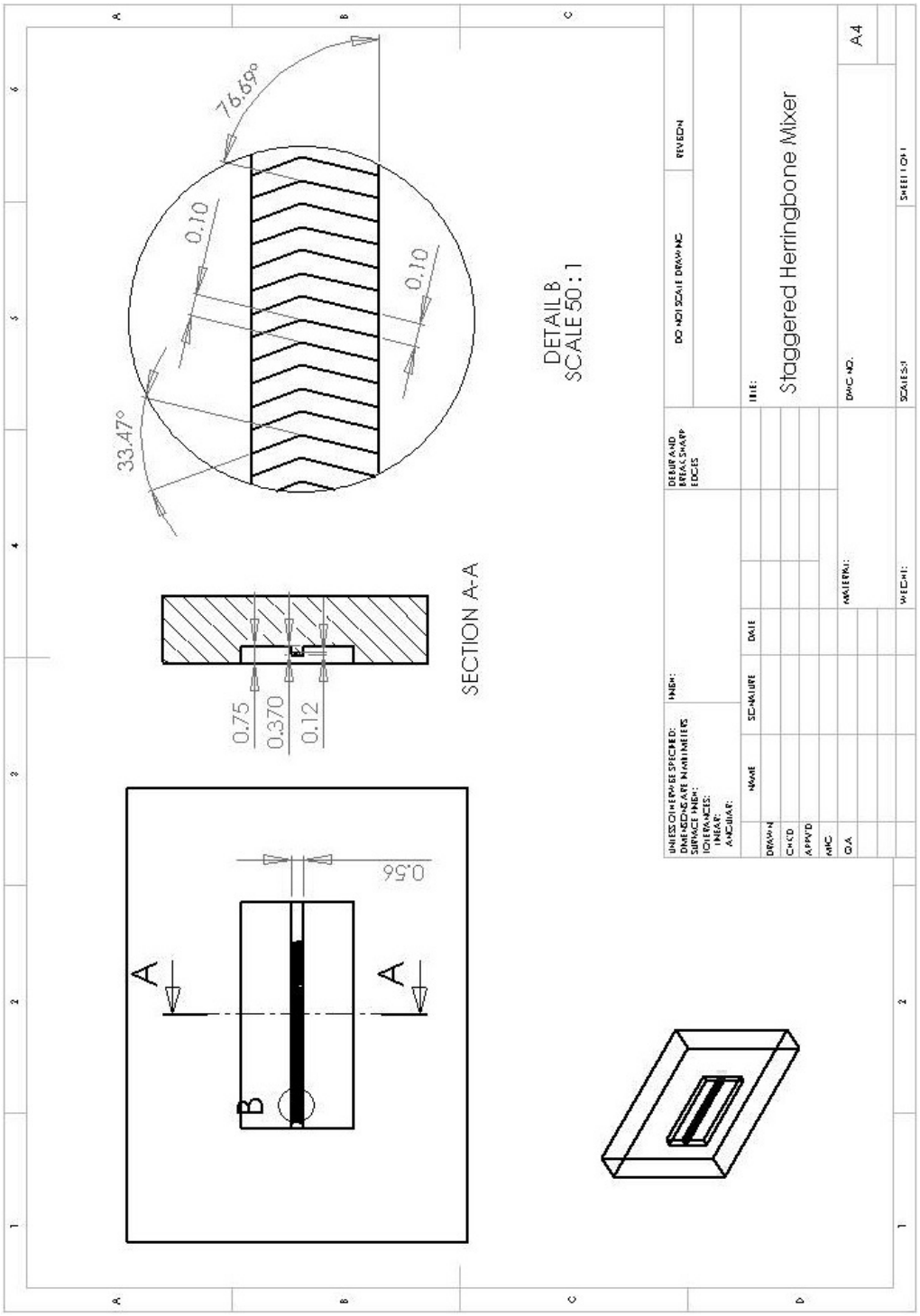

Figure B.15: Mould for staggered herringbone mixer - Jointly developed with Dr. B. O'Sullivan. Dimensions in mm.

B.5 Material and part list & drawings for the microfabricated cell culture device used in chapter 3

Material and part list required to fabricate and assemble the microfabricated cell culture device and the low hydrodynamic shear stress microfluidic layer used in chapter 3. Please note that the frame and the sockets for the fittings are the same as the ones used for the second generation packaging system (compare with section B.2).

Table B.4: Part list for the microfabricated cell culture device used in chapter 3

Part	Cat. No.	Supplier
Poly(carbonate) sheet 3 mm thick	681-637	RS Components
Poly(carbonate) sheet 5 mm thick	681-659	RS Components
Dow Corning Sylgard 184	634165S	VWR International
M3×6 Stainless Steel Socket Head Cap Screw	187-1207	RS Components
M3×8 Stainless Steel Countersink Screw	187-1213	RS Components

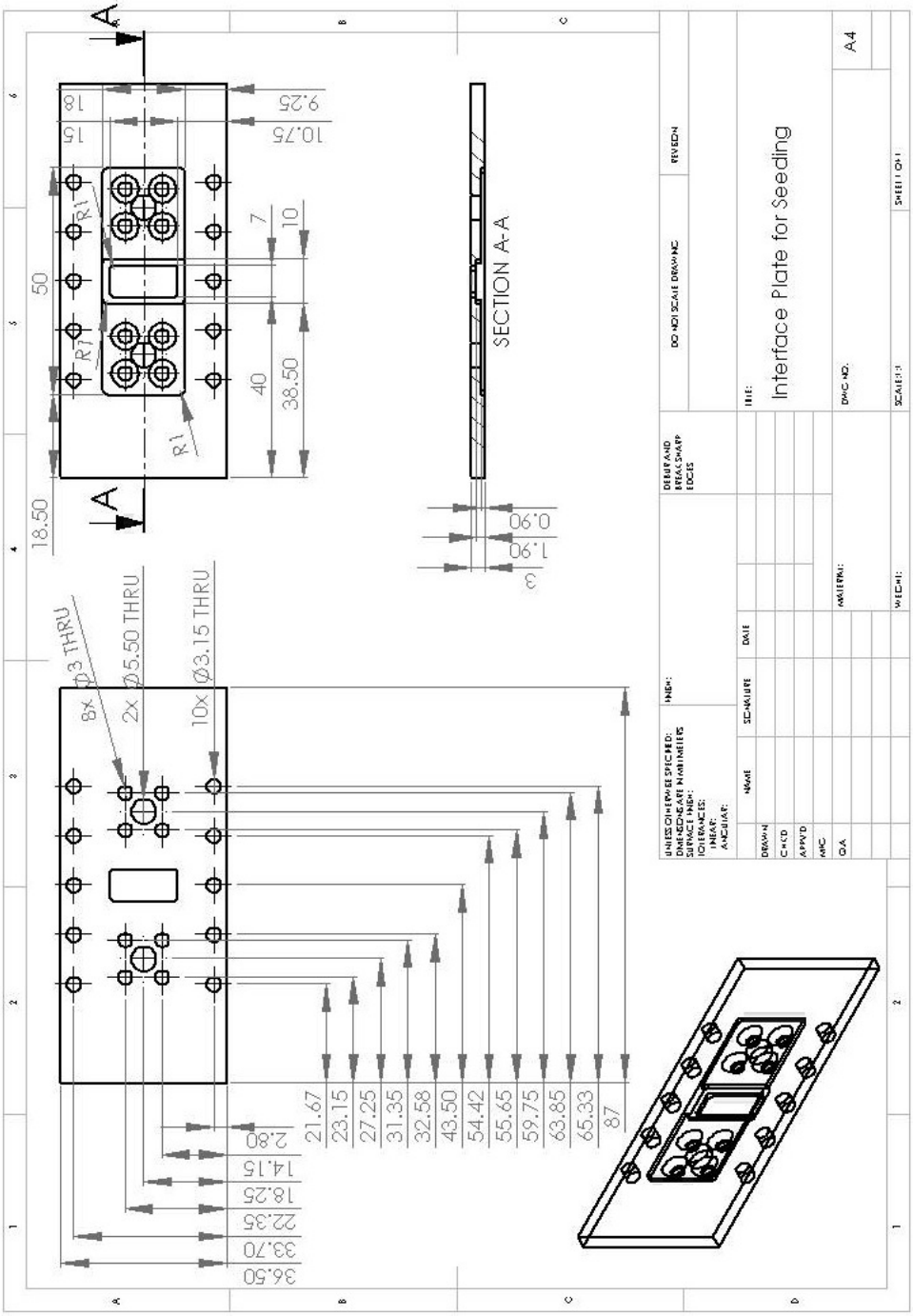

Figure B.16: Interface plate for the third generation packaging system - Dimensions in mm.

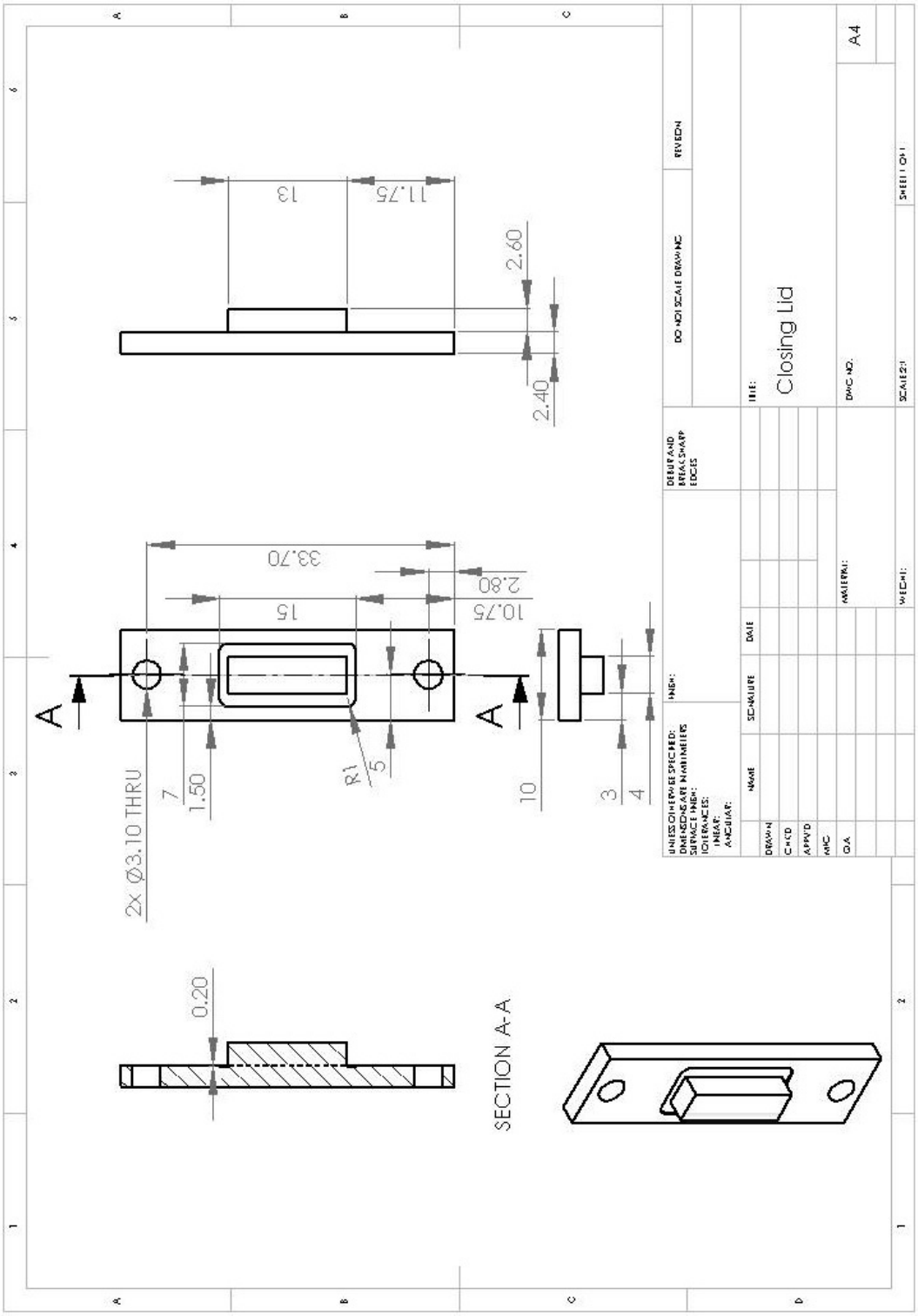

Figure B.17: Closing lid for the microfabricated cell culture device used in chapter 3 - Dimensions in mm.

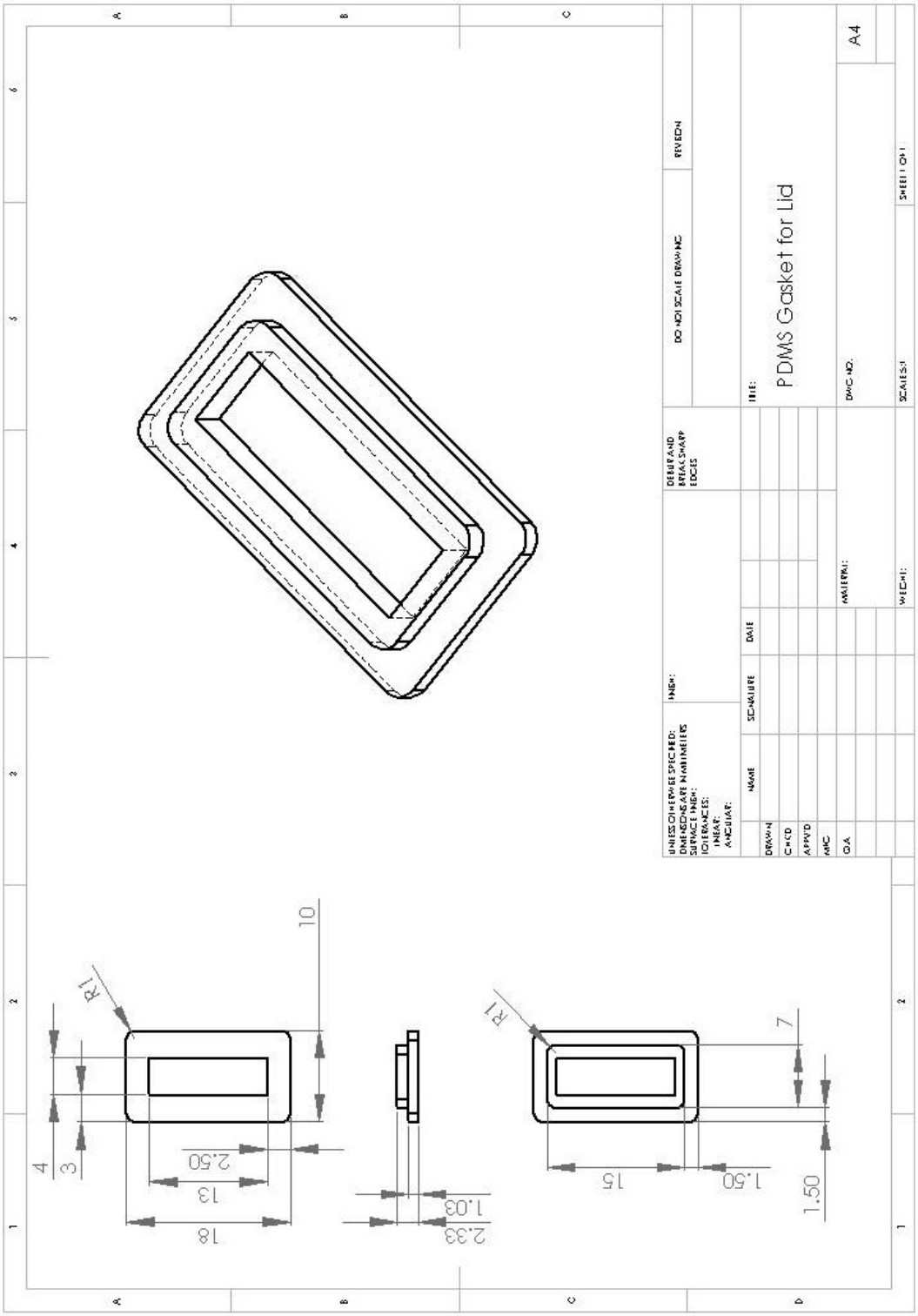

Figure B.18: PDMS gasket for the microfabricated cell culture device used in chapter 3 - Dimensions in mm.

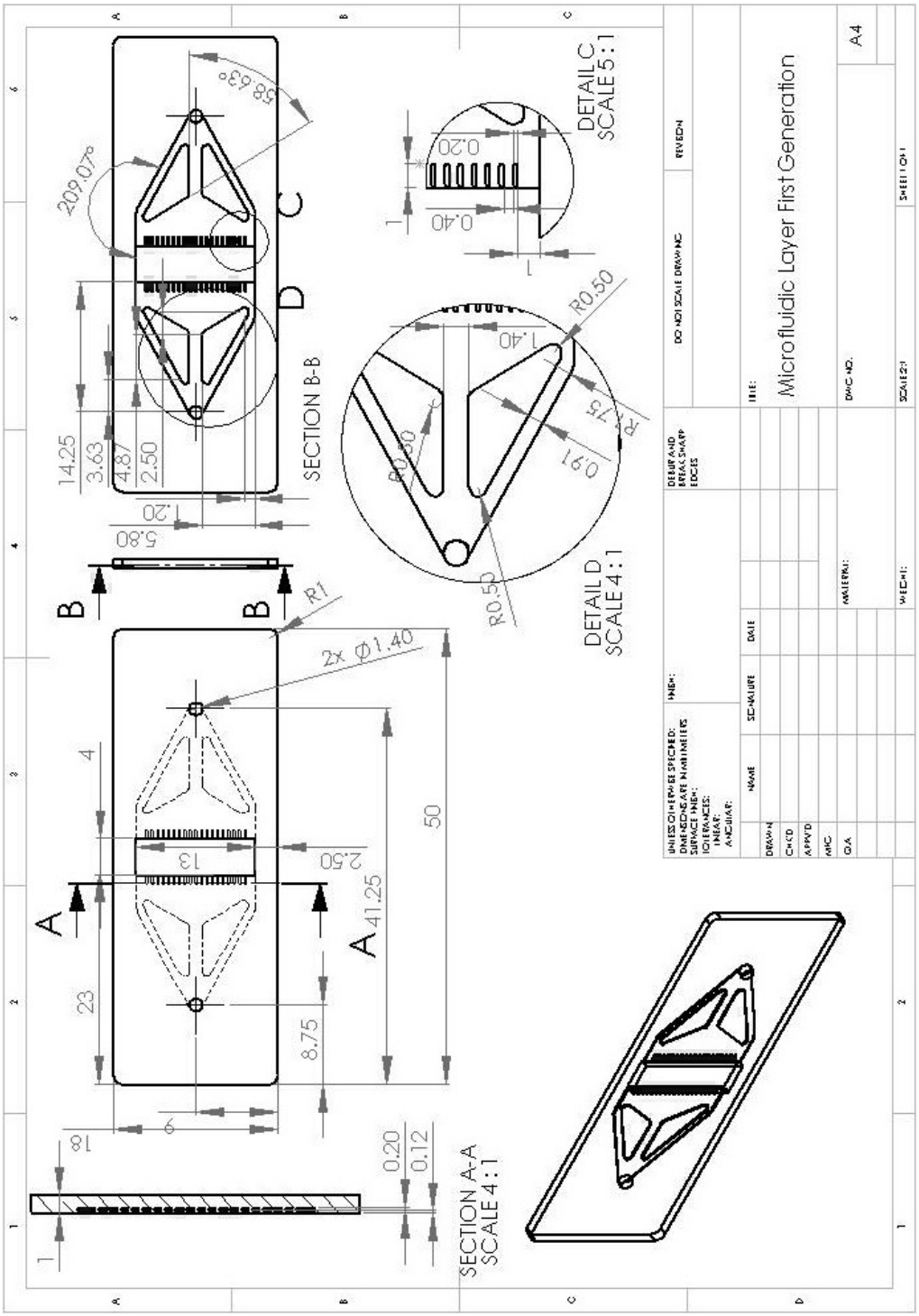

Figure B.19: First generation microfluidic layer used in chapter 3 - Dimensions in mm.

B.6 Material and part list & drawings for the microfluidic platform used in chapter 4

Material and part list required to fabricate and assemble the microfabricated cell culture device used for the platform, improved versions of the low hydrodynamic shear stress microfluidic layer used in chapter 3, the preheat section and the bubble trap. Please note that the sockets for the fittings are the same as the ones used for the third generation packaging system (compare with section **??**).

Table B.5: Part list for the microfabricated cell culture device used in chapter 4

Part	Cat. No.	Supplier
Poly(carbonate) sheet 3 mm thick	681-637	RS Components
Poly(carbonate) sheet 5 mm thick	681-659	RS Components
Poly(carbonate) sheet 8 mm thick	258-6629	RS Components
Aluminium sheet 3 mm thick	ALU-35	HABA
Dow Corning Sylgard 184	634165S	VWR International
M3×8 Stainless Steel Socket Head Cap Screw	187-1213	RS Components
M3×10 Stainless Steel Socket Head Cap Screw	660-4636	RS Components

B.6.1 Microfabricated cell culture device

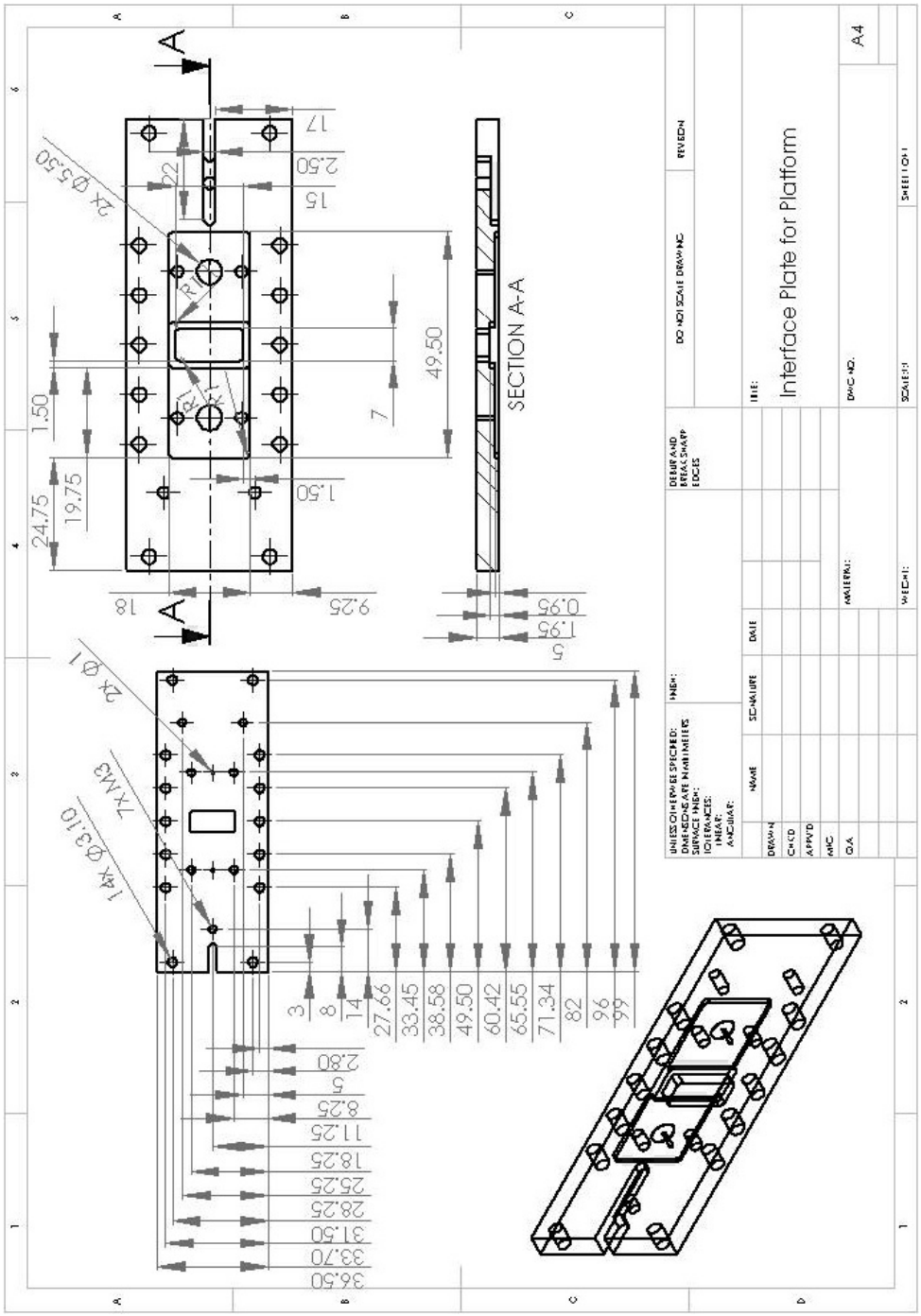

Figure B.20: Interface plate for the microfluidic platform - Dimensions in mm.

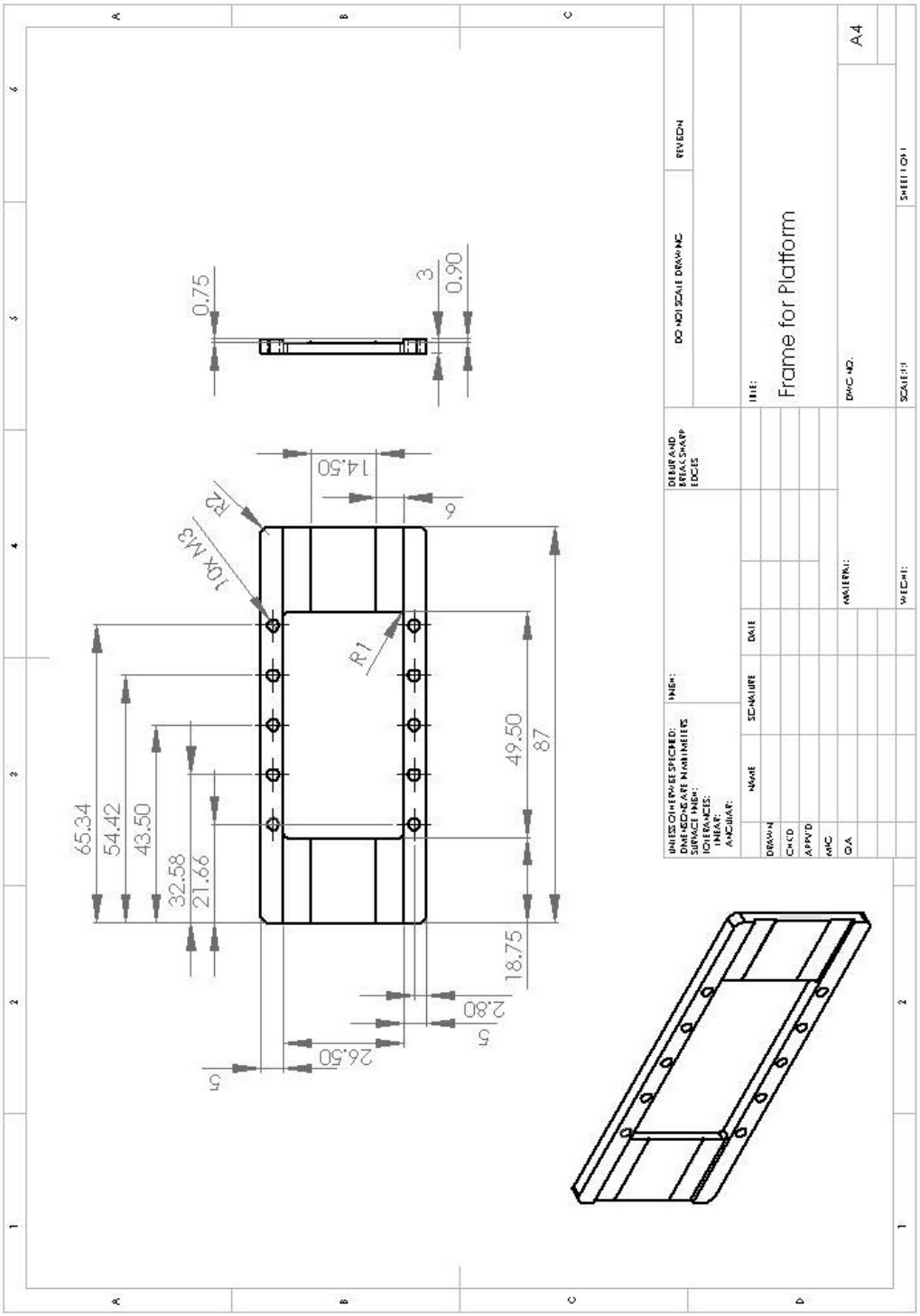

Figure B.21: Frame for the microfluidic platform - Dimensions in mm.

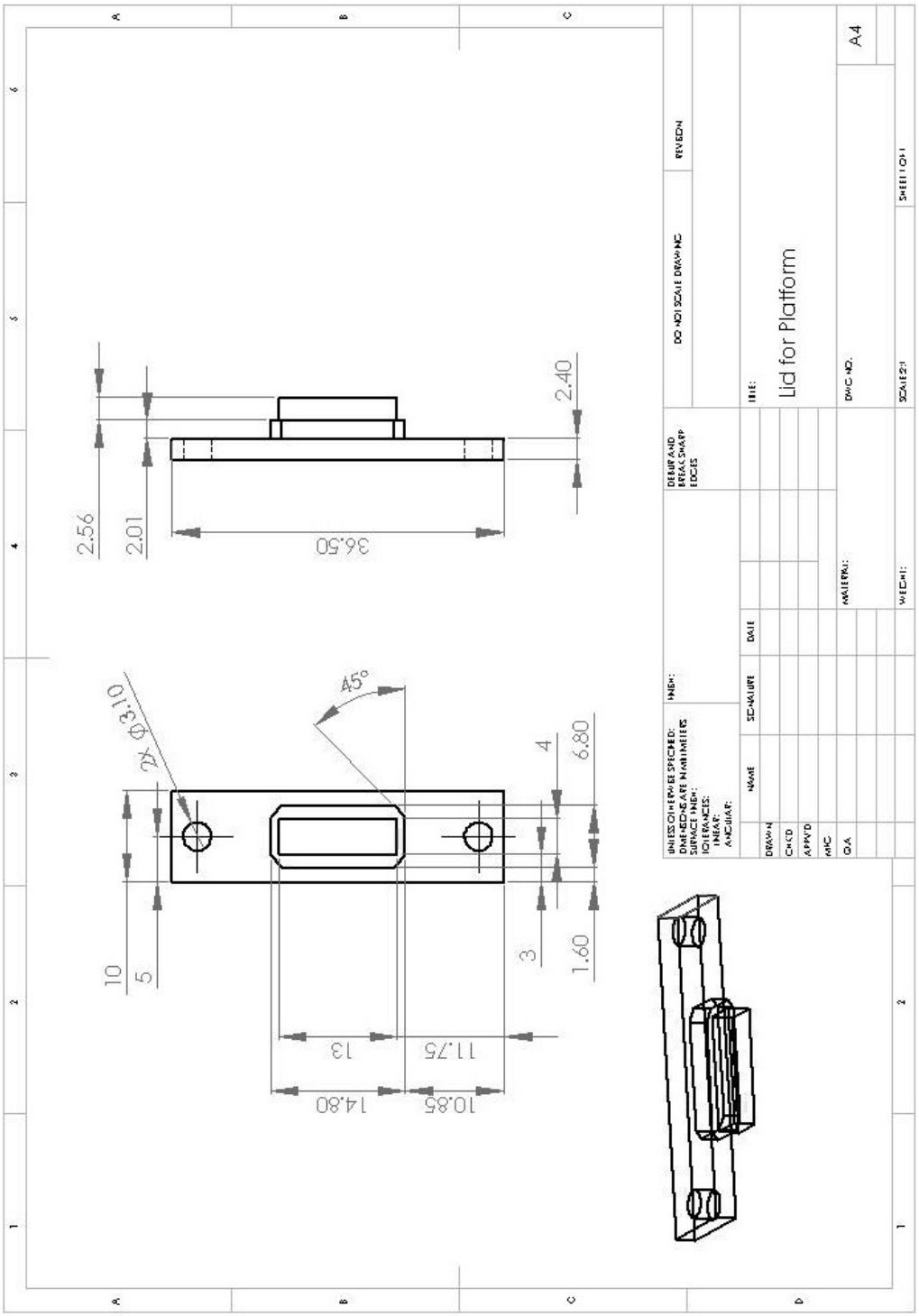

Figure B.22: Closing lid for the microfabricated cell culture device used in chapter 4 - Dimensions in mm.

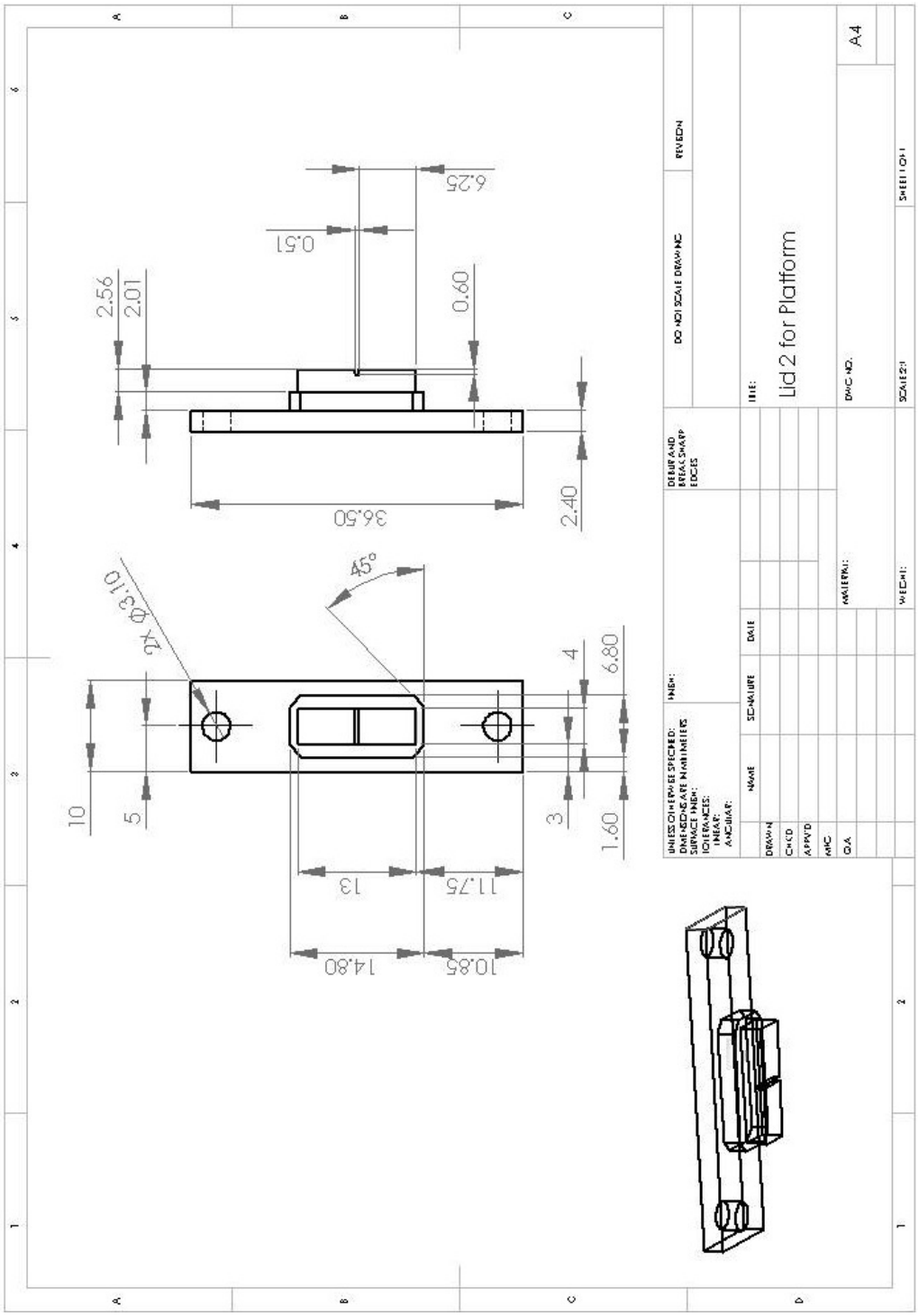

Figure B.23: Closing lid for the microfluidic chip used in chapter 4 - Dimensions in mm.

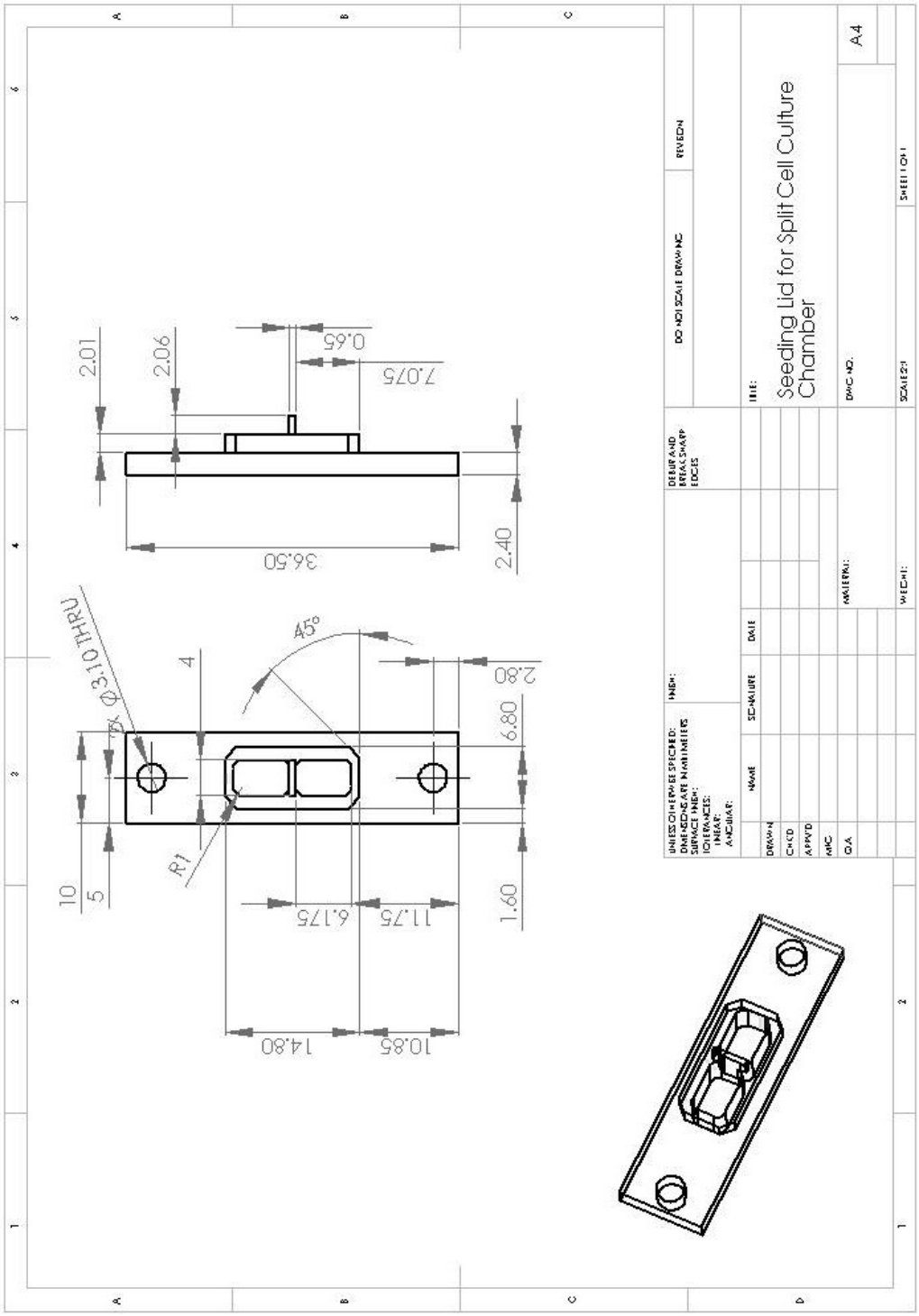

Figure B.24: Seeding lid for the split microfluidic chip used in chapter 4 - Dimensions in mm.

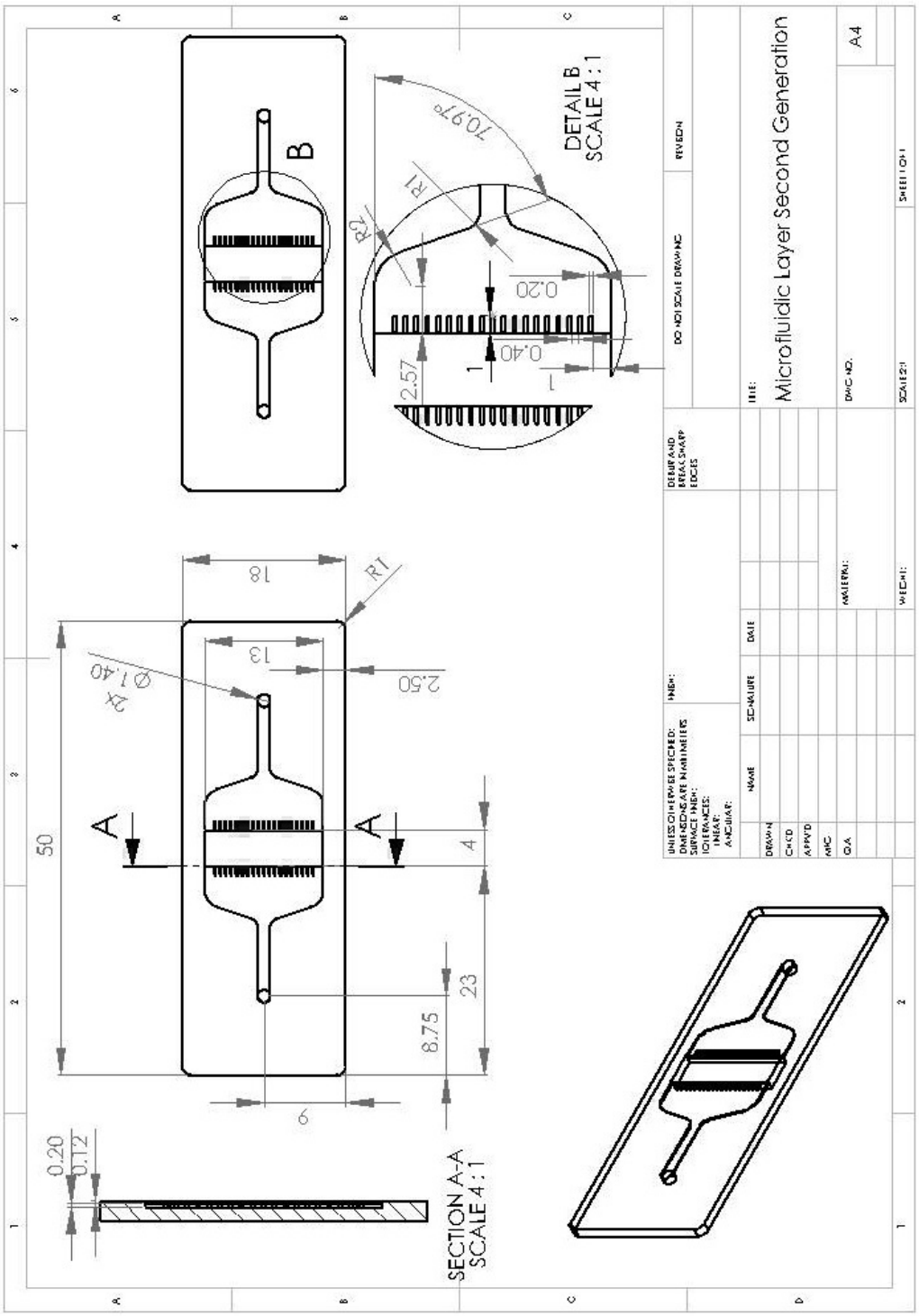

Figure B.25: Second generation microfluidic layer used in chapter 4 - Dimensions in mm.

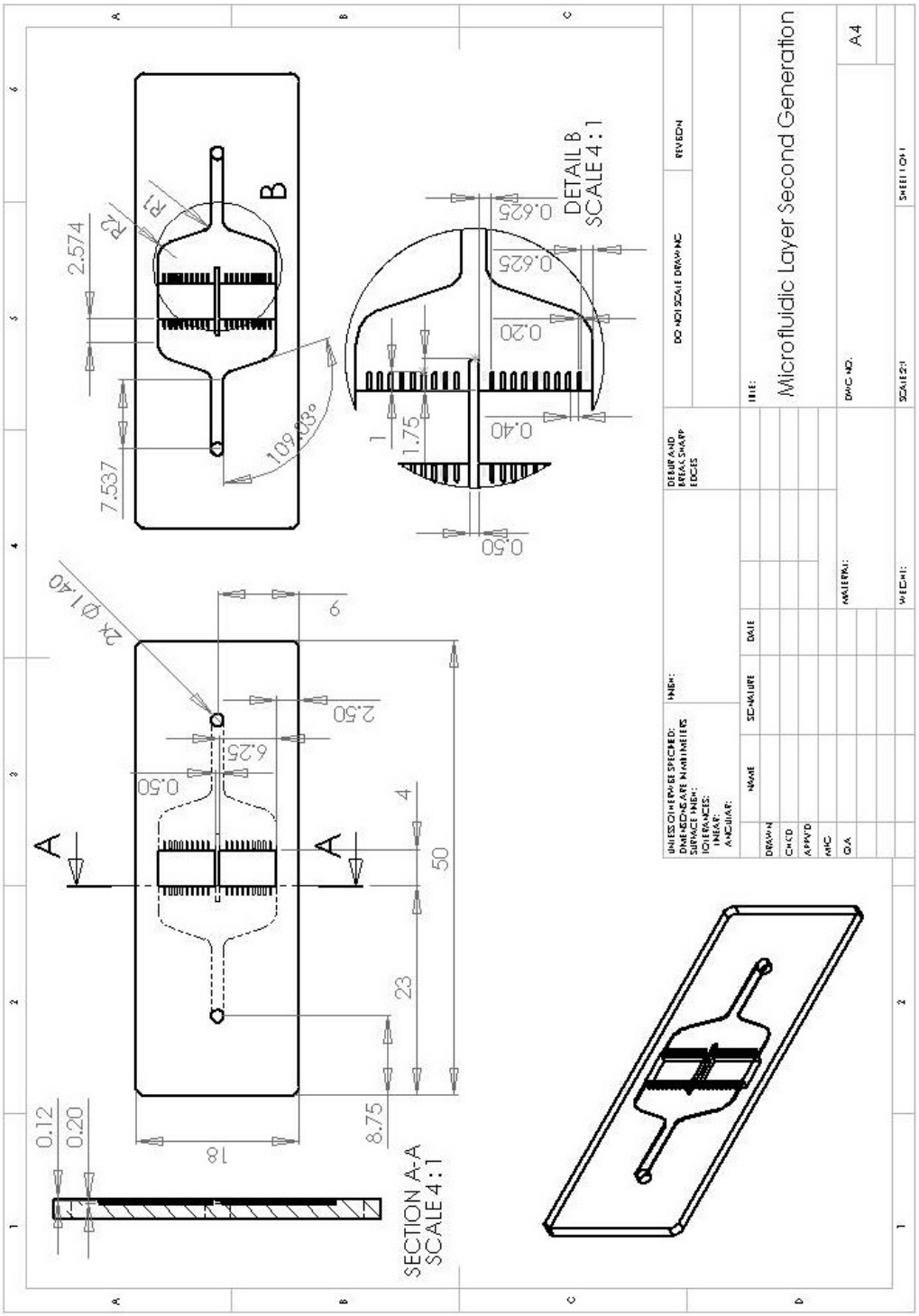

Figure B.26: Split microfluidic layer used in chapter 4 - Dimensions in mm.

B.6.2 Bubble trap

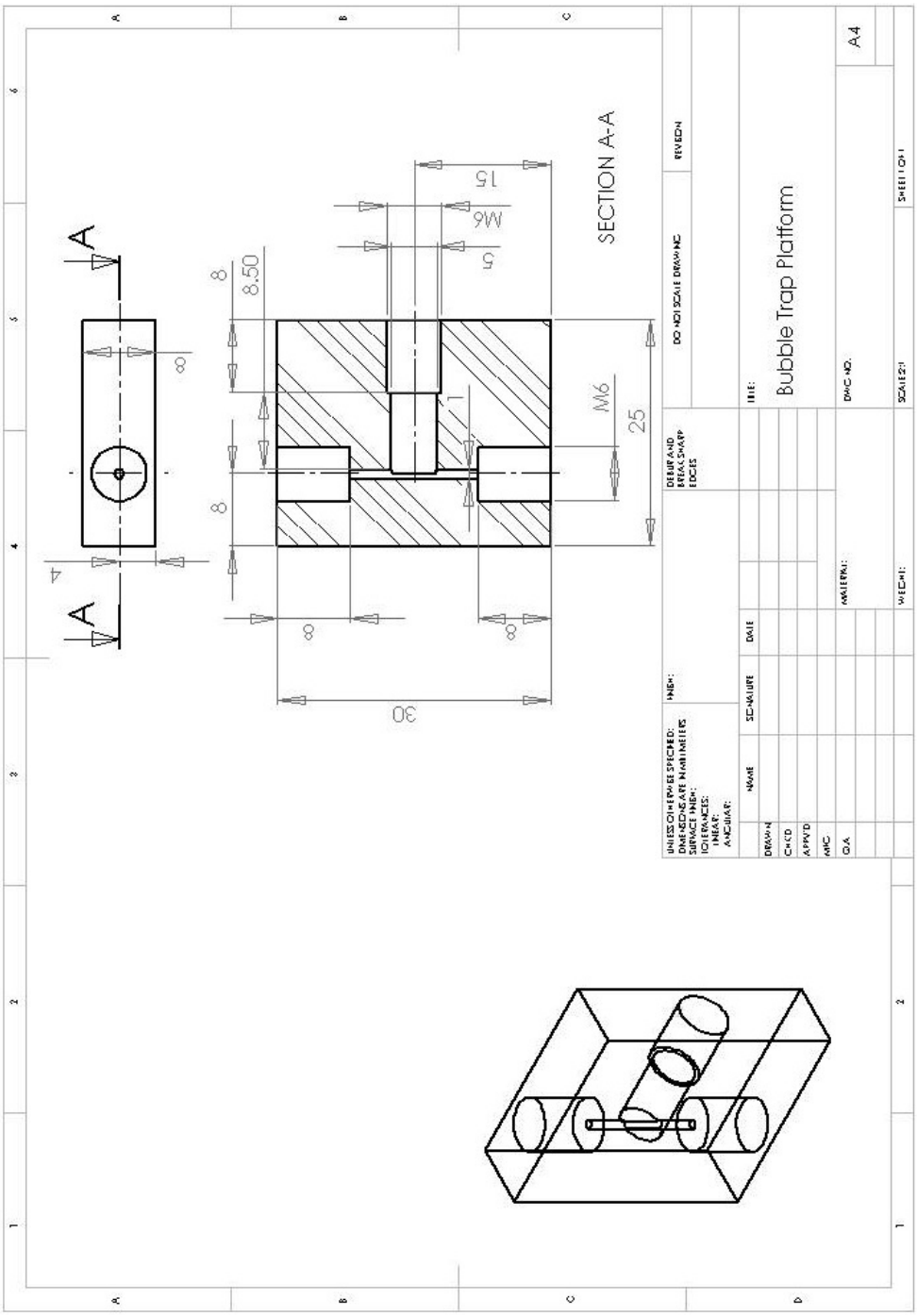

Figure B.27: Bubble trap used in chapter 4 - Dimensions in mm.

B.6.3 Preheat

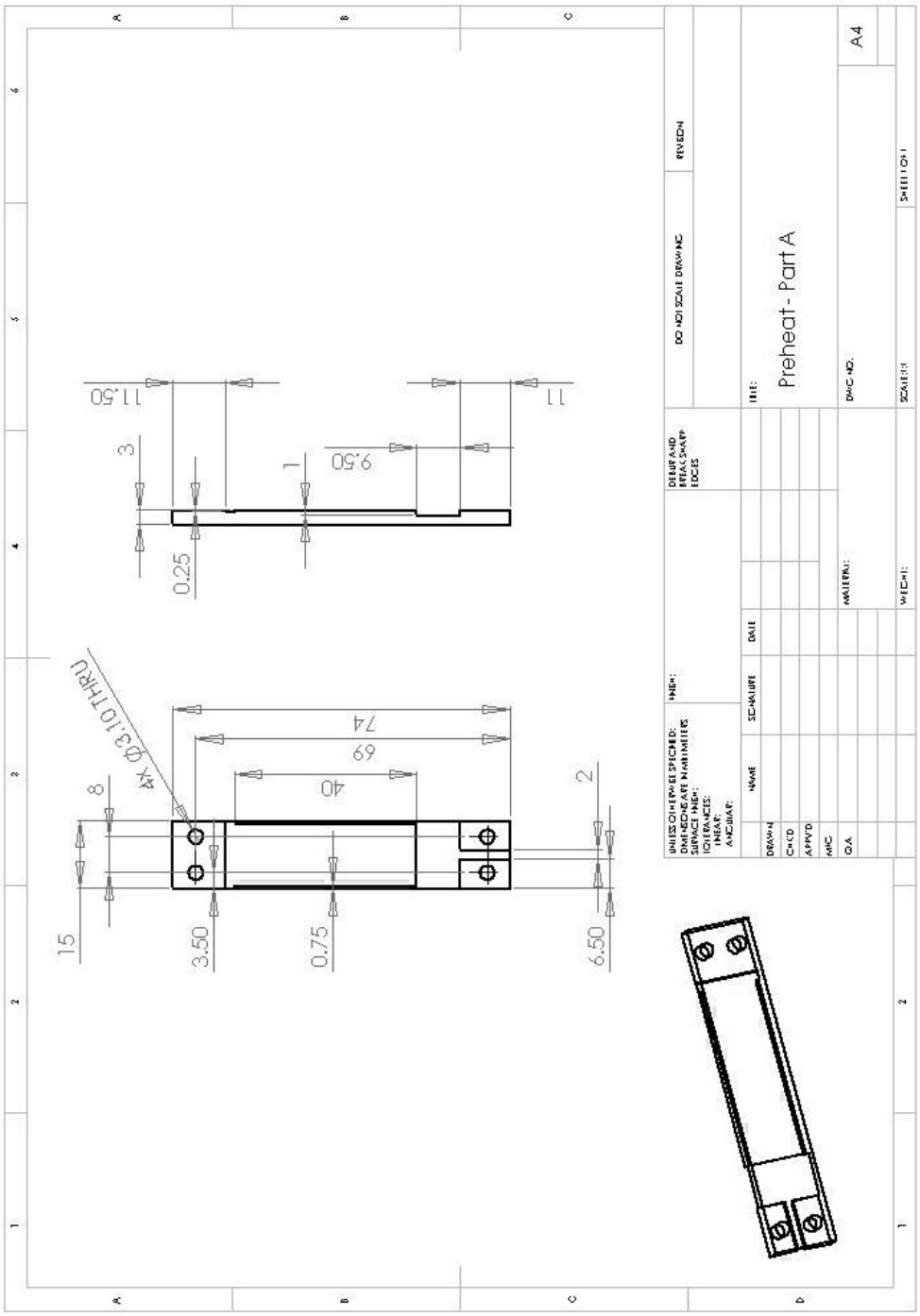

Figure B.28: Part A of the preheat used in chapter 4 - Dimensions in mm.

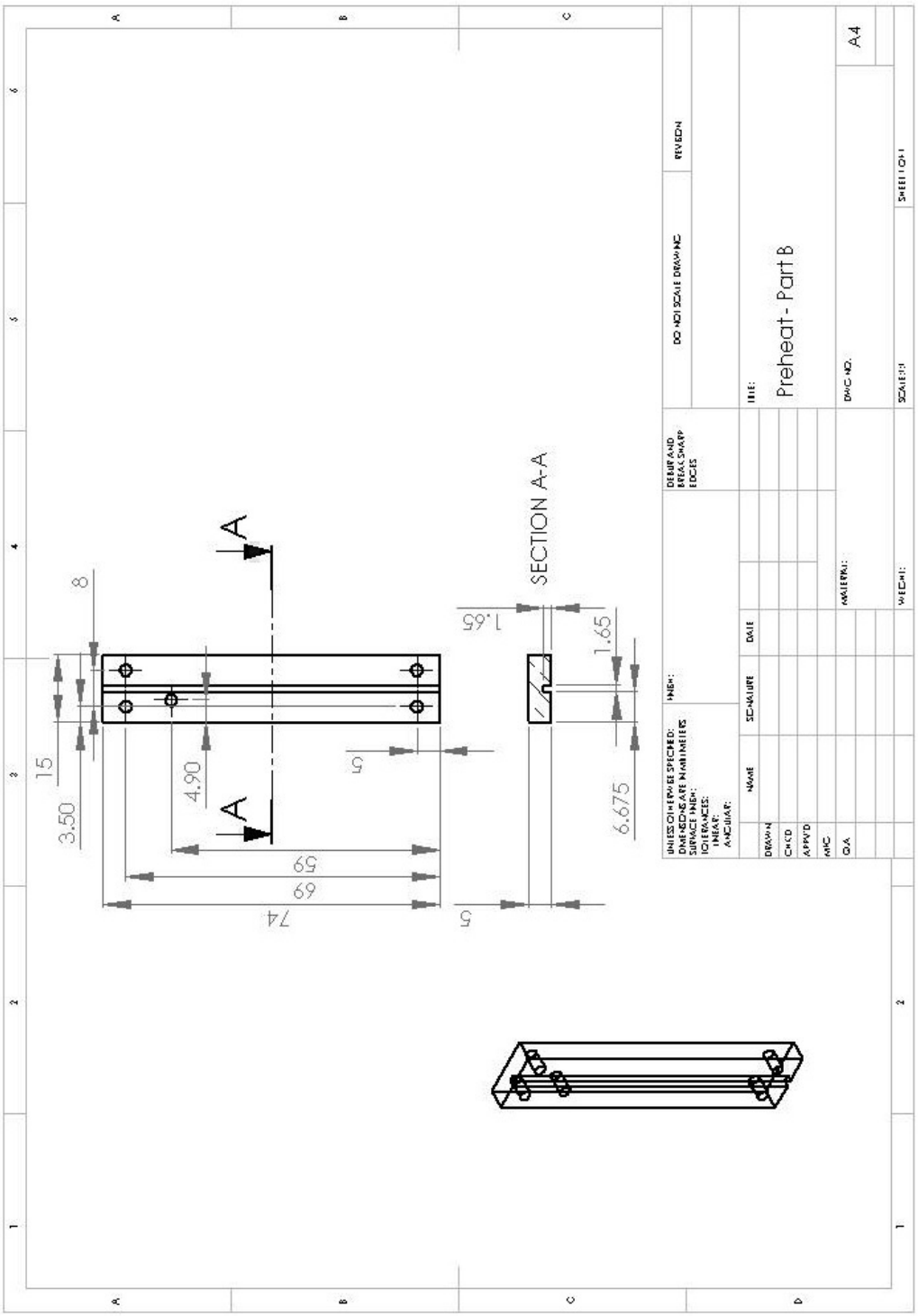

Figure B.29: Part B of the preheat used in chapter 4 - Dimensions in mm.

B.7 Electrical circuits

Table B.6: Parts for thermistor circuit - PCB board and wires are not included.

Part	Cat. No.	Supplier
LM324N	268-0002	RS Components
2N2907	349-9043	RS Components
2 way PCB vertical mount terminal	220-4260	RS Components
IC Socket 16 pins	226-3843	RS Components

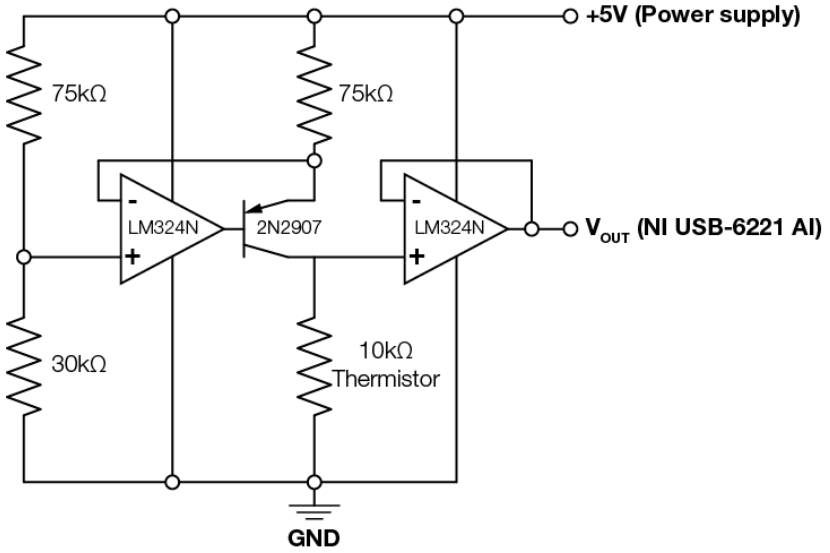

Figure B.30: Circuit to read out a thermistor - Standard circuit to read out thermistors on the microfabricated cell culture device, preheat and the cooling plate.

Table B.7: Parts for valve circuit - PCB board and wires are not included.

Part	Cat. No.	Supplier
DS3658N	1652422	Farnell
IC Socket 16 pins	226-3843	RS Components
2 way PCB vertical mount terminal	220-4260	RS Components
3 way PCB vertical mount terminal	220-4276	RS Components
4 way PCB vertical mount terminal	290-1286	RS Components

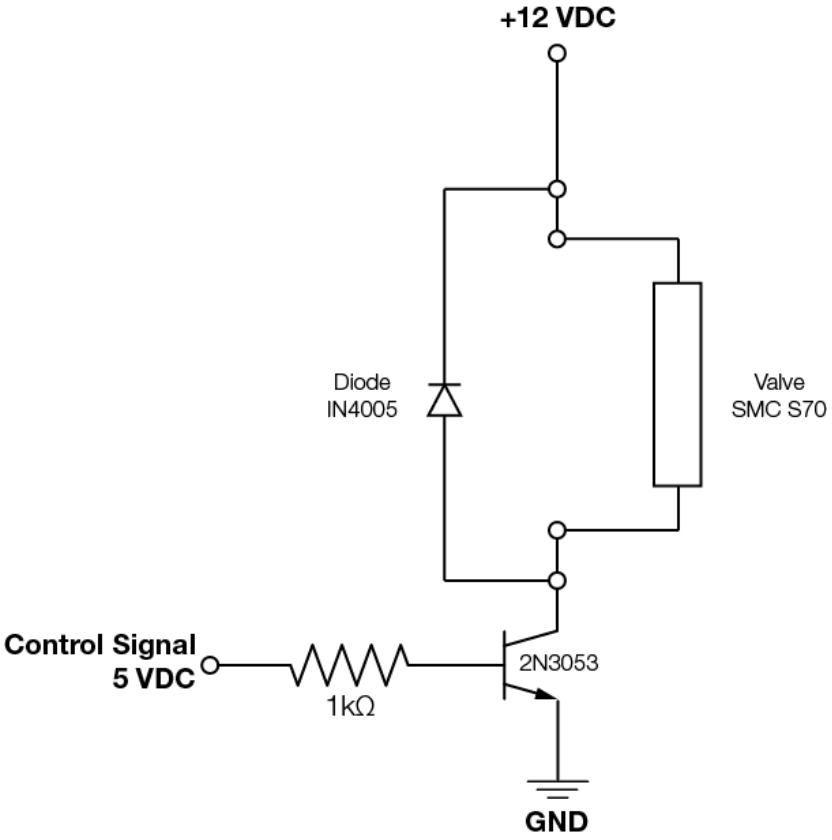

Figure B.31: Circuit to control valves of the pump - Circuit to control the pneumatic valves SMC S070B-6CC in the media handling module. The diode and the transistor are included in the DS3658N IC.

Appendix C

Mathematical derivation of the shear stress equation in a rectangular microchannel

Microfluidic cell culture devices have to be designed such that viable cells are not washed out or undergo undesired phenotype changes. The estimation of characteristic numbers of a bioreactor, such as hydrodynamic shear stress levels and medium residence time (MRT), is thus a vital tool to predict the performance of a bioreactor or to refine its design.

To describe the properties and behaviour of a microfluidic system, an appropriate formulation of the mechanics has to be chosen first. Continuum mechanics can be applied for *Knudsen* numbers[1] below 0.01, which is the case for microfluidic cell culture devices (Nguyen, 2004). The discussion of conservation of mass and momentum for incompressible flows of *Newtonian* fluids[2] is accurate enough to describe the flow properties in microfluidic devices.

For instance, the density ρ is constant in the flow field, which means that the equation for conservation of mass simplifies from

$$\nabla \cdot (\rho \mathbf{u}) = 0 \tag{C.1}$$

[1]The *Knudsen* number is the dimensionless ratio of the mean free path to the representative physical lenght scale. If the ratio is close to 1 or bigger than 1, the continuum assumption is no longer an accurate enough approximation.

[2]A *Newtonian* fluid is a fluid which has a linear relationship between stress and strain rate.

to

$$\nabla \cdot \mathbf{u} = 0 \tag{C.2}$$

where ρ is the density of the fluid and $\mathbf{u}$ the velocity field.

Newton's second law of motion is used to derive the governing equations for microfluidics:

$$m\frac{d\mathbf{v}}{dt} = \mathbf{F} \tag{C.3}$$

where m is the mass of the object, $\frac{d\mathbf{v}}{dt}$ is the acceleration and $\mathbf{F}$ is the net force acting on the object. The net force may consist of gravitational forces, pressure and viscous stresses. The conservation of linear momentum is described by the *Cauchy momentum* equation:

$$\rho\frac{D\mathbf{u}}{Dt} = \underbrace{\rho\mathbf{g}}_{BodyForce} \underbrace{-\nabla P + \nabla \cdot \tau}_{StressTensor} \tag{C.4}$$

where ρ is the density of the continuum, $\mathbf{u}$ the velocity vector field which depends on time and space, $\mathbf{g}$ the gravitational acceleration, $-\nabla P$ the pressure tensor and $\nabla \cdot \tau$ the deviatoric stress tensor.

For Newtonian fluids, i.e. fluids which show a linear relationship between viscous stress and rate of strain, the rate-of-strain tensor τ relates viscous stresses with material properties such as the dynamic viscosity μ and the rate of strain γ. For an incompressible fluid, the viscous stress is represented by:

$$\tau = 2\mu\Gamma = \mu[\nabla v + (\nabla v)^t] \tag{C.5}$$

An important special case is that of a Newtonian fluid with constant density and viscosity, where the shear tensor can be written thus as:

$$\nabla \cdot \tau = \mu\nabla^2\mathbf{v} \tag{C.6}$$

By replacing the expression for viscous stresses in C.4 with C.6, the *Navier-Stokes* equation is obtained:

$$\rho\frac{D\mathbf{u}}{Dt} = \rho\mathbf{g} - \nabla P + \mu\nabla^2\mathbf{v} \tag{C.7}$$

These equations are the basis for deriving analytical solutions for flow in microchannels, and to predict, for example, hydrodynamic shear stress levels and distribution within a microchannel.

C.0.1 Analytical solutions for unidirectional flow in rectangular microchannels

To design microfluidic devices with low hydrodynamic shear stress, analytical solutions of the Navier-Stokes equations can be used to predict shear stress levels in a first approximation. Analytical solutions for different cross-sectional channel geometries have been derived (Bruus, 2004). The microchannel cross-sections for a microfluidic bioreactor will be rectangular due to the fabrication method used. The derivation of the analytical solutions is therefore limited to a rectangular cross-section.

Considering a microchannel with the dimension $h, w << l$ and $h << w$ and flow in positive y direction, the solution of the Navier-Stokes equation is reduced to the y component because $v_x = v_z = 0$ and can be expressed with a Fourier expansion as:

$$v_y(x,z) = \frac{4 \cdot h^2}{\pi^3 \cdot \mu} \cdot \frac{dp}{dy} \sum_{n,odd}^{\infty} \frac{1}{n^3} \left[1 - \frac{cosh\left(n \cdot \pi \cdot \frac{y}{h}\right)}{cosh\left(n \cdot \pi \cdot \frac{w}{2h}\right)} \right] \cdot sinh\left(n \cdot \pi \cdot \frac{z}{h}\right) \tag{C.8}$$

For simplicity however, the velocity profile is well approximated by infinite, parallel plates, particularly for microchannels with high channel aspect ratios (> 10). The flow is considered steady and fully developed, which simplifies the Navier-Stokes equations to:

$$0 = -\frac{dP}{dy} + \mu \cdot \frac{\partial^2 v_y}{\partial z^2} \frac{\partial^2 v_y}{\partial z^2} = \frac{dP}{dy} \cdot \frac{1}{\mu} \tag{C.9}$$

and with no slip at the boundaries $v_y(0) = v_y(h) = 0$, so the velocity can be expressed after rearranging and integration as:

$$v_y(z) = \frac{1}{2 \cdot \mu} \frac{dP}{dy} [h - z] \cdot z \tag{C.10}$$

The average velocity in the microchannel can be calculated by integrating the velocity over the inlet area and dividing by the same:

$$\overline{v} = \frac{1}{A} \int_0^w dx \int_0^h dz \; \frac{1}{2 \cdot \mu} \frac{dP}{dy} [h - z] \cdot z = \frac{h^2}{12 \cdot \mu} \frac{dP}{dy} \tag{C.11}$$

Replacing the pressure gradient in equation C.10 with the expression obtained from equation C.11, the velocity is then:

$$v_y(z) = \frac{6}{h^2} \cdot \overline{v} [h - z] \cdot z \tag{C.12}$$

The average velocity can be replaced with the volumetric flow rate Q and equation C.12 reduces to:

$$Q = \overline{v} \cdot A \tag{C.13}$$

$$v_y(z) = \frac{6}{h^3 \cdot w} \cdot Q\,[h - z] \cdot z \tag{C.14}$$

Hydrodynamic shear stress is a critical parameter in a microfluidic culture device. The viscous stress tensor reduces to one dimension in unidirectional flow. Note that the shear stress $\tau_{wall} \neq 0$, even though $v_y = 0$ at the boundaries:

$$\tau = -\mu \cdot \frac{\partial \mathbf{v}}{\partial z} \tag{C.15}$$

Shear stress at the wall in a rectangular channel can be expressed as a function of flow rate Q and channel dimensions h and w by replacing the velocity derivative in z direction in equation C.15 with the according derivative of equation C.14:

$$\tau_{wall} = 6 \cdot \mu \cdot \frac{Q}{h^2 \cdot w} \tag{C.16}$$

Appendix D

Continuous culture of hESC in a straight channel microfluidic cell culture device

A first generation packaging system served as basis for the microfluidic cell culture device which used the same concept described in section 3.3. An interface plate with an opening allowed access to the TC-PS slide for coating with ECM and seeding of cells. Once cell seeding was completed and cells attached to the ECM on the cell growth surface, the interface plate with the opening and the microfluidic gasket was removed and replaced with a closed interface plate and microfluidic layer. Both microfluidic layers were made from PDMS in a casting process using moulds (see Figure D.1).

To culture feeder-attached hESCs in the microfabricated cell culture device, inactivated MEFs were seeded on day 1 using a standard laboratory pipette. After one day of incubation, medium was aspirated and fresh hESC medium added. hESC colonies were manually dissected and added into the open microfluidic cell culture device on day 2. After another day of incubation, the interface plates and microfluidic layers were exchanged and continuous culture started (see Figure D.2).

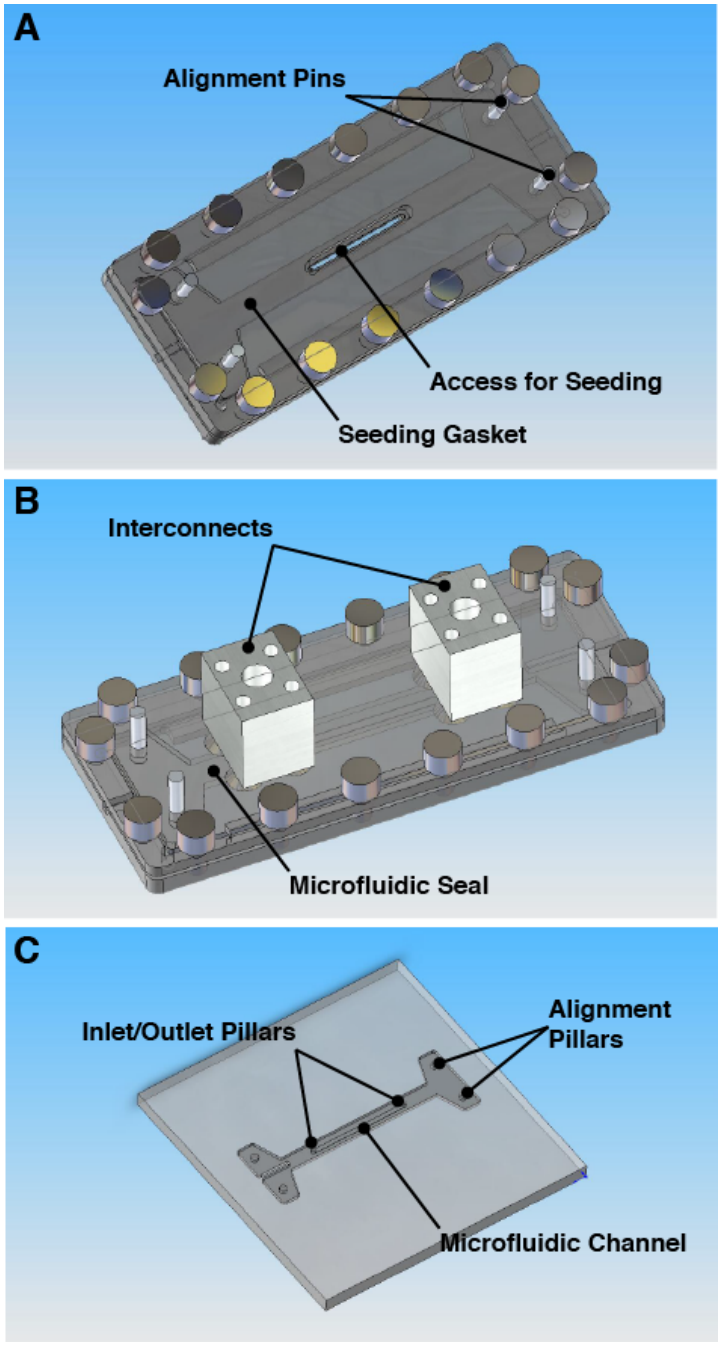

Figure D.1: Design and configurations of the microfabricated cell culture device - The straight channel microfluidic cell culture device had two exchangeable lids. One lid was used for seeding and had an access to the culture plane to seed cells with a pipette (**A**). Once feeder cells and hESC colonies were attached, the seeding lid was replaced by the perfusion lid (**B**) and perfusion started. The seeding gasket and the microfluidic seal were both casted using a micro-milled mould (**C**)

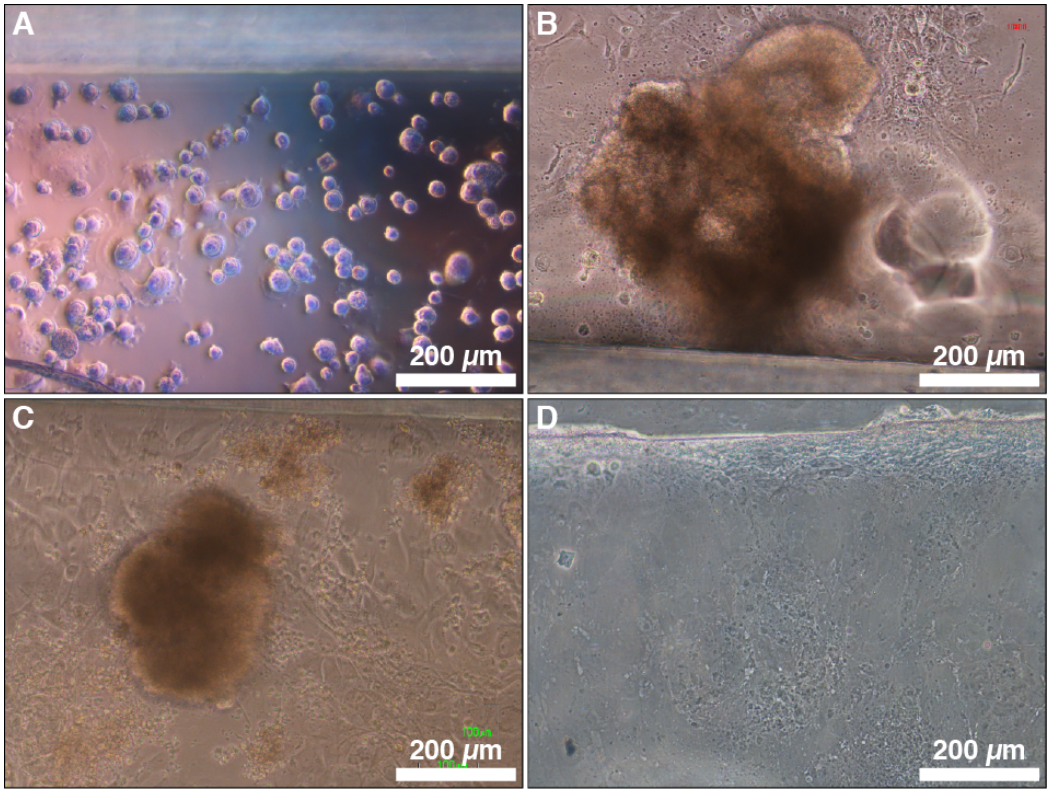

Figure D.2: Seeding and continuous culture experiments in a straight channel with hESC - Inactivated MEFs were seeded on day 1 in the open configuration on a 0.1 % (w/v) gelatine coated TC-PS slide (**A**). hESC colonies were seeded on d2 (**B**). On d3, hESC colonies attached and started growing (**C**). On d3, hESC colonies were washed out with flow rates as low as 100 μl h^{-1} (**D**)

Appendix E

Additional characterisation

E.1 Fabrication characterisation of moulds

Characterisation of the aluminium mould to cast first generation microfluidic low shear layers demonstrated a high spatial fidelity and accuracy (see figure E.1). Profilometer measurements have shown that the flow restrictors and dividers in the mould had a height of 202 μm +/- 1 μm, which represented an error of 1% of the nominal height of 200 μm. The PDMS microfluidic chip cast from the mould had a channel height of 202 μm +/- 1 μm, corresponding to the measurements of the mould. These results compare well with the results obtained in section 2.4.2. Scanning electron microscopy (SEM) was used to inspect the moulds for burrs and surface quality. Burrs caused by milling were minimal and did not affect the de-moulding of the PDMS microfluidic chip, resulting in 100% yield of PDMS microfluidic chips (see figure E.2).

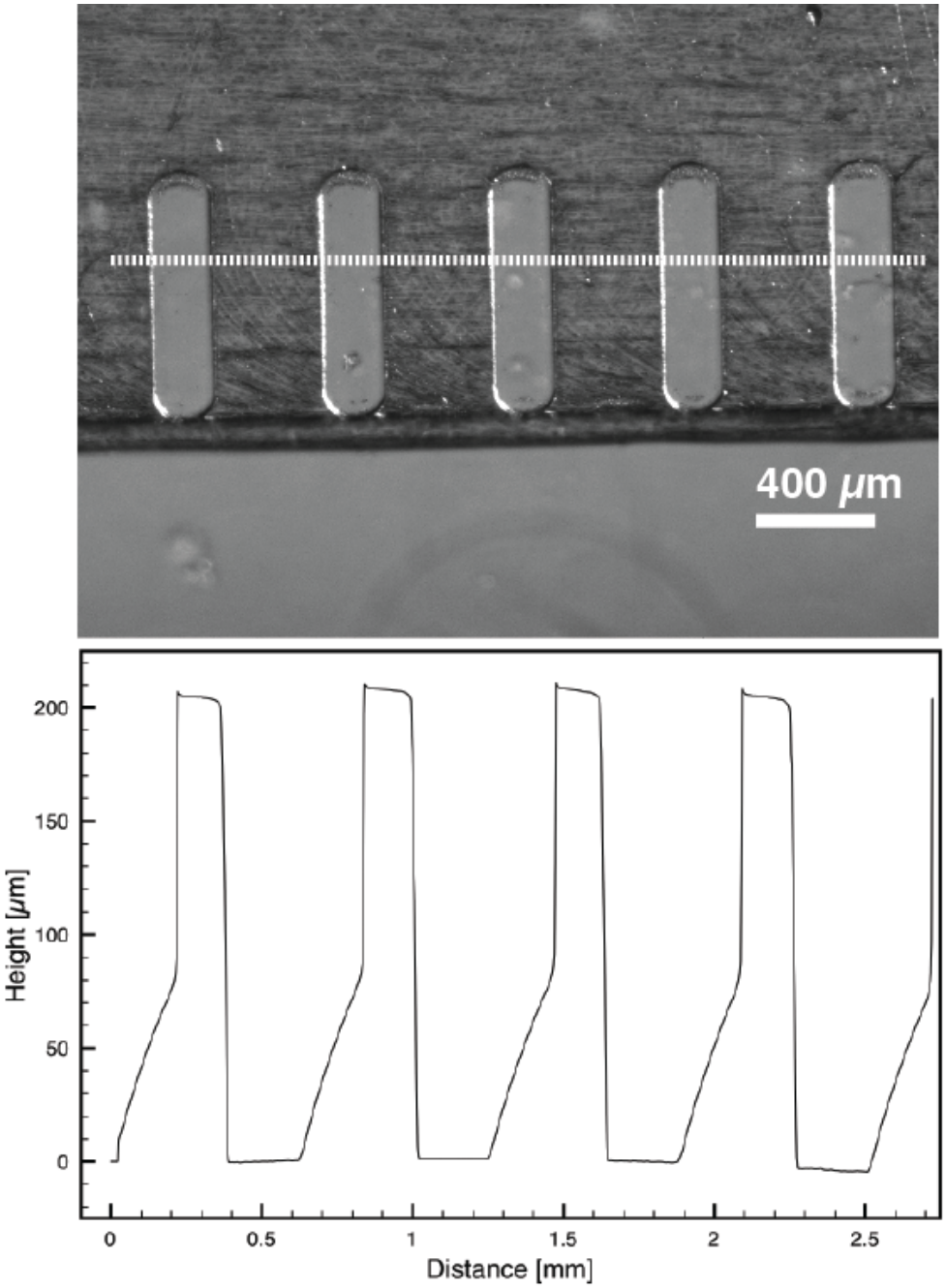

Figure E.1: Profilometer measurements of the flow restrictors in the PDMS cast - The dashed line in the picture indicates the scan from left to right.

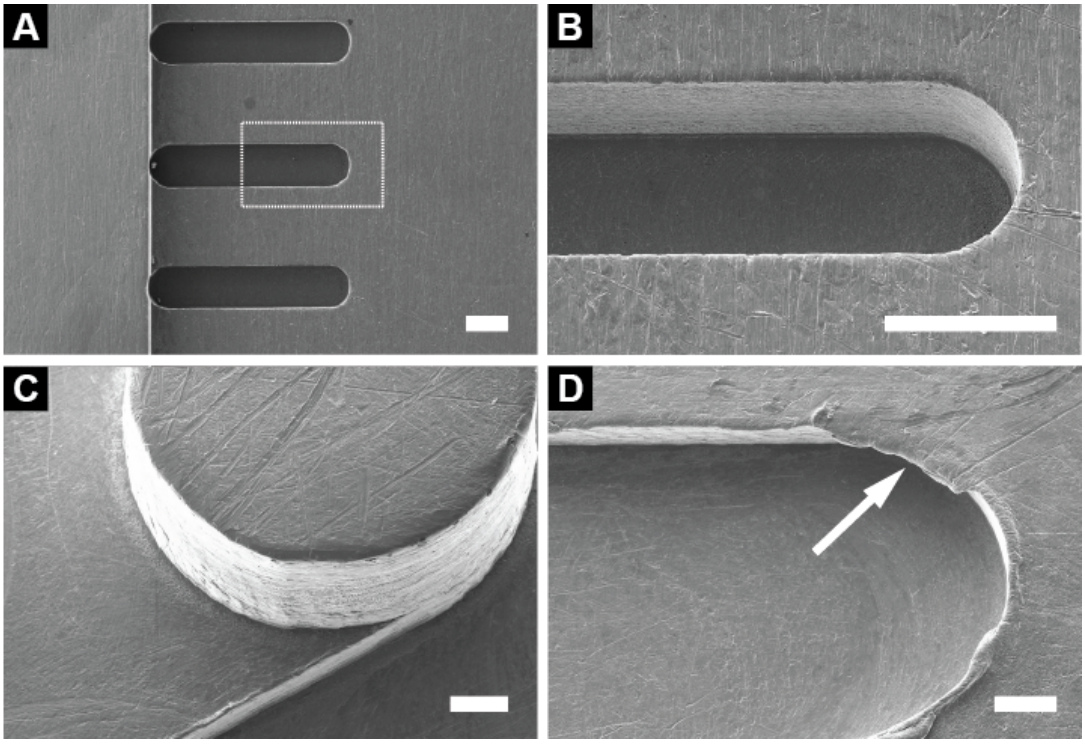

Figure E.2: SEM images mould - Characterisation of the first generation low hydrodynamic shear stress microfluidic layer. (**A**) shows a SEM picture of a section of the flow restrictors in the mould and (**B**) one flow restrictor. No burrs were observed at the inlet (**C**). However, some burrs (indicated by arrow) occurred at the flow splitter (**D**). The scale bar is 200 μm long.

E.2 Thermal imaging of an ITO microscope glass slide

The knowledge on the temperature distribution across an indium tin oxide (ITO) microscope slide was limited during development of the heater for the microfluidic bioreactor. However, it was important to determine where to position the thermocouple in the microfluidic bioreactor and if cells would be exposed to a temperature gradient.

A thermal imaging handheld camera (ThermaCAM SC360, FLIR Systems, Sweden) was used to visualise the infrared signature of an ITO microscope slide (see figure E.3). Images were analysed using ImageJ (Version 1.43, NIH, USA). Temperature distribution was measured in x and y direction. For each direction, 3 measurements were taken and mean and standard deviation calculated.

In y direction, the temperature only deviated 4.8 % from the average temperature.

In x direction the temperature deviated approximately 7 % in the relevant area.

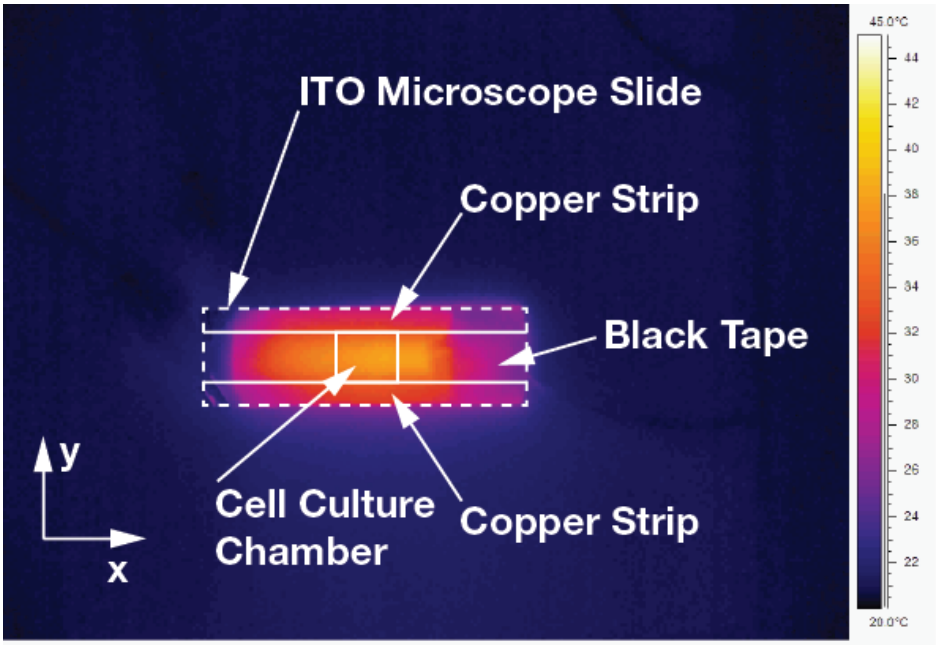

Figure E.3: Infrared image of an ITO microscope slide used as a heater - The temperature distribution where the cell culture chamber is located varies in y direction only 4.8 % and in x direction 7 %. The black tape holds the thermocouple in place and appears therefore as cold area.

E.3 FEM analysis of microfluidic layers used in chapter 4

A FEM analysis with the same parameters described in chapter 3 was conducted to verify that the modification of the inlet and outlet manifold of the second generation microfluidic layer has not affected hydrodynamic shear stress levels.

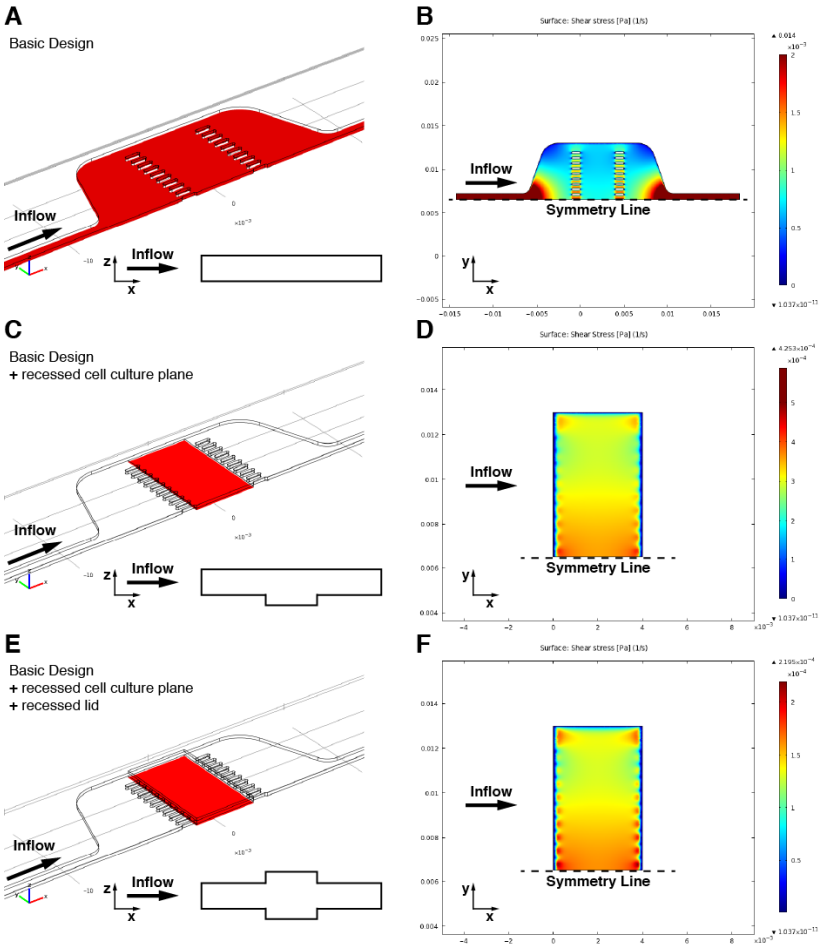

Figure E.4: Hydrodynamic shear stress in the improved microfluidic chip - To measure the influence of different channel heights, the microfluidic chip was analysed in a basic configuration (**A**, **B**), the basic design and a recessed cell culture plane (**C**, **D**) and the basic design with a recessed cell culture plane and lid (**E**, **F**). Due to symmetry, only one half of the chip was simulated. Flow rate was chosen 300 μl h^{-1}.

E.4 Flow rate generated in a syringe pump versus the proposed pump

The flow rate generated in the pressurised medium reservoir has been compared to a standard laboratory syringe pump (Model 100, KD Scientific, USA). Compared to the syringe pump, the pump described in chapter 4 responds immediately and is able to follow changes immediately. The syringe pump is troubled by lag times of up to 15 minutes to generate the dialled flow rate or stop flow. Water has been used as medium for both pumps.

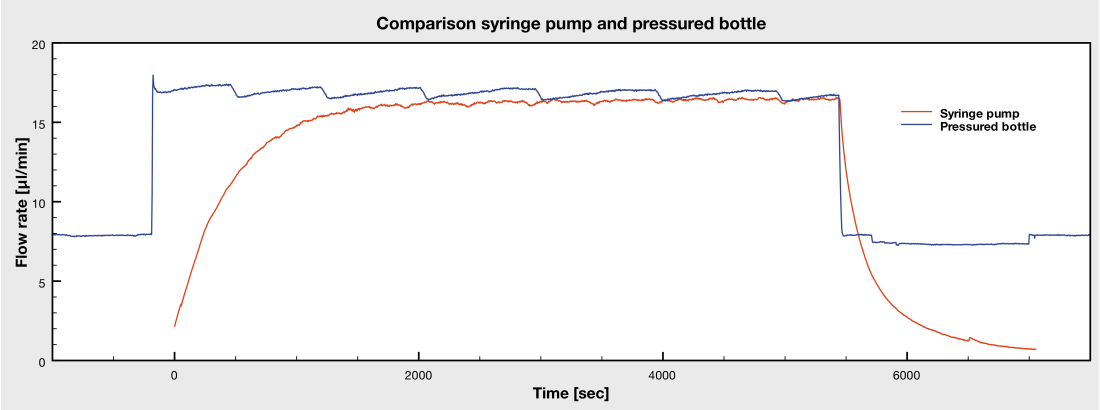

Figure E.5: Comparison of flow rates generated in a syringe pump and the pump described in chapter 4 - Both pumps were turned on, left running for an hour and then stopped. The red line depicts the temporal course of the flow rate generated by the syringe pump, while the blue line represents the temporal course of the flow rate generated by the pump presented in chapter 4

Appendix F

Calibration of thermistors & PID heater settings

F.1 Calibration of thermistors

Thermistor coefficients have been calculated using the Stein-Hart equation in two point or three point calibrations by measuring the resistance of the thermistor when exposed to three different temperatures. Temperatures included 0°C, room temperature and 37°C of a water bath. The calibration values were optimised using the least-square error method.

$$\frac{1}{T} = A + B \cdot ln(R) + C \cdot (ln(R))^3 \tag{F.1}$$

Table F.1: Thermistor calibration - Thermistor coefficients obtained in a two point calibration at room temperature and 37°C

	Cooling element	Preheat Element	MB 1	MB 2	MB 3
A	0.00097536	0.00117487	0.000491747	0.000491747	0.000491747
B	0.00025823	0.00023688	0.000310421	0.000310421	0.000310421
C	0.00000000	0.00000000	0.000000000	0.000000000	0.000000000

F.2 PID heater settings

PID settings were obtained by using the auto-tuning routine developed by (Li, 2008b).

Table F.2: PID settings for all heaters and cooling elements

	Cooling element	Preheat Element	MB 1	MB 2	MB 3
P	388436.40418	44.5415	67.437	57.465	67.437
I	8.000951	18.6748	3.585	2.914	3.585
D	1.60019	3.73496	0.717	0.583	0.717

Appendix G

Publications

Results of this thesis have been presented in several conference proceedings of international conferences. The holistic rapid prototyping approach described and characterised in chapter 2 has been presented at the 6th international conference on the microtechnologies in medicine and biotechnology (MMB) 2011 in Lucerne, Switzerland.

The results of chapter 3 have been published in conference proceedings of the 13th international conference on micro total analysis (mTAS) 2009 in Jeju, Korea and of the 6th international conference on the microtechnologies in medicine and biotechnology (MMB) 2011 in Lucerne, Switzerland.

The microfluidic platform described in chapter 4 has been presented in the proceedings of the 14th international conference on micro total analysis (mTAS) 2010 in Groningen, The Netherlands and of the 6th international conference on the microtechnologies in medicine and biotechnology (MMB) 2011 in Lucerne, Switzerland.

HUMAN EMBRYONIC STEM CELL CULTURING IN A MICROFLUIDIC PERFUSION SYSTEM WITH A REVERSIBLY SEALABLE LID

Marcel Reichen, Ludmila Ruban, Farlan Singh Veraitch, Nicolas Szita
University College London, Biochemical Engineering, UNITED KINGDOM
(n.szita@ucl.ac.uk)

ABSTRACT

We present a modularly configured microfluidic system for human embryonic stem cells (hESC) enabling controlled seeding of intact hESC colonies, continuous perfusion of hESC colonies cultured on feeder cells without cell wash-out, and seamless integration with standard analytical methods for endpoint assays. Immunocytochemistry performed after 48 hours of continuous medium perfusion indicates for the first time that co-cultured hESCs remain pluripotent during continuous perfusion.

KEYWORDS: Microfluidic perfusion, human embryonic stem cells, pluripotent proliferation

INTRODUCTION

Human embryonic stem cells (hESCs) can be expanded indefinitely and can retain their pluripotency, i.e. the ability to differentiate into any of the three germ layers. Thus, they potentially allow to obtain specialised cells in unlimited quantity for developmental biology research, drug discovery, and cell based therapies. Parallelised microfluidic cell culture systems with their potentially greater control over the culture conditions than, for example, automated microwell platforms [1] could be an ideal tool to investigate the complex interplay between culturing conditions and stem cell properties. Previously, different seeding techniques for hESCs have been demonstrated, including the seeding of hESCs suspensions from an upstream port into a cell culture chamber via microfluidic channels and microfluidic selection ports [2, 3], and direct cell seeding of hESCs into 'open' chambers [4]. Microfluidic culturing of hESCs was performed with periodic stop-flow medium feeds, microwells recessed in microchannels, and hESCs encapsulated in gels, but pluripotency was not shown [2, 4]. Recently, pluripotent proliferation of hESCs was reported using intermittent medium re-feed schedules [3], but the use of intermittent medium re-feed schedules to maintain pluripotency prevents the study of hESC behaviour under continuous perfusion, hence under steady-state conditions.

DESIGN AND OPERATION OF THE MICROFLUIDIC SYSTEM

The modular microfluidic perfusion system consists of a reusable interface system and a disposable microfluidic chip (Figure 1). The microfluidic poly(dimethylsiloxane) (PDMS) chip contains a culture chamber with a rectangular footprint (4 mm x 13 mm), a microfluidic manifold using flow equalisation barriers [5] for uniform culture medium perfusion over the entire chamber, and the cell culture is recessed with respect to the medium flow plane to reduce the hydro-

978-0-9798064-2-1/μTAS2009/$20

dynamic shear stress on the cells. The reusable interface system includes a top plate and a bottom frame made from polycarbonate (PC) which press the microfluidic chip on a tissue culture polystyrene (TC-PS) slide when they are clamped together. The interface also hosts 2 interconnects (Aluminium) to link the chip with external medium feed, and a lid (PC) and gasket (PDMS) to reversibly seal the chamber.

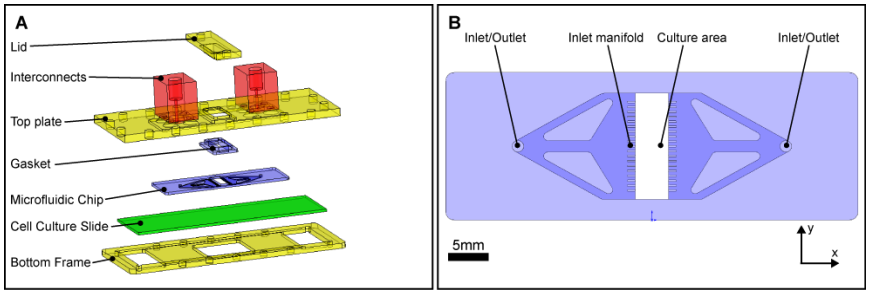

Figure 1. (A) Rendering of the modular microfluidic perfusion system shown in exploded view. (B) Top view of the microfluidic chip architecture.

Using the reversibly sealable lid, the system can be configured to 'open' culture chamber mode for cell seeding with standard laboratory pipettes (Figure 2). We coated the TC-PS slide with a 0.1% gelatine solution and seeded approximately 20'000 growth-arrested fibroblasts in 200 µℓ of medium. The fibroblasts were allowed to attach to the gelatine for 24 hours. Then 6-8 hESC colonies were pipetted into the chamber and allowed to attach to the growth-arrested fibroblasts. On the third day, the culture chamber was closed with the lid and medium perfusion started. A syringe pump delivered medium via gas permeable tubing at a flowrate of 300 µℓ/h, resulting in complete medium exchange approximately every 5 minutes.

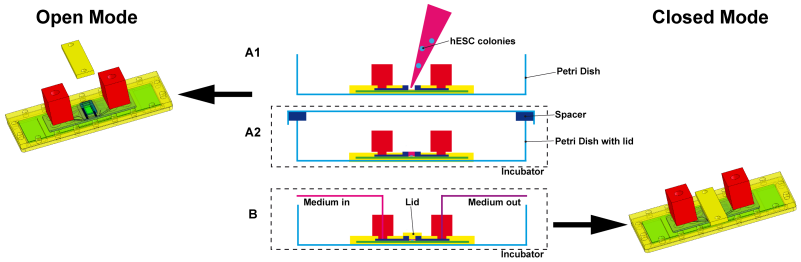

Figure 2. Illustration of the seeding operation with an 'open' microfluidic system using standard laboratory pipettes (A1), and perfusion with the 'closed' microfluidic system (B). After seeding, the cells were allowed to attach in the open configuration within a Petri-dish (A2).

RESULTS AND DISCUSSION

The fibroblasts attached and uniformly spread across the culture chamber to attain their characteristic morphology within 24 hours. After seeding of the hESC

colonies, the hESCs attached to the fibroblasts and their morphology was similar to the one of the hESCs in the static control dishes. During perfusion of the hESCs for 48 hours, no wash-out of hESC colonies or feeder cells was observed and hESC colonies maintained a similar colony shape and morphology compared to the static control dishes (Figure 3A). Finally, after 48 hours of perfusion, the hESC colonies stained positively for different pluripotency markers which strongly indicates that the hESCs retained their pluripotency (Figure 3B).

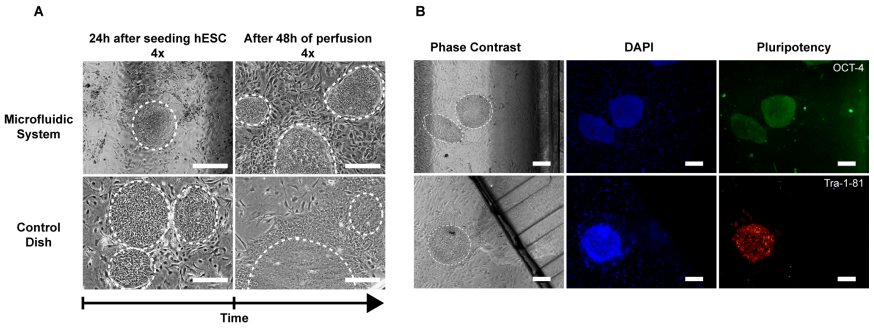

Figure 3. (A) Comparison of morphology of microfluidic perfusion system and control dish. (B) Images of hESC colonies in the microfluidic perfusion system in phase contrast, stained for DAPI and pluripotency markers OCT-4 and Tra-1-81. Scale bars are 200µm long.

CONCLUSIONS

The results obtained indicate that continuous perfusion of intact hESC colonies on typical cell growth substrate can be performed in the presented microfluidic system.

ACKNOWLEDGEMENTS

The authors would like to acknowledge the EPSRC for funding. We also thank Minal Patel, Emily Culme-Seymour and Alexandra Hemsley for their help with the maintenance of the inactivated fibroblasts and hESC colonies.

REFERENCES

[1] J. El-Ali, P.K. Sorger, K.F. Jensen, Nature, 442, pp. 403-411, (2006).
[2] N. Korin, A. Bransky, U. Dinnar and S. Levenberg, Biomedical Microdevices, 11, pp. 87-94, (2009).
[3] K.-I. Kamei, S. Guo, Z. T. Yu, H. Takahashi, E. Gschweng, C. Suh, X. Wang, J. Tang, J. McLaughlin, O. N. Witte, K. B. Lee and H. R. Tseng, Lab Chip, 9, pp. 555-563, (2009).
[4] E. Figallo, C. Cannizzaro, S. Gerecht, J. A. Burdick, R. Langer, N. Elvassore and G. Vunjak-Novakovic, Lab Chip, 7, pp. 710-719, (2007).
[5] S. Petronis, M. Stangegaard, C.B.V. Christensen, M. Dufva, BioTechniques, 40, pp. 368-376, (2006).

AN AUTOMATED AND MULTIPLEXED MICROFLUIDIC BIOREACTOR PLATFORM WITH TIME-LAPSE IMAGING FOR CULTIVATION OF EMBRYONIC STEM CELLS AND ON-LINE ASSESSMENT OF MORPHOLOGY AND PLURIPOTENCY MARKERS

Marcel Reichen, Farlan Singh Veraitch, Nicolas Szita*
University College London, Biochemical Engineering, UNITED KINGDOM

ABSTRACT

An automated and multiplexed microfluidic bioreactor platform with time-lapse imaging for cultivation of embryonic stem (ES) cells is reported. Media temperature is controlled in the storage container and before entering the microbioreactors. Furthermore, the temperature in the microbioreactor is regulated to maintain cells at culture temperature over prolonged periods of time. Flow control is implemented in the platform to vary flowrates and to switch between two different media bottles in one experiment. Morphology and pluripotency of mouse embryonic stem (mES) cells were monitored with the integrated time-lapse imaging.

KEYWORDS: Time-lapse imaging, microbioreactor, embryonic stem cells (ESCs), cell culture monitoring

INTRODUCTION

Data-rich experimentation requires monitoring and controlling of important process parameters. Various input parameters such as media composition, medium replacement times and temperature affect the proliferation or differentiation of embryonic stem (ES) cells. Output from the cells, for example changes in their morphology and pluripotency/differentiation needs thus to be monitored/controlled to correlate the results with the tested parameter. To monitor and control all these input and output parameters, particularly for long-term experiments, automated fluid handling, time lapse imaging and tight control of the microenvironment are required. Different systems have been developed, which address the optical monitoring, but do not include automated liquid handling. For example, a microfluidic culture system compatible with plate readers has been recently reported to measure fluorescent intensities [1]. However, analysis of cell morphology, a daily routine task in cell culture, has to be carried out on a microscope. A charged-coupled device (CCD) has also been directly attached to a microfluidic cell culture device for counting cells [2]. For high quality imaging, a microfluidic culture chamber with a transparent heater has been implemented on an inverted microscope to monitor HeLa cell cultures at defined temperatures [3]. We present a multiplexed microfluidic platform which combines automated brightfield and fluorescent imaging with flow control. This will allow the on-line study of the complex and dynamic cellular processes, under controlled culture conditions.

EXPERIMENTAL

The platform consists of a 'microscope module' and a 'media handling module', both automated via a LabView™ routine as shown in Figure 1A. The microscope module includes three microfluidic bioreactors, a flow splitter to feed the three microfluidic bioreactors, a media preheat element to heat up cooled media and a box for the temperature control of the microbioreactors as shown in Figure 1B.

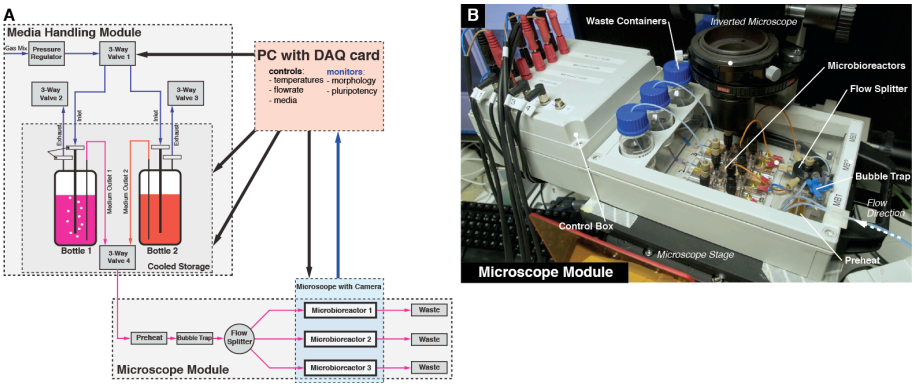

Figure 1: (A) schematic representation of all modules and components of the microfluidic ES cell culture platform. (B) shows the microscope module and its components.

The microfluidic bioreactors used for this platform are based on a previously presented design where we demonstrated perfusion culture of feeder-attached human ES cells [4]. In this design as shown in Figure 2A and 2B, the temperature in each microfluidic bioreactor can be controlled individually. An indium tin oxide (ITO) microscope slide is

used as a resistive heating element and - coated with gelatin - serves as the culture surface for ES cells. A temperature feedback control loop implemented in LabView™ monitors and controls the resistive heating by pulse-width modulation. The culture chamber of each bioreactor is split in two compartments to accommodate two mESC lines with a different green fluorescent protein (GFP) marker each.

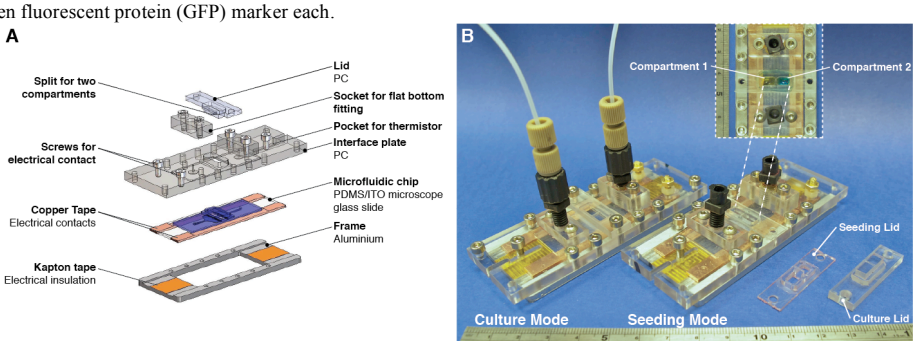

Figure 2: (A) Exploded view of all parts of the microfluidic bioreactor for the cell culture platform. (B) shows the two modes of operation, seeding and culture mode of the microbioreactor [4], and the corresponding lid. The microfluidic bioreactor has two compartments to seed different populations, and both compartments can be directly accessed with standard laboratory pipettes.

The media handling module includes two media bottles, a cooling plate, a pressure regulator and a set of valves as shown in figure 1A. To avoid media decomposition during long term cultures, the media bottles are stored on the cooling plate (using the same temperature control loop as for the microbioreactors). The pressure regulator is used to control the head pressure in the media bottle and therefore the media flow. A set of valves is used to switch between the media bottles. An inverted microscope with a CCD camera was used for imaging cell morphology and fluorescent markers. Phase contrast images were automatically taken every 15 minutes with a LabView™ routine. Images of the fluorescent markers were taken daily.

All three microbioreactor and medium flasks were autoclaved before each experiment. Tubing was sterilized by flowing ethanol through for 20 min followed by a PBS wash. Sterile filters were used to seal the inlet and outlet for the pressurized gas. Prior to seeding, an 0.1% (w/v) gelatine solution was used to coat the glass slides. Two mESC lines were used, an Oct4-GFP reporter line to monitor pluripotency seeded in one compartment, and a Sox-1-GFP reporter line for early neuronal differentiation in the other. Cells were statically seeded with a pipette to a seeding density of approximately 100,000 cells/cm^2. 24h after seeding, the microbioreactors were changed from seeding mode into culture mode by sealing the culture chambers with a lid. Tubing was connected first to the media bottles and then to the microbioreactors, which had been placed into the microscope module in a laminar flow hood. After priming, the microscope module was transferred to the inverted microscope and mounted on the microscope stage. The temperature for all microbioreactors was set at 37°C and the flowrate controlled to maintain approximately 300 µl/h in each microbioreactor .

RESULTS AND DISCUSSION

The microfluidic bioreactor platform consists of 6 culture chambers. Each chamber can be accessed individually with a laboratory pipette and different types of cells can be seeded without cross-contamination. Culture programs with physical parameters such as temperatures and flow rates can be automatically read into the LabView™ routine and altered manually during the experiments. Flow rates and temperatures can be accurately controlled as shown in Figure 3A and B.

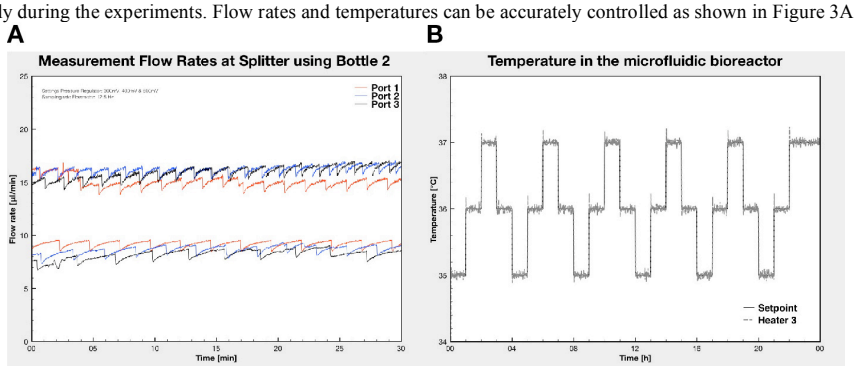

Figure 3: Flow rates after the flow splitter using bottle 2 at different head pressures measured with a flow sensor (A). Temperature of the culture surface in a microfluidic bioreactor (B).

Preliminary results with the microfluidic platform show that the cells grow under low shear perfusion and that cell proliferation and marker expression can be monitored (Figure 4A and B). During culture, cells moved over the culture area as shown in Figure 4C and D. Such information on cell migration and proliferation can only be obtained from real time cell culture monitoring, which illustrates the importance of an automated time-lapse imaging routine.

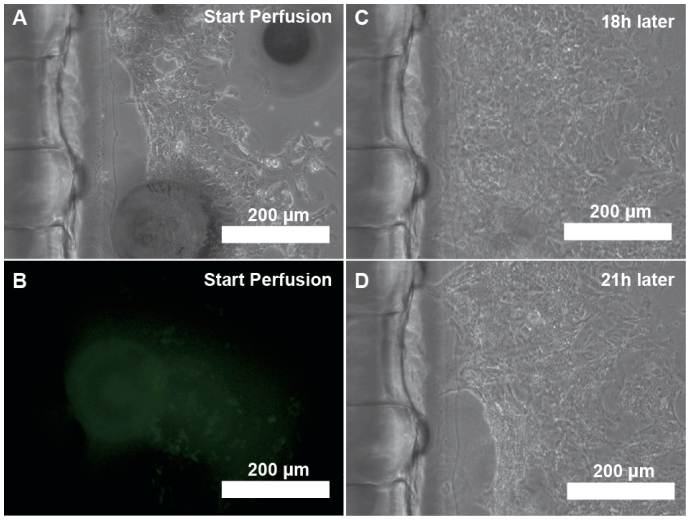

Figure 4: Representative images of a cell culture compartment. Phase contrast images at different time points (A,C,D) and fluorescent Oct-4 marker image (B).

CONCLUSION

An automated, versatile microfluidic platform for long-term cell culture has been devoloped to monitor cell morphology, migration and proliferation from phase contrast images, and pluripotency and differentiation markers from fluorescence images. The microbioreactors have a culture chamber with two compartments which allows to monitor simultaneously and under identical culture conditions two GFP-reporter mES cell line. A deeper insight in cellular processes and data-rich experiments can be gained by modulating flow, extracellular matrix and media composition using such a microfluidic platform with its integrated optical monitoring. Future work includes the implementation of advanced imaging algorithms for on-line analysis and long-term experiments.

ACKNOWLEDGEMENTS

The authors gratefully acknowledge the Department of Biochemical Engineering, UCL, for providing funding during Marcel Reichen's PhD studentship. We would also like to thank Matthew Li for the programming of the LabView™ routines. Finally we would like to thank the UK Joint Infrastructure Fund (JIF), the Science and Research Investment Fund (SRIF), and the Gatsby Charitable Foundation for funds to establish the UCL Centre for Micro Biochemical Engineering.

REFERENCES

[1] Y. Wen, X. Zhang and S.-T. Yang, "Microplate-reader compatible perfusion bioreactor array for modular tissue culture and cytotoxicity assays", *Biotech. Prog.*, DOI10.1002/btpr.423, 2010.
[2] A. Ozcan and U. Demirci, "Ultra wide-field lens-free monitoring of cells on-chip", *Lab Chip*, vol. 8, pp. 98-106, 2008.
[3] S. Petronis, M. Stangegaard, C. B. Christensen and M. Dufva, "Transparent polymeric cell culture chip with integrated temperature control and uniform media perfusion", *Biotechniques*, vol. 40, pp. 368-375, 2005.
[4] M. Reichen, L. Ruban, F. S. Veraitch and N.Szita, Human embryonic stem cell culturing in a microfluidic perfusion system with a reversibly sealable lid, Proc. Micro Total Analysis Systems 2009, pp. 1829-1831, (2009).

CONTACT

*N.Szita, Tel: +44 (0)20 7679 4418; n.szita@ucl.ac.uk

MICROFLUIDIC PLATFORM FOR THE AUTOMATED CULTIVATION AND TIME-LAPSE IMAGING OF EMBRYONIC STEM CELLS

M. Reichen, F. S. Veraitch and N. Szita
Department of Biochemical Engineering, University College London (UCL), London, UK

ABSTRACT

A microfluidic bioreactor platform for the automated cultivation of embryonic stem cells is presented. The individual microbioreactors have a reversibly sealable culture chamber and seamlessly integrate with typical laboratory procedures: cells are seeded in static culture, e.g. on gelatin-coated tissue culture (TC-PS); for end-point assays, cells can be fixed on a standard microscope slide. The automated platform includes the temperature control for the individual microbioreactors, the delivery of culture medium at desired flow rates and the on-line time-lapse imaging of cell morphology and pluripotency markers on an inverted microscope.

KEY WORDS: Microbioreactor, Embryonic Stem Cells (ESCs), Time-Lapse Imaging, Modular Microfluidics

INTRODUCTION

Numerous biological, physical and chemical factors influence stem cell fate [1, 2]. Therefore, a large number of multivariable experiments will be needed to precisely define what combination of factors are required, the relative contribution of each during target cell derivation, and how these factors are best controlled. Microfluidic bioreactors offer greater control over the cellular microenvironment than, for example, automated microwells. To perform these multivariable experiments, it is necessary to precisely control (and monitor) the operational parameters of the microfluidic bioreactor. These include the culture medium flow rate, cell culture temperature, the culture medium composition (including the gaseous tensions), as well as cell seeding densities, use of culture substrate and deposited extracellular matrices. These operational parameters must then be correlated with the output from the cells, for example their changes in morphology and level of expression markers, and potentially the composition of the spent medium. Different systems have been developed, which address the optical monitoring of cells, but do not include automated liquid handling. For example, a microfluidic culture system compatible with plate readers has been recently reported to measure fluorescent intensities [3]. For high quality imaging, a microfluidic culture chamber with a transparent heater has been implemented on an inverted microscope to monitor HeLa cell cultures at defined temperatures [4]. We present a multiplexed microfluidic platform that combines automated brightfield and fluorescent imaging with flow control, and microbioreactors where different culture substrates can be integrated.

DESIGN AND OPERATION OF THE MICROBIOREACTOR

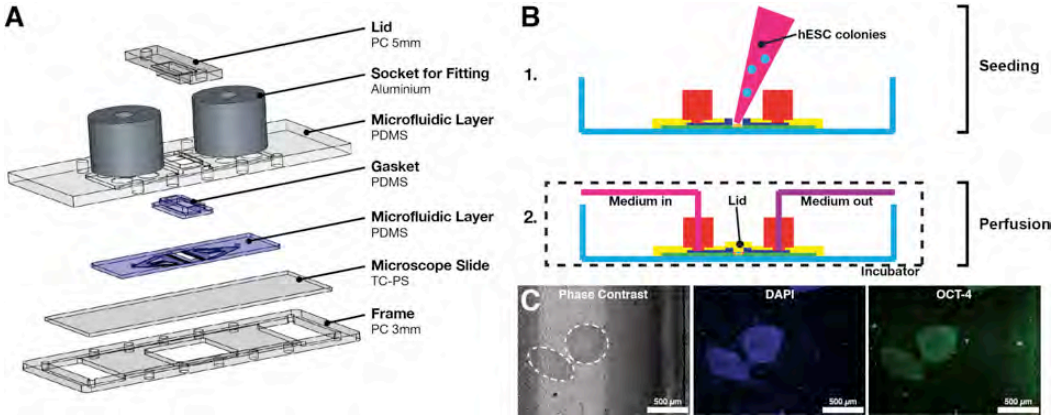

Figure 1: (A) Exploded view of all parts of the microbioreactors. (B) shows the two modes of operation, seeding and culture/perfusion mode of the microbioreactor. The culture chamber of the microbioreactors can be directly accessed with standard laboratory pipettes [5]. (C) Images of hESC colonies (following static seeding and subsequent 2-day perfusion) in phase contrast, stained for DAPI, and pluripotency marker OCT-4.

The microbioreactor consists of a disposable microfluidic chip made of poly(dimethylsiloxane) (PDMS), a culture slide in microscope slide format, and a reusable interface (Fig. 1A). The microfluidic chip made of poly(dimethylsiloxane) (PDMS) defines the sidewalls of the cell culture chamber, and the microfluidic structures that control the fluid flow of the culture medium through the chamber. The reusable interface provides all interfaces with the macro-world, aligns all parts, and enables reliable operation of the reactor. It is made of several parts including an interface plate made of polycarbonate (PC), a bottom frame, two interconnects sockets (PC), and finally a lid (PC) with a corresponding gasket (PDMS). The lid allows repeated access to the culture chamber for cell protocols (Fig. 1B), for

example cell seeding according to typical laboratory procedures. Perfusion experiments in an incubator with an external syringe drive demonstrated that hESC colonies are not washed out of the microbioreactor and retain the expression of pluripotency markers (Fig. 1C) [5].

AUTOMATED CULTIVATION PLATFORM WITH TIME-LAPSE IMAGING

Three microbioreactors fit into the platform which is designed to fit onto a stage of an inverted fluorescence microscope. To separate flow control and cell culture imaging, the platform consists of a 'microscope module' and a 'media handling module', both automated via a LabView™ routine (Figure 2). Medium is delivered from a pressurized reservoir *via* a flow splitter to the three microfluidic bioreactors. To enable long-term perfusion without medium degradation, the reservoirs can be cooled. Prior to reaching the cell culture, the medium is preheated to the desired temperature. Preliminary results are shown in Figure 2C. Cells started to proliferate and were pluripotent (Oct-4) after seeding. Real-time information about the growth and proliferation of cells can only be obtained with an automated cell culture platform and the time-lapse imaging routines.

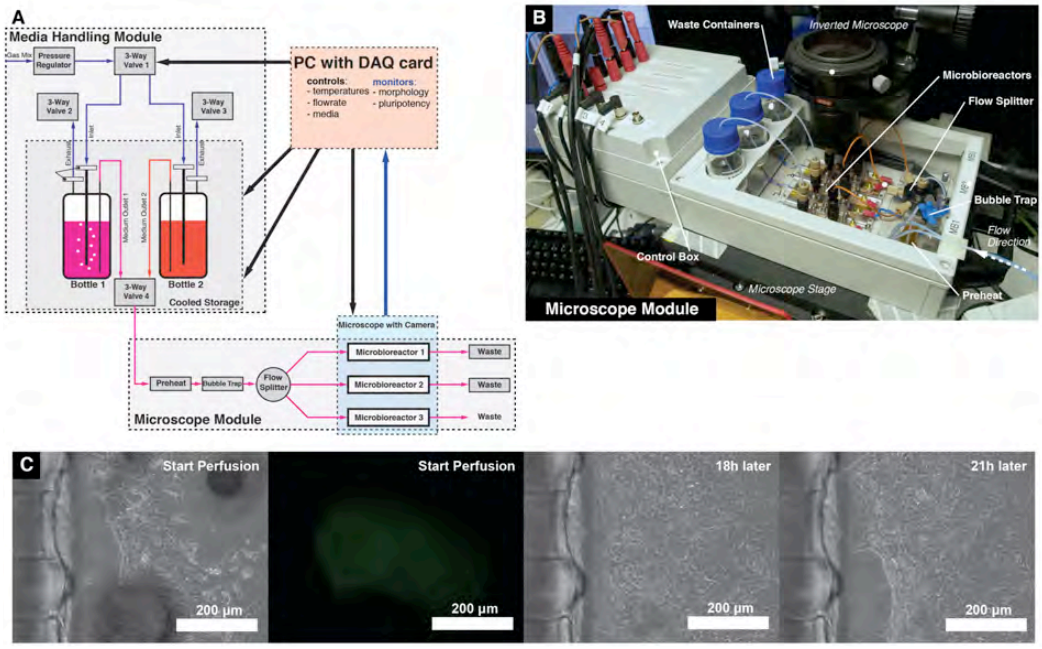

Figure 2: (A) schematic representation of all modules and components of the microfluidic ES cell culture platform. (B) shows the microscope module and its components. (C) Representative images of a cell culture in the microbioreactor showing phase contrast images and fluorescent Oct-4 marker images at different time points (0h, 18h, and 21h).

CONCLUSION

An automated, versatile microfluidic platform for long-term cell culture has been developed to monitor cell morphology, migration and proliferation from phase contrast images, and pluripotency and differentiation markers from fluorescence images. The microbioreactors have a reversibly sealable culture chamber which enables seamless integration with the typically employed seeding protocols and end-point assays in cell culture laboratories. A deeper insight into cellular processes and data-rich experiments can be gained by modulating flow, extracellular matrix and media composition using such a microfluidic platform with its integrated optical monitoring. Future work includes the implementation of advanced imaging algorithms for on-line analysis and long-term experiments.

REFERENCES

[1] D. E. Discher, D. J. Mooney, P. W. Zandstra, "Growth factors, matrices, and forces combine and control stem cells", *Science*, vol. 324, pp. 1673-1677, 2009.

[2] D. C. Kirouac and P. W. Zandstra, "The systematic production of cells for cell therapies", *Cell Stem Cell*, vol. 3, pp. 369-381, 2008.

[3] Y. Wen, X. Zhang, S.-T. Yang, "Microplate-reader compatible perfusion microbioreactor array for modular tissue culture and cytotoxicity assasys", *Biotech. Prog.*, vol. 26, pp. 1135-1144, 2010.

[4] S. Petronis, M. Stangegaard, C. B. V. Christensen, M. Dufva, "Transparent polymeric cell culture chip with integrated temperature control and uniform media perfusion", *Biotechniques*, vol. 40, pp. 368-375, 2006.

[5] M. Reichen, L. Ruban, F. S. Veraitch, N. Szita, "Human embryonic stem cell culturing in a microfluidic perfusion system with a reversibly sealable lid" In *Proc. microTAS 2009*, Jeju, Korea, November 1-5, 2009, pp. 1829-1831.

A MODULAR PACKAGING SYSTEM WITH A RAPID FABRICATION METHOD OF DISPOSABLE MICROFLUIDIC CHIPS

M. Reichen, B. O'Sullivan, T.V. Kirk and N. Szita
Department of Biochemical Engineering, University College London (UCL), London, UK

ABSTRACT

We present a rapid prototyping method for the fabrication of polymeric microfluidic devices which consist of a disposable, fully customisable silicone microfluidic chip, and a modular, reusable, interconnect and packaging system. All device components and mould masters were fabricated with a low-cost, readily available micro-milling machine. The short turnaround time (two days) from design to finished working prototype allows rapid verification of microfluidic design concepts. To demonstrate the abilities and flexibility of our prototyping approach, we fabricated devices with multiple inlets and outlets, three-dimensional chips and staggered herringbone mixers.

KEY WORDS: Rapid Prototyping, Packaging, World-to-Chip Interface, PDMS, Micro-Milling

INTRODUCTION

In order to increase the uptake of microfluidic techniques by biologists and other non-engineering specialists, there must be readily available microfluidic devices that have reliable and robust world-to-chip interfaces, packaging and standardised chips, but that also allow the researcher some flexibility in designing their microfluidic system [1].

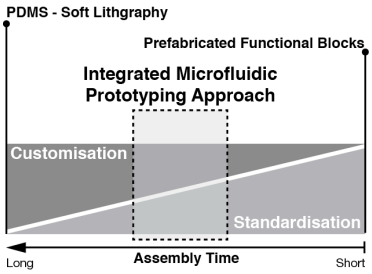

Figure 1: An ideal microfluidic rapid prototyping approach offers a high degree of customisation and a short assembly time due to standardisation.

Currently, the casting of polydimethylsiloxane (PDMS) in moulds created by photolithographic techniques is a commonly used fabrication method for disposable microfluidic chips, offering the ability to fabricate highly customised microfluidic network layouts [2]. However, the need for special equipment such as a mask aligner for photolithography and the lack of a standardised world-to-chip interface and packaging solutions discourage potential end-users of employing microfluidic technology. Functional microfluidic blocks and units made from thermoplastics allow a simple and rapid assembly for microfluidic systems, but the customisation and optimisation of individual blocks is difficult to implement rapidly [3,4].

A rapid prototyping approach which combined simple fabrication of customisable microfluidic channel networks with stadardised world-to-chip interfaces and packaging, would open up the world of microfluidics to non-specialists, allowing them to design, build and optimise their own systems, tailoring the microfluidics to their own research interests. (see figure 1).

DESIGN AND FABRICATION METHOD

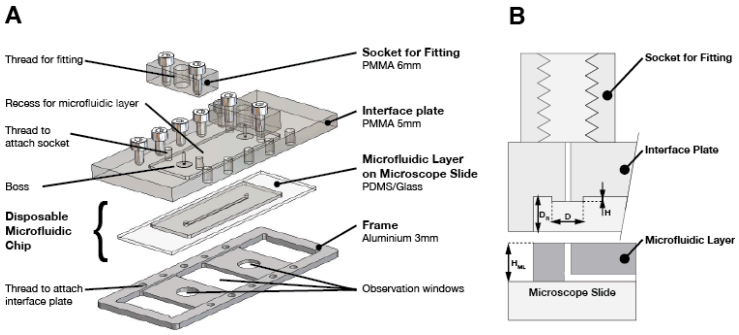

Figure 2: (A) Exploded view of the microfluidic system with the reusable parts of the interconnect system and the disposable microfluidic chip consisting of a PDMS layer bonded to a microscope slide. (B) Schematic of the interconnect, showing dimensions of the boss (D, H) and recess (D_R, H_{ML}).

The microfluidic system presented consists of a reusable interface plate (5 mm PMMA) and a bottom frame (2 mm aluminium) and a disposable PDMS microfluidic chip (see figure 2A). The packaging of the microfluidic chip is based on the compression of the microfluidic chip. Leak-tight fluidic connection with the microfluidic chip is ensured by a boss in the interface plate (see figure 2B). The critical dimensions are the diameter and height of the boss (D, H), and the depth of the recess in the interface plate (D_R) and the height of the microfluidic layer (H_{ML}). The sockets can be used with different fitting types, for example standard adapters (figure 2A, 3), or they can be modified for custom-made inter-connects if required. All parts can be precisely fabricated using a low-cost micro-milling machine. To cast a PDMS microfluidic chip, a mould (including all channel features including inlet and outlet ports) is machined from a rigid substrate such as aluminium, brass or PMMA. The mould also defines the outer dimensions of the microfluidic chip thus facilitating alignment of multiple layers in multi-layer chips. After casting and curing the PDMS, the layer can be released from the mould without the need for further post-processing. The dimensional fidelity of micro-milled parts and moulds was characterized by contact profilometry and image analysis.

RESULTS

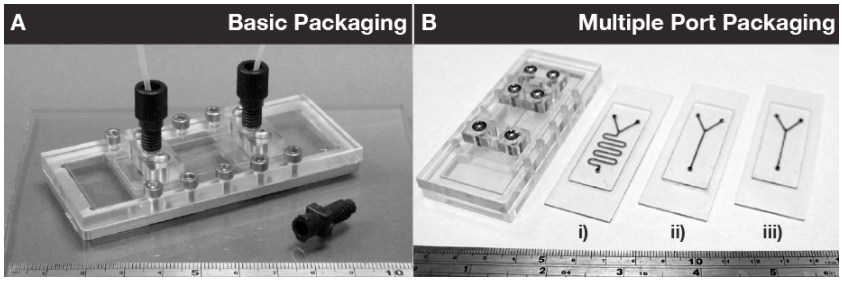

Figure 3: (A) An assembled microfluidic system in a basic packaging configuration with different types of fittings. (B) Multiple ports can be realised, for example for mixer chips with different mixing lengths i), ii) and with added passive mixer structure iii).

The standardised packaging design and corresponding rapid fabrication method enables the rapid, reliable implementation of a wide range of microfluidic designs, without having to re-develop and re-test the world-to-chip interfaces and packaging for every new device. The packaging system enables the simple insertion and alignment of disposable PDMS/glass chips (see figure 3). The system is compatible with the standard microscope slide format (3 x 1 inches), which could be employed to use different commercially available materials, such as tissue culture polystyrene (TC-PS). The latter is particularly useful for microfluidic devices for cell culture where a growth substrate consisting of TC-PS is desirable. The packaging does not rely on adhesives, which are often not biocompatible. The micro-milling fabrication method delivers accurate and precise microfluidic chips with a deviation of less than 7.5% from the nominal dimension (obtained with a low-cost micromilling machine). Burst pressures as high as 7.26 bar have been achieved by varying the dimensions of the boss. Moulds and PDMS with feature sizes smaller than 35 µm were created using our fabrication method by reproducing staggered herringbone mixer structures (see figure 4). As an example for the degree of complexity the fabrication and packaging approach allows, we have developed three-dimensional chips with through holes. The well-defined, outer dimensions of the two PDMS layers allow a precise and simple alignment of the two PDMS layers. The turnaround time from the design idea to this working prototype was 2 days (see figure 5).

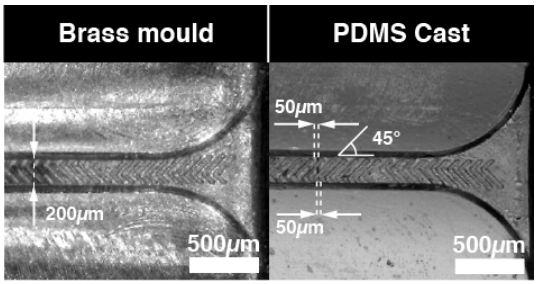

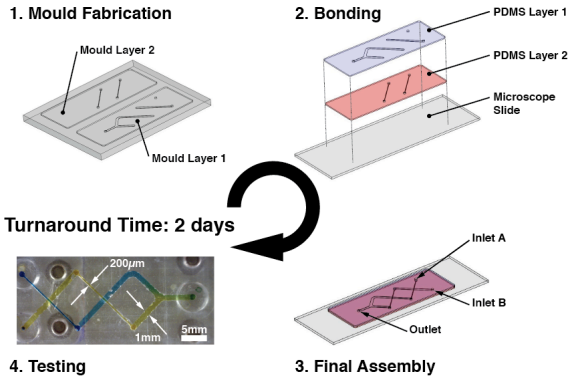

Figure 5: From the design idea to a working prototype in 2 days. Rapid fabrication of the mould and casting of PDMS chips (step 1) and subsequent bonding (Step 2) on day 1. Assembly in the multiple port packaging system (step 3) allows the testing of microfluidic chips (step 4) on day 2.

CONCLUSION

An integrated rapid prototyping approach has been developed and characterised, which offers a simple but comprehensive route to large numbers of ready-to-use microfluidic devices. The system consists of a casting method to deliver microfluidic prototype chips within two days, and a modular, robust, and adhesive-free interconnect and packaging system to rapidly test microfluidic chips. All materials and tools are widely available and at low cost, opening up the possibilities of microfluidic device design to non-specialists such as biologists or chemists.

REFERENCES

[1] G. M. Whitesides, "What comes next?", *Lab Chip*, 11(2), 191, 2011.
[2] D. C. Duffy, J. Cooper McDonald, O. J. A. Schueller and G. M. Whitesides, "Rapid prototyping of microfluidic systems in poly(dimethlysiloxane)", *Anal. Chem.*, 70(23), pp. 4974-4984, 1998.
[3] M. Rhee & M. A. Burns, "Microfluidic assembly blocks", *Lab Chip*, 8(8), pp.1365-1373, 2008.
[4] P.K. Yuen, "SmartBuild - A truly plug-n-play modular microfluidic system" *Lab Chip*, 8(8), pp. 1374-1378, 2008.

References

(2009). Regenerative medicine glossary. *Regenerative Medicine*, **4**, S1–S88. 4

Abhyankar, V.V. & Beebe, D.J. (2007). Spatiotemporal micropatterning of cells on arbitrary substrates. *Analytical Chemistry*, **79**, 4066–4073. 30, 73

Ahmed, T.A. & Hincke, M.T. (2010). Strategies for articular cartilage lesion repair and functional restoration. *Tissue Engineering Part B: Reviews*, **16**, 305–329. 13

Ahsan, T. & Nerem, R.M. (2010). Fluid shear stress promotes an endothelial-like phenotype during the early differentiation of embryonic stem cells. *Tissue Engineering Part A*, **16**, 3547–3553. 18

Alam, M.N.H.Z., Schaepper, D. & Gernaey, K.V. (2010). Embedded resistance wire as a heating element for temperature control in microbioreactors. *Journal of Micromechanics and Microengineering*, **20**, 055014. 117

Albrecht, D.R., Underhill, G.H., Resnikoff, J., Mendelson, A., Bhatia, S.N. & Shah, J.V. (2010). Microfluidics-integrated time-lapse imaging for analysis of cellular dynamics. *Integrative Biology*, **2**, 278–287. 102, 116

Alper, J. (2009). Geron gets green light for human trial of es cell-derived product. *Nature Biotechnology*, **27**, 213–214. 11

Améen, C., Strehl, R., Björquist, P., Lindahl, A., Hyllner, J. & Sartipy, P. (2008). Human embryonic stem cells: current technologies and emerging industrial applications. *Critical Reviews in Oncology/Hematology*, **65**, 54–80. 9

Amit, M. & Itskovitz-Eldor, J. (2006). Feeder-free culture of human embryonic stem cells. In I. Klimanskaya & R. Lanza, eds., *Stem Cell Tools and Other Experimental Protocols*, vol. 420 of *Methods in Enzymology*, 37–49, Academic Press, New York, NY, USA, New York, NY, USA. 7

Amit, M., Margulets, V., Segev, H., Shariki, K., Laevsky, I., Coleman, R. & Itskovitz-Eldor, J. (2003). Human feeder layers for human embryonic stem cells. *Biology of Reproduction*, **68**, 2150–2156. 7

Amit, M., Chebath, J., Margulets, V., Laevsky, I., Miropolsky, Y., Shariki, K., Peri, M., Blais, I., Slutsky, G., Revel, M. & Itskovitz-Eldor, J. (2010). Suspension culture of undifferentiated human embryonic and induced pluripotent stem cells. *Stem Cell Reviews and Reports*, **6**, 248–259. 24

Andersson, H. & van den Berg, A. (2003). Microfluidic devices for cellomics: a review. *Sensors and Actuators B*, **92**, 315–325. 27

Andersson, H. & van den Berg, A. (2006). Where are the biologists? *Lab on a Chip*, **6**, 467–470. 28, 46

Andersson, H. & van den Berg, A. (2007). Single cells or large populations? *Lab on a Chip*, **7**, 544–546. 29

Andrade-Zaldívar, H., Santos, L. & De León Rodríguez, A. (2008). Expansion of human hematopoietic stem cells for transplantation: trends and perspectives. *Cytotechnology*, **56**, 151–160. 23

Angers, S. & Moon, R.T. (2009). Proximal events in wnt signal transduction. *Nature Reviews Molecular Cell Biology*, **AOP**. 15

Anisimov, S.V., Morizane, A. & Correia, A.S. (2010). Risks and mechanisms of oncological disease following stem cell transplantation. *Stem Cell Reviews and Reports*, **6**, 411–424. 11

Appelbaum, F.R. (2007). Hematopoietic-cell transplantation at 50. *The New England Journal of Medicine*, **357**, 1472–1475. 10

Arathoon, W. & Birch, J. (1986). Large-scale cell culture in biotechnology. *Science*, **232**, 1390–1395. 24

Arii, K., Kobayashi, H., Kai, T. & Kokuba, Y. (1999). Degradation kinetics of L-glutamine in aqueous solution. *European Journal of Pharmaceutical Sciences*, **9**, 75–78. 34

Atala, A. (2009). Engineering organs. *Current Opinion in Biotechnology*, **20**, 575–592. 13

Atencia, J., Cooksey, G.A., Jahn, A., Zook, J.M., Vreeland, W.N. & Locascio, L.E. (2010). Magnetic connectors for microfluidic applications. *Lab on a Chip*, **10**, 246–249. 45

Aubrey, P., Arber, S. & Tyler, M. (2008). The organ donor crisis: The missed organ donor potential from the accident and emergency departments. *Transplantation Proceedings*, **40**, 1008–1011. 10

Aunins, J., Bader, B., Caola, A., Griffiths, J., Katz, M., Licari, P., Ram, K., Ranucci, C. & Zhou, W. (2003). Fluid mechanics, cell distribution, and environment in CellCube bioreactors. *Biotechnology Progress*, **19**, 2–8. 89

Azizi, F. & Mastrangelo, C.H. (2008). Generation of dynamic chemical signals with pulse code modulators. *Lab on a Chip*, **8**, 907–912. 139

Baraniak, P.R. & McDevitt, T.C. (2010). Stem cell paracrine actions and tissue regeneration. *Regenerative Medicine*, **5**, 121–143. 17

Barrett, T.A., Wu, A., Zhang, H., Levy, M.S. & Lye, G.J. (2010). Microwell engineering characterization for mammalian cell culture process development. *Biotechnology and Bioengineering*, **105**, 260–275. 26

Beaulieu, I., Geissler, M. & Mauzeroll, J. (2009). Oxygen plasma treatment of polystyrene and zeonor: Substrates for adhesion of patterned cells. *Langmuir*, **25**, 7169–7176. 35

Becerra, J., Santos-Ruiz, L., Andrades, J.A. & Marí-Beffa, M. (2010). The stem cell niche should be a key issue for cell therapy in regenerative medicine. *Stem Cell Reviews and Reports*, 1–8. 15

Becker, H. & Gärtner, C. (2008). Polymer microfabrication technologies for microfluidic systems. *Analytical and Bioanalytical Chemistry*, **390**, 89–111. 43

Bhagat, A.A.S., Jothimuthu, P., Pais, A. & Papautsky, I. (2007). Re-usable quick-release interconnect for characterization of microfluidic systems. *Journal of Micromechanics and Microengineering*, **17**, 42–49. 45

Boettcher, M., Jaeger, M., Kirschbaum, M., Mueller, T., Schnelle, T. & Duschl, C. (2008). Gravitation-driven stress-reduced cell handling. *Analytical and Bioanalytical Chemistry*, **390**, 857–863. 73

Bongso, A., Fong, C. & Gauthaman, K. (2008). Taking stem cells to the clinic: Major challenges. *Journal of Cellular Biochemistry*, **105**, 1352–1360. 11

Braam, S.R., Passier, R. & Mummery, C.L. (2009). Cardiomyocytes from human pluripotent stem cells in regenerative medicine and drug discovery. *Trends in Pharmacological Sciences*, **30**, 536–545. 13

Braun, S.M. & Jessberger, S. (2010). Crossing boundaries: Direct programming of fibroblasts into neurons. *Cell Stem Cell*, **6**, 189–191. 8

Brown, L., Koerner, T., Horton, J.H. & Oleschuk, R.D. (2006). Fabrication and characterization of poly(methylmethacrylate) microfluidic devices bonded using surface modifications and solvents. *Lab on a Chip*, **6**, 66–73. 43

Bruus, H. (2004). Theoretical microfluidics. DTU, lecture notes. 184

Bundgaard, F., Perozziello, G. & Geschke, O. (2006). Rapid prototyping tools and methods for all-Topas® cyclic olefin copolymer fluidic microsystems. *Proceedings of the Institution of Mechanical Engineers, Part C: Journal of Mechanical Engineering Science*, **220**, 1625–1632. 43

Burdick, J.A. & Vunjak-Novakovic, G. (2008). Engineered microenvironments for controlled stem cell differentiation. *Tissue Engineering - Part A*, **15**, 205–219. 18

Burdon, T., Smith, A. & Savatier, P. (2002). Signalling, cell cycle and pluripotency in embryonic stem cells. *Trends in Cell Biology*, **12**, 432–438. 17

Caplan, A.I. (2010). Mesenchymal stem cells: The past, the present, the future. *Cartilage*, **1**, 6–9. 5

Carpenter, M.K. & Couture, L.A. (2010). Regulatory considerations for the development of autologous induced pluripotent stem cell therapies. *Regenerative Medicine*, **5**, 569–579. 8

Carpenter, M.K., Frey-Vasconcells, J. & Rao, M.S. (2009). Developing safe therapies from human pluripotent stem cells. *Nature Biotechnology*, **27**, 606–613. 11

Carré, A. & Lacarrièe, V. (2010). How substrate properties control cell adhesion. a physical-chemical approach. *Journal of Adhesion Science and Technology*, **24**, 815–830. 35

Chalfie, M. (2009). GFP: Lighting up life. *Proceedings of the National Academy of Sciences of the United States of America*, **106**, 10073–10080. 101

Chan, E.M., Ratanasirintrawoot, S., Park, I., Manos, P.D., Loh, Y., Huo, H., Miller, J.D., Hartung, O., Rho, J., Ince, T.A., Daley, G.Q. & Schlaeger, T.M. (2009). Live cell imaging distinguishes bona fide human iPS cells from partially reprogrammed cells. *Nature Biotechnology*, **27**, 1033–1037. 101

Charvin, G., Oikonomou, C. & Cross, F. (2010). Long-term imaging in microfluidic devices. In J.M. Walker & D.B. Papkovsky, eds., *Live Cell Imaging*, vol. 591 of *Methods in Molecular Biology*, 229–242, Humana Press, New York, NY, USA, New York, NY, USA. 102

Chien, K.R. (2008). Regenerative medicine and human models of human disease. *Nature*, **453**, 302–305. 9

Chin, V.I., Taupin, P., Sanga, S., Scheel, J., Gage, F.H. & Bhatia, S.N. (2004). Microfabricated platform for studying stem cell fates. *Biotechnology and Bioengineering*, **88**, 399–415. 136

Choi, Y.Y., Chung, B.G., Lee, D.H., Khademhosseini, A., Kim, J.H. & Lee, S.H. (2010). Controlled-size embryoid body formation in concave microwell arrays. *Biomaterials*, **31**, 4296 – 4303. 26

Choo, A.B., Padmanabhan, J., Chin, A.C. & Oh, S.K. (2004). Expansion of pluripotent human embryonic stem cells on human feeders. *Biotechnology and Bioengineering*, **88**, 321–331. 7

Chung, B.G., Park, J.W., Hu, J., Huang, C., Monuki, E. & Jeon, N.L. (2007). A hybrid microfluidic-vacuum device for direct interfacing with conventional cell culture methods. *BMC Biotechnology*, **7**, 60. 73

Clarke, J. (2009). Live imaging of development in fish embryos. *Seminars in Cell & Developmental Biology*, **20**, 942–946. 101

Condic, M.L. & Rao, M. (2010). Alternative sources of pluripotent stem cells: Ethical and scientific issues revisited. *Stem Cells and Development*, **19**, 1121–1129. 8

Crane, M.M., Chung, K., Stirman, J. & Lu, H. (2010). Microfluidics-enabled phenotyping, imaging, and screening of multicellular organisms. *Lab on a Chip*, **10**, 1509–1517. 42

Czechowicz, A. & Weissman, I.L. (2011). Purified hematopoietic stem cell transplantation: The next generation of blood and immune replacement. *Hematology/Oncology Clinics of North America*, **25**, 75–87. 6

Daar, A.S. & Greenwood, H.L. (2007). A proposed definition of regenerative medicine. *Journal of Tissue Engineering and Regenerative Medicine*, **1**, 179–184. 10

Daley, W.P., Peters, S.B. & Larsen, M. (2008). Extracellular matrix dynamics in development and regenerative medicine. *Journal of Cell Science*, **121**, 255–264. 19

Dalton, C. & Kaler, K.V. (2007). A cost effective, re-configurable electrokinetic microfluidic chip platform. *Sensors and Actuators B: Chemical*, **123**, 628–635. 45

Darr, H. & Benvenisty, N. (2006). Human embryonic stem cells: the battle between self-renewal and differentiation. *Regenerative Medicine*, **1**, 317–325. 2, 15

Desai, S.P., Freeman, D.M. & Voldman, J. (2009). Plastic masters-rigid templates for soft lithography. *Lab on a Chip*, **9**, 1631–1637. 62

DiMasi, J.A., Feldman, L., Seckler, A. & Wilson, A. (2010). Trends in risks associated with new drug development: Success rates for investigational drugs. *Clinical Pharmacology & Therapeutics*, **87**, 272–277. 9

Discher, D.E., Mooney, D.J. & Zandstra, P.W. (2009). Growth factors, matrices, and forces combine and control stem cells. *Science*, **324**, 1673–1677. 15

Domansky, K., Inman, W., Serdy, J., Dash, A., Lim, M.H.M. & Griffith, L.G. (2010). Perfused multiwell plate for 3D liver tissue engineering. *Lab on a Chip*, **10**, 51–58. 116

Domogatskaya, A., Rodin, S., Boutaud, A. & Tryggvason, K. (2008). Laminin-511 but not -332, -111, or -411 enables mouse embryonic stem cell self-renewal in vitro. *Stem Cells*, **26**, 2800–2809. 20

Doran, M.R., Frith, J.E., Prowse, A.B., Fitzpatrick, J., Wolvetang, E.J., Munro, T.P., Gray, P.P. & Cooper-White, J.J. (2010). Defined high protein content surfaces for stem cell culture. *Biomaterials*, **31**, 5137–5142. 20

Draper, J.S., Moore, H.D., Ruban, L.N., Gokhale, P.J. & Andrews, P.W. (2004). Culture and characterization of human embryonic stem cells. *Stem Cells and Development*, **13**, 325–336. 7

Drews, J. (2000). Drug discovery: A historical perspective. *Science*, **287**, 1960–1964. 9

Easley, C.J., Benninger, R.K.P., Shaver, J.H., Head, W.S. & Piston, D.W. (2009). Rapid and inexpensive fabrication of polymeric microfluidic devices via toner transfer masking. *Lab on a Chip*, **9**, 1119. 42

Ebert, A.D. & Svendsen, C.N. (2010). Human stem cells and drug screening: Opportunities and challenges. *Nature Reviews Drug Discovery*, **9**, 367–372. 9

Eddings, M.A., Johnson, M.A. & Gale, B.K. (2008). Determining the optimal PDMS–PDMS bonding technique for microfluidic devices. *Journal of Micromechanics and Microengineering*, **18**, 067001. 64

El-Ali, J., Sorger, P.K. & Jensen, K.F. (2006). Cells on chips. *Nature*, **442**, 403–411. 27

Ellis, S. & Tanentzapf, G. (2010). Integrin-mediated adhesion and stem-cell-niche interactions. *Cell and Tissue Research*, **339**, 121–130. 19

Ellison, D., Munden, A. & Levchenko, A. (2009). Computational model and microfluidic platform for the investigation of paracrine and autocrine signaling in mouse embryonic stem cells. *Molecular BioSystems*, **5**, 1004–1012. 30

Engler, A.J., Sen, S., Sweeney, H.L. & Discher, D.E. (2006). Matrix elasticity directs stem cell lineage specification. *Cell*, **126**, 677–689. 19

Erickson, D. (2005). Towards numerical prototyping of labs-on-chip: Modeling for integrated microfluidic devices. *Microfluidics and Nanofluidics*, **1**, 301–318. 42

Evans, M.J. & Kaufman, M.H. (1981). Establishment in culture of pluripotential cells from mouse embryos. *Nature*, **292**, 154–156. 6

Fan, C.G., Zhang, Q.j. & Zhou, J.r. (2011). Therapeutic potentials of mesenchymal stem cells derived from human umbilical cord. *Stem Cell Reviews and Reports*, **7**, 195–207. 6

Feng, X., Du, W., Luo, Q. & Liu, B. (2009). Microfluidic chip: Next-generation platform for systems biology. *Analytica Chimica Acta*, **650**, 83–97. 27

Figallo, E., Cannizzaro, C., Gerecht, S., Burdick, J.A., Langer, R., Elvassore, N. & Vunjak-Novakovic, G. (2007). Micro-bioreactor array for controlling cellular microenvironments. *Lab on a Chip*, **7**, 710–719. 30, 73, 89

Fingar, D.C. & Blenis, J. (2004). Target of rapamycin (TOR): an integrator of nutrient and growth factor signals and coordinator of cell growth and cell cycle progression. *Oncogene*, **23**, 3151–3171. 17

Fiorini, G. & Chiu, D. (2005). Disposable microfluidic devices: Fabrication, function, and application. *BioTechniques*, **38**, 429–446. 43

Firestone, A. & Chen, J. (2010). Controlling destiny through chemistry: Small-molecule regulators of cell fate. *ACS Chemical Biology*, **5**, 15–34. 17

Fok, E.Y.L. & Zandstra, P.W. (2005). Shear-controlled single-step mouse embryonic stem cell expansion and embryoid Body-Based differentiation. *Stem Cells*, **23**, 1333–1342. 23

Fong, W.J., Tan, H.L., Choo, A. & Oh, S.K.W. (2005). Perfusion cultures of human embryonic stem cells. *Bioprocess and Biosystems Engineering*, **27**, 381–387. 25

Frantz, C., Stewart, K.M. & Weaver, V.M. (2010). The extracellular matrix at a glance. *Journal of Cell Science*, **123**, 4195–4200. 19

Fredrickson, C.K. & Fan, Z.H. (2004). Macro-to-micro interfaces for microfluidic devices. *Lab on a Chip*, **4**, 526–533. 44

Fu, Y., Kedziorek, D. & Kraitchman, D.L. (2009). Recent developments and future challenges on imaging for stem cell research. *Journal of Cardiovascular Translational Research*, **3**, 24–29. 101

Fung, W., Beyzavi, A., Abgrall, P., Nguyen, N. & Li, H. (2009). Microfluidic platform for controlling the differentiation of embryoid bodies. *Lab on a Chip*, **9**, 2591–2595. 30

Gad, S.C. (2005). Drug discovery in the 21st century. In S.C. Gad, ed., *Drug Discovery Handbook*, John Wiley & Sons, Inc., Hoboken, NJ, USA. 9

Gervais, T., El-Ali, J., Gunther, A. & Jensen, K.F. (2006). Flow-induced deformation of shallow microfluidic channels. *Lab on a Chip*, **6**, 500–507. 55

Gimble, J.M. & Guilak, F. (2003). Adipose-derived adult stem cells: Isolation, characterization, and differentiation potential. *Cytotherapy*, **5**, 362–369. 6

Gögel, S., Gubernator, M. & Minger, S.L. (2011). Progress and prospects: Stem cells and neurological diseases. *Gene Therapy*, **18**, 1–6. 12, 13

Gomez-Sjoberg, R., Leyrat, A., Pirone, D., Chen, C. & Quake, S. (2007). Versatile, fully automated, microfluidic cell culture system. *Analytical Chemistry*, **79**, 8557–8563. 72

Gonez, L.J. & Knight, K.R. (2010). Cell therapy for diabetes: Stem cells, progenitors or beta-cell replication? *Molecular and Cellular Endocrinology*, **323**, 55–61. 13

Gray, B.L., Jaeggi, D., Mourlas, N.J., van Drieënhuizen, B.P., Williams, K.R., Maluf, N.I. & Kovacs, G.T.A. (1999). Novel interconnection technologies for integrated microfluidic systems. *Sensors and Actuators A: Physical*, **77**, 57–65. 45

Greenlee, A., Kronenwetter-Koepel, T., Kaiser, S. & Liu, K. (2005). Comparison of Matrigel(TM) and gelatin substrata for feeder-free culture of undifferentiated mouse embryonic stem cells for toxicity testing. *Toxicology in Vitro*, **19**, 389–397. 20

Grigoryan, A. & Kruglyakov, P. (2009). Murine embryonic stem cells as a model for human embryonic stem-cell research. *Cell and Tissue Biology*, **3**, 199–212. 7

Griffith, M., Jagasia, M. & Jagasia, S. (2010). Diabetes mellitus after hematopoietic stem cell transplantation. *Endocrine Practice*, **16**, 699–706. 11

Gu, W., Zhu, X., Futai, N., Cho, B.S. & Takayama, S. (2004). Computerized microfluidic cell culture using elastomeric channels and braille displays. *Proceedings of the National Academy of Sciences of the United States of America*, **101**, 15861–15866. 116

Guilak, F., Cohen, D.M., Estes, B.T., Gimble, J.M., Liedtke, W. & Chen, C.S. (2009). Control of stem cell fate by physical interactions with the extracellular matrix. *Cell Stem Cell*, **5**, 17 – 26. 19

Gupta, K., Kim, D., Ellison, D., Smith, C., Kundu, A., Tuan, J., Suh, K. & Levchenko, A. (2010). Lab-on-a-chip devices as an emerging platform for stem cell biology. *Lab on a Chip*, **10**, 2019. 28

Gutierrez, E., Petrich, B.G., Shattil, S.J., Ginsberg, M.H., Groisman, A. & Kasirer-Friede, A. (2008). Microfluidic devices for studies of shear-dependent platelet adhesion. *Lab on a Chip*, **8**, 1486–1495. 73

Hagenmüller, H., Hofmann, S., Kohler, T., Merkle, H., Kaplan, D., Vunjak-Novakovic, G., Müller, R. & Meinel, L. (2007). Non-invasive time-lapsed monitoring and quantification of engineered bone-like tissue. *Annals of Biomedical Engineering*, **35**, 1657–1667. 21

Hamill, K.J., Kligys, K., Hopkinson, S.B. & Jones, J.C.R. (2009). Laminin deposition in the extracellular matrix: a complex picture emerges. *Journal of Cell Science*, **122**, 4409–4417. 20

Han, K.H. & Frazier, A. (2005). Reliability aspects of packaging and integration technology for microfluidic systems. *IEEE Transactions on Device and Materials Reliability*, **5**, 452 – 457. 43

Harms, P., Kostov, Y. & Rao, G. (2002). Bioprocess monitoring. *Current Opinion in Biotechnology*, **13**, 124–127. 21

Hernandez, D., Ruban, L. & Mason, C. (2011). Feeder-free culture of human embryonic stem cells for scalable expansion in a reproducible manner. *Stem Cells and Development*, **AOP**. 7

Ho, A.D. (2005). Kinetics and symmetry of divisions of hematopoietic stem cells. *Experimental Hematology*, **33**, 1–8. 2

Hoffman, L.M. & Carpenter, M.K. (2005). Characterization and culture of human embryonic stem cells. *Nature Biotechnology*, **23**, 699–708. 7

Hossain, M.M., Shimizu, E., Saito, M., Rao, S.R., Yamaguchi, Y. & Tamiya, E. (2010). Non-invasive characterization of mouse embryonic stem cell derived cardiomyocytes based on the intensity variation in digital beating video. *The Analyst*, **135**, 1624–1630. 22

Hovatta, O., Mikkola, M., Gertow, K., Stromberg, A., Inzunza, J., Hreinsson, J., Rozell, B., Blennow, E., Andang, M. & Ahrlund-Richter, L. (2003). A culture system using human foreskin fibroblasts as feeder cells allows production of human embryonic stem cells. *Human Reproduction*, **18**, 1404–1409. 7

Hu, Y. (2008). Compatibility study for fibroblasts on micro-milled surface on a macro- and microscale. MSc thesis, UCL Biochemical Engineering. 137

Huang, C. & Lee, G. (2007). A microfluidic system for automatic cell culture. *Journal of Micromechanics and Microengineering*, **17**, 1266–1274. 119

Huang, S.B., Wu, M.H., Wang, S.S. & Lee, G.B. (2011). Microfluidic cell culture chip with multiplexed medium delivery and efficient cell/scaffold loading mechanisms for high-throughput perfusion 3-dimensional cell culture-based assays. *Biomedical Microdevices*, **13**, 1–16. 139

Hughes, C.S., Postovit, L.M. & Lajoie, G.A. (2010). Matrigel: A complex protein mixture required for optimal growth of cell culture. *Proteomics*, **10**, 1886–1890. 20

Hung, P.J., Lee, P.J., Sabounchi, P., Lin, R. & Lee, L.P. (2005). Continuous perfusion microfluidic cell culture array for high-throughput cell-based assays. *Biotechnology and Bioengineering*, **89**, 1–8. 89

Hynes, R.O. (2009). The extracellular matrix: Not just pretty fibrils. *Science*, **326**, 1216–1219. 19

James, S. (2007). Characterisation of oxygen permeability within two types of poly(dimethylsiloxane); C6-570 liquid silicone rubber and Sylgard 184. MEng Thesis, UCL Biochemical Engineering. 90

Jenkins, D. (2009). Hedgehog signalling: Emerging evidence for non-canonical pathways. *Cellular Signalling*, **21**, 1023–1034. 15

Jo, B., Lerberghe, L.V., Motsegood, K. & Beebe, D. (2000). Three-dimensional micro-channel fabrication in polydimethylsiloxane (PDMS) elastomer. *Journal of Microelectromechanical Systems*, **9**, 76–81. 52

Jones, M.B., Chu, C.H., Pendleton, J.C., Betenbaugh, M.J., Shiloach, J., Baljinnyam, B., Rubin, J.S. & Shamblott, M.J. (2010). Proliferation and pluripotency of human embryonic stem cells maintained on type I collagen. *Stem Cells and Development*, **19**, 1923–1935. 20

Joyce, N., Annett, G., Wirthlin, L., Olson, S., Bauer, G. & Nolta, J.A. (2010). Mesenchymal stem cells for the treatment of neurodegenerative disease. *Regenerative Medicine*, **5**, 933–946. 6

Jung, W., Heo, Y., Yoon, G., Shin, K., Chang, S., Kim, G. & Cho, M. (2007). Micro machining of injection mold inserts for fluidic channel of polymeric biochips. *Sensors*, **7**, 1643–1654. 44

Kamei, K., Guo, S., Yu, Z.T.F., Takahashi, H., Gschweng, E., Suh, C., Wang, X., Tang, J., McLaughlin, J., Witte, O.N., Lee, K. & Tseng, H. (2009). An integrated microfluidic culture device for quantitative analysis of human embryonic stem cells. *Lab on a Chip*, **9**, 555–563. 30, 36, 72, 73

Khademhosseini, A., Yeh, J., Eng, G., Karp, J., Kaji, H., Borenstein, J., Farokhzad, O.C. & Langer, R. (2005). Cell docking inside microwells within reversibly sealed microfluidic channels for fabricating multiphenotype cell arrays. *Lab on a Chip*, **5**, 1380–1386. 30

Khan, W.S., Johnson, D.S. & Hardingham, T.E. (2010). The potential of stem cells in the treatment of knee cartilage defects. *The Knee*, **17**, 369–374. 6

Khoury, M., Bransky, A., Korin, N., Konak, L., Enikolopov, G., Tzchori, I. & Levenberg, S. (2010). A microfluidic traps system supporting prolonged culture of human embryonic stem cells aggregates. *Biomedical Microdevices*, **12**, 1001–1008. 30

Kim, H.S., Oh, S.K., Park, Y.B., Ahn, H.J., Sung, K.C., Kang, M.J., Lee, L.A., Suh, C.S., Kim, S.H., Kim, D. & Moon, S.Y. (2005). Methods for derivation of human embryonic stem cells. *Stem Cells*, **23**, 1228–1233. 6

Kim, L., Vahey, M.D., Lee, H. & Voldman, J. (2006). Microfluidic arrays for logarithmically perfused embryonic stem cell culture. *Lab on a Chip*, **6**, 394–406. 29, 30, 72, 92

Kim, L., Toh, Y., Voldman, J. & Yu, H. (2007). A practical guide to microfluidic perfusion culture of adherent mammalian cells. *Lab on a Chip*, **7**, 681–694. 70, 71, 93

Kim, S.U. & de Vellis, J. (2009). Stem cell-based cell therapy in neurological diseases: A review. *Journal of Neuroscience Research*, **87**, 2183–2200. 12, 13

King, J.A. & Miller, W.M. (2007). Bioreactor development for stem cell expansion and controlled differentiation. *Current Opinion in Chemical Biology*, **11**, 394–398. 21

Kino-oka, M. & Taya, M. (2009). Recent developments in processing systems for cell and tissue cultures toward therapeutic application. *Journal of Bioscience and Bioengineering*, **108**, 267–276. 21

Kirouac, D.C. & Zandstra, P.W. (2008). The systematic production of cells for cell therapies. *Cell Stem Cell*, **3**, 369–381. 14

Klank, H., Kutter, J.P. & Geschke, O. (2002). CO_2-laser micromachining and back-end processing for rapid production of PMMA-based microfluidic systems. *Lab on a Chip*, **2**, 242–246. 43

Kleinman, H.K. & Martin, G.R. (2005). Matrigel: basement membrane matrix with biological activity. *Seminars in Cancer Biology*, **15**, 378–386. 20

Kola, I. & Landis, J. (2004). Can the pharmaceutical industry reduce attrition rates? *Nature Reviews Drug Discovery*, **3**, 711–716. 9

Koller, M., Bender, J., Papoutsakis, E. & Miller, W. (1992). Beneficial effects of reduced oxygen tension and perfusion in long-term hematopoietic cultures. *Annals of the New York Academy of Sciences*, **665**, 105–116. 24

Koller, M., Bender, J., Miller, W. & Papoutsakis, E. (1993a). Expansion of primitive human hematopoietic progenitors in a perfusion bioreactor system with IL-3, IL-6, and stem cell factor. *Nature Biotechnology*, **11**, 358–363. 24

Koller, M., Emerson, S. & Palsson, B. (1993b). Large-scale expansion of human stem and progenitor cells from bone marrow mononuclear cells in continuous perfusion cultures. *Blood*, **82**, 378–384. 24

Korin, N., Bransky, A., Dinnar, U., Levenberg, S. & Nicolau, D.V. (2006). The culture of human embryonic stem cells in microchannel perfusion bioreactors. In *Biomedical Applications of Micro- and Nanoengineering III*, vol. 6416, 64160N–1–64160N–4, SPIE, Adelaide, Australia. 73

Korin, N., Bransky, A., Dinnar, U. & Levenberg, S. (2009a). Periodic "flow-stop" perfusion microchannel bioreactors for mammalian and human embryonic stem cell long-term culture. *Biomedical Microdevices*, **11**, 87–94. 73, 78, 92

Korin, N., Bransky, A., Khoury, M., Dinnar, U. & Levenberg, S. (2009b). Design of well and groove microchannel bioreactors for cell culture. *Biotechnology and Bioengineering*, **102**, 1222–1230. 30, 73, 91

Krawetz, R., Taiani, J.T., Liu, S., Meng, G., Li, X., Kallos, M.S. & Rancourt, D.E. (2010). Large-scale expansion of pluripotent human embryonic stem cells in stirred-suspension bioreactors. *Tissue Engineering Part C: Methods*, **16**, 573–582. 23

Kretzmer, G. (2000). Influence of stress on adherent cells. In H.J. Henzler, P.M. Kieran, G. Kretzmer, P.F. MacLoughlin, D.M. Malone, W. Schumann, P.A. Shamlou & S.S. Yim, eds., *Influence of Stress on Cell Growth and Product Formation*, vol. 67 of *Advances in Biochemical Engineering/Biotechnology*, 123–137, Springer Berlin / Heidelberg. 24

Kristensen, D., Kalisz, M. & Nielsen, J. (2005). Cytokine signalling in embryonic stem cells. *APMIS*, **113**, 756–772. 17

Kroon, E., Martinson, L.A., Kadoya, K., Bang, A.G., Kelly, O.G., Eliazer, S., Young, H., Richardson, M., Smart, N.G., Cunningham, J., Agulnick, A.D., D'Amour, K.A., Carpenter, M.K. & Baetge, E.E. (2008). Pancreatic endoderm derived from human embryonic stem cells generates glucose-responsive insulin-secreting cells in vivo. *Nature Biotechnology*, **26**, 443–452. 7

Lee, K.S. & Ram, R.J. (2009). Plastic-PDMS bonding for high pressure hydrolytically stable active microfluidics. *Lab on a Chip*, **9**, 1618–1624. 64

Lee, P.J., Ghorashian, N., Gaige, T.A. & Hung, P.J. (2007). Microfluidic system for automated cell-based assays. *Journal of the Association for Laboratory Automation*, **12**, 363–367. 29

Lee, S.T., Yun, J.I., Jo, Y.S., Mochizuki, M., van der Vlies, A.J., Kontos, S., Ihm, J.E., Lim, J.M. & Hubbell, J.A. (2010). Engineering integrin signaling for

promoting embryonic stem cell self-renewal in a precisely defined niche. *Biomaterials*, **31**, 1219–1226. 19

Lei, T., Jacob, S., Ajil-Zaraa, I., Dubuisson, J., Irion, O., Jaconi, M. & Feki, A. (2007). Xeno-free derivation and culture of human embryonic stem cells: Current status, problems and challenges. *Cell Research*, **17**, 682–688. 7

Lemon, E.W. (2009). Properties of water. In D.R. Lide & W.M. Haynes, eds., *CRC Handbook of Chemsitry and Physics*, chap. 6-1, CRC Press, Boca Raton, FL, USA, Boca Raton, FL, USA, 90th edn. 79

Li, D. (2008a). Microfluidic systems. In D. Li, ed., *Encyclopedia of Microfluidics and Nanofluidics*, 1221–1221, Springer US, New York, NY, USA, New York, NY, USA. 27

Li, M. (2008b). Automated routines for a microfluidic cell culture platform. MSc thesis, UCL Biochemical Engineering. 117, 120, 123, 195

Li, S. & Chen, S. (2003). Polydimethylsiloxane fluidic interconnects for microfluidic systems. *IEEE Transactions on Advanced Packaging*, **26**, 242–247. 45

Li, W. & Ding, S. (2010). Small molecules that modulate embryonic stem cell fate and somatic cell reprogramming. *Trends in Pharmacological Sciences*, **31**, 36–45. 17

Li, Y., Lin, C., Wang, L., Liu, Y., Mu, X., Ma, Y. & Li, L. (2009). Maintenance of human embryonic stem cells on gelatin. *Chinese Science Bulletin*, **54**, 4214–4220. 20

Lii, J., Hsu, W., Parsa, H., Das, A., Rouse, R. & Sia, S.K. (2008). Real-time microfluidic system for studying mammalian cells in 3D microenvironments. *Analytical Chemistry*, **80**, 3640–3647. 30

Lin, J., Wu, M., Kuo, C., Lee, K. & Shen, Y. (2010). Application of indium tin oxide (ITO)-based microheater chip with uniform thermal distribution for perfusion cell culture outside a cell incubator. *Biomedical Microdevices*, **12**, 389–398. 117

Lindvall, O. & Kokaia, Z. (2010). Stem cells in human neurodegenerative disorders - time for clinical translation? *Journal of Clinical Investigation*, **120**, 29–40. 12

Liu, K., Pitchimani, R., Dang, D., Bayer, K., Harrington, T. & Pappas, D. (2008). Cell culture chip using low-shear mass transport. *Langmuir*, **24**, 5955–5960. 74

Liu, L., Luo, C., Ni, X., Wang, L., Yamauchi, K., Nomura, S., Nakatsuji, N. & Chen, Y. (2010). A micro-channel-well system for culture and differentiation of embryonic stem cells on different types of substrate. *Biomedical Microdevices*, **12**, 505–511. 35

Lu, H., Koo, L.Y., Wang, W.M., Lauffenburger, D.A., Griffith, L.G. & Jensen, K.F. (2004). Microfluidic shear devices for quantitative analysis of cell adhesion. *Analytical Chemistry*, **76**, 5257–5264. 73

Lu, J., Hou, R., Booth, C.J., Yang, S. & Snyder, M. (2006). Defined culture conditions of human embryonic stem cells. *Proceedings of the National Academy of Sciences of the United States of America*, **103**, 5688–5693. 20

Ludwig, T.E., Bergendahl, V., Levenstein, M.E., Yu, J., Probasco, M.D. & Thomson, J.A. (2006). Feeder-independent culture of human embryonic stem cells. *Nature Methods*, **3**, 637–646. 7

Lutolf, M.P., Gilbert, P.M. & Blau, H.M. (2009). Designing materials to direct stem-cell fate. *Nature*, **462**, 433–441. 19

Macchiarini, P., Jungebluth, P., Go, T., Asnaghi, M.A., Rees, L.E., Cogan, T.A., Dodson, A., Martorell, J., Bellini, S., Parnigotto, P.P., Dickinson, S.C., Hollander, A.P., Mantero, S., Conconi, M.T. & Birchall, M.A. (2008). Clinical transplantation of a tissue-engineered airway. *The Lancet*, **372**, 2023–2030. 5

Mack, G.S. (2011). ReNeuron and StemCells get green light for neural stem cell trials. *Nature Biotechnology*, **29**, 95–97. 11

Mair, D.A., Geiger, E., Pisano, A.P., Frechet, J.M.J. & Svec, F. (2006). Injection molded microfluidic chips featuring integrated interconnects. *Lab on a Chip*, **6**, 1346–1354. 43, 45, 57

Mallon, B.S., Park, K., Chen, K.G., Hamilton, R.S. & McKay, R.D. (2006). Toward xeno-free culture of human embryonic stem cells. *The International Journal of Biochemistry & Cell Biology*, **38**, 1063–1075. 7

Manz, A., Graber, N. & Widmer, H.M. (1990). Miniaturized total chemical analysis systems: A novel concept for chemical sensing. *Sensors and Actuators B: Chemical*, **1**, 244–248. 27

Margolin, K. (2008). Cytokine therapy in cancer. *Expert Opinion on Biological Therapy*, **8**, 1495–1505. 1

Martin, G.R. (1981). Isolation of a pluripotent cell line from early mouse embryos cultured in medium conditioned by teratocarcinoma stem cells. *Proceedings of the National Academy of Sciences of the United States of America*, **78**, 7634–7638. 6

Martin, I., Wendt, D. & Heberer, M. (2004). The role of bioreactors in tissue engineering. *Trends in Biotechnology*, **22**, 80–86. 21

Martínez, E., Lagunas, A., Mills, C., Rodríguez-Seguí, S., Estévez, M., Oberhansl, S., Comelles, J. & Samitier, J. (2009). Stem cell differentiation by functionalized micro- and nanostructured surfaces. *Nanomedicine*, **4**, 65–82. 18

Mason, C. & Dunnill, P. (2009). Quantities of cells used for regenerative medicine and some implications for clinicians and bioprocessors. *Regenerative Medicine*, **4**, 153–157. 11

Mason, C. & Hoare, M. (2007). Regenerative medicine bioprocessing: Building a conceptual framework based on early studies. *Tissue Engineering*, **13**, 301–11. 13

Maul, T., Chew, D., Nieponice, A. & Vorp, D. (2011). Mechanical stimuli differentially control stem cell behavior: Morphology, proliferation, and differentiation. *Biomechanics and Modeling in Mechanobiology*, 1–15. 18

McDonald, J.C. & Whitesides, G.M. (2002). Poly(dimethylsiloxane) as a material for fabricating microfluidic devices. *Accounts of Chemical Research*, **35**, 491–499. 43

McDonald, J.C., Duffy, D.C., Anderson, J.R., Chiu, D.T., Wu, H., Schueller, O.J.A. & Whitesides, G.M. (2000). Fabrication of microfluidic systems in poly(dimethylsiloxane). *Electrophoresis*, **21**, 27–40. 44

McKenna, D.H. & Brunstein, C.G. (2011). Umbilical cord blood: current status and future directions. *Vox Sanguinis*, **100**, 150–162. 6

McKernan, R., McNeish, J. & Smith, D. (2010). Pharma's developing interest in stem cells. *Cell Stem Cell*, **6**, 517–520. 11

McNeish, J.D. (2007). Stem cells as screening tools in drug discovery. *Current Opinion in Pharmacology*, **7**, 515–520. 9

Mecomber, J.S., Stalcup, A.M., Hurd, D., Halsall, H.B., Heineman, W.R., Seliskar, C.J., Wehmeyer, K.R. & Limbach, P.A. (2006). Analytical performance of polymer-based microfluidic devices fabricated by computer numerical controlled machining. *Analytical Chemistry*, **78**, 936–941. 44

Melin, J. & Quake, S.R. (2007). Microfluidic large-scale integration: The evolution of design rules for biological automation. *Annual Review of Biophysics and Biomolecular Structure*, **36**, 213–231. 38, 116

Melkoumian, Z., Weber, J.L., Weber, D.M., Fadeev, A.G., Zhou, Y., Dolley-Sonneville, P., Yang, J., Qiu, L., Priest, C.A., Shogbon, C., Martin, A.W., Nelson, J., West, P., Beltzer, J.P., Pal, S. & Brandenberger, R. (2010). Synthetic peptide-acrylate surfaces for long-term self-renewal and cardiomyocyte differentiation of human embryonic stem cells. *Nature Biotechnology*, **28**, 606–610. 20

Melton, D.A. & Cowen, C. (2009). "Stemness": definitions, criteria, and standards. In R. Lanza, ed., *Essentials of Stem Cell Biology*, Elsevier, Amsterdam, The Netherlands, Amsterdam, The Netherlands, 2nd edn. 3

Metallo, C.M., Vodyanik, M.A., de Pablo, J.J., Slukvin, I.I. & Palecek, S.P. (2008). The response of human embryonic stem cell-derived endothelial cells to shear stress. *Biotechnology and Bioengineering*, **100**, 830–837. 73

Micheletti, M. & Lye, G.J. (2006). Microscale bioprocess optimisation. *Current Opinion in Biotechnology*, **17**, 611–618. 25

Miserendino, S. & Tai, Y. (2008). Modular microfluidic interconnects using photodefinable silicone microgaskets and MEMS o-rings. *Sensors and Actuators, A: Physical*, **143**, 7–13. 45

Mohr, J.C., Zhang, J., Azarin, S.M., Soerens, A.G., de Pablo, J.J., Thomson, J.A., Lyons, G.E., Palecek, S.P. & Kamp, T.J. (2010). The microwell control of embryoid body size in order to regulate cardiac differentiation of human embryonic stem cells. *Biomaterials*, **31**, 1885–1893. 26

Mohyeldin, A., Garzo-Muvdi, T. & Quinones-Hinojosa, A. (2010). Oxygen in stem cell biology: A critical component of the stem cell niche. *Cell Stem Cell*, **7**, 150–161. 18, 37

Mondragon-Teran, P., Lye, G.J. & Veraitch, F.S. (2009). Lowering oxygen tension enhances the differentiation of mouse embryonic stem cells into neuronal cells. *Biotechnology Progress*, **25**, 1480–1488. 23

Morizane, A., Li, J. & Brundin, P. (2007). From bench to bed: The potential of stem cells for the treatment of parkinson's disease. *Cell and Tissue Research*, **331**, 323–336. 1, 12

Morrison, S.J. & Kimble, J. (2006). Asymmetric and symmetric stem-cell divisions in development and cancer. *Nature*, **441**, 1068–1074. 2

Mukhopadhyay, R. (2009). Microfluidics: On the slope of enlightenment. *Analytical Chemistry*, **81**, 4169–4173. 46

Murphy, M.J., Wilson, A. & Trumpp, A. (2005). More than just proliferation: Myc function in stem cells. *Trends in Cell Biology*, **15**, 128 – 137. 15

Muruganandan, S., Roman, A. & Sinal, C. (2009). Adipocyte differentiation of bone marrow-derived mesenchymal stem cells: Cross talk with the osteoblastogenic program. *Cellular and Molecular Life Sciences*, **66**, 236–253. 6

Nath, P., Fung, D., Kunde, Y.A., Zeytun, A., Branch, B. & Goddard, G. (2010). Rapid prototyping of robust and versatile microfluidic components using adhesive transfer tapes. *Lab on a Chip*, **10**, 2286–2291. 42

Neganova, I. & Lako, M. (2008). G1 to s phase cell cycle transition in somatic and embryonic stem cells. *Journal of Anatomy*, **213**, 30–44. 17

Nguyen, N. (2004). *Mikrofluidik - Entwurf, Herstellung und Charakterisierung*. Vieweg & Teubner, Stuttgart/Leipzig/Wiesbaden, Germany, Stuttgart/Leipzig/Wiesbaden, Germany. 182

Nienow, A. (2006). Reactor engineering in large scale animal cell culture. *Cytotechnology*, **50**, 9–33. 23

Nirmalanandhan, V.S. & Sittampalam, G.S. (2009). Stem cells in drug discovery, tissue engineering, and regenerative medicine: Emerging opportunities and challenges. *Journal of Biomolecular Screening*, **14**, 755–768. 1

Nittis, V., Fortt, R., Legge, C.H. & de Mello, A.J. (2001). A high-pressure interconnect for chemical microsystem applications. *Lab on a Chip*, **1**, 148–152. 45

Ogonczyk, D., Wegrzyn, J., Jankowski, P., Dabrowski, B. & Garstecki, P. (2010). Bonding of microfluidic devices fabricated in polycarbonate. *Lab on a Chip*, **10**, 1324–1327. 43

Oh, S. & Choo, A. (2006). Human embryonic stem cells: Technological challenges towards therapy. *Clinical and Experimental Pharmacology and Physiology*, **33**, 489–495. 12

Oh, S.K., Chen, A.K., Mok, Y., Chen, X., Lim, U.M., Chin, A., Choo, A.B. & Reuveny, S. (2009). Long-term microcarrier suspension cultures of human embryonic stem cells. *Stem Cell Research*, **2**, 219–230. 24

Okita, K. & Yamanaka, S. (2006). Intracellular signalling pathways regulating pluripotency of embryonic stem cells. *Current Stem Cell Research and Therapy*, **1**, 103–111. 17

Okita, K., Nakagawa, M., Hyenjong, H., Ichisaka, T. & Yamanaka, S. (2008). Generation of mouse induced pluripotent stem cells without viral vectors. *Science*, **322**, 949–953. 8

Okumoto, S. (2010). Imaging approach for monitoring cellular metabolites and ions using genetically encoded biosensors. *Current Opinion in Biotechnology*, **21**, 45–54. 101

Oswald, J., Boxberger, S., Jørgensen, B., Feldmann, S., Ehninger, G., Bornhäuser, M. & Werner, C. (2004). Mesenchymal stem cells can be differentiated into endothelial cells in vitro. *Stem Cells*, **22**, 377–384. 6

Ouyang, A. & Yang, S. (2008). A two-stage perfusion fibrous bed bioreactor system for mass production of embryonic stem cells. *Expert Opinion on Biological Therapy*, **8**, 895–909. 25

Ozcan, A. & Demirci, U. (2008). Ultra wide-field lens-free monitoring of cells on-chip. *Lab on a Chip*, **8**, 98–106. 102

Paguirigan, A.L. & Beebe, D.J. (2008). Microfluidics meet cell biology: Bridging the gap by validation and application of microscale techniques for cell biological assays. *BioEssays*, **30**, 811–821. 28

Pal, R., Mandal, A., Rao, H., Rao, M. & Khanna, A. (2007). A panel of tests to standardize the characterization of human embryonic stem cells. *Regenerative Medicine*, **2**, 179–192. 7

Paliwal, S., Wang, C.J. & Levchenko, A. (2008). Pulsing cells: How fast is too fast? *HFSP Journal*, **2**, 251–256. 139

Pankov, R. & Yamada, K.M. (2002). Fibronectin at a glance. *Journal of Cell Science*, **115**, 3861–3863. 20

Park, I., Arora, N., Huo, H., Maherali, N., Ahfeldt, T., Shimamura, A., Lensch, M.W., Cowan, C., Hochedlinger, K. & Daley, G.Q. (2008). Disease-specific induced pluripotent stem cells. *Cell*, **134**, 877–886. 10

Paul, S.M., Mytelka, D.S., Dunwiddie, C.T., Persinger, C.C., Munos, B.H., Lindborg, S.R. & Schacht, A.L. (2010). How to improve R&D productivity: The pharmaceutical industry's grand challenge. *Nature Reviews Drug Discovery*, **9**, 203–214. 9

Peerani, R. & Zandstra, P.W. (2010). Enabling stem cell therapies through synthetic stem cell–niche engineering. *Journal of Clinical Investigation*, **120**, 60–70. 15, 18

Pera, M. & Tam, P. (2010). Extrinsic regulation of pluripotent stem cells. *Nature*, **465**, 713–720. 15

Perozziello, G., Bundgaard, F. & Geschke, O. (2008). Fluidic interconnections for microfluidic systems: A new integrated fluidic interconnection allowing plug'n'play functionality. *Sensors and Actuators B: Chemical*, **130**, 947–953. 45

Petronis, S., Stangegaard, M., Christensen, C.B. & Dufva, M. (2006). Transparent polymeric cell culture chip with integrated temperature control and uniform media perfusion. *Biotechniques*, **40**, 368–375. 74, 89, 102, 117, 119

Placzek, M.R., Chung, I., Macedo, H.M., Ismail, S., Blanco, T.M., Lim, M., Cha, J.M., Fauzi, I., Kang, Y., Yeo, D.C., Ma, C.Y.J., Polak, J.M., Panoskaltsis, N. & Mantalaris, A. (2009). Stem cell bioprocessing: Fundamentals and principles. *Journal of the Royal Society Interface*, **6**, 209–232. 13

Plews, J.R., Li, J., Jones, M., Moore, H.D., Mason, C., Andrews, P.W. & Na, J. (2010). Activation of pluripotency genes in human fibroblast cells by a novel mRNA based approach. *PLoS ONE*, **5**, e14397. 8

Polak, J. & Mantalaris, S. (2008). Stem cells bioprocessing: An important milestone to move regenerative medicine research into the clinical arena. *Pediatric Research*, **63**, 461–466. 15

Pouton, C. & Haynes, J. (2005). Pharmaceutical applications of embryonic stem cells. *Advanced Drug Delivery Reviews*, **57**, 1918–1934. 9

Power, C. & Rasko, J.E. (2008). Whither prometheus' liver? greek myth and the science of regeneration. *Annals of Internal Medicine*, **149**, 421–426. 10

Prowse, A.B., Chong, F., Gray, P.P. & Munro, T.P. (2011). Stem cell integrins: Implications for ex-vivo culture and cellular therapies. *Stem Cell Research*, **6**, 1–12. 19

Puccinelli, J., Su, X. & Beebe, D. (2010). Automated High-Throughput microchannel assays for cell biology: Operational optimization and characterization. *Journal of the Association for Laboratory Automation*, **15**, 25–32. 138

Qi, H., Chen, T., Yao, L. & Zuo, T. (2009). Micromachining of microchannel on the polycarbonate substrate with CO_2 laser direct-writing ablation. *Optics and Lasers in Engineering*, **47**, 594 – 598. 43

Quaglio, M., Canavese, G., Giuri, E., Marasso, S.L., Perrone, D., Cocuzza, M. & Pirri, C.F. (2008). Evaluation of different PDMS interconnection solutions for silicon, pyrex and COC microfluidic chips. *Journal of Micromechanics and Microengineering*, **18**, 055012. 45

Rao, R.R., Calhoun, J.D., Qin, X., Rekaya, R., Clark, J.K. & Stice, S.L. (2004). Comparative transcriptional profiling of two human embryonic stem cell lines. *Biotechnology and Bioengineering*, **88**, 273–286. 7

Rayment, E.A. & Williams, D.J. (2010). Mind the gap: Challenges in characterising and quantifying cell- and tissue-based therapies for clinical translation. *Stem Cells*, **28**, 996–1004. 11

Raymond, K., Deugnier, M., Faraldo, M.M. & Glukhova, M.A. (2009). Adhesion within the stem cell niches. *Current Opinion in Cell Biology*, **21**, 623–629. 19

Rees, S. & Wise, A. (2008). The industrialisation of cellular screening. *Expert Opinion on Drug Discovery*, **3**, 715–723. 25

Regehr, K., Domenech, M., Koepsel, J., Carver, K., Ellison-Zelski, S., Murphy, W., Schuler, L., Alarid, E. & Beebe, D. (2009). Biological implications of polydimethylsiloxane-based microfluidic cell culture. *Lab on a Chip*, **9**, 2132–2139. 90, 135

Reilly, G.C. & Engler, A.J. (2010). Intrinsic extracellular matrix properties regulate stem cell differentiation. *Journal of Biomechanics*, **43**, 55–62. 19

Reubinoff, B.E., Pera, M.F., Fong, C., Trounson, A. & Bongso, A. (2000). Embryonic stem cell lines from human blastocysts: Somatic differentiation in vitro. *Nature Biotechnology*, **18**, 399–404. 7, 34

Reubinoff, B.E., Itsykson, P., Turetsky, T., Pera, M.F., Reinhartz, E., Itzik, A. & Ben-Hur, T. (2001). Neural progenitors from human embryonic stem cells. *Nature Biotechnology*, **19**, 1134–1140. 7

Reynolds, B. & Weiss, S. (1992). Generation of neurons and astrocytes from isolated cells of the adult mammalian central nervous system. *Science*, **255**, 1707–1710. 6

Rhee, M. & Burns, M.A. (2008). Microfluidic assembly blocks. *Lab on a Chip*, **8**, 1365. 43

Richards, M., Fong, C., Chan, W., Wong, P. & Bongso, A. (2002). Human feeders support prolonged undifferentiated growth of human inner cell masses and embryonic stem cells. *Nature Biotechnology*, **20**, 933–936. 7

Rodin, S., Domogatskaya, A., Strom, S., Hansson, E.M., Chien, K.R., Inzunza, J., Hovatta, O. & Tryggvason, K. (2010). Long-term self-renewal of human pluripotent stem cells on human recombinant laminin-511. *Nature Biotechnology*, **28**, 611–615. 20

Rosler, E.S., Fisk, G.J., Ares, X., Irving, J., Miura, T., Rao, M.S. & Carpenter, M.K. (2004). Long-term culture of human embryonic stem cells in feeder-free conditions. *Developmental Dynamics*, **229**, 259–274. 7

Ross, J.J. & Verfaillie, C.M. (2008). Evaluation of neural plasticity in adult stem cells. *Philosophical Transactions of the Royal Society B: Biological Sciences*, **363**, 199–205. 5

Rossi, S.L. & Keirstead, H.S. (2009). Stem cells and spinal cord regeneration. *Current Opinion in Biotechnology*, **20**, 552–562. 12

Rowland, T.J., Miller, L.M., Blaschke, A.J., Doss, E.L., Bonham, A.J., Hikita, S.T., Johnson, L.V. & Clegg, D.O. (2010). Roles of integrins in human induced pluripotent stem cell growth on matrigel and vitronectin. *Stem Cells and Development*, **19**, 1231–1240. 20

Rozario, T. & DeSimone, D. (2010). The extracellular matrix in development and morphogenesis: A dynamic view. *Developmental Biology*, **341**, 126–140. 19

Rubin, L.L. (2008). Stem cells and drug discovery: The beginning of a new era? *Cell*, **132**, 549–552. 9, 10, 22

Rubin, R.R. & Peyrot, M. (2001). Psychological issues and treatments for people with diabetes. *Journal of Clinical Psychology*, **57**, 457–478. 10

Saarela, V., Franssila, S., Tuomikoski, S., Marttila, S., Östman, P., Sikanen, T., Kotiaho, T. & Kostiainen, R. (2006). Re-usable multi-inlet PDMS fluidic connector. *Sensors and Actuators B: Chemical*, **114**, 552–557. 45

Sabourin, D., Snakenborg, D. & Dufva, M. (2009). Interconnection blocks: A method for providing reusable, rapid, multiple, aligned and planar microfluidic interconnections. *Journal of Micromechanics and Microengineering*, **19**, 035021. 45

Sahni, V. & Kessler, J.A. (2010). Stem cell therapies for spinal cord injury. *Nature Reviews Neurology*, **6**, 363–372. 12

Saias, L., Autebert, J., Malaquin, L. & Viovy, J.L. (2011). Design, modeling and characterization of microfluidic architectures for high flow rate, small footprint microfluidic systems. *Lab on a Chip*, **11**, 822–832. 137

Sakai, Y., Yoshiura, Y. & Nakazawa, K. (2011). Embryoid body culture of mouse embryonic stem cells using microwell and micropatterned chips. *Journal of Bioscience and Bioengineering*, **111**, 85–91. 27

Schäpper, D., Alam, M., Szita, N., Eliasson Lantz, A. & Gernaey, K. (2009). Application of microbioreactors in fermentation process development: a review. *Analytical and Bioanalytical Chemistry*, **395**, 679–695. 25

Schwarz, S.C. & Schwarz, J. (2010). Translation of stem cell therapy for neurological diseases. *Translational Research*, **156**, 155–160. 12

Séguin, C., McLachlan, J.M., Norton, P.R. & Lagugné-Labarthet, F. (2010). Surface modification of poly(dimethylsiloxane) for microfluidic assay applications. *Applied Surface Science*, **256**, 2524–2531. 137

Serra, M., Brito, C., Sousa, M.F., Jensen, J., Tostões, R., Clemente, J., Strehl, R., Hyllner, J., Carrondo, M.J. & Alves, P.M. (2010). Improving expansion of pluripotent human embryonic stem cells in perfused bioreactors through oxygen control. *Journal of Biotechnology*, **148**, 208–215. 25

Shenghui, H., Nakada, D. & Morrison, S.J. (2009). Mechanisms of stem cell self-renewal. *Annual Review of Cell and Developmental Biology*, **25**, 377–406. 2

Sia, S.K. & Whitesides, G.M. (2003). Microfluidic devices fabricated in poly(dimethylsiloxane) for biological studies. *Electrophoresis*, **24**, 3563–3576. 44

Simon, M.C. & Keith, B. (2008). The role of oxygen availability in embryonic development and stem cell function. *Nature Reviews Molecular Cell Biology*, **9**, 285–296. 18

Singh, A.M. & Dalton, S. (2009). The cell cycle and myc intersect with mechanisms that regulate pluripotency and reprogramming. *Cell Stem Cell*, **5**, 141 – 149. 15, 17

Skafte-Pedersen, P., Sabourin, D., Dufva, M. & Snakenborg, D. (2009). Multi-channel peristaltic pump for microfluidic applications featuring monolithic PDMS inlay. *Lab on a Chip*, **9**, 3003–3006. 127

Skelley, A.M. & Voldman, J. (2008). An active bubble trap and debubbler for microfluidic systems. *Lab on a Chip*, **8**, 1733–1737. 137

Skottman, H. & Hovatta, O. (2006). Culture conditions for human embryonic stem cells. *Reproduction*, **132**, 691–698. 7

Smith, D. (2010). Commercialization challenges associated with induced pluripotent stem cell-based products. *Regenerative Medicine*, **5**, 593–603. 8

Smith, K.P., Luong, M.X. & Stein, G.S. (2009). Pluripotency: Toward a gold standard for human ES and iPS cells. *Journal of Cellular Physiology*, **220**, 21–29. 2, 4

Snakenborg, D., Perozziello, G., Geschke, O. & Kutter, J.P. (2007). A fast and reliable way to establish fluidic connections to planar microchips. *Journal of Micromechanics and Microengineering*, **17**, 98–103. 45

Spiller, D.G., Wood, C.D., Rand, D.A. & white, M.R.H. (2010). Measurement of single-cell dynamics. *Nature*, **465**, 736–745. 29

Stadtfeld, M. & Hochedlinger, K. (2010). Induced pluripotency: History, mechanisms, and applications. *Genes & Development*, **24**, 2239–2263. 8

Stadtfeld, M., Nagaya, M., Utikal, J., Weir, G. & Hochedlinger, K. (2008). Induced pluripotent stem cells generated without viral integration. *Science*, **322**, 945–949. 8

Stangegaard, M., Petronis, S., Jorgensen, A.M., Christensen, C.B.V. & Dufva, M. (2006). A biocompatible micro cell culture chamber (μCCC) for the culturing and on-line monitoring of eukaryote cells. *Lab on a Chip*, **6**, 1045–1051. 89

Steiner, D., Khaner, H., Cohen, M., Even-Ram, S., Gil, Y., Itsykson, P., Turetsky, T., Idelson, M., Aizenman, E., Ram, R., Berman-Zaken, Y. & Reubinoff, B. (2010). Derivation, propagation and controlled differentiation of human embryonic stem cells in suspension. *Nature Biotechnology*, **28**, 361–364. 24

Stewart, M.H., Bendall, S.C. & Bhatia, M. (2008). Deconstructing human embryonic stem cell cultures: Niche regulation of self-renewal and pluripotency. *Journal of Molecular Medicine*, **86**, 875–886. 15

Sui, R., Liao, X., Zhou, X. & Tan, Q. (2011). The current status of engineering myocardial tissue. *Stem Cell Reviews and Reports*, **7**, 172–180. 13

Sung, J.H., Choi, J.r., Kim, D. & Shuler, M.L. (2009). Fluorescence optical detection in situ for real-time monitoring of cytochrome p450 enzymatic activity of liver cells in multiple microfluidic devices. *Biotechnology and Bioengineering*, **104**, 516–525. 29

Szita, N., Boccazzi, P., Zhang, Z., Boyle, P., Sinskey, A.J. & Jensen, K.F. (2005). Development of a multiplexed microbioreactor system for high-throughput bioprocessing. *Lab on a Chip*, **5**, 819–826. 31

Taipale, J. & Beachy, P.A. (2001). The Hedgehog and Wnt signalling pathways in cancer. *Nature*, **411**, 349–354. 15

Takahashi, K. & Yamanaka, S. (2006). Induction of pluripotent stem cells from mouse embryonic and adult fibroblast cultures by defined factors. *Cell*, **126**, 663–676. 8

Takahashi, K., Tanabe, K., Ohnuki, M., Narita, M., Ichisaka, T., Tomoda, K. & Yamanaka, S. (2007). Induction of pluripotent stem cells from adult human fibroblasts by defined factors. *Cell*, **131**, 861–872. 8

Tamanaha, C.R., Malito, M.P., Mulvaney, S.P. & Whitman, L.J. (2009). Reusable, compression-sealed fluid cells for surface mounting to planar substrates. *Lab on a Chip*, **9**, 1468 –1471. 73

Tang, L., Min, J., Lee, E., Kim, J. & Lee, N. (2010). Targeted cell adhesion on selectively micropatterned polymer arrays on a poly(dimethylsiloxane) surface. *Biomedical Microdevices*, **12**, 13–21. 137

Terstegge, S., Laufenberg, I., Pochert, J., Schenk, S., Itskovitz-Eldor, J., Endl, E. & Brüstle, O. (2007). Automated maintenance of embryonic stem cell cultures. *Biotechnology and Bioengineering*, **96**, 195–201. 23, 26

Terstegge, S., Rath, B.H., Laufenberg, I., Limbach, N., Buchstaller, A., Schütze, K. & Brüstle, O. (2009). Laser-assisted selection and passaging of human pluripotent stem cell colonies. *Journal of Biotechnology*, **143**, 224–230. 23

Thomas, R.J., Anderson, D., Chandra, A., Smith, N.M., Young, L.E., Williams, D. & Denning, C. (2008). Automated, scalable culture of human embryonic stem cells in feeder-free conditions. *Biotechnology and Bioengineering*, **102**, 1636–1644. 26

Thompson, J. (2009). Process development for rapid prototyping of microfluidic devices from thermoplastic polyurethanes. MEng Thesis, UCL Biochemical Engineering. 90

Thomson, J.A., Itskovitz-Eldor, J., Shapiro, S.S., Waknitz, M.A., Swiergiel, J.J., Marshall, V.S. & Jones, J.M. (1998). Embryonic stem cell lines derived from human blastocysts. *Science*, **282**, 1145–1147. 6

Thorgeirsson, S.S. & Grisham, J.W. (2006). Hematopoietic cells as hepatocyte stem cells: A critical review of the evidence. *Hepatology*, **43**, 2–8. 6

Thorsen, T., Maerkl, S.J. & Quake, S.R. (2002). Microfluidic large-scale integration. *Science*, **298**, 580–584. 38

Tilles, A.W., Baskaran, H., Partha, R., Yarmush, M. & Toner, M. (2001). Effects of oxygenation and flow on the viability and function of rat hepatocytes cocultered in a microchannel flat-plate bioreactor. *Biotechnology and Bioengineering*, **73**, 379–389. 73

Tkachenko, E., Gutierrez, E., Ginsberg, M.H. & Groisman, A. (2009). An easy to assemble microfluidic perfusion device with a magnetic clamp. *Lab on a Chip*, **9**, 1085–1095. 73

Toepke, M.W. & Beebe, D.J. (2006). PDMS absorption of small molecules and consequences in microfluidic applications. *Lab on a Chip*, **6**, 1484–1486. 90

Toh, Y., Zhang, C., Zhang, J., Khong, Y.M., Chang, S., Samper, V.D., van Noort, D., Hutmacher, D.W. & Yu, H. (2007). A novel 3D mammalian cell perfusion-culture system in microfluidic channels. *Lab on a Chip*, **7**, 302–309. 74

Torisawa, Y.s., Chueh, B.h., Huh, D., Ramamurthy, P., Roth, T.M., Barald, K.F. & Takayama, S. (2007). Efficient formation of uniform-sized embryoid bodies using a compartmentalized microchannel device. *Lab on a Chip*, **7**, 770–776. 30

Torsney, E. & Xu, Q. (2011). Resident vascular progenitor cells. *Journal of Molecular and Cellular Cardiology*, **50**, 304–311. 6

Tremml, G., Singer, M. & Malavarca, R. (2008). Culture of mouse embryonic stem cells. In *Current Protocols in Stem Cell Biology*, SUPPL. 5, John Wiley & Sons, Inc. 7

Trivedi, P., Tray, N., Nguyen, T., Nigam, N. & Gallicano, G.I. (2010). Mesenchymal stem cell therapy for treatment of cardiovascular disease: Helping people sooner or later. *Stem Cells and Development*, **19**, 1109–1120. 6

Tsang, K., Cheung, M., Chan, D. & Cheah, K. (2010). The developmental roles of the extracellular matrix: Beyond structure to regulation. *Cell and Tissue Research*, **339**, 93–110. 17

Tsien, R.Y. (1998). The green fluorescent protein. *Annual Reviews of Biochemistry*, **67**. 101

Valamehr, B., Jonas, S.J., Polleux, J., Qiao, R., Guo, S., Gschweng, E.H., Stiles, B., Kam, K., Luo, T.M., Witte, O.N., Liu, X., Dunn, B. & Wu, H. (2008). Hydrophobic surfaces for enhanced differentiation of embryonic stem cell-derived embryoid bodies. *Proceedings of the National Academy of Sciences of the United States of America*, **105**, 14459–14464. 18

van Noort, D., Ong, S.M., Zhang, C., Zhang, S., Arooz, T. & Yu, H. (2009). Stem cells in microfluidics. *Biotechnology Progress*, **25**, 52–60. 28

Veraitch, F.S., Scott, R., Wong, J., Lye, G.J. & Mason, C. (2008). The impact of manual processing on the expansion and directed differentiation of embryonic stem cells. *Biotechnology and Bioengineering*, **99**, 1216–1229. 23, 93

Vidarsson, H., Hyllner, J. & Sartipy, P. (2010). Differentiation of human embryonic stem cells to cardiomyocytes for in vitro and in vivo applications. *Stem Cell Reviews*, **6**, 108–120. 7

Vierbuchen, T., Ostermeier, A., Pang, Z.P., Kokubu, Y., Südhof, T.C. & Wernig, M. (2010). Direct conversion of fibroblasts to functional neurons by defined factors. *Nature*, **463**, 1035–1041. 8

Villa-Diaz, L.G., Torisawa, Y., Uchida, T., Nogueira-de-Souza, N.C., O'Shea, K.S., Takayama, S. & Smith, G.D. (2009). Microfluidic culture of single human embryonic stem cell colonies. *Lab on a Chip*, **9**, 1749–1755. 29, 30, 74

Villa-Diaz, L.G., Nandivada, H., Ding, J., Nogueira-de-Souza, N.C., Krebsbach, P.H., O'Shea, K.S., Lahann, J. & Smith, G.D. (2010). Synthetic polymer coatings for long-term growth of human embryonic stem cells. *Nature Biotechnology*, **28**, 581–583. 20

Wagers, A.J. & Weissman, I.L. (2004). Plasticity of adult stem cells. *Cell*, **116**, 639–648. 5

Watabe, T. & Miyazono, K. (2009). Roles of TGF-β family signaling in stem cell renewal and differentiation. *Cell Research*, **19**, 103–115. 15

Webster, A., Dyer, C.E., Haswell, S.J. & Greenman, J. (2010). A microfluidic device for tissue biopsy culture and interrogation. *Analytical Methods*, **2**, 1005–1007. 139

Wen, Y., Zhang, X. & Yang, S. (2010). Microplate-reader compatible perfusion microbioreactor array for modular tissue culture and cytotoxicity assays. *Biotechnology Progress*, **26**, 1135–1144. 29

Wen, Y., Chen, B. & Ildstad, S.T. (2011). Stem cell-based strategies for the treatment of type 1 diabetes mellitus. *Expert Opinion on Biological Therapy*, **11**, 41–53. 13

Wert, G.d. & Mummery, C. (2003). Human embryonic stem cells: Research, ethics and policy. *Human Reproduction*, **18**, 672–682. 8

White, J. & Dalton, S. (2005). Cell cycle control of embryonic stem cells. *Stem Cell Reviews*, **1**, 131–138. 17

Whitesides, G.M. (2006). The origins and the future of microfluidics. *Nature*, **442**, 368–373. 27

Whitesides, G.M. (2011). What comes next? *Lab on a Chip*, **11**, 191. 42

Whyte, J.L., Ball, S.G., Shuttleworth, C.A., Brennan, K. & Kielty, C.M. (2011). Density of human bone marrow stromal cells regulates commitment to vascular lineages. *Stem Cell Research*, **In Press, Accepted Manuscript**. 34

Wilson, M.E., Kota, N., Kim, Y., Wang, Y., Stolz, D.B., LeDuc, P.R. & Ozdoganlar, O.B. (2011). Fabrication of circular microfluidic channels by combining mechanical micromilling and soft lithography. *Lab on a Chip*, **11**, 1550–1555. 62

Wong, I. & Ho, C. (2009). Surface molecular property modifications for poly(dimethylsiloxane) (PDMS) based microfluidic devices. *Microfluidics and Nanofluidics*, **7**, 291–306. 90

Wong, R., Pera, M. & Pébay, A. (2008). Role of gap junctions in embryonic and somatic stem cells. *Stem Cell Reviews*, **4**, 283–292. 17

Wong, S.S. & Bernstein, H.S. (2010). Cardiac regeneration using human embryonic stem cells: producing cells for future therapy. *Regenerative Medicine*, **5**, 763–775. 13

Wu, Z. & Hjort, K. (2009). Surface modification of PDMS by gradient-induced migration of embedded pluronic. *Lab on a Chip*, **9**, 1500–1503. 90

Xu, C., Inokuma, M.S., Denham, J., Golds, K., Kundu, P., Gold, J.D. & Carpenter, M.K. (2001). Feeder-free growth of undifferentiated human embryonic stem cells. *Nature Biotechnology*, **19**, 971–974. 20

Xu, C., Rosler, E., Jiang, J., Lebkowski, J.S., Gold, J.D., O'Sullivan, C., Delavan-Boorsma, K., Mok, M., Bronstein, A. & Carpenter, M.K. (2005). Basic fibroblast growth factor supports undifferentiated human embryonic stem cell growth without conditioned medium. *Stem Cells*, **23**, 315–323. 7

Yamashita, Y.M. (2010). Cell adhesion in regulation of asymmetric stem cell division. *Current Opinion in Cell Biology*, **22**, 605–610. 19

Yang, M.T., Fu, J., Wang, Y.K., Desai, R.A. & Chen, C.S. (2011). Assaying stem cell mechanobiology on microfabricated elastomeric substrates with geometrically modulated rigidity. *Nature Protocols*, **6**, 187–213. 18

Yin, H., Zhang, X., Pattrick, N., Klauke, N., Cordingley, H.C., Haswell, S.J. & Cooper, J.M. (2007). Influence of hydrodynamic conditions on quantitative cellular assays in microfluidic systems. *Analytical Chemistry*, **79**, 7139–7144. 28

Yin, H., Pattrick, N., Zhang, X., Klauke, N., Cordingley, H.C., Haswell, S.J. & Cooper, J.M. (2008). Quantitative comparison between microfluidic and microtiter plate formats for cell-based assays. *Analytical Chemistry*, **80**, 179–185. 28

Ying, Q., Stavridis, M., Griffiths, D., Li, M. & Smith, A. (2003). Conversion of embryonic stem cells into neuroectodermal precursors in adherent monoculture. *Nature Biotechnology*, **21**, 183–186. 34, 70

Young, E.W.K. & Beebe, D.J. (2010). Fundamentals of microfluidic cell culture in controlled microenvironments. *Chemical Society Reviews*, **39**, 1036–1048. 27

Young, E.W.K., Berthier, E., Guckenberger, D.J., Sackmann, E., Lamers, C., Meyvantsson, I., Huttenlocher, A. & Beebe, D.J. (2011). Rapid prototyping of arrayed microfluidic systems in polystyrene for cell-based assays. *Analytical Chemistry*, **83**, 1408–1417. 43

Yu, J., Vodyanik, M.A., Smuga-Otto, K., Antosiewicz-Bourget, J., Frane, J.L., Tian, S., Nie, J., Jonsdottir, G.A., Ruotti, V., Stewart, R., Slukvin, I.I. & Thomson, J.A. (2007). Induced pluripotent stem cell lines derived from human somatic cells. *Science*, **318**, 1917–1920. 8

Yue, X., Drakakis, E., Lim, M., Radomska, A., Ye, H., Mantalaris, A., Panoskaltsis, N. & Cass, A. (2008). A real-time multi-channel monitoring system for stem cell culture process. *IEEE Transactions on Biomedical Circuits and Systems*, **2**, 66–77. 21

Yuen, P.K. (2008). SmartBuild–A truly plug-n-play modular microfluidic system. *Lab on a Chip*, **8**, 1374–1378. 43

Yuen, P.K. & Goral, V.N. (2010). Low-cost rapid prototyping of flexible microfluidic devices using a desktop digital craft cutter. *Lab on a Chip*, **10**, 384–387. 42

Zampetaki, A., Kirton, J.P. & Xu, Q. (2008). Vascular repair by endothelial progenitor cells. *Cardiovascular Research*, **78**, 413–421. 6

Zhang, Y. & Ozdemir, P. (2009). Microfluidic DNA amplification – a review. *Analytica Chimica Acta*, **638**, 115–125. 117

Zhao, T. & Xu, Y. (2010). p53 and stem cells: new developments and new concerns. *Trends in Cell Biology*, **20**, 170–175. 17

Zhou, H., Wu, S., Joo, J.Y., Zhu, S., Han, D.W., Lin, T., Trauger, S., Bien, G., Yao, S. & Zhu, Y. (2009). Generation of induced pluripotent stem cells using recombinant proteins. *Cell Stem Cell*, **4**, 381–384. 8